

JADOMYCIN B AFFECTS CYCLOOXYGENASE-2 RELATED SIGNALLING AND
ACTS SYNERGISTICALLY WITH CELECOXIB TO KILL HUMAN BREAST
CANCER CELLS

by

Brendan Timothy McKeown

Submitted in partial fulfilment of the requirements
for the degree of Doctor of Philosophy

at

Dalhousie University
Halifax, Nova Scotia
March 2024

Dalhousie University is located in Mi'kma'ki, the
ancestral and unceded territory of the Mi'kmaq.
We are all Treaty people.

© Copyright by Brendan Timothy McKeown, 2024

Dedication

To Amanda.

“There was a man who sat each day looking out through a narrow vertical opening where a single board had been removed from a tall wooden fence. Each day a wild ass of the desert passed outside the fence and across the narrow opening – first the nose, then the head, the forelegs, the long brown back, the hindlegs, and lastly the tail. One day, the man leaped to his feet with the light of discovery in his eyes and he shouted for all who could hear him: ‘It’s obvious! The nose causes the tail!’”

-Frank Herbert, *Heretics of Dune*

Table of Contents

List of Tables	ix
List of Figures	xii
Abstract	xvi
List of Abbreviations and Symbols Used	xvii
Acknowledgements	xxiii
Chapter 1: Introduction	1
1.1: History of Cancer.....	1
1.2: Cancer Incidence, Mortality, and Cost	6
1.3: Cancer	9
1.3.1: Hallmarks of Cancer	11
1.3.1.1: Sustaining Proliferative Signalling	13
1.3.1.2: Evading Growth Suppressors.....	13
1.3.1.3: Resisting Cell Death	14
1.3.1.4: Enabling Replicative Immortality.....	14
1.3.1.5: Inducing Angiogenesis	15
1.3.1.6: Activating Invasion and Metastasis	15
1.3.1.7: Reprogramming Energy Metabolism.....	16
1.3.1.8: Evading Immune Destruction	17
1.3.1.9: Unlocking Phenotypic Plasticity.....	17
1.3.1.10: Genome Instability and Mutation	18
1.3.1.11: Tumour Promoting Inflammation	18
1.3.1.12: Nonmutational Epigenetic Reprogramming	18
1.3.1.13: Polymorphic Microbiomes	19
1.4: Breast Anatomy and Introduction to Breast Cancer	19
1.4.1: Classification of Breast Cancer.....	24

1.4.2: Triple Negative Breast Cancer.....	35
1.4.3: Experimental Models of Breast Cancer	35
1.4.3.1: <i>in vivo</i> Models of Breast Cancer	36
1.4.3.2: <i>in vitro</i> Models of Breast Cancer	38
1.4.4: Treatment Options for Breast Cancer	41
1.4.4.1: Surgery.....	41
1.4.4.2: Radiation Therapy.....	42
1.4.4.3: Targeted Therapy.....	43
1.4.4.4: Hormone Therapy	44
1.4.4.5: Immunotherapy	49
1.4.4.6: Chemotherapy	50
1.4.5: Multidrug Resistance in Breast Cancer	54
1.4.5.1: Drug Efflux Transporters.....	56
1.4.5.2: Drug Influx Transporters	58
1.4.5.3: Drug Inactivation	58
1.4.5.4: Modification of Drug Targets	59
1.4.5.5: DNA Damage Repair.....	60
1.4.5.6: Avoidance of Apoptosis and Increased Survival Signalling	61
1.4.6: The Role of Prostaglandins in Breast Cancer	62
1.5: Natural Products in Drug Discovery and Development	65
1.5.1: Natural Products in the Treatment of Cancer	69
1.6: Jadomycins: Source, Structure, and Diversity	70
1.6.1: Antimicrobial Activity of Jadomycins.....	75
1.6.2: Anticancer Effects of Jadomycins <i>in vitro</i>	76
1.6.2.1: Jadomycins and Liver Cancer.....	81
1.6.2.2: Jadomycins and Myeloma	81

1.6.2.3: Jadomycins and Lung Cancer	82
1.6.2.4: Jadomycins and Cervical Cancer	83
1.6.2.5: Jadomycins and Melanoma.....	83
1.6.2.6: Jadomycins and Colon Cancer.....	84
1.6.2.7: Jadomycins and Brain Cancer.....	85
1.6.2.8: Jadomycins and Stomach Cancer	85
1.6.2.9: Jadomycins and Pancreatic Cancer.....	86
1.6.2.10: Jadomycins and Prostate Cancer.....	86
1.6.2.11: Jadomycins and Breast Cancer	86
1.6.3: Anticancer Effects of Jadomycins <i>in vivo</i>	89
1.6.4: Proposed Jadomycin Mechanisms of Action.....	90
1.6.4.1: Apoptosis Induction.....	92
1.6.4.2: Cell Cycle Alteration	94
1.6.4.3: Aurora-B Kinase Inhibition	95
1.6.4.4: DNA Cleavage.....	97
1.6.4.5: Reactive Oxygen Species Formation.....	98
1.6.4.6: Topoisomerase II Inhibition.....	100
1.7: Drug-Drug Combination Therapy	106
1.7.1: Mathematical Models for Determining Synergy	106
1.7.4.1: Loewe Additivity	107
1.7.4.2: Chou-Talalay Combination Index	108
1.7.4.3: Bliss Independence	110
Chapter 2: Research Rationale, General Hypothesis, and Objectives.....	112
Chapter 3: Materials and Methods	114
3.1: Chemical and Biological Materials.....	114
3.2: Production of Jadomycins.....	117

3.3: Cell Lines.....	118
3.4: Cell Culture.....	119
3.5: MTT Viability Assays	119
3.6: Jadomycin B Aging and Evaluation of Potency and Chemical Stability	120
3.7: Combination Index and Drug Reduction Index Calculation	121
3.8: Flow Cytometry and Cell Cycle Analysis	122
3.9: <i>In Vivo</i> Complex of Enzyme Assay.....	122
3.10: RNA Isolation, Reverse Transcription, and Quantitative Real-Time Polymerase Chain Reaction	123
3.11: RT ² Profiler PCR Array.....	126
3.12: Immunoblot Analysis.....	126
3.13: PGE ₂ ELISA	127
3.14: Cellular Lipid Profile Analysis	127
3.15: Calculation of Lipogenesis Indices and Estimated Desaturase Enzyme Activity	128
3.16: Purified COX2 Enzyme Activity Assay	129
3.17: Synergy Score Calculation.....	130
3.18: Molecular Docking of Molecules of Interest to the COX2 Active Site <i>In Silico</i>	130
3.19: Cell Spheroid Formation.....	130
3.20: Acid Phosphatase Assay for Spheroid Viability.....	131
3.21: Statistical Analysis.....	132
Chapter 4: Results.....	133
4.1: Comparison of Potency Between Jadomycin B Produced Commercially and Synthesized Locally	133
4.2: Determination of Jadomycin B Cytotoxic Effect Stability Following Long-Term Storage at 25 °C and 37 °C.....	135
4.3: Effect of Jadomycin B on Accumulation of Cells in Phases of the Cell Cycle....	139

4.4: TOP2 Cleavage Complex Accumulation in the Presence of Jadomycin B	141
4.5: Synergy Between Jadomycin B and Topoisomerase Poisons	144
4.6: Assessment of Resistance in 231-JB and 231-MITX Cells	151
4.7: Changes in <i>TOP2</i> mRNA Expression in 231-JB and 231-MITX Cells	156
4.8: Association of Resistance and Increased mRNA Expression of ABC Transporters	158
4.9: Changes in mRNA Expression of Human Cancer Drug Targets in 231-JB Cells	160
4.10: COX2 Protein Expression in 231-JB Cells	162
4.11: EP4 Protein Expression in 231-CON Cells Following Transient Jadomycin B Exposure	164
4.12: Concentrations of PGE ₂ in 231-CON Growth Medium Following Exposure to Jadomycin B	166
4.13: Alterations to Cellular Lipid Profiles Following Jadomycin B Exposure	168
4.14: Lipogenesis Assessment by Calculation of Enzyme Indices	180
4.15: Assessment of Synergy Between Jadomycin B and Celecoxib in COX2 Enzyme Activity Assays	183
4.16: <i>in silico</i> Modeling of Jadomycin B Binding to the Active Site of COX2	186
4.17: Determination of Synergistic Reduction of Cellular Viability with Jadomycin B and COX2 Inhibitors	189
4.18: Cell Spheroid Formation and Viability Assessment	195
4.19: Measurement of PI3K Signalling	202
Chapter 5: Discussion	206
5.1: Characterization of the Similarity of Jadomycin B Obtained from Multiple Sources and Initial Stability Assessment	208
5.2: Jadomycin B Behaves Differently as Compared to Established TOP2 Poisons	209
5.3: Resistance to Jadomycin B is Differentially Mediated as Compared to Mitoxantrone Resistance	212
5.4: Jadomycin B Resistance is Correlated to Increased COX2 Expression	214

5.5: Jadomycin B Abolishes PGE ₂ Accumulation and Alters Cellular Lipid Profiles	217
5.6: Celecoxib and Jadomycin B Act Synergistically to Inhibit COX2 Activity and Result in an Enhanced Cytotoxic Effect	218
5.7: Formation of Cell Spheroids is Inhibited by Jadomycin B Exposure.....	221
5.8: Jadomycin B Induces Minor Changes to PI3K/AKT Intracellular Signalling	222
5.9: Limitations and Future Directions	223
5.10: Conclusion	227
References	229
Appendix A: Copyright Permissions.....	271
Appendix B: Supplementary Figures.....	284
Appendix C: Supplementary Tables	305

List of Tables

Table 1.1: Hallmarks and Enabling Characteristics of Cancer	12
Table 1.2: 10-Year Probability of Breast Cancer Diagnosis or Death	23
Table 1.3: Scoring of Histological Grade in Breast Cancer	27
Table 1.4: Determination of Histological Grade	28
Table 1.5: Criteria for Primary Tumour Size (T) Classifications	29
Table 1.6: Criteria for Lymph Node Metastases (N) Classifications	30
Table 1.7: Criteria for Metastases (M) Classifications	32
Table 1.8: TNM Anatomic Stage Groups	33
Table 1.9: Immunohistochemical Criteria for Defining Breast Cancer Subtypes.....	34
Table 1.10: ABC Transporters Involved in Multidrug Resistance	57
Table 1.11: Jadomycin IC₅₀ Values Reported in Breast Cancer Cell Lines	77
Table 1.12: Jadomycin IC₅₀ Values Reported in All Other Cancer Cell Lines.....	79
Table 3.1: Primary and Secondary Antibodies used for Immunoblotting Assays	116
Table 3.2: PCR Primers Used in this Work	125
Table 4.1: Comparison of IC₅₀s after 72 h Exposure to Synthesized or Commercial Jadomycin B in 231-CON cells	134
Table 4.2: Calculated Median Effect Parameters for Combinations of Drugs against 231-CON Cell Viability	146
Table 4.3: Interpolated Combination Index Values for Drugs Tested Against 231-CON Viability	147

Table 4.4: The Cytotoxic Effects of Control Drugs and Jadomycins in Drug Sensitive and Drug Resistant Cells	152
Table C.1: Interpolated Dose Reduction Index Values for a Combination of Jadomycin B and Doxorubicin	305
Table C.2: Interpolated Dose Reduction Index Values for a Combination of Jadomycin B and Mitoxantrone	306
Table C.3: Interpolated Dose Reduction Index Values for a Combination of Jadomycin B and SN-38	307
Table C.4: Interpolated Dose Reduction Index Values for a Combination of Jadomycin B and MG132	308
Table C.5: Interpolated Dose Reduction Index Values for a Combination of Doxorubicin and Mitoxantrone	309
Table C.6: Interpolated Dose Reduction Index Values for a Combination of Doxorubicin and SN-38	310
Table C.7: Interpolated Dose Reduction Index Values for a Combination of Doxorubicin and MG132	311
Table C.8: Interpolated Dose Reduction Index Values for a Combination of Mitoxantrone and SN-38	312
Table C.9: Interpolated Dose Reduction Index Values for a Combination of Mitoxantrone and MG132.....	313
Table C.10: Interpolated Dose Reduction Index Values for a Combination of SN-38 and MG132.....	314
Table C.11: Expression Changes Found with Human Cancer Drug Target Array	315
Table C.12: Jadomycin B and Celecoxib Act Synergistically to Inhibit COX2	318
Table C.13: Synergy Scores for Jadomycin B and Celecoxib in 231-CON Cells	319
Table C.14: Synergy Scores for Jadomycin B and Ibuprofen in 231-CON Cells	320

Table C.15: Synergy Scores for Jadomycin B Naproxen in 231-CON Cells	321
Table C.16: Synergy Scores for Jadomycin B and Celecoxib in 231-JB Cells	322
Table C.17: Synergy Scores for Jadomycin B and Ibuprofen in 231-JB Cells	323
Table C.18: Synergy Scores for Jadomycin B and Naproxen in 231-JB Cells	324
Table C.19: Synergy Scores for Jadomycin B and Celecoxib in MCF-7 Cells.....	325

List of Figures

Figure 1.1: Breast Anatomy	22
Figure 1.2: Hormone Therapy Mechanisms of Action	48
Figure 1.3: Molecular Structures of Example Chemotherapeutics.....	53
Figure 1.4: Overview of Mechanisms of Drug Resistance in Cancer Cells	55
Figure 1.5: Development of Natural Products to Pharmaceutical Agents	68
Figure 1.6: Morphology and Life Cycle of <i>Streptomyces venezuelae</i>.....	73
Figure 1.7: Molecular Structures of Example Jadomycin Analogues	74
Figure 1.8: Previously Proposed Mechanisms of Action of Jadomycons in Human Breast Cancer Cells.....	91
Figure 1.9: DNA and RNA Topological Problems Managed by Topoisomerases ...	104
Figure 1.10: Topoisomerase II Cleavage Complex Formation.....	105
Figure 4.1: Change in Jadomycin B Potency Following Aging	136
Figure 4.2: Jadomycin B Changes Colour Following Aging at 25 °C.....	137
Figure 4.3: Jadomycin B Changes Colour Following Aging at 37 °C.....	138
Figure 4.4: Alterations in Cell Cycle Distribution Following Jadomycin B or Mitoxantrone Exposure.....	140
Figure 4.5: Jadomycin B Does Not Cause Accumulation of TOP2 Cleavage Complexes.....	142
Figure 4.6: Jadomycin B Does Not Cause Accumulation of TOP1 Cleavage Complexes.....	143
Figure 4.7: Isobiograms Representing Dose Reduction or Increase Needed When Drugs are Used in Combination with Jadomycin B	149

Figure 4.8: Isobiograms Representing Dose Reduction or Increase Needed For All Other Drugs Combinations.....	150
Figure 4.9: IC₅₀ Plots for Data Reported in Table 4.4.....	153
Figure 4.10: Dose Response Curves for Jadomycin IC₅₀ Values Reported in Table 4.4	154
Figure 4.11: Dose Response Curves for Other IC₅₀ Values Reported in Table 4.4.....	155
Figure 4.12: <i>TOP2</i> mRNA Expression Does Not Significantly Change in 231-JB Cells	157
Figure 4.13: Resistance to mitoxantrone, but not to jadomycin B, is associated with increased mRNA expression of <i>ABCG2</i>.....	159
Figure 4.14: Expression of <i>COX2</i> mRNA is increased in 231-JB cells.....	161
Figure 4.15: Expression of COX2 Protein is Increased in 231-JB cells	163
Figure 4.16: Expression of EP4 Protein Decreases with Jadomycin B	165
Figure 4.17: Growth Medium Concentration of PGE₂ with Jadomycin B.....	167
Figure 4.18: Biosynthesis of n-6 and n-3 Fatty Acids	169
Figure 4.19: Representative GFCID Chromatograms For 24 h Fatty Acid Analysis	173
Figure 4.20: Representative GFCID Chromatograms For 48 h Fatty Acid Analysis	177
Figure 4.21: Changes in Cellular Levels of n-6 Fatty Acids Following Exposure to Jadomycin B.....	178
Figure 4.22: Changes in Cellular Levels of n-3 Fatty Acids Following Exposure to Jadomycin B.....	179
Figure 4.23: Calculations of Lipogenesis	181
Figure 4.24: Estimation of Desaturase Activity	182

Figure 4.25: Jadomycin B Enhances Inhibition of COX2 by Celecoxib	184
Figure 4.26: Jadomycin B and Celecoxib Act Synergistically to Inhibit COX2	185
Figure 4.27: Jadomycons Occur in a Diastereomeric Mixture of 3a<i>S</i> and 3a<i>R</i> forms.....	187
Figure 4.28: Molecular Docking of Arachidonic Acid, Jadomycin B, and Known Inhibitors of COX2.....	188
Figure 4.29: Synergy Scores for Jadomycin B and Celecoxib, Ibuprofen, or Naproxen in 231-CON Cells.....	190
Figure 4.30: Synergy Scores for Jadomycin B and Celecoxib, Ibuprofen, or Naproxen in 231-JB Cells.....	191
Figure 4.31: Synergy Scores for Jadomycin B and Celecoxib Across an Expanded Range of Concentrations in 231-CON and 231-JB Cells	193
Figure 4.32: Synergy Scores for Jadomycin B and Celecoxib in MCF-7 Cells	194
Figure 4.33: Effects of Jadomycin B on Spheroid Formation and Viability	196
Figure 4.34: Representative Microscopic Images of Cell Spheroids Following Exposure to Jadomycin B.....	198
Figure 4.35: Effects of Jadomycin B Preexposure on Spheroid Formation and Viability.....	199
Figure 4.36: Representative Microscopic Images of Cell Spheroids Following Preexposure to Jadomycin B.....	201
Figure 4.37: Expression of PI3K Protein with Jadomycin B	203
Figure 4.38: Expression of AKT Protein with Jadomycin B	204
Figure 4.39: Expression of mTOR Protein with Jadomycin B	205
Figure 5.1: Summary of Novel Observations on the COX2 Related Activity of Jadomycin B Described in this Work.....	207
Figure B.1: Graphical Representation of IC₅₀ Values Reported in Table 4.1.....	284

Figure B.2: Dose Response Curves for Jadomycin B Aged at 25 °C.....	285
Figure B.3: Dose Response Curves for Jadomycin B Aged at 37 °C.....	286
Figure B.4: Jadomycin B Absorbance at 550 nm.....	287
Figure B.5: Dose Response Curves for Combination Index Calculations Involving Jadomycin B.....	288
Figure B.6: Dose Response Curves for All Other Combination Index Calculations	289
Figure B.7: Changes in Other Cellular Levels of Fatty Acids Following Exposure to Jadomycin B.....	296
Figure B.8: Pre-Incubation of Jadomycin B with COX2 Does Not Affect Enzyme Inhibition.....	297
Figure B.9: Synergistic Activity of Jadomycins with Celecoxib, Naproxen, and Ibuprofen in 231-CON cells	299
Figure B.10: Synergistic Activity of Jadomycins with Celecoxib, Naproxen, and Ibuprofen in 231-JB cells	301
Figure B.11: Synergistic Activity of Jadomycins with Celecoxib Across an Expanded Range of Concentrations in 231-CON cells	302
Figure B.12: Synergistic Activity of Jadomycins with Celecoxib Across an Expanded Range of Concentrations in 231-JB cells	303
Figure B.13: Synergistic Activity of Jadomycins with Celecoxib in MCF-7 cells.....	304

Abstract

Breast cancer affects 1 in 8 Canadian women and 10-20% of advanced breast cancers are triple negative. Triple negative breast cancers (TNBC) lack receptors required for hormone and targeted therapy and, thus, require cytotoxic therapy as first line treatment. Development of multi-drug resistance (MDR) is expected with long term chemotherapy, leading to eventual treatment failure. One mechanism of MDR involves removal of the cytotoxic substance by efflux transporters, namely P-glycoprotein (ABCB1) and breast cancer resistance protein (ABCG2). Jadomycin B remains effective in killing many different types of breast cancer cells, including MDR and TNBC. While increased expression of ABCB1 or ABCG2 transporters do not result in resistance to jadomycin B, it is important to identify possible pathways for the development of jadomycin B resistance as this will aid our understanding of how jadomycin B exerts a cytotoxic effect.

Jadomycin B is a compound produced by the soil bacterium *Streptomyces venezuelae* and has previously been shown to exert a cytotoxic effect through induction of reactive oxygen species (ROS) and to interact with topoisomerase 2 (TOP2). While each of these pathways are supported, neither fully explains the observed cytotoxic effect of jadomycin B *in vitro*. The goal of this project was, therefore, to elucidate and describe further pharmacological mechanism(s) through which jadomycin B may exert anticancer activity.

By selecting for jadomycin B resistance in the MDA-MB-231 human TNBC cell line, increased cyclooxygenase 2 (COX2) expression was observed suggesting jadomycin B may affect COX2 signalling. COX2 is found in many solid tumours where its expression is associated with increased inflammation, proliferation, metastasis, apoptosis avoidance, and poor patient outcome. These effects are mediated by prostaglandin E₂ (PGE₂) which is synthesized by COX2 from arachidonic acid (AA). Additional studies showed that jadomycin B exposure in control breast cancer cells increased cellular AA levels and decreased media levels of PGE₂. Jadomycin B alone did not inhibit COX2 but acted synergistically with the known COX2 inhibitor celecoxib. COX2 inhibitors were subsequently used to determine that a synergistic cytotoxic effect with jadomycin B occurred *in vitro*. This synergistic interaction was observed in control MDA-MB-231, jadomycin B-resistant cells, and MCF-7 breast cancer cells. Finally, jadomycin B was shown to decrease the formation of MCF-7 cell spheroids, indicating an inhibitory effect toward cancer stem cells.

This work has identified a novel interaction between jadomycin B and the known chemotherapy target COX2 in cellular models of breast cancer. By better understanding this anticancer effect, jadomycin B continues to show promise as a potential therapy for MDR breast cancer.

List of Abbreviations and Symbols Used

°C – degrees Celsius

15-PGDH – 15-prostaglandin dehydrogenase

2D – two dimensional

231-CON – control MDA-MB-231 cells

231-JB – jadomycin-resistant MDA-MB-231 cells

231-MITX – mitoxantrone-resistant MDA-MB-231 cells

231-TXL – paclitaxel-resistant MDA-MB-231 cells

3D – three dimensional

4T1-TXL – paclitaxel-resistant 4T1 cells

γ H2AX – phosphorylated histone H2AX

Δ 5D – Δ 5 desaturase

Δ 6D – Δ 6 desaturase

μ g – microgram

μ L – microliter

μ m – micrometer

μ M – micromolar

AA – arachidonic acid

ABC – adenosine triphosphate-binding cassette superfamily drug efflux transporters

ABK – aurora-B kinase

AKT – protein kinase B

ATCC – American Tissue Culture Collection

ATM – ataxia telangiectasia mutated serine/threonine kinase gene

ATP – adenosine triphosphate

BCE – before current era

Bcl-2 – B-cell lymphoma 2 protein

BCRP – breast cancer resistance protein, alternative to ABCG2

BCT – breast conserving therapy

BH3 – Bcl-2-homology-3

BRCA1 – breast cancer susceptibility gene 1

BRCA2 – breast cancer susceptibility gene 2

BRIP1 – BRCA1 interacting protein 1 gene

BSA – bovine serum albumin

Cas-9 – CRISPR-associated protein 9

CCND1 – cyclin-D1 gene

CE – current era

CHK – checkpoint kinase 2 gene

CI – combination index

cm – centimeter

COX1 – cyclooxygenase-1

COX2 – cyclooxygenase-2

CRISPR – clustered regularly interspaced short palindromic repeats

DMEM – Dulbecco’s modified Eagle’s medium

DMSO – dimethyl sulfoxide

DNA – deoxyribonucleic acid

dNTPs – deoxynucleoside triphosphates

DPD – dihydropyrimidine dehydrogenase

DTT – dithiothreitol

E1 – estrone

E2 – estradiol

E3 – estriol

EGFR – epidermal growth factor receptor

EMT – epithelial-mesenchymal transition

EP1 – prostaglandin E₂ receptor-1

EP2 – prostaglandin E₂ receptor-2

EP3 – prostaglandin E₂ receptor-3

EP4 – prostaglandin E₂ receptor-4

ER – estrogen receptor

ER⁻ – estrogen receptor negative

ER⁺ – estrogen receptor positive

ERBB2 – human epidermal growth factor receptor 2 gene

ERK – extracellular signal-regulated kinase

f_a – fraction affected

FBS – fetal bovine serum

G – gravity

GCFID – gas chromatograph and flame ionization detector

h – hours

HeLa – Henrietta Lacks cervical carcinoma cell line

HER2 – human epidermal growth factor receptor 2

HER2⁻ – human epidermal growth factor receptor 2 negative

HER2⁺ – human epidermal growth factor receptor 2 positive

HMEC – human microvascular epithelial cells

IC₅₀ – half maximal inhibitory concentration

ICE – *in vivo* complex of enzyme

ISP – International *Streptomyces* Project

kg – kilogram

Ki67 – antigen kiel 67

LDH – lactate dehydrogenase

LHRH – luteinizing hormone releasing hormone

MAPK – mitogen-activated protein kinase

MCF-7 – Michigan Cancer Foundation breast cancer cell line 7

MCF-7-ETP – etoposide-resistant MCF-7 cells

MCF-7-MITX – mitoxantrone-resistant MCF-7 cells

MCF-7-TXL – paclitaxel-resistant MCF-7 cells

MDA-MB-231 – MD Anderson metastatic breast cancer cell line 231

MDR – multidrug resistance

MDR1 – multidrug resistance protein 1, alternative to ABCB1

mg – milligram

min – minutes

mL – milliliter

mM – millimolar

MRP1 – multidrug resistance-associated protein 1, alternative to ABCC1

MRP4 – multidrug resistance-associated protein 4, alternative to ABCC4

MRSA – methicillin-resistant *Staphylococcus aureus*

MSM – mineral salts medium

mTOR – mechanistic target of rapamycin kinase

MTT – thiazolyl blue methyltetrazolium bromide

MXR1 – mitoxantrone resistance protein 1, alternative to ABCG2

MYC – C-Myc gene

MYM agar – maltose, yeast extract, malt extract agar

NF κ B – nuclear factor kappa-light-chain-enhancer of activated B cells

nm – nanometer

NSAID – non-steroidal anti-inflammatory drug

P-gp – permeability-glycoprotein, alternative to ABCB1

P53 – tumour protein 53

PALB2 – partner and localizer of BRCA2 gene

PBS – phosphate buffered saline

PD – Culture Bureau of Park, Davis and Company

PD-1 – programmed cell death receptor 1

PD-L1 – programmed cell death ligand 1

PGE₂ – prostaglandin E₂

PGT – prostaglandin transporter

PI3K – phosphatidylinositol 3-kinase

PI3KCA – phosphatidylinositol 3-kinase gene

PLA₂ – phospholipase A₂

PR – progesterone receptor

PR⁻ – progesterone receptor negative

PR⁺ – progesterone receptor positive

PTEN – phosphatase and tensin homolog gene

RAD50 – RAD50 double strand break repair protein gene

RB – retinoblastoma protein gene

RFC – reduced folate carrier

RFU – relative fluorescence units

ROS – reactive oxygen species

RPM – revolutions per minute

SCL – solute carrier

SDS – sodium dodecyl sulfate

SERD – selective estrogen receptor degrader

SERM – selective estrogen receptor modulator

sp. – species

TBS – tris-buffered saline

TERT – telomerase reverse transcriptase

TMED – N,N,N',N'-Tetramethylethylenediamine

TNBC – triple negative breast cancer

TNF – tumour necrosis factor

TOP1 – topoisomerase I

TOP1MT – mitochondrial topoisomerase I

TOP2 – topoisomerase II

TP53 – tumour protein 53 gene

v/v – volume per volume

w/v – weight per volume

Acknowledgements

This work would not have been possible without the help and dedication of many people. I would first like to say thank you to Dr. Kerry Goralski for acting as my mentor and supervisor. You have pushed me to become a better scientist and a more well rounded person. Your hard work and positive attitude have been an inspiration and I hope to follow your example. I will always hold on to the lessons you have taught me.

To Drs. Susan Howlett, Christian Lehmann, George Robertson, and Paola Marcato, thank you for your time and attention across committee meetings and my comprehensive exam. You have pushed me to my limit and forced me to grow where growth was needed.

To Drs. Amy Fulton, Paola Marcato, and Denis Dupré, thank you for offering your time to read this work and prepare the questions for my defence.

To Drs. David Jakeman, Michael Beh, and Wasundara Fernando, thank you for the technical support offered in conducting this work. You had a direct hand in helping collect these results. Each of you have played an essential role in making this possible.

To Steve, Antonios, Jaime, Shanukie, Esther, and Hailey, who have been my lab mates and fellow residents of the Burbidge Building: thank you all for your ideas, inspiration, support, and the laughs along the way.

For the financial support that made this project possible, I want to thank the Department of Pharmacology, the College of Pharmacy, the Pharmacy Endowment Fund, the NSERC CREATE BioActives program (grant number 510963), the Beatrice Hunter Cancer Research Institute, the Saunders Matthey Foundation for Cancer Research, and the Terry Fox Research Institute.

Finally, I want to thank my family. You've listened to my rambling in person and on the phone, and you have been there for my ups and downs. To Amanda, my fiancée, thank you for everything you've done across the years. I would not have gotten here without you.

Chapter 1: Introduction

The first chapter of this work introduces the history of cancer, followed by a description of cancer incidence, mortality, and the disease itself. It then further defines breast cancer as a specific subset of cancer, describing its characteristics and the typical treatment approaches commonly used. The idea of using natural products to develop new therapeutic options follows, along with a description of the group of compounds known as jadomycins and their biological activity. A comprehensive review of anticancer effects of jadomycins establish what is currently known about this group of natural products.

1.1: History of Cancer

Cancer is a disease which has been known of throughout history and has been consistently present throughout the course of life on earth. By exploring the history of cancer a greater appreciation of our current understanding of cancer and its treatments, both historic and in development, can be gained from those who came before.

The history of cancer predates *Homo sapiens* with the oldest incidence of tumours discovered in dinosaurs (Rothschild et al., 2003). These tumours were identified in the fossilized bones of hadrosaurs dating from the late Cretaceous period, approximately 70 million years ago (Rothschild et al., 2003). Among hominids, the earliest identified benign tumour was found in a thoracic vertebra of Malapa Hominin 1, the type specimen of *Australopithecus sediba*, dated to 1.9 million years ago (Randolph-Quinney et al., 2016). These findings provide evidence that cancers have been present throughout the history of life on Earth.

The oldest malignant tumour was found in a metatarsal of an unidentified hominin dated at 1.6 – 1.8 million years old (Odes et al., 2016). This marks the first known instance of cancer in the genus *Homo*. These ancient cancers appear throughout history, with other early examples of malignancy found in modern-day Austria, dated to 4000 BCE, and Nubia, dated to 1200 BCE (Strouhal and Kritscher, 1990; Binder et al., 2014).

The ancient Egyptians provide some of the earliest written records of cancer. The Edwin Papyrus was written in approximately 1600 BCE but may be a copy of an earlier

document from around 3000 BCE (Breasted, 1930; Hajdu, 2011a). In it the author describes the diagnosis of tumours of the breast, which were deemed to be a severe disease without possible treatment (Breasted, 1930; Hajdu, 2011a). These ancient scholars began to differentiate between tumours resulting from injury, inflammation, and cancerous growth, detailing different courses of treatment for each (Diamandopoulos, 1996). Modern examination of Egyptian mummified remains has led to proposed diagnoses of nasopharyngeal, testicular, uterine, breast, colorectal, ovarian, leukemic, and cervical cancers and metastases (Wells, 1963; Molto and Sheldrick, 2018). Although ancient evidence of soft tumours has proven difficult to find, accurate diagnoses of prostate cancer, for instance, have been made based on patterns of metastatic invasion in the pelvis and spine (Prates et al., 2011).

Ancient evidence of cancer is not limited to Africa and Europe. Indian manuscripts such as the Ramayana or cuneiform inscription tablets from Babylonia, both dated to around 800 BCE, describe tumours in the breasts of women and propose treatment by surgical excision or application of an arsenic containing paste (Diamandopoulos, 1996). The Chinese doctor Hong Ge (281-341 CE) provides the first medical writing on breast cancer from East Asia, describing a hard lump resembling a walnut which became larger and seemed fixed as if by roots (Yan, 2013).

The Greek physician Hippocrates (460-370 BCE) is considered the “Father of Medicine” and wrote about his diagnoses and treatment of tumours based on his clinical observations (Diamandopoulos, 1996; Karpozilos and Pavlidis, 2004). He classified tumours based on behaviour, either benign (which likely included both non-neoplastic and neoplastic lesions) or malignant (Gallucci, 1985; Diamandopoulos, 1996). Referring to the malignant cancers, he held that it was preferable not to treat these as patients die quickly following any available intervention (Gallucci, 1985; Diamandopoulos, 1996; Karpozilos and Pavlidis, 2004). Hippocrates also makes specific mention of ailments of the uterus which lead to small tumours in the breast and can become “hidden” cancers (Gallucci, 1985; Karpozilos and Pavlidis, 2004). As a proponent of the humoral theory, Hippocrates believed that health and disease were governed by the blending and mixing of four biological counterparts: blood, phlegm, yellow bile, and black bile (Diamandopoulos, 1996). Cancer, he proposed, was the result of excess of black bile that

was prevented from draining from a tissue and that this was associated with the cessation of menses in women (Gallucci, 1985; Diamandopoulos, 1996). Throughout this and subsequent periods where the humoral theory dominated, treatments were primarily based around surgery, lancing, or blood letting; a rational approach as these treatments could release the accumulation of humor causing the disease (Gallucci, 1985).

Hippocrates was the first to use the term “*Karkinos*,” Greek for “crab,” to describe the disease and the Roman physician Galen (130-200 CE) adopted the Latin analogue “cancer” (Diamandopoulos, 1996; Hajdu, 2011a). Paul of Aegina (625-690 CE), a physician in the East Roman Empire, offered two explanations as to why Hippocrates and Galen used this descriptor: that cancer was particularly frequent in the breasts of women and that the protruding veins stretched around the mass like the feet of a crab, or that it adheres to the tissue around it like the grip of a crab’s claw (Diamandopoulos, 1996; Hajdu, 2011a). Understanding the root of the words used to describe a disease can help define the surrounding thoughts and feelings experienced by those treating it and suffering from it. The Chinese physician Dong Xuan was the first to ascribe a specific name to cancer, differentiating it from swellings caused by injury or infection, calling it “*ai*” (癌) which is phonetically similar to the word for sorrow (Yan, 2013).

Nomenclature was not the only area where Galen followed Hippocrates. Galen built upon the Hippocratic view of cancer and was the first to describe metastasis as the spread of cancer to distant sites (Diamandopoulos, 1996). Galen was also first to propose that a relationship between diet, environment, and cancer exists (Karpozilos and Pavlidis, 2004). The ideas of Galen and Hippocrates would dominate medical thought and action for 16 centuries in Europe, Western Asia, and Northern Africa (Diamandopoulos, 1996).

Physicians of the East Roman Empire like Aetius (527-565) developed new surgical techniques like cauterization and mastectomies to remove cancerous growths (Hajdu, 2011a). The teachings of the Greeks and Romans were brought to Western Asia, leading to the Golden Age of Arab Medicine from 850-1050 CE (Diamandopoulos, 1996). Avicenna of Persia (980-1037) advanced cancer treatment by wrapping a wire around the cancer and gradually tightening it until the growth fell off (Hajdu, 2011a). Knowledge was preserved in this region before travelling back to Europe.

The universities of Europe were founded in the Middle Ages (900-1300) and preserved findings from practical evaluation and experience, for instance allowing the diagnosis of rectal cancer by digital examination for the first time (Diamandopoulos, 1996; Hajdu, 2011a). Unfortunately, it was also in this time period that the Papacy prohibited surgery; seen as causing unnecessary harm to patients (Hajdu, 2011a).

As Europe entered the Renaissance (1300-1700) the theories of antiquity attributing cancer to black bile gave way to new ideas. The invention of the printing press in 1450 by Johannes Guttenberg (1395-1468) allowed knowledge to be distributed, and the first medical book was printed in 1478 (Hajdu, 2011b). Paracelsus (1493-1541) pioneered chemistry and chemotherapy, introducing heavy metals for cancers but warning that concentration and dose distinguish the poisonous from the non-poisonous (Hajdu, 2011b). René Descartes (1596-1650) contributed to the lymph theory which proposed benign tumours arose from coagulated lymph that had escaped the lymphatic vessels and malignant tumours developed due to its fermentation or degeneration (Diamandopoulos, 1996). Zacutus Lusitani (1575-1642) and Nicholas Tulp (1539-1674) independently came to the erroneous conclusion that cancer was contagious due to the observation that breast cancer would often appear in members of the same family (Hajdu, 2011b). By 1700, incidence of specific cancers became associated with profession: lung cancer was common in miners while breast cancer was common in nuns (Hajdu, 2011b).

The modern period of medicine saw further transition away from humoral theories and toward the idea that cancer could be caused by changes in cells and tissues, therefore necessitating new approaches in its treatment. Joseph Recamier (1774-1852) popularized the idea of metastasis as the means by which cancer could spread throughout the body, making observations that cancer could invade blood vessels and that similar cancers appearing in successive generations of a family may indicate a hereditary component to the disease (Hajdu, 2012a). In 1838 Theodor Schwann (1810-1882) and Johannes Müller (1801-1858) formalized the cellular basis of cancer (Diamandopoulos, 1996; Hajdu, 2012a). Their discoveries, along with those of Rudolf Virchow (1821-1878) and Karl von Rokitanski (1804-1878) recognized two distinct components of tumours: the parenchyma, describing the mass of uncontrollably replicating cells, and the stroma, comprised of supporting tissues and vasculature (Diamandopoulos, 1996). These observations directly

influence the way tumours are classified today, based on microscopic morphology (Gallucci, 1985; David, 1988; Diamandopoulos, 1996; Hajdu, 2012a).

By the 1860s it was commonly accepted that microscopically distinct, malignant tumours could arise in any organ, however, a single progenitor cell had not been identified (Hajdu, 2012b). Developments in anesthesia, aseptic technique, and endoscopy allowed for increasingly complex and invasive surgeries for the removal of cancerous tissue (Hajdu, 2012b). Radical mastectomy, for example, removed the entire breast and pectoralis major muscle without interrupting lymphatic channels and improved median 3-year survival from 5% in the 18th century to 42% in 1891 (Halsted, 1907; Hajdu, 2012b).

The discovery of x-rays by Wilhelm C. Rontgen (1845-1923) led to diagnostic radiology in 1896 and quickly progressed to x-ray radiation therapy for the treatment of inoperable breast cancer in 1897 (Hajdu, 2012b). Pierre Curie (1859-1906) and Marie Sklodowska Curie (1867-1934) described radioactive decay which led to the use of radium in the treatment of skin cancer in 1903 (Hajdu, 2012b). As radiologic treatment advanced, so too did chemotherapeutic treatment. Paul Ehrlich (1854-1915) described his observations on chemical agents capable of killing cancer cells in 1909 (Hajdu, 2012b).

By 1914, the first successful tissue culture of a human cancer was grown *in vitro*, establishing an essential model for research (Losee and Ebeling, 1914; Hajdu and Darvishian, 2013). Use of cellular and animal models led to the discovery of the roles of estrogen and progesterone in the development of breast cancer, that estrogen could induce breast cancer in female and male mice, and provided evidence that hormonal therapies could benefit breast cancer patients (Burrows, 1935; Lacassagne, 1936; Hajdu and Darvishian, 2013).

Developments in screening made cancer diagnoses easier and more accurate (Papanicolaou and Traut, 1941; Diamandopoulos, 1996; Hajdu and Vadmal, 2013). Mammography, for instance, became common in the 1950s and a 1962 trial demonstrated that mammograms combined with manual examination reduced breast cancer related mortality to a third of that in the control group (Strax et al., 1967; Shapiro et al., 1971; Hajdu and Darvishian, 2013; Hajdu and Vadmal, 2013). Positron emission tomography and computed tomography were developed from the 1950s to 1970s and allowed for highly detailed imaging (Hajdu and Vadmal, 2013).

The National Cancer Act in the United States of America was introduced in 1971, granting national support to cancer research and improving in clinical outcomes for patients (Hajdu et al., 2015). Discovery of the structure of deoxyribonucleic acid (DNA) had enabled a greater understanding of carcinogenesis (Watson and Crick, 1953; Hajdu and Vadmal, 2013; Hajdu et al., 2015). By the 1980s several oncogenes and tumour suppressors associated with cancer development had been identified, for instance, human epidermal growth factor 2 (HER2) which plays a role in breast cancer and tumour protein 53 (p53) which is the most commonly mutated gene across many types of cancer (Slamon et al., 1987; Nigro et al., 1989; Hajdu et al., 2015).

As early as 1894, attempts were made to induce the immune system to help prevent the growth of cancer (Coley, 1894; Hajdu, 2012b; Hajdu et al., 2015). No real progress was made until the 1980s when immune cells became a focus of research and treatments inducing immune activity were therapeutically adopted (Hajdu et al., 2015).

By 1995 the standard of care had changed from radical surgery alone to combination therapy involving surgery, radiation, immunotherapy, and chemotherapeutics depending on the cancer type (Hajdu et al., 2015). Even within the bounds of chemotherapy, combinations of different agents with complementary mechanisms of action improved clinical response while minimizing adverse effects (Hajdu et al., 2015). This brings us to the modern science of cancer therapy where complex combinations of therapies are used in well defined algorithms to maximize patient response while minimizing adverse effects of treatment. The present day understanding of cancer and approaches used to treat it continue to develop and expand.

1.2: Cancer Incidence, Mortality, and Cost

An estimated 19.3 million new cancer diagnoses and 10 million cancer deaths are believed to have occurred worldwide in 2020 (Sung et al., 2021). By 2040, it is estimated that there will be 28.4 million new cases globally per year (Sung et al., 2021). Cancer is among the leading causes of death worldwide; an analysis of World Health Organization data from 2019 gathered from 183 countries showed cancer as the leading cause of death in 57 countries while cardiovascular disease was first and cancer second in 70 countries

(Bray et al., 2021). This trend remains true in Canada and the United States of America. In Canada, cancer is the leading cause of death at 28.2%, followed by cardiovascular disease at 18.5% mortality (CCS, 2021). The reverse is true in the United States, where cancer is responsible for 18% of deaths and 21% are attributed to cardiovascular disease (Siegel et al., 2023). In real numbers, an estimated 233,900 new cancer diagnoses were made in Canada in 2022 and 1,958,310 new diagnoses in the United States in 2023 (Brenner et al., 2022; Siegel et al., 2023). This translates to approximately 43% of Canadians and 40.9% of Americans expected to receive a cancer diagnosis in their lifetime (Brenner et al., 2022; Siegel et al., 2023).

Different forms of cancer have different incidence and mortality rates, with some being much more common or deadly than others. Female breast cancer is the most commonly diagnosed form of cancer globally, at 11.7% of all new cases (Sung et al., 2021). This is followed by lung (11.4%), colorectal (10.0%), prostate (7.3%), and stomach (5.6%) cancers to comprise the top 5 diagnoses worldwide, regardless of sex (Sung et al., 2021). In Canada, the most commonly diagnosed forms of cancer are lung (12.8%), female breast (12.2%), prostate (10.5%), and colorectal (10.4%), regardless of sex (Brenner et al., 2022). Among Canadians assigned male at birth, prostate cancer is the most common diagnosis (1 in 5 among new diagnoses) while breast cancer is the most common diagnosis (1 in 4) among those assigned female at birth (Brenner et al., 2022). In terms of mortality, more Canadians will die of lung cancer (5% of overall mortality, or 24.3% of cancer related mortality) than any other type (CCS, 2021; Brenner et al., 2022). Following lung, colorectal (11.0% of cancer related mortality), pancreatic (6.7%), female breast (6.5%), and prostate (5.4%) cancer have the highest mortality rates regardless of sex (Brenner et al., 2022). The fact that female breast cancer and prostate cancer appear in the top five causes of cancer related death demonstrates that an individual's experience with cancer can vary greatly depending on factors such as biological sex and environment.

Cancer does not affect all people in North America equally. Race is associated with differing risk and outcome in cancer, however, these racial disparities are also correlated to disparities in healthcare access, quality of care, risk factor exposure, availability of screening, and access to treatment (Siegel et al., 2023). Generally, black

individuals have lower survival rates than white individuals diagnosed with similar cancers (Siegel et al., 2023). In Canada, geography has been associated with differing cancer incidence. Cancer rates are typically highest in the central and eastern provinces with Newfoundland and Labrador having the highest rate (559.8 per 100,000) followed by Ontario (545.9 per 100,000), and Nova Scotia (539.8 per 100,000) when standardized to both age and sex (CCS, 2021). Age is the most important risk factor for cancer development, with 90% of Canadian cancer diagnoses occurring after age 50 (CCS, 2021). This correlation to age explains the rise in cancer incidence, however, when corrected for age and population the risk of developing or dying from cancer has been decreasing in Canada since 1988 (CCS, 2021). Finally, males are at a greater risk of developing and dying from cancer than females (CCS, 2021). This difference between males and females has been attributed to greater exposure to environmental risk factors (Siegel et al., 2023).

An important distinction can be made between cancer diagnoses and prevalence. Diagnoses and mortality inform the change in number of patients, while prevalence reflects the number of individuals diagnosed and still alive (CCS, 2022). Female breast (19.4%), prostate (17.8%), and colorectal (11.3%) cancers are the three most prevalent forms of cancer among those who have lived with cancer for 25+ years (CCS, 2022). Regardless of time since diagnosis, prostate cancer was most prevalent (37.1%) among males while breast cancer was the most prevalent (37.1%) among females (CCS, 2022). Due to advances in early detection and treatment cancer prevalence has been increasing in Canada over time, with more than 1.5 million Canadians living with cancer in 2018 (CCS, 2022). The needs of those diagnosed with cancer change over time, where individuals in the first 2 years following diagnosis are undergoing primary treatment, from 2-5 years monitoring for recurrence prevails, and after 5+ years treatment is usually complete but monitoring may persist for the remainder of their lives (CCS, 2022).

In addition to the effect on human health, cancer also presents a significant economic burden to society. Annual cancer related costs have risen from \$2.9 billion spent by Canadians in 2005 to \$7.5 billion spent in 2012 to \$20.6 billion spent in 2020 (de Oliveira et al., 2018; Ruan et al., 2023). Using data from the Canadian Cancer Registry, it has been estimated that cancer incidence will increase by 40% between 2020

and 2040, resulting in an increase to \$31.4 billion in costs projected for Canadians by 2040 (Ruan et al., 2023). The increasing costs of hospital care, chemotherapy, and radiation therapy have been identified as the leading factors contributing to this increase (de Oliveira et al., 2018).

1.3: Cancer

It is now understood that cancer is not a single disease, but rather a group of unrelated diseases which exhibit similarities in symptoms and progression (CCS, 2021). Many factors have been associated with cancer risk including sun exposure, radiation, tobacco use, chemical exposure, hormone levels, alcohol use, viral/bacterial/fungal/parasitic infection, dietary choices, environmental irritants, sedentary lifestyle, obesity, genetic predisposition, and exercise, among others (Blackadar, 2016). Of the genetic mutations contributing to an individual's risk for developing cancer, some occur in a heritable manner, passed down from one generation to the next. Long term studies in twins demonstrate a significant familial risk for both overall cancer development and specific cancer type including prostate, breast, ovarian, uterine, and melanoma (Mucci et al., 2016). Using breast cancer as an example, mutations in genes like breast cancer susceptibility protein 1 (*BRCA1*) and breast cancer susceptibility protein 2 (*BRCA2*) were identified as conferring a greater than 10-fold increase in breast cancer risk (Turnbull and Rahman, 2008). The *BRCA1* and *BRCA2* genes normally facilitate DNA double strand break repair, and mutations to these genes were reported as strongly linked to breast cancer development (Hall et al., 1990; Miki et al., 1994; Wooster et al., 1995; Turnbull and Rahman, 2008).

Regardless of the inciting event, development of cancer involves damage to the genetic material resulting in changes to the cell's ability to control proliferation (Hanahan and Weinberg, 2000). An accumulation of genetic changes has been associated with increased aggressiveness of the resulting cancer. Typically, the changes can be categorized as either gain-of-function mutations to proto-oncogenes or loss-of-function mutations to tumour suppressor genes (Lee and Muller, 2010; Kontomanolis et al., 2020). In the context of breast cancer only a few genes are frequently mutated, however, many

genes can be infrequently mutated (Lee and Muller, 2010). This diversity of mutations can partially explain the heterogeneity of disease between individuals.

In normal cells, proto-oncogenes have regulatory functions controlling cell growth, signalling, and transcription. Mutations to these proto-oncogenes result in their becoming oncogenes, which stimulate growth, division, and survival in an uncontrolled manner (Lee and Muller, 2010; Kontomanolis et al., 2020). This is therefore described as a gain-of-function mutation because the resulting oncogenes have an increased ability to perform their function as compared to the unmutated proto-oncogene. Mutations to proto-oncogenes can be categorized as either resulting in an alteration to protein structure following translation, or deregulation of protein expression (Kontomanolis et al., 2020). Commonly deregulated oncogenes in breast cancer include human epidermal growth factor receptor 2 (*ERBB2*), phosphatidylinositol 3-kinase (*PI3KCA*), C-Myc (*MYC*), and cyclin-D1 (*CCND1*) (Lee and Muller, 2010).

In contrast to proto-oncogenes, tumour suppressor genes normally slow or stop cell division, repair DNA damage, and signal unrepairable cells to undergo programmed cell death. In this way, a variety of genes with different functions work together to prevent the development of cancers (Lee and Muller, 2010; Kontomanolis et al., 2020). Mutations to tumour suppressor genes are described as loss-of-function because they decrease or eliminate activity, allowing cells which would otherwise have been regulated to bypass checkpoints (Kontomanolis et al., 2020). Commonly altered tumour suppressor genes in breast cancer include retinoblastoma protein (*RB*), *BRCA1*, *BRCA2*, *p53*, phosphatase and tensin homolog (*PTEN*), ataxia telangiectasia mutated serine/threonine kinase (*ATM*), RAD50 double strand break repair protein (*RAD50*), partner and localizer of BRCA2 (*PALB2*), and BRCA1 interacting protein 1 (*BRIP1*) (Lee and Muller, 2010).

In addition to genetic mutations to proto-oncogenes and tumour suppressor genes, epigenetic deregulation can also contribute to abnormal expression of these genes in ways which promote cancer development (Lee and Muller, 2010; Baylin and Jones, 2016). Epigenetic changes which can lead to the development of cancer include abnormal patterns of DNA methylation, changes to enzymes responsible for histone modification, changes to enzymes responsible for chromatin remodelling, and changes in microRNA expression (Baylin and Jones, 2016). Alterations in the epigenome can contribute to the

silencing of tumour suppressor genes and, therefore, remove barriers preventing the development of cancer without directly altering the DNA sequence.

1.3.1: Hallmarks of Cancer

Cellular proliferation normally consists of a strictly controlled sequence of events describing growth, division, and death; however, cancer cells can continue the process of growth and proliferation in an unregulated manner under conditions which would normally cause cells to undergo apoptosis. Hanahan and Weinberg initially proposed 6 “hallmarks of cancer” describing shared characteristics between forms of cancer which define cancerous cells and provide an approach to targeting and treating cancer as a disease (Hanahan and Weinberg, 2000). These hallmarks have since been expanded to include additional hallmarks and enabling characteristics which are summarized in **Table 1.1** (Hanahan and Weinberg, 2011; Hanahan, 2022). Each of the hallmarks and enabling characteristics will herein be discussed.

Table 1.1: Hallmarks and Enabling Characteristics of Cancer

List of the hallmarks and enabling characteristics of cancer as described by Hanahan and Weinberg (Hanahan and Weinberg, 2000; Hanahan and Weinberg, 2011; Hanahan, 2022).

Hallmarks	Enabling Characteristics
Sustaining proliferative signalling	Genome instability and mutation
Evading growth suppressors	Tumour-promoting inflammation
Resisting cell death	Nonmutational epigenetic reprogramming
Enabling replicative immortality	Polymorphic microbiomes
Inducing angiogenesis	
Activating invasion and metastasis	
Reprogramming energy metabolism	
Evading immune destruction	
Unlocking phenotypic plasticity	

1.3.1.1: Sustaining Proliferative Signalling

In normal cells, growth signals transmitted from the extracellular environment to the cell *via* ligand specific transmembrane receptors are required to produce and sustain proliferation. Many oncogenes act in ways which mimic these normal growth signals, freeing cells from the need for exogenous stimulation and normal homeostatic control. This is the principle behind *sustaining proliferative signalling* as a hallmark of cancer (Hanahan and Weinberg, 2000; Hanahan and Weinberg, 2011). Dysregulation of proliferative signalling can occur in several ways. Cancer cells may acquire the ability to synthesize growth factors that they themselves are responsive to, for instance insulin-like growth factor or transforming growth factor- β , creating a feedback loop where cells signal themselves and their neighbours to proliferate (Witsch et al., 2010). Alternatively, overexpression of transmembrane receptors for these signals may allow cells to become hyperresponsive to growth factors which would not typically be sufficient to induce proliferation. Mutations can also arise which allow receptors to elicit ligand-independent signalling, or the signalling pathways downstream of the receptors may change in ways which allow them to activate without any receptor involvement. For instance, the p21 Ras protein can become altered such that activation by upstream receptors is no longer needed for signalling (Medema and Bos, 1993). The final way in which proliferative signalling can be sustained is through the involvement of surrounding non-cancerous cells in the tumour microenvironment; these normal cells can be induced to release growth signals.

1.3.1.2: Evading Growth Suppressors

In addition to the growth signals used to stimulate proliferation, normal tissues also use several antiproliferative signals to maintain homeostasis. By *evading growth suppressors* cells acquire the second of the hallmarks of cancer (Hanahan and Weinberg, 2000; Hanahan and Weinberg, 2011). These growth suppressors include both soluble signals in the extracellular fluid and bound inhibitors in the extracellular matrix or on the surfaces of neighbouring cells which produce a form of contact inhibition that prevents overcrowding (Pavel et al., 2018). As with the growth signals, inhibitory signals are detected by transmembrane receptors which convey signals into the cell. When inhibitory

signals are activated cells can be alternatively forced into a quiescent state, from which they may re-enter into active proliferation later, or a permanent post-mitotic state. Failure to respond to these signals results in continued proliferation.

1.3.1.3: Resisting Cell Death

Proliferative signalling alone is not sufficient for a population of cancerous cells to increase; *resisting cell death* represents the third hallmark and allows cancer cells to accumulate in number (Hanahan and Weinberg, 2000; Hanahan and Weinberg, 2011). There are many triggers in normal cells which initiate a tightly controlled series of events culminating in apoptosis, or programmed cell death. For instance, elimination of the p53 tumour suppressor removes an important pro-apoptotic regulatory factor (Ozaki and Nakagawara, 2011). The cellular factors involved in apoptosis can be described as either upstream regulators or downstream effectors. Regulators can either detect extracellular signals, the extrinsic pathway, or intracellular signals, the intrinsic pathway, which begin a complex cascade that results in activation of the effectors. The role of the regulators is to detect cellular damage that is beyond the capacity for repair, for example extensive DNA damage or oncogenic activity. Stressful conditions, like hypoxia or the loss of cell-to-cell adhesion can also be sufficient to initiate the apoptotic process. Effectors respond to this cascade of signals and destroy subcellular structures, organelles, and DNA. By accumulating mutations to genes controlling apoptosis, cancer cells avoid activation of this process and so the cells remain viable long enough to continue acquiring additional hallmarks.

1.3.1.4: Enabling Replicative Immortality

Normal cells are limited in their capacity to divide beyond the need for proliferative signalling alone. After having undergone a finite number of divisions normal cells will become senescent, an irreversible state wherein cells remain viable and function as part of a tissue but can no longer divide, or enter into a state known as crisis which results in cell death. *Enabling replicative immortality* allows cancer cells to overcome this limitation (Hanahan and Weinberg, 2000; Hanahan and Weinberg, 2011).

Immortalization is accomplished in 85-90% of cancer cells through upregulation of telomerase expression. Telomerase is an enzyme which extends the number of repeats of a short, 6 base pair sequence at the ends of DNA (Blasco, 2005). Telomeres consist of thousands of these repeats which serve to protect the ends of chromosomal DNA from sequence loss during replication. Telomere repeats are needed because the genome would otherwise be shortened during replication due to the inability of DNA polymerase to completely replicate the 3' end. When the telomeres have degraded beyond a critical threshold cell death or senescence occurs to prevent accumulation of additional damage. By increasing telomerase activity, cancer cells can undergo unlimited replication.

1.3.1.5: Inducing Angiogenesis

The previous hallmarks of resisting cell death and enabling replicative immortality result in an accumulation of cells that would otherwise have been removed. This results in an increased need for oxygen and nutrients which must be supplied by *inducing angiogenesis* (Hanahan and Weinberg, 2000; Hanahan and Weinberg, 2011). All cells in a tissue must live within 100 μm of a capillary to receive oxygen, energy, and dispose of metabolic wastes. In normal development, angiogenesis occurs in a carefully regulated manner which is not typically activated in most adult tissues. The exceptions to this, under circumstances of wound healing or female reproductive cycling, are transient in nature. Cancer cells can induce and sustain angiogenesis by altering the balance of angiogenic inducers and suppressors to support tumour growth. Vascular endothelial growth factor, for instance, normally promotes embryonic angiogenesis and wound healing but is commonly upregulated in solid tumours (Carmeliet, 2005).

1.3.1.6: Activating Invasion and Metastasis

Thus far, the hallmarks have characterized cancer cell's ability to grow at their site of origin. By *activating invasion and metastasis* cancer cells gain the ability to spread throughout the body and colonize new tissues (Hanahan and Weinberg, 2000; Hanahan and Weinberg, 2011). By metastasizing to new sites, cancer cells encounter new environments without the nutritional or space limitations present in the primary tumour.

This kind of metastatic growth is responsible for the majority of cancer related deaths. Invasion and metastasis are complex processes which involve changes to a cancer cell's interaction with its microenvironment through disruption of proteins involved in cell-cell or cell-extracellular matrix interactions. E-cadherin, for example, is involved in coupling adjacent cells together (Berx and van Roy, 2009). When coupled, antigrowth signals are conveyed to both cells. By inactivating E-cadherin, or other similar proteins, cancer cells can detach from the primary tumour and travel to distant sites via the blood or lymphatic systems.

1.3.1.7: Reprogramming Energy Metabolism

Originally proposed as an emerging hallmark, *reprogramming energy metabolism* has since been recognized as a core hallmark describing how cancer differs from normal cells (Hanahan and Weinberg, 2011; Hanahan, 2022). As was alluded to when discussing angiogenesis and metastasis, unchecked proliferation of cells has broad consequences on metabolic needs. Normally, cells process glucose for energy by first converting it to pyruvate in the cytosol via glycolysis and then further processing it in the mitochondria to carbon dioxide as a waste product. The second step of this process, mitochondrial conversion of pyruvate, requires oxygen and is the key energy producing step in aerobic respiration. Under anaerobic conditions glycolysis is favoured with little pyruvate transported to the mitochondria. Cancer cells enter a state of aerobic glycolysis, wherein they largely limit their energy production to glycolysis even in the presence of oxygen. This propensity in cancer cells has been termed the Warburg Effect after its original describer (Warburg, 1930; Warburg, 1956b; Warburg, 1956a). Aerobic glycolysis is approximately 18-fold less efficient than oxidative phosphorylation, however, cancer cells compensate for this through increased expression of glucose transporters. Furthermore, glycolysis allows for increased production of glycolytic intermediary structures which can be used by cancer cells in biosynthetic pathways generating amino acids, nucleosides, and lipids. In this way, preferentially undergoing aerobic glycolysis allows cancer cells greater access to the components needed to sustain increased proliferation.

1.3.1.8: Evading Immune Destruction

While the concept of avoiding apoptosis has been discussed, cancer cells are also at risk of identification and removal by cells of the immune system. *Evading immune destruction* was identified as an emerging hallmark and like energy metabolism has since come to be recognized as a core hallmark in its own right (Hanahan and Weinberg, 2011; Hanahan, 2022). The immune system represents a barrier to tumour formation and progression by identifying and eliminating cancer cells as they first develop. One key mechanism by which tumours avoid immune detection is through a process termed immunoediting, where the immune system successfully detects and kills a majority of cancer cells which are immunogenic (Smyth et al., 2006). The remaining cells, with mutations that make them weakly immunogenic, survive and proliferate which results in a population less susceptible to immune detection. Changes to antigen presentation or secretion of immunosuppressive factors by cancer cells can contribute to this effect.

1.3.1.9: Unlocking Phenotypic Plasticity

The most recently proposed hallmark is *unlocking phenotypic plasticity* (Hanahan, 2022). Terminal differentiation describes the end result of cellular differentiation where normal cells undergo a process of specialization to become part of distinct tissues of the body. These terminally differentiated cells are commonly incapable of proliferation except under specific circumstances such as wound healing. Cancer cells which originate from partially or fully differentiated cells may undergo a process deemed dedifferentiation, converting back to a progenitor-like state. Alternatively, cancer cells originating from undifferentiated or partially differentiated progenitors can accumulate mutations that block differentiation and maintain their progenitor-like state. A third possibility is that differentiated cancer cells were originally committed to one developmental pathway but acquire traits that allow them to switch to an entirely independent secondary developmental pathway, deemed transdifferentiation. Transdifferentiation, in particular, can lead to increased cancer cell resistance to treatments targeting lineage-specific traits.

1.3.1.10: Genome Instability and Mutation

In addition to the hallmarks describing features shared by cancer cells, there are four enabling characteristics which contribute to cancer cells' ability to develop the hallmarks. Enabling characteristics differ from hallmarks in that they represent mechanisms by which the hallmarks can accumulate. The first enabling characteristic is *genome instability and mutation* (Hanahan and Weinberg, 2000; Hanahan and Weinberg, 2011). Most changes in cancer cells are acquired through genetic mutation, however, the rate of mutation in normal cells is typically low. This is confounded by tightly controlled cellular checkpoints which operate at critical stages of mitosis to detect and repair alterations to DNA. Specific mutations can predispose cancer cells to further mutations, such as those which decrease expression or activity of DNA repair proteins. Examples again include p53 which has a role in monitoring for DNA damage or the aurora kinase proteins which mediate passage through the mitotic checkpoint (Yao and Dai, 2014).

1.3.1.11: Tumour Promoting Inflammation

The immune system can identify and destroy cancer cells; however, immune activation can also be tumour promoting. *Tumour promoting inflammation* results from a chronic inflammatory state (Hanahan and Weinberg, 2011). Inflammation increases the supply of bioactive molecules needed by cancer cells for proliferation. These can include growth and survival factors, proangiogenic factors, and extracellular matrix modifying enzymes (Grivennikov et al., 2010). Additionally, inflammation can cause the release of reactive oxygen species (ROS) which cause potentially mutagenic DNA damage.

1.3.1.12: Nonmutational Epigenetic Reprogramming

In addition to the genetic changes brought on by genomic instability and increased access to bioactive molecules supplied by inflammation, *nonmutational epigenetic reprogramming* is the third enabling characteristic of cancer (Hanahan, 2022). Epigenetic changes occur as a result of mutations to genes controlling chromatin architecture or DNA methylation. Non-mutational changes analogous to mutations discussed above can

similarly alter expression of key factors leading to hallmark development. Hypoxia, for instance, is common in tumours and has been associated with hypermethylation of DNA (Thienpont et al., 2016).

1.3.1.13: Polymorphic Microbiomes

The final enabling characteristic is *polymorphic microbiomes* (Hanahan, 2022). The microbiome refers to the diverse microorganisms resident on the tissues of the body. These include both the epidermis and internal mucosa of the gastrointestinal tract, urogenital system, lungs, and other tissues. Individuals show huge variability in their microbiomes and changes to an individual's microbiome can occur over time. These differences can have profound effects on cancer development, progression, and response to therapy. Bacterial toxins can elicit mutagenesis in epithelial tissues on which they are living. For instance the cytolethal distending toxin expressed by *Campylobacter jejuni* and certain *E. coli* strains causes DNA damage to exposed human cells (Rosadi et al., 2016). Immunomodulatory factors, which can act locally or systemically, may also be released or induced by microorganisms and affect cancers throughout the body.

Taken together, the hallmarks and enabling characteristics of cancer describe the ways cancer cells differ from the normal cells of the body. These provide a general explanation of cancer as a group of similar diseases, but it is important to remember that each cancer is unique. Even cancers in the same organ or tissue can result from different changes and need individual diagnoses and treatment approaches.

1.4: Breast Anatomy and Introduction to Breast Cancer

The focus of the research described in this work is on breast cancer. As such, the remainder of this section will be restricted to describing breast cancer and its variations. A key component in understanding the differences present in breast cancer is a basic knowledge of the anatomical composition of the normal breast (**Figure 1.1**). The human breast forms early in fetal development from ectodermal tissue which divides into 15-20 epithelial columns that give rise to a corresponding 15-20 lactiferous ducts (Pandya and Moore, 2011; Bazira et al., 2022). This epithelial system becomes surrounded by

mesenchyme which develops into the stromal, supportive connective tissue and fat of the breast (Bazira et al., 2022). Prior to puberty the male and female breast are similar, with differences in structure and function arising in the female in response to hormonal signals. Estradiol, an estrogen steroid, induces proliferation and branching of the lactiferous ducts and maturation of the breast; estradiol and progesterone act in combination to mature the secretory lobules, which produce milk, during pregnancy (Bazira et al., 2022). As such, the normal tissues of the breast are innately sensitive to female sex hormones.

The mature female breast (hereafter “breast” unless otherwise indicated) is located on the anterior thoracic wall and surrounded by two layers of fascia, one separating it from the skin and another from the underlying pectoralis major muscle (Pandya and Moore, 2011; Bazira et al., 2022). Secretory lobules are collected into 15-20 lactiferous lobes, with each lobe draining into a dedicated lactiferous duct. These ducts then combine to a common lactiferous sinus which opens to the nipple (Pandya and Moore, 2011; Bazira et al., 2022). Blood is supplied to the breast *via* 3 major routes: the internal thoracic artery provides approximately 60%, the lateral thoracic artery provides approximately 30%, and the posterior intercostal arteries supply the remainder (Pandya and Moore, 2011). Drainage of blood occurs through the internal thoracic vein, posterior intercostal veins, and axillary vein (Pandya and Moore, 2011). In addition to the blood supply, lymphatic drainage of the breast occurs primarily (approximately 75%) through the axillary lymph nodes (Pandya and Moore, 2011; Bazira et al., 2022). There are 20-30 lymph nodes in the axillary region, and lymph typically drains from the breast in an ipsilateral manner.

Among those assigned female at birth, breast cancer is the most common form of cancer globally at 11.7% of all newly diagnosed cases and representing 6.9% of all cancer-related deaths (Sung et al., 2021). The American Cancer Society predicts that 1 in 8 female Americans will be diagnosed with breast cancer in their lifetime, and that 1 in 39 will die from it (Giaquinto et al., 2022). The risk of diagnosis and death between 2017 and 2019, stratified by age (**Table 1.2**), demonstrates that risk increases over time (Giaquinto et al., 2022). The numbers are similar for Canadians. In Canada, it is estimated that 1 in 8 (12%) females will be diagnosed with breast cancer at some point in their lives and 1 in 4 (25%) new diagnoses of cancer will be breast cancer (CCS, 2021). Among all female Canadians, 1 in 34 (3%) are expected to die from breast cancer and this represents

14% of all cancer associated deaths (CCS, 2021). Cancer diagnosis is more common among females aged 25-59 years than among males despite males experiencing greater rates of diagnosis in all other age groups; this is largely because 38% of breast cancers are diagnosed in patients aged 30-59 years (CCS, 2021). Rates of female breast cancer follow the same geographic distributions as other types of cancer in Canada, with the highest rates on the east coast (CCS, 2021).

Although breast cancer is known to occur in males, it is extremely rare and accounts for less than 1% of all breast cancer diagnoses (Yalaza et al., 2016). Differences in volume of breast tissue and hormonal profiles are the main factors contributing to this difference in incidence (Yalaza et al., 2016). When breast cancer does occur in males it is typically more similar to postmenopausal, as opposed to premenopausal, breast cancer in females in that it exhibits a similar age of onset and favourable hormone receptor-positive expression (Anderson et al., 2004). Therefore, the focus of this work will be on female breast cancer.

Breast tumours can be benign (non-cancerous) or malignant (cancerous). Benign tumours are groups of cells dividing uncontrollably in the same way as cancerous tumours, but remain in their primary location (Patel, 2020). Benign tumours are more common than malignant tumours, are typically slow growing, and have distinct borders separating them from surrounding tissue. As a result, benign tumours do not generally represent an immediate risk to the patient. Malignant tumours, in contrast, can grow quickly and rapidly spread to other regions of the body (Patel, 2020). They have irregular borders and invade nearby tissues, gaining access to the blood or lymphatic system by which they disperse to the body. Most breast cancers are carcinomas, forming from the epithelial tissue of the ducts or lobules (do Nascimento and Otoni, 2020). Ductal carcinomas account for approximately 75% of all breast cancers while lobular carcinomas account for approximately 15% (Li et al., 2003; Li et al., 2005; do Nascimento and Otoni, 2020). Breast sarcomas, primary cancers originating from the muscle, fat, or connective tissue of the breast, are very uncommon and represent less than 0.1% of all malignant tumours found in the breast (Adem et al., 2004). As such, carcinomas will be the primary focus within this work.

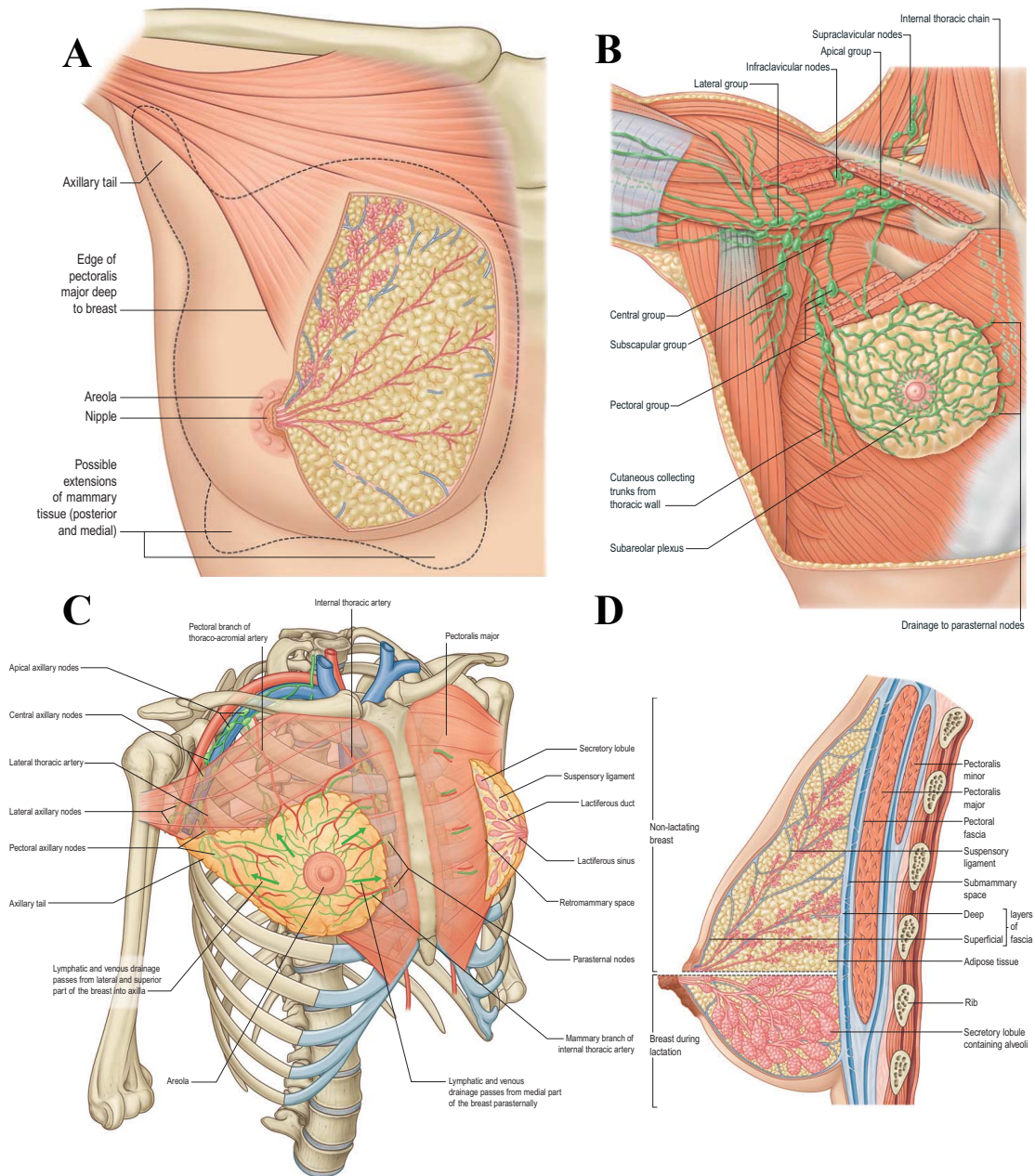


Figure 1.1: Breast Anatomy

Major anatomical features of the female breast including (A) external anatomy and breast margins, (B) musculature and lymphatic vessels, (C) arterial and venous vessels, and (D) comparison of lobule development in the non-lactating and lactating breast. Figure reproduced, with permission (**Appendix A.1**), from Standing (2016).

Table 1.2: 10-Year Probability of Breast Cancer Diagnosis or Death

Age stratified 10-year probability of breast cancer diagnosis or death in female Americans as determined for 2017-2019. Table reproduced, with permission (**Appendix A.2**), from Giaquinto et al. (2022).

Age (years)	Occurrence of Diagnosis	Occurance of Death
20	0.1% (1 in 1439)	<0.1% (1 in 18,029)
30	0.5% (1 in 204)	<0.1% (1 in 2945)
40	1.6% (1 in 63)	0.1% (1 in 674)
50	2.4% (1 in 41)	0.3% (1 in 324)
60	3.5% (1 in 28)	0.5% (1 in 203)
70	4.1% (1 in 24)	0.7% (1 in 137)
80	3.0% (1 in 33)	1.0% (1 in 100)
Lifetime Risk	12.9% (1 in 8)	2.5% (1 in 39)

1.4.1: Classification of Breast Cancer

Breast cancer is a heterogeneous group of diseases which can be classified several different ways. Classification of breast cancer by type considers cellular characteristics to determine the tissue of origin (do Nascimento and Otoni, 2020). The most commonly diagnosed type of breast cancer, at 75% of diagnoses, is invasive ductal carcinoma with no specific type (Li et al., 2003; do Nascimento and Otoni, 2020). The possible specific types include invasive lobular, adenoid cystic, apocrine, infiltrating ductal with osteoclastic giant cells, medullary, metaplastic, micropapillary, mucinous, neuroendocrine, invasive cribriform, tubular, secretory, lipid-rich, and glycogen-rich clear cell carcinomas (Masood, 2016; ACS, 2017; do Nascimento and Otoni, 2020). The term adenocarcinoma is used to describe any carcinoma arising from glandular tissue of the ducts or lobules. Both invasive ductal carcinoma and invasive lobular carcinoma are capable of invading nearby tissues and metastasis to distant parts of the body.

Following determination of type, breast cancer is graded to determine how closely it resembles healthy breast tissue and identify how rapidly the cancer cells are dividing. The system of grading recommended by the American College of Surgeons is the Nottingham combined histological grade (Elston and Ellis, 1991; ACS, 2017). In this system, the grade is determined by assessing 3 morphological features (tubule formation, nuclear pleomorphism, and calibrated mitotic count) and assigning a value from 1 (favourable) to 3 (unfavourable) to each feature (**Table 1.3**). Feature scores are then added to generate an overall tumour grade (**Table 1.4**). As tumour grade increases, so do differences from healthy cells. Grade 1 cancer cells are “well differentiated,” appearing similar to normal cells with normal tubule formation, normal nuclear morphology, and slower growth. Grade 2 cells are “moderately differentiated,” with accumulating differences that have not yet reached the severity of Grade 3. Grade 3 cells are “poorly differentiated” and are fast growing with the fewest similarities to normal cells.

The tumour-node-metastasis (TNM) classification system is also important in determining the anatomical extent of a cancer. This system was originally developed for use in all solid tumours by Pierre Denoix in a series of technical manuals published between 1944 and 1952 (UICC, 2017). The TNM system currently in use assigns a

category in each of 3 distinct areas used to measure extent of disease. Primary tumour (T) assesses the size of the mass as an estimate of volume, as well as the degree to which the tumour has invaded nearby tissues (**Table 1.5**), ranging on a scale of 0-4 (ACS, 2017; UICC, 2017; Giuliano et al., 2017). Characterization of lymph nodes (N) differs based on clinical or pathological measurement (**Table 1.6**). Clinical measurements are based on physical examination, imaging, or biopsy while pathological measurements are based on surgically removed tissue and clinical information together (ACS, 2017; Giuliano et al., 2017). Finally, distant metastases (M) are assessed (**Table 1.7**) as being present or absent (ACS, 2017; UICC, 2017; Giuliano et al., 2017). These categories can determine an anatomical stage ranging from I to IV (**Table 1.8**) which is used to express the overall severity of disease (ACS, 2017; UICC, 2017; Giuliano et al., 2017). Of note, this method of anatomical staging is only appropriate to use in regions where further biomarker classification is not possible. As such, biomarkers will next be discussed before returning to staging.

The 3 most important molecular markers in breast cancer classification are the estrogen receptor (ER), progesterone receptor (PR) and HER2. As discussed earlier, normal breast development is controlled in part by estrogen and progesterone signalling through the ER and PR (Bazira et al., 2022). Breast cancers can inappropriately overexpress ER and PR, inducing them to increased growth and proliferation. As cancers advance they lose the need for external receptor stimulation by estrogen and internal cellular signalling drives replication. Therefore, ER positive (ER⁺) or PR positive (PR⁺) cancers are associated with better prognosis and decreased risk of mortality than ER negative (ER⁻) or PR negative (PR⁻) cancers because of this continued need for external growth stimulation (Dunnwald et al., 2007; ACS, 2017). HER2 is a common oncogene in breast cancer, occurring in approximately 20% of breast cancers with gene amplification the most frequent cause of overexpression (Krishnamurti and Silverman, 2014). Cancer cells which overexpress HER2 are deemed HER2 positive (HER2⁺) and have increased capacity to activate intracellular signalling pathways which promote cell proliferation and survival (Krishnamurti and Silverman, 2014). As with the ER and PR, HER2 negative (HER2⁻) cancers show worse prognosis and increased mortality (Slamon et al., 1987). ER⁺, PR⁺, and HER2⁺ cancers are also considered prognostically positive as they afford

greater options for treatment. Targeting these receptors, when present, provides a more selective approach to cancer therapy (Dunnwald et al., 2007; Krishnamurti and Silverman, 2014). Breast cancers can be any combination of ER⁺/ER⁻, PR⁺/PR⁻, and HER2⁺/HER2⁻ phenotypes.

In addition to the above, breast cancer is molecularly classified based on biomarker expression. Molecular classification began with the theory that phenotypic diversity in breast cancer was associated with a corresponding diversity of gene expression that could be classified into similar groups (Perou et al., 2000). Using these biomarkers, at least 6 distinct subtypes of breast cancer can be identified (Holliday and Speirs, 2011; Eroles et al., 2012). Each of the 6 subtypes are described in **Table 1.9**. These subtypes are defined by the expression of ER, PR, and HER2 receptors, antigen kiel 67 (Ki67), p53, claudin-3, -4, -7, and other markers (Goldhirsch et al., 2011; Holliday and Speirs, 2011; Eroles et al., 2012). Ki67 is a nuclear protein associated with cellular proliferation expressed as cells proceed through the cell cycle (Inwald et al., 2013). As such, Ki67 is used as a proliferation marker. Claudin-3, -4, and -7 (along with other proteins like E-cadherin) are involved in maintaining cell-cell adhesion; decreased expression of these proteins is characteristic of aggressive disease and can lead to increased capacity for cell invasion, migration, and metastasis (Yadav et al., 2022). Luminal A is the most common of the 6 subtypes at 50-60% of all breast cancers, followed by HER2-enriched at 15-20%, luminal B and Basal-like at 10-20% each, claudin-low at 12-14%, and normal breast-like at 5-10% (Eroles et al., 2012).

All of the above categorizations are taken into consideration for cancer staging. Tumours are staged on a scale of I to IV, where a higher stage indicates greater severity of disease (ACS, 2017). Early stages (IA, IB, or IIA) are characterized by small tumour size and limited or no spread to lymph nodes. Locally advanced cancers (stages IIB, IIA, IIIB, or IIIC) are larger in size and may have invaded nearby tissues and lymph nodes. Any metastatic spread of breast cancer to distant sites of the body is considered stage IV regardless of primary tumour size. An additional Stage 0 is used to describe a benign tumour which has not grown beyond the duct or lobule in which it originated.

Table 1.3: Scoring of Histological Grade in Breast Cancer

Semiquantitative scoring method used in the Nottingham combined histological grade for assessment of breast cancer histological grade. Table reproduced, with permission (**Appendix A.3**), from Elston and Ellis (1991).

Feature	Score
Tubule formation	
Majority of tumour (>75%)	1
Moderate degree (10-75%)	2
Little or none (<10%)	3
Nuclear pleomorphism	
Small, regular uniform cells	1
Moderate increase in size and variability	2
Marked variation	3
Mitotic Counts	
Dependent on microscope field area	1-3

Table 1.4: Determination of Histological Grade

Determination of histological grade based on semiquantitative scoring (**Table 1.3**) for breast cancer. Table reproduced, with permission (**Appendix A.3**), from Elston and Ellis (1991).

Score	Grade
3-5 points	grade I - well differentiated
6-7 points	grade II - moderately differentiated
8-9 points	grade III - poorly differentiated

Table 1.5: Criteria for Primary Tumour Size (T) Classifications

Criteria for primary tumour size (T) classification as defined by the American Joint Commission on Cancer. Table reproduced, with permission (**Appendix A.4**), from Giuliano et al. (2017).

T Category	T Criteria
TX	Primary tumour cannot be assessed
T0	No evidence of primary tumour
Tis (DCIS)	Ductal carcinoma <i>in situ</i> (DCIS)
Tis (Paget)	Paget disease of the nipple NOT associated with invasive carcinoma and/or carcinoma <i>in situ</i> (DCIS) in the underlying breast parenchyma. Carcinomas in the breast parenchyma associated with Paget disease are categorized based on the size and characteristics of the parenchymal disease, although the presence of Paget disease should still be noted.
T1	Tumour \leq 20 mm in greatest dimension
T1mi	Tumour \leq 1 mm in greatest dimension
T1a	Tumour $>$ 1 mm but \leq 5 mm in greatest dimension (round any measurement from $>$ 1.0-1.9 mm to 2 mm)
T1b	Tumour $>$ 5 mm but \leq 10 mm in greatest dimension
T1c	Tumour $>$ 10 mm but \leq 20 mm in greatest dimension
T2	Tumour $>$ 20 mm but \leq 50 mm in greatest dimension
T3	Tumour $>$ 50 mm in greatest dimension
T4	Tumour of any size with direct extension to the chest wall and/or to the skin (ulceration or macroscopic nodules); invasion of the dermis alone does not qualify as T4
T4a	Extension to the chest wall; invasion or adherence to pectoralis muscle in the absence of invasion of chest wall structures does not qualify as T4
T4b	Ulceration and/or ipsilateral macroscopic satellite nodules and/or edema (including <i>peau d'orange</i>) of the skin that does not meet the criteria for inflammatory carcinoma
T4c	Both T4a and T4b are present
T4d	Inflammatory carcinoma

Table 1.6: Criteria for Lymph Node Metastases (N) Classifications

Criteria for clinical (cN) and pathological (pN) lymph node metastases classification as defined by the American Joint Commission on Cancer. Table reproduced, with permission (**Appendix A.4**), from Giuliano et al. (2017). Continued on next page.

N Category	N Criteria
cN	Clinical lymph node classification
cNX	Regional lymph nodes cannot be assessed (eg, previously removed)
cN0	No regional lymph node metastases (by imaging or clinical examination)
cN1	Metastases to movable ipsilateral level I and II axillary lymph node(s)
cN1mi	Micrometastases (approximately 200 cells, larger than 0.2 mm, but none larger than 2.0 mm)
cN2	Metastases in ipsilateral level I and II axillary lymph nodes that are clinically fixed or matted; <i>or</i> in ipsilateral internal mammary lymph nodes in the absence of axillary lymph node metastases
cN2a	Metastases in ipsilateral level I and II axillary lymph nodes fixed to one another (matted) or to other structures
cN2b	Metastases only in ipsilateral internal mammary lymph nodes in the absence of axillary lymph node metastases
cN3	Metastases in ipsilateral infraclavicular (level III axillary) lymph node(s) with or without level I and II axillary lymph node involvement; <i>or</i> in ipsilateral internal mammary lymph node(s) with level I and II axillary lymph node metastases; <i>or</i> metastases in ipsilateral supraclavicular lymph node(s) with or without axillary or internal mammary lymph node involvement
cN3a	Metastases in ipsilateral infraclavicular lymph node(s)
cN3b	Metastases in ipsilateral internal mammary lymph node(s) and axillary lymph node(s)
cN3c	Metastases in ipsilateral supraclavicular lymph node(s)

Table 1.6 (continued)

N Category	N Criteria
pN	Pathological lymph node classification
pNX	Regional lymph nodes cannot be assessed (eg, not removed for pathological study or previously removed)
pN0	No regional lymph node metastases identified or isolated tumour cells only
pN0(i+)	Isolated tumour cells only (malignant cell clusters no larger than 0.2 mm) in regional lymph node(s)
pN0(mol+)	Positive molecular findings by reverse transcriptase-polymerase chain reaction (RT-PCR); no isolated tumour cells detected
pN1	Micrometastases; or metastases in 1-3 axillary lymph nodes; and/or clinically negative internal mammary lymph nodes with micrometastases or macrometastases by sentinel lymph node biopsy
pN1mi	Micrometastases (approximately 200 cells, larger than 0.2 mm, but none larger than 2.0 mm)
pN1a	Metastases in 1-3 axillary lymph nodes, at least one metastasis larger than 2.0 mm
pN1b	Metastases in ipsilateral internal mammary lymph nodes, excluding isolated tumour cells
pN1c	pN1a and pN1b combined
pN2	Metastases in 4-9 axillary lymph nodes; or positive ipsilateral internal mammary lymph nodes by imaging in the absence of axillary lymph node metastases
pN2a	Metastases in 4-9 axillary lymph nodes (at least one tumour deposit larger than 2.0 mm)
pN2b	Metastases in clinically detected internal mammary lymph nodes with or without microscopic confirmation; with pathologically negative axillary lymph nodes
pN3	Metastases in 10 or more axillary lymph nodes; <i>or</i> in infraclavicular (level III axillary) lymph nodes; <i>or</i> positive ipsilateral internal mammary lymph nodes by imaging in the presence of one or more positive level I or II axillary lymph nodes; <i>or</i> in ipsilateral supraclavicular lymph nodes
pN3a	Metastases in 10 or more axillary lymph nodes (at least one tumour deposit larger than 2.0 mm); <i>or</i> metastases to the infraclavicular (level III axillary lymph) nodes
pN3b	pN1a or pN2a in the presence of pN2b (positive internal mammary lymph nodes by imaging); <i>or</i> pN2a in the presence of pN1b
pN3c	Metastases in ipsilateral supraclavicular lymph nodes

Table 1.7: Criteria for Metastases (M) Classifications

Criteria for metastases classification as defined by the American Joint Commission on Cancer. Table reproduced, with permission (**Appendix A.4**), from Giuliano et al. (2017).

M Category	M Criteria
M0	No clinical or radiographic evidence of distant metastases
cM0(i+)	No clinical or radiographic evidence of distant metastases in the presence of tumour cells and/or no deposits greater than 0.2 mm detected microscopically or by using molecular techniques in circulating blood, bone marrow, or other nonregional lymph node tissue in a patient without symptoms or signs of metastases
M1	Distant metastases detected by clinical or radiographic means (cM) and/or histologically proven metastases larger than 0.2 mm (pM)

Table 1.8: TNM Anatomic Stage Groups

Determination of TNM anatomic stage group as defined by the American Joint Commission on Cancer. Table reproduced, with permission (**Appendix A.4**), from Giuliano et al. (2017).

When T is...	And N is...	And M is...	Stage Group
Tis	N0	M0	0
T1	N0	M0	IA
T0	N1mi	M0	IB
T1	N1mi	M0	IB
T0	N1	M0	IIA
T1	N1	M0	IIA
T2	N0	M0	IIA
T2	N1	M0	IIB
T3	N0	M0	IIB
T1	N2	M0	IIIA
T2	N2	M0	IIIA
T3	N1	M0	IIIA
T3	N2	M0	IIIA
T4	N0	M0	IIIB
T4	N1	M0	IIIB
T4	N2	M0	IIIB
Any T	N3	M0	IIIC
Any T	Any N	M1	IV

Table 1.9: Immunohistochemical Criteria for Defining Breast Cancer Subtypes

Immunohistochemical criteria used to differentiate between breast cancer subtypes. Table reproduced, with permission (**Appendix A.5**), from Holliday and Speirs (2011).

Subtype	Immunoprofile	Other Characteristics
Normal	ER ⁺ , PR ⁺ , HER2 ⁻	
Luminal A	ER ⁺ , PR ^{+/-} , HER2 ⁻	Ki67 low
Luminal B	ER ⁺ , PR ^{+/-} , HER2 ⁻	Ki67 high
Basal	ER ⁻ , PR ⁻ , HER2 ⁻	EGFR positive and/or cytokeratin 5/6 positive; Ki67 high
Claudin-low	ER ⁻ , PR ⁻ , HER2 ⁻	Ki67 low; E-cadherin low; claudin-3, -4, and -7 low
HER2	ER ⁻ , PR ⁻ , HER2 ⁺	Ki67 high

1.4.2: Triple Negative Breast Cancer

One especially important categorization of breast cancers is based on the expression of ER, PR, and HER2. Tumours which lack ER and PR expression, and lack overexpression of HER2 are termed triple negative breast cancer (TNBC) and grouped based on a shared poor prognostic outcome despite being an otherwise heterogeneous group by other methods of classification (Alluri and Newman, 2014; Jhan and Andrechek, 2017). Importantly, TNBC and basal-like breast cancer are not synonymous, with the latter expressing a distinct set of basal cell markers (Eroles et al., 2012; Alluri and Newman, 2014). Approximately 15-20% of all invasive breast cancers are TNBC (Ismail-Khan and Bui, 2010; Li et al., 2017). These TNBCs are more common in women below age 40 and among black or Hispanic women (Bauer et al., 2007; Millikan et al., 2008). Furthermore, women with TNBC have poorer odds of survival than those with other forms of breast cancer due to a more aggressive pattern of growth and metastatic spread (Bauer et al., 2007; Ismail-Khan and Bui, 2010; Li et al., 2017). The four most common sites of metastasis are the bone, lung, brain, and liver (ACS, 2017). Treatment of TNBC is made more complex because of the lack of receptor expression. While receptor positive breast cancers can be effectively treated using endocrine or HER2-targeting therapies, systemically administered cytotoxic chemotherapeutics remain the only option available for TNBC (Alluri and Newman, 2014; Jhan and Andrechek, 2017; Li et al., 2017).

1.4.3: Experimental Models of Breast Cancer

Experimental models are necessary for basic and translational research on the development, course of disease, and treatment of breast cancer. Ideally, these models closely mimic clinical conditions found in human breast cancer: arising spontaneously from similar tissues, behaving in a pathologically similar manner, and responding similarly to therapeutic treatment (Zeng et al., 2020). These models can be divided between *in vivo* animal models and *in vitro* cell based models, each of which are used to study specific aspects of disease.

1.4.3.1: *in vivo* Models of Breast Cancer

Non-mammalian species are commonly used in the study of breast cancer despite the obvious drawback that they lack the breast tissues from which breast cancer develops. The fruit fly, *Drosophelia melanogaster*, has been extensively used in cancer research to learn about the molecular basis of the disease (Mirzoyan et al., 2019; Sajjad et al., 2021). Their short generational time and low cost of maintenance allow for their application in genetic studies of many different diseases. Other invertebrates such as *Caenorhabditis elegans*, a nematode, have similarly been used for genetic and functional studies to provide insight into the pathways and conditions which become dysregulated in cancer development (Kirienko et al., 2010).

Moving to distantly related vertebrates, animals like the zebrafish *Danio rerio* have been successfully used to model cancer development and to screen anticancer drugs for effectiveness and toxicity (Veinotte et al., 2014; Wertman et al., 2016; Sajjad et al., 2021). Zebrafish larvae are permeable to small molecules and do not fully develop adaptive immunity until 28 days of life; this allows transplantation of human cancer cells without immune suppression in a model which can then be monitored for tumour growth or cell migration following exposure to experimental small molecules (Lam et al., 2004; Veinotte et al., 2014; McKeown et al., 2022). Zebrafish have low innate tumour incidence, but can be genetically modified to express cancer markers or spontaneously develop tumours similar to those found in humans (Sajjad et al., 2021).

The most common animal models for breast cancer research are rodents (Zeng et al., 2020). Mice, *Mus musculus*, have long been used as a model in drug testing to determine pharmacokinetics and toxicity of novel therapeutics when establishing safety and feasibility of future efficacy studies (Andes and Craig, 2002; McKeown et al., 2022). When studying efficacy of novel therapeutic agents, there are thousands of different mouse strains available to choose from depending on the specific needs of the researcher (Borowsky, 2011). Genetically engineered mouse models of breast cancer can be categorized as either transgenic, where a specific oncogene is being overexpressed, or gene-targeted, where a tumour suppressor gene has been knocked out (Borowsky, 2011).

Some of these models are inducible through the introduction of a chemical or viral agent, allowing the researcher to initiate tumour development and thus measure differences between a trial and control group more easily. Chemical carcinogens such as 7,12-dimethylbenzanthracene (DMBA) or N-methyl-N-nitrosourea (MNU) can be used to induce tumour development at the site of injection (Russo and Russo, 1996; Thompson and Singh, 2000; Zeng et al., 2020). This can be combined with transgenic techniques to produce a more predictable effect. Tetracycline, for instance, can be used to control gene promoter activity in transgenic mice, selectively activating gene expression linked to cancer development (Gunther et al., 2002; Borowsky, 2011).

Another approach is the transplantation of cancer cells into disease free mice. Syngeneic transplant models are available where a mammary tumour occurring in a clonal mouse strain can be cultured and transplanted to other, genetically identical, mice. The 4T1 mouse mammary carcinoma cell line is an example of this, where a spontaneous tumour isolated from a Balb/C mouse can be cultured *in vitro* prior to injection into the mammary pad of an immunocompetent female Balb/C mouse wherein it will develop into an aggressive tumour which closely parallels human metastatic breast carcinoma (Dexter et al., 1978; Aslakson and Miller, 1992; Pulaski and Ostrand-Rosenberg, 1998; Pulaski and Ostrand-Rosenberg, 2000). Alternatively, immunodeficient mice such as NOD/SCID can be xenotransplanted with human breast cancer cells to more closely model human cells *in vitro* (Borowsky, 2011; Marcato et al., 2015). Mice have historically been viewed as the ideal xenotransplant model due to their small size and corresponding economical husbandry requirements, along with their high degree of similarity to humans and the presence of analogous anatomical features (Wertman et al., 2016).

A major drawback to mouse models of metastasis is that they are almost exclusively pulmonary, whereas the lung is only one possible site of metastasis in humans along with the liver, brain, and bone which are rarely observed in mice (Borowsky, 2011). The 4T1 cell line represents a rare exception to this, as it is capable of metastasizing to the lung, liver, bone, and brain *via* blood circulation (Heppner et al., 2000). This, in combination with the incidence of cancer being largely artificial through genetic alteration, induction, or transplantation, remains a challenge for those wishing to study cancer in as natural a model as possible.

1.4.3.2: *in vitro* Models of Breast Cancer

Several human breast cancer cell lines have been developed to fill the needs which remain unmet with animal models or can be used in combination with animals to produce more robust models. Immortalized human cell lines were developed as a natural progression of earlier experiments successfully culturing the embryonic tissues of frogs and chickens *in vitro*, which demonstrated that growth of cells outside the body was possible and outlined the techniques through which further lines could be established (Harrison, 1908; Carrel and Burrows, 1911; Mirabelli et al., 2019).

The first human cell line was established from samples taken from Henrietta Lacks, a young black woman diagnosed with cervical carcinoma. These cells were called HeLa, in reference to her name, and have been used as a standard cellular cancer model since their establishment (Scherer et al., 1953; Mirabelli et al., 2019). While the methods used in establishing and maintaining HeLa cells became the standard through which other adherent cell lines could be cultured, other methods were quickly developed for the cultivation of suspension cell lines with the establishment of RAJI lymphoma cells (Pulvertaft, 1964; Mirabelli et al., 2019). These cells, and those which followed them, have been extensively used in screening for new anticancer agents and in modeling cancer as a means to develop new treatments or gain further insight into the ways it develops and progresses (Mirabelli et al., 2019). A breast cancer cell line was first successfully cultured in 1958 with the establishment of the BT-20 line from an invasive ductal carcinoma taken from a 74 year old, white, female breast cancer patient (Lasfargues and Ozzello, 1958; Dai et al., 2017).

Today we have access to many different breast cancer cell lines, as such the remainder of this section will be confined to those used in the experimental sections which follow. One commonly used model of ER⁺/PR⁺ breast cancer is the MCF-7 cell line. MCF-7 cells were first established in 1973 at the Michigan Cancer Foundation, from which they get their name, from a 69 year old, white, female patient who had previously underwent a mastectomy of her left breast for malignant mammary adenocarcinoma and re-presented with a pleural effusion from which the cells were taken (Soule et al., 1973; Comşa et al., 2015). The MCF-7 line has been characterized as belonging to the luminal

A subtype and is generally considered to be poorly aggressive with low metastatic potential (Comşa et al., 2015). There are some concerns over the genetic stability of MCF-7 cells, as they demonstrate the capacity to develop clonal variations with differing genomic expression levels (Nugoli et al., 2003; Comşa et al., 2015). This can be used to the researcher's advantage through the development of treatment resistant sublines as a consequence of gradual, chronic exposure to known cytotoxic agents as a means to understand the development of resistance to chemotherapy (Schneider et al., 1994; Issa et al., 2014). To avoid unwanted genetic changes from the baseline MCF-7 cell lineage it is important to maintain a low passage number in cell culture; cryopreserving a large number of cell aliquots and repeatedly replacing cells after a set time in culture with "fresh" cell stocks to minimize genetic drift (Briske-Anderson et al., 1997; Chang-Liu and Woloschak, 1997; Esquetet et al., 1997; Wenger et al., 2004).

In addition to growing well as an adherent, 2D monolayer, MCF-7 cells are capable of growing as 3D spheroids or mammospheres (Comşa et al., 2015; Greenshields et al., 2015). Adapting a cell line from growth as a monolayer to a 3D architecture more closely simulates the environment found within a tumour, generating a mass of cells with a hypoxic core that does not have immediate access to the nutrient containing medium. By using spheroids, cell culture can be used to assess efficacy of anticancer agents previously tested in 2D culture as an intermediary step toward animal models. Additionally, spheroid formation can be used to assess differential effects of cytotoxic agents on differing populations of cell, for instance targeting cancer stem cells and thereby preventing spheroid formation (Yousefnia et al., 2019).

The MCF-7 line represents an important model of breast cancer because it remains ER⁺, an uncommon feature among cultured breast cancer cells, allowing it to be used in both experiments targeting the ER as well as validating that non-targeted therapeutics will remain effective in hormone sensitive cells (Comşa et al., 2015; Lee et al., 2015).

A continuing need in the treatment of breast cancer is the development of agents which can target TNBC and avoid common mechanisms of drug resistance. To this end, the primary cellular model of breast cancer used throughout this work is the MDA-MB-231 human breast cancer cell line. MDA-MB-231 human breast cancer cells were originally isolated in 1973 at the University of Texas MD Anderson Cancer Center from a

51 year old, white, female patient presenting with a pleural effusion containing metastatic breast cancer cells, hence the name MDA-MB-231, after an earlier radical mastectomy of her right breast (Cailleau et al., 1974). MDA-MB-231 cells are a claudin-low, TNBC cell line representing poorly differentiated and highly aggressive, invasive disease (Liu et al., 2003; Chavez et al., 2010; Holliday and Speirs, 2011). Similar to MCF-7 cells, resistance can be selected for through gradual exposure to cytotoxic agents (Schneider et al., 1994; Hall et al., 2017). Furthermore, MDA-MB-231 cells have been widely utilized in xenotransplantation models of breast cancer, increasing translatability from cellular to animal studies (Holliday and Speirs, 2011; Marcato et al., 2015; Lim et al., 2018; McKeown et al., 2022). This makes MDA-MB-231 cells ideal for screening new drugs intended to target difficult-to-treat cancers.

While cell lines provide enormous power in their potential to model cancer economically and specifically to many different conditions, there are several drawbacks to their usage. Cross-contamination can occur where one cell line can infiltrate another and become a co-culture with, or completely replace, the original through errors in handling and labeling (Nelson-Rees et al., 1981; Mirabelli et al., 2019). Contaminations by *Mycoplasma*, a genus of bacteria lacking a cell wall and responsible for a number of human infections, are also common (Mirabelli et al., 2019). *Mycoplasma* species gain nutrients from the cell culture medium and cellular metabolites, altering the culture environment leading to inconsistent conditions as compared to uncontaminated cultures. As with cross-contamination, poor technique can increase risk of cell culture infections. Finally, tightly controlled growth conditions needed for successful cell culture are not necessarily representative of the normal tumour microenvironment in patients. Most breast cancer cell culture takes place as 2D monolayers which do not experience the same pressures present in a 3D tumour. While this can be partially alleviated by the use of 3D spheroid cultures, there is still a lack of ancillary immune and non-cancerous cells which play a vital role in disease development and progression. Nevertheless, cell culture is among the most powerful tools used to understand the basic biology of cancer and pharmacology of cancer therapy in a high throughput and low cost model.

1.4.4: Treatment Options for Breast Cancer

Breast cancer treatments vary widely depending on the staging of the cancer present, but can be categorized as locally or systemically acting (Waks and Winer, 2019). Local treatments, for instance surgery or radiation, target a specific region of the body where the tumour is found and have limited effects elsewhere. Systemic treatments, for instance cytotoxic chemotherapy, are transported throughout the body by the blood and affect any cell with susceptibility to them. Most commonly, a combination of different treatment approaches are used, where surgical removal may be combined with systemic therapy preoperatively (neoadjuvant), postoperatively (adjuvant), or both (Waks and Winer, 2019). Radiation can be used prior to surgical intervention to help decrease tumour mass or postoperatively to eliminate remaining cancer cells. Systemic therapy can differ depending on progression and spread of the cancer (Waks and Winer, 2019).

All cancer treatments come with adverse effects which can affect quality of life and recovery. The goal in cancer therapy is to eliminate as much of the cancer as possible while keeping these adverse effects to a level of acceptable tolerability by the patient. In nonmetastatic disease, this means eradication of the tumour and prevention of metastatic recurrence. Metastatic breast cancer currently remains incurable and therefore therapeutic goals are limited to prolonging life and relieving symptoms (Waks and Winer, 2019).

1.4.4.1: Surgery

Typical treatment for breast cancer will involve surgical removal of the primary tumour for nonmetastatic cancers, although, systemic therapy may be started immediately for advanced, metastatic disease. Surgical approaches are broadly characterized into two types: breast conserving therapy (BCT), alternatively called a lumpectomy and involving the removal of as little tissue as possible, or mastectomy, where the entire affected breast is removed (Waks and Winer, 2019; Riis, 2020). BCT is the preferred approach when possible, as it is a more cosmetically acceptable intervention without compromising efficacy of the intervention. The primary requirement for BCT is the presence of a well defined, tumour free surgical margin to reduce the risk of recurrence (Waks and Winer,

2019; Riis, 2020). BCT is typically combined with postsurgical radiation to further reduce the risk of recurrence.

If a patient is not a good candidate for BCT, a mastectomy may be recommended instead. A mastectomy involves the complete removal of breast tissue from the affected breast and may also involve removal of underlying tissues as well. Malignant breast tumours in young patients, typically presenting as TNBC, are generally more aggressive and have worse prognosis than tumours in older patients. As a result, mastectomy has historically been the surgical approach of choice in this population (Riis, 2020). Despite the more medically extensive nature of a mastectomy, adjuvant radiation or systemic therapy may still be required.

The third surgical intervention is removal of axillary lymph nodes. The benefits to axillary lymph node resection are twofold, eliminating cancer cells which have spread to those nodes and allowing extensive histopathological examination to better assess metastatic potential (Riis, 2020).

Current recommendations in surgical treatment of breast cancer call for aggressive screening and public awareness campaigns such that cancers can be detected early and minimally invasive BCT will be an option for patients. Despite this, there is a trend toward patients increasingly electing for mastectomy in an attempt to minimize their risk of recurrence (Dragun et al., 2012).

1.4.4.2: Radiation Therapy

Radiation therapy is a common addition to surgery. Radiation can be delivered to the whole breast or a portion of the breast (following BCT), the chest wall (following mastectomy), and the regional lymph nodes depending on the surgical option elected (Waks and Winer, 2019). For instance, whole breast radiation is a standard component of BCT (Waks and Winer, 2019). In the simplest terms, radiation therapy involves the bombardment of cancer cells with high energy, gamma radiation to cause cellular damage resulting in cell death. Radiation can be delivered by means of external beam, where radiation is delivered from an instrument and focused to the area affected by cancer. Alternatively, although more rarely used, an internal radioactive device can be

temporarily implanted at the site of tumour removal to deliver localized radiation termed brachytherapy (Shah et al., 2018). Radiation is commonly used in tandem with surgical intervention, while neoadjuvant or adjuvant systemic therapy is commonplace in addition to radiation.

1.4.4.3: Targeted Therapy

Targeted therapies specifically target known breast cancer biomarkers such as HER2, and the biochemical pathways associated with them. Systemic use of targeted therapies allows for their use against both the primary tumour as well as any metastatic sites to which cancer cells may have spread throughout the body. By targeting specific proteins overexpressed by cancer cells, targeted therapies can be useful in limiting off target effects on other rapidly dividing, healthy cell populations like those comprising mucous membranes or bone marrow.

HER2 overexpression in the 20-25% of breast cancers which are HER2⁺ has been exploited to develop therapies which can specifically target that receptor (Wang and Xu, 2019). Trastuzumab, for example, is a monoclonal antibody which binds to the extracellular domain of the HER2 receptor, preventing its activation and subsequent downstream signalling (Molina et al., 2001; Wang and Xu, 2019). As an antibody, trastuzumab is delivered intravenously and has been used as both an adjuvant to surgical approaches and for metastatic disease. Cardiac toxicity and heart failure have been associated with trastuzumab treatment and represents the most limiting factor influencing the choice to use it (Seidman et al., 2002; Smith et al., 2006; Perez, 2008).

Small molecule inhibitors of HER2 are another approach used in targeted therapy. Lapatinib is a tyrosine kinase inhibitor which acts at both HER2 and the epidermal growth factor receptor (EGFR) to prevent phosphorylation and subsequent activation of proliferation pathways (Wang and Xu, 2019). Lapatinib is particularly useful in patients with advanced stage breast cancer when given in combination with trastuzumab as the two therapies act in different ways on the same HER2 receptor to produce a synergistic effect (Baselga et al., 2012; Wang and Xu, 2019).

Combining a HER2 selective antibody with a chemotherapeutic agent can provide additional benefits. The first such combination to receive approval was trastuzumab

emtansine, where the fungal derived toxin emtansine was conjugated to the trastuzumab antibody (Peddi and Hurvitz, 2014; Koster et al., 2022). Emtansine alone, while more potent than chemotherapeutic agents currently in use such as paclitaxel, could not be clinically implemented due to concerns over toxicity (Peddi and Hurvitz, 2014). By conjugating emtansine to trastuzumab, emtansine is selectively delivered to HER2⁺ cancer cells where it can interrupt microtubule polymerization and have minimal effect on cells not expressing high levels of HER2 (Peddi and Hurvitz, 2014).

Downstream of ER, PR, and HER2 are intracellular signalling cascades regulating growth and proliferation. One such signalling cascade which can be targeted is the phosphatidylinositol 3-kinase (PI3K)/protein kinase B (AKT)/mechanistic target of rapamycin kinase (mTOR) pathway (Wang and Xu, 2019). Everolimus, an orally delivered small molecule inhibitor of mTOR, is an example of one such drug undergoing clinical trials (André et al., 2014; Hurvitz et al., 2015; Wang and Xu, 2019).

While initially highly effective, the greatest drawback to targeted therapies is that they are, by their very nature, dependent on the overexpression of proteins like HER2. In advanced, TNBC which lack HER2 overexpression these targeted therapies are of no use.

1.4.4.4: Hormone Therapy

Hormone therapy, alternatively called endocrine therapy, is used in breast cancers which are ER⁺ and/or PR⁺. Broadly speaking, hormone therapy can be a specific type of targeted therapy which involves receptors for the female sex hormones, or directly affects production of the female sex hormones in an untargeted manner. Normal breast tissue growth and differentiation is controlled by estrogens and progesterone: steroid hormones primarily produced in the ovaries in premenopausal women and in adipose tissue after menopause (Tremont et al., 2017). The 3 forms of estrogen, in order of potency, are estradiol (E₂), estrone (E₁), and estriol (E₃); all of which are derived from androgenic precursors (Birkhauser, 1996; Bennink, 2004). The estrogens and progesterone then interact with ERs and PRs expressed by cancer cells to promote proliferation (**Figure 1.2**). Hormone therapies are used to interrupt this signalling.

The first group of drugs used to modify estrogen signalling in cancer cells are the selective estrogen receptor modulators (SERMs) which act as ER antagonists in breast tissue, yet can act as partial agonists in other tissues like bone (An, 2016). By selectively antagonizing ERs on breast cancer cells, tumour growth can be slowed; simultaneous agonism of ERs in bone help to maintain bone density which is beneficial in postmenopausal patients (Swaby et al., 2007; An, 2016). Tamoxifen is one such SERM currently in use for the treatment of ER⁺ breast cancer. Tamoxifen is orally delivered as a pro-drug which is converted by cytochrome P450 3A4 and 2D6 to biologically active metabolites (Desta et al., 2004). Adjuvant use of tamoxifen for 5 years in patients with ER⁺ breast cancer has been shown to decrease mortality by 31% throughout the following 15 years (Davies et al., 2011; Tremont et al., 2017). The benefits to be gained from use of SERMs must still be balanced against possible adverse effects. SERMs can be agonistic to uterine tissue and therefore increase the risk of endometrial cancers, although the degree of risk varies depending on which SERM is used (Jordan, 2003; An, 2016). Other common adverse effects associated with SERMs are those typically associated with menopause due to the disruption of estrogen signalling; they include hot flashes, cramps, and increased risk of thromboembolism (An, 2016).

Selective estrogen receptor degraders (SERDs) comprise the next group of drugs used to modify estrogen signalling. SERDs behave much like SERMs, binding to the ER of cancer cells and thereby preventing signal propagation (Patel and Bihani, 2018). SERDs differ, however, in that they act as global ER antagonists which competitively bind the ER with high affinity and remain bound leading to proteasomal degradation of the receptor (Johnston and Cheung, 2010; Patel and Bihani, 2018). Fulvestrant is an example of a SERD which binds to ER monomers, preventing dimerization of the ER which prevents signalling from occurring (Patel and Bihani, 2018). The difference in mechanism of action means that Fulvestrant can remain effective in cancer cells which have become resistant to tamoxifen (Hu et al., 1993; Patel and Bihani, 2018). The adverse effects associated with SERDs are similar to those associated with SERMs.

While SERMs and SERDs target the ER, estrogen can be lowered directly by a group of drugs called aromatase inhibitors. In premenopausal women estrogen is primarily produced by the ovaries, however, estrogen can also be produced peripherally

from androgenic precursors by aromatase (Chumsri et al., 2011). This is especially important in breast cancer patients who have undergone menopause, surgery, or chemical therapy which would otherwise reduce the estrogen produced by the ovaries. Aromatase is a cytochrome P450 enzyme found in tissues throughout the body and has been demonstrated to be expressed in breast cancer cells at levels sufficient to produce enough estrogen to stimulate tumour growth (Smith and Dowsett, 2003; Chumsri et al., 2011; Tremont et al., 2017). Aromatase inhibitors prevent this peripheral synthesis of estrogen, thereby interrupting ER signal transduction by reducing the available ligand for the receptors. For this reason, aromatase inhibitors are most effective in postmenopausal women or those undergoing therapy for ovarian suppression. Letrozole, anastrozole, and exemestane are the 3 aromatase inhibitors currently in use. Early aromatase inhibitors were effective against breast cancer but also inhibited the production of other steroid hormones like cortisol and aldosterone, leading to significant adverse effects (Chumsri et al., 2011). Third generation aromatase inhibitors are generally better tolerated, with the most common adverse effects being hot flashes, vaginal dryness, and headache (Smith and Dowsett, 2003).

The final option for hormone therapy is ovarian ablation or suppression. Ovarian ablation refers specifically to the physical removal or destruction of the ovaries by surgical or radiological means, while ovarian suppression refers to the use of transient inhibition of hormone production elicited through pharmacological means (Prowell and Davidson, 2004). Premenopausal women can reduce estrogen and progesterone production by removing or suppressing the ovaries, effectively making them postmenopausal. Suppression of the ovaries can be beneficial in broadening the therapeutic choices available to patients, in the case of aromatase inhibitors, as well as limiting the production of estrogen and progesterone available to interact with ERs and PRs on cancer cells. Oophorectomy is the surgical removal of the ovaries and was the original systemic therapy used to treat hormonally sensitive cancers (Prowell and Davidson, 2004). While reliably reducing hormone levels, oophorectomy is irreversible, causes loss of fertility, premature menopause (and related risks), and is an invasive surgical procedure. Ovarian irradiation is an alternative approach, being less invasive and available as an outpatient procedure, but otherwise carrying similar drawbacks (Prowell

and Davidson, 2004). Chemical suppression of the ovaries can be accomplished with luteinizing hormone releasing hormone (LHRH) analogues. LHRH regulates release of gonadotropins from the pituitary, which then stimulate estrogen production by the ovaries (Prowell and Davidson, 2004). LHRH analogues cause an initial surge in gonadotropins and estrogens, followed by a decline in estrogens to postmenopausal levels (Harvey et al., 1985; Prowell and Davidson, 2004). Reversibility is the greatest advantage to LHRH analogues, while the largest disadvantage is recurrence of tumour growth following discontinuation. Lastly, chemotherapy can unpredictably result in ovarian toxicity as an adverse effect when administered (Prowell and Davidson, 2004). While beneficial, this damage may or may not be reversible and chemotherapy is not typically used explicitly for this purpose.

Most of the hormone targeting therapies discussed have focused on interrupting signalling through the ER. The need for ER⁺/PR⁺ expression in cancer cells is the largest drawback to hormonal therapy as a concept, with more advanced, TNBC, and aggressive cancers not expressing ER/PR and therefore not benefiting from these treatments. ER⁻/PR⁺ breast cancer is associated with worse prognosis than ER⁺/PR⁺ or ER⁺/PR⁻ cancer, but represents only a very small proportion of breast cancer subtypes (Li et al., 2022). Estrogens are capable of binding to PRs as well as ERs, and this has been associated with increased breast cancer risk (Hasan et al., 2011). Development of agents which specifically target progesterone and PR is an area of ongoing research, however, none are currently in clinical use (Klijn et al., 2000).

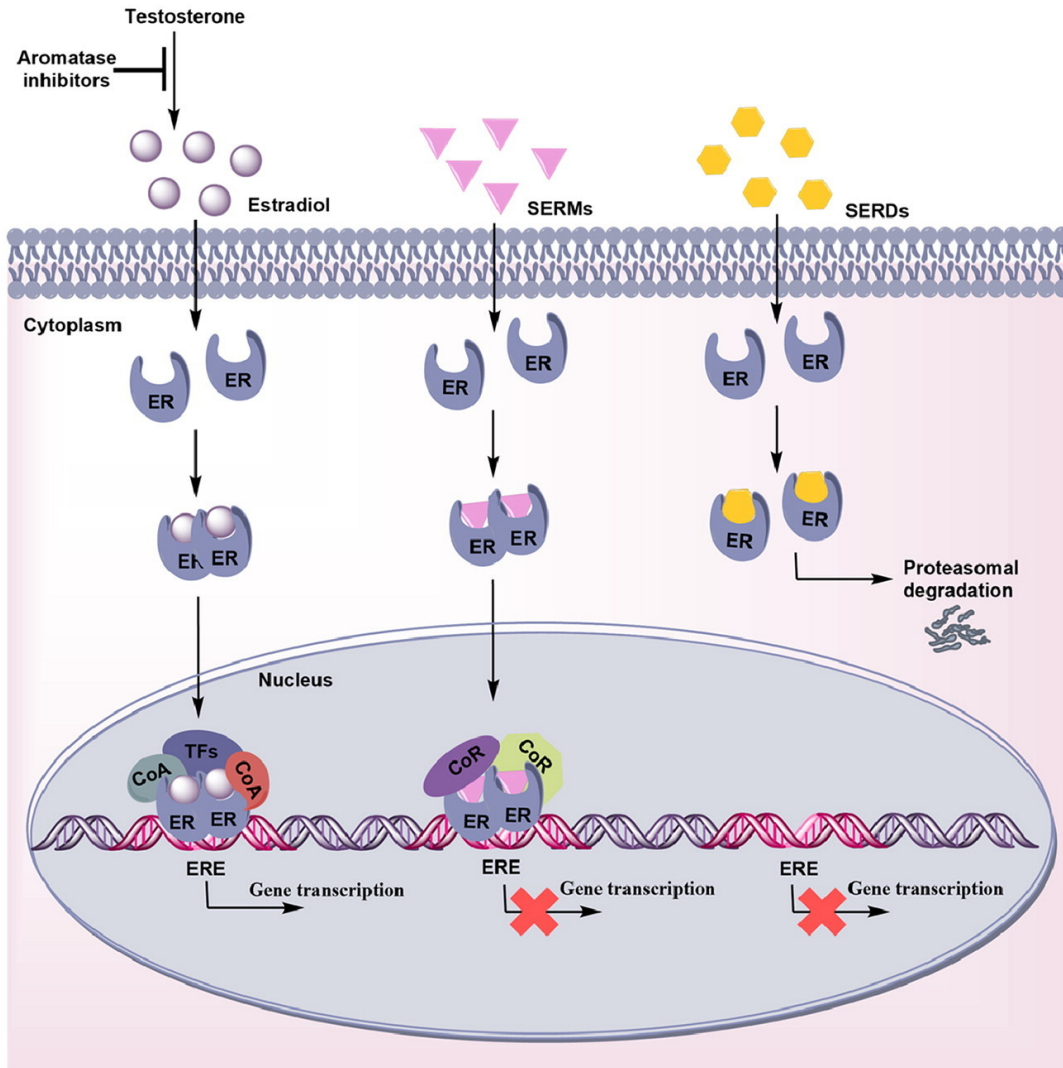


Figure 1.2: Hormone Therapy Mechanisms of Action

Hormone therapy can interrupt growth and proliferation of ER⁺ breast cancer cells. Aromatase inhibitors can prevent peripheral synthesis of estrogens from precursor androgens, thus interfering with ER signal transduction. SERMs antagonize ER, preventing activation of downstream transcription. SERDs bind ER and lead to proteasomal degradation without inducing downstream transcription. Figure reproduced, under creative commons fair use (**Appendices A.6 and A.7**), from Patel and Bihani (2018).

1.4.4.5: Immunotherapy

Immunotherapy for cancer involves the use of the patient's own immune system to identify and destroy cancer cells. An immune response can be stimulated by inducing the immune system to recognize proteins expressed on the surface of cancer cells or by masking these proteins such that immune cells are no longer inactivated by them. For breast cancer, an approach using immune checkpoint inhibitors therapy is used (Vonderheide et al., 2017; Disis and Stanton, 2018; Adams et al., 2019). Healthy cells express checkpoint proteins which interact with receptors on T cells that prevent the immune system from activating and targeting healthy tissue. When these checkpoint proteins are expressed on cancer cells they are capable of avoiding immune detection. One example of a checkpoint protein is the programmed cell death receptor 1 (PD-1) protein expressed on T cells and the corresponding programmed cell death ligand 1 (PD-L1) which can be expressed on breast cancer cells (Emens et al., 2016; Vonderheide et al., 2017; Disis and Stanton, 2018; Adams et al., 2019). When PD-1 successfully recognizes PD-L1 an inhibitory signal is released to prevent T cell activation. Monoclonal antibodies targeting PD-1, for example pembrolizumab, or PD-L1, for example atezolizumab, selectively bind to their target and prevent interaction between PD-1 and PD-L1 (Vonderheide et al., 2017; Disis and Stanton, 2018; Adams et al., 2019).

A second approach to utilizing the immune system to attack cancer cells is the development of therapeutic vaccines. Phase I clinical trials are ongoing to evaluate the possibility of developing vaccines against known molecular markers for breast cancer (Disis et al., 2023). The idea is to elicit active immunity against tumour specific antigens, allowing T cells to seek out cancer directly (Disis and Stanton, 2018; Disis et al., 2023). While still in initial phases of testing, vaccines show promise as a future therapy.

HER2⁺ and TNBCs in particular are associated with increased tumour infiltration by lymphocytes, providing a basis for the use of immunotherapy in these subtypes (Emens et al., 2016). By developing checkpoint inhibitors, another tool is becoming available to treat breast cancers which have historically had limited therapeutic options available. Unfortunately, immunotherapy is not without risks of its own. These agents

remove a defence against autoimmune attack of healthy tissue and, thus, can result in serious adverse effects.

1.4.4.6: Chemotherapy

While the aforementioned approaches of targeted, hormone, and immune therapy are all selective toward cells expressing particular biomarkers or receptors, chemotherapies are systemically acting drugs which broadly effect all cells of the body. The important distinction is that chemotherapy is more harmful to rapidly dividing, as opposed to slowly dividing, cells and therefore will have the greatest effect on tumours or tissues with a high rate of cellular division. It is for this reason that the adverse effects of chemotherapy tend to most affect areas of rapid cellular turnover like immune cells or the mucosal epithelia. Likewise, slowly growing cancers are less susceptible to chemotherapy (Tesarova, 2012; O'Shaughnessy et al., 2015; Prihantono and Faruk, 2021). Different tumours can lend themselves to different types of chemotherapy, which can be initiated either before or after surgery.

If chemotherapy is delivered following surgery it is deemed as adjuvant, with the intended goal being to eliminate any remaining cancerous cells at the primary site or disseminated throughout the body (Waks and Winer, 2019; Montemurro et al., 2020). If delivered prior to surgery, deemed neoadjuvant, there may be several different possible goals. Neoadjuvant chemotherapy for breast cancer was first introduced in the late 1970s as a means to treat inoperable, advanced disease with the hope of making it operable (Rubens et al., 1980; EBCTCG, 2018). Neoadjuvant therapy has since been used to decrease tumour size, allowing for better outcomes with BCT (Clough et al., 2015; Mougalian et al., 2015; EBCTCG, 2018). For advanced, metastatic breast cancers chemotherapy used alone is a common treatment option, with its use limited to symptomatic relief as opposed to being curative (Mayer and Burstein, 2007).

Chemotherapy is a broad categorization, with many different possible targets, and can be administered orally, intravenously, or intrathecally (Mayer and Burstein, 2007). One important group are the anthracyclines (**Figure 1.3A, B, C**), such as doxorubicin and epirubicin, which cause DNA damage leading to apoptosis. Anthracyclines have been

proposed to act by intercalating into DNA, resulting in inhibition of macromolecular biosynthesis, free radical formation, DNA cross linking, interruption of DNA strand separation and helicase activity, and inhibition of topoisomerase II (TOP2) activity (Gewirtz, 1999). Anthracyclines may be used at any stage in breast cancer therapy, from early disease through advanced metastatic spread (Mayer and Burstein, 2007).

Taxanes (**Figure 1.3D, E**), such as paclitaxel and docetaxel, are a second group of drugs commonly used in the treatment of breast cancer. Taxanes stabilize microtubules and thereby inhibit vesicle transport, transcription factor trafficking, mitochondrial function, and chromosome separation during cell division (Fitzpatrick and de Wit, 2014). When chromosome separation is prevented in this way, the affected cell will undergo apoptosis. Taxanes are primarily used in the treatment of solid tumours and are an option for first-line therapy in metastatic breast cancer (Mayer and Burstein, 2007).

Another group of drugs are the antimetabolites (**Figure 1.3F, G**) such as 5-fluorouracil and gemcitabine. Antimetabolites are drugs which are similar to essential biomolecules needed for the biosynthesis of cellular structures (Longley et al., 2003). In the case of 5-fluorouracil, it is a pyrimidine antagonist which mimics the uracil base needed for assembly of DNA and RNA. Due to the incorporated fluorine atom, 5-fluorouracil disrupts RNA synthesis and prevents the biosynthesis of thymidylate which is needed for DNA replication and repair (Longley et al., 2003).

Finally, alkylating agents (**Figure 1.3H**), such as cyclophosphamide, and platinum-containing compounds (**Figure 1.3I, J**), such as cisplatin and carboplatin, also act by targeting DNA. Metabolites of cyclophosphamide cause DNA damage through alkylation, which in turn initiates apoptosis in the affected cell (Voelcker, 2020). Similarly, platinum-containing agents are used to form covalent DNA-DNA or DNA-protein bonds (de Sousa et al., 2014). These permanent bonds prevent DNA replication and ultimately result in cell cycle arrest and apoptosis (de Sousa et al., 2014).

Ultimately, the representative chemotherapeutic agents described above highlight the diversity of approaches used to elicit a cytotoxic response in cancer cells. Chemotherapy can be delivered as a single agent, but more commonly combinations of chemotherapy drugs are used (Mayer and Burstein, 2007; Waks and Winer, 2019). By combining multiple differently acting chemotherapies, the dose delivered can be reduced

while increasing or maintaining the efficacy of individual agents and decreasing adverse effects (Fisusi and Akala, 2019).

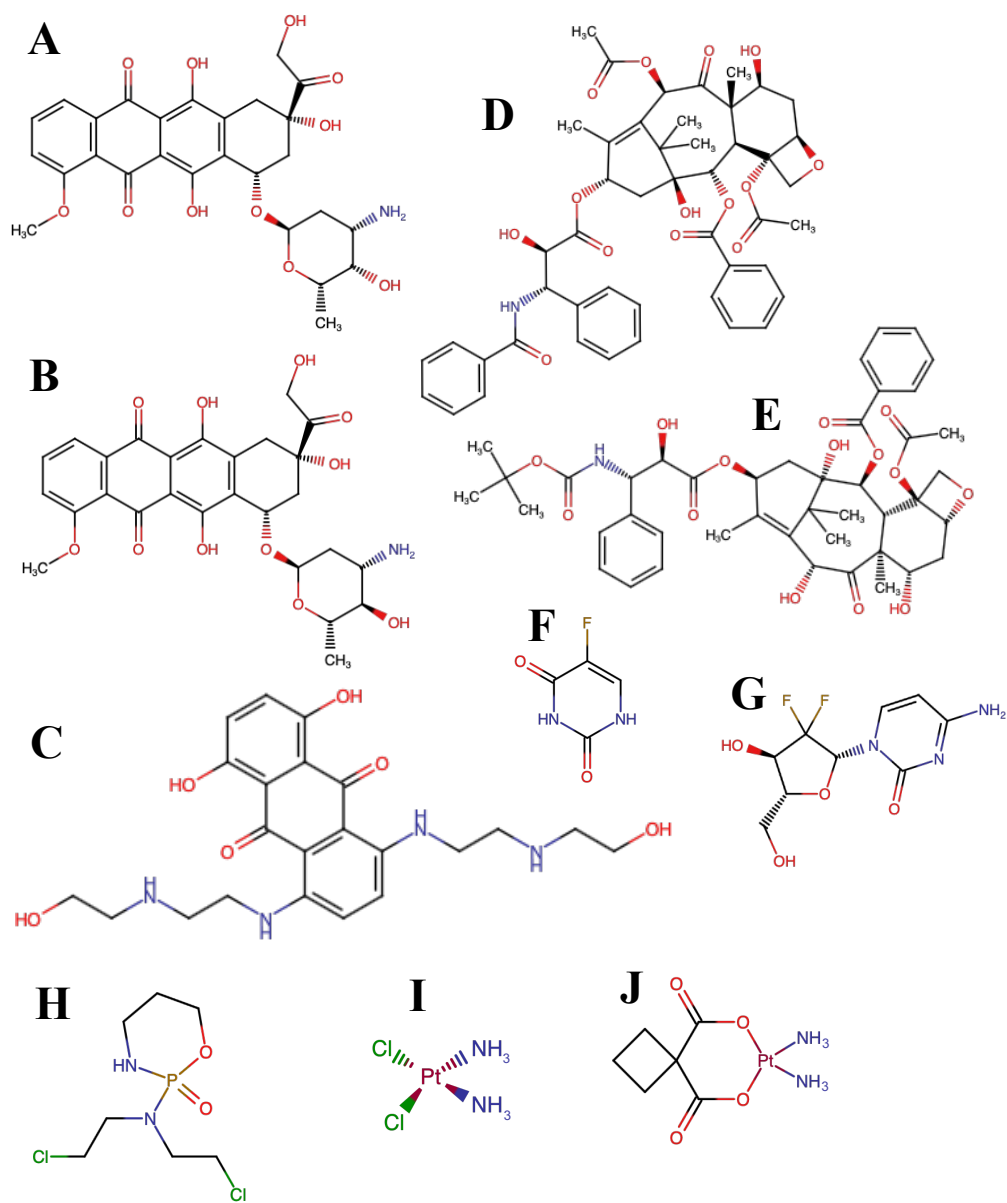


Figure 1.3: Molecular Structures of Example Chemotherapeutics

Molecular structures are depicted for example chemotherapeutics. The anthracyclines are represented by (A) doxorubicin, (B) epirubicin, and (C) mitoxantrone (which is not therapeutically used). Taxanes are represented by (D) paclitaxel and (E) docetaxel. Antimetabolites include (F) 5-fluorouracil and (G) gemcitabine. An example alkylating agent is (H) cyclophosphamide. Finally, (I) cisplatin and (J) carboplatin represent platinum-containing compounds.

1.4.5: Multidrug Resistance in Breast Cancer

Treatment options for breast cancer have been progressing and accumulating as our understanding has improved. Unfortunately, for those patients with advanced and recurrent disease, drug resistance can occur with prolonged or repeated exposure to chemotherapy (Longley and Johnston, 2005; Coley, 2008; Marquette and Nabell, 2012). This resistance may become acquired over time, or cancer cells may have developed attributes which happen to confer resistance before they are ever exposed to chemotherapy (Longley and Johnston, 2005). If randomly acquired mutations happen to confer an advantage toward resistance, it is termed innate drug resistance, whereas resistance arising from the selective killing of the most susceptible cancer cells gradually selecting for a more resistant subpopulation is termed acquired resistance (Coley, 2008). Furthermore, development of resistance to one chemotherapeutic may confer resistance to another, a trait termed multidrug resistance (MDR). Regardless of how it is acquired, treatment failure in 90% of metastatic breast cancer patients has been attributed to drug resistance (Longley and Johnston, 2005; Coley, 2008). The acquisition of drug resistance occurs quickly. First line therapies for metastatic breast cancer, like anthracyclines and taxanes, initially have a 30-70% response rate but disease progression following treatment is expected to occur in 6-10 months (Bonnetterre et al., 2004; Vassilomanolakis et al., 2005; Coley, 2008). Following disease progression, the response to chemotherapeutics is as low as 20-30% with a median response duration less than 6 months (Porkka et al., 1994; Coley, 2008). MDR represents a major hurdle to the treatment of advanced, TNBC and therefore the development of new chemotherapeutic agents which are not susceptible to the same mechanism of resistance are needed. MDR can develop in a variety of ways, including increased drug efflux, decreased drug influx, drug inactivation, modification of drug targets, DNA damage repair, avoidance of apoptosis, and increased survival signalling (**Figure 1.4**). Importantly, MDR is not limited to any one of the following mechanisms and can result from any combination of factors involving multiple different pathways to resistance.

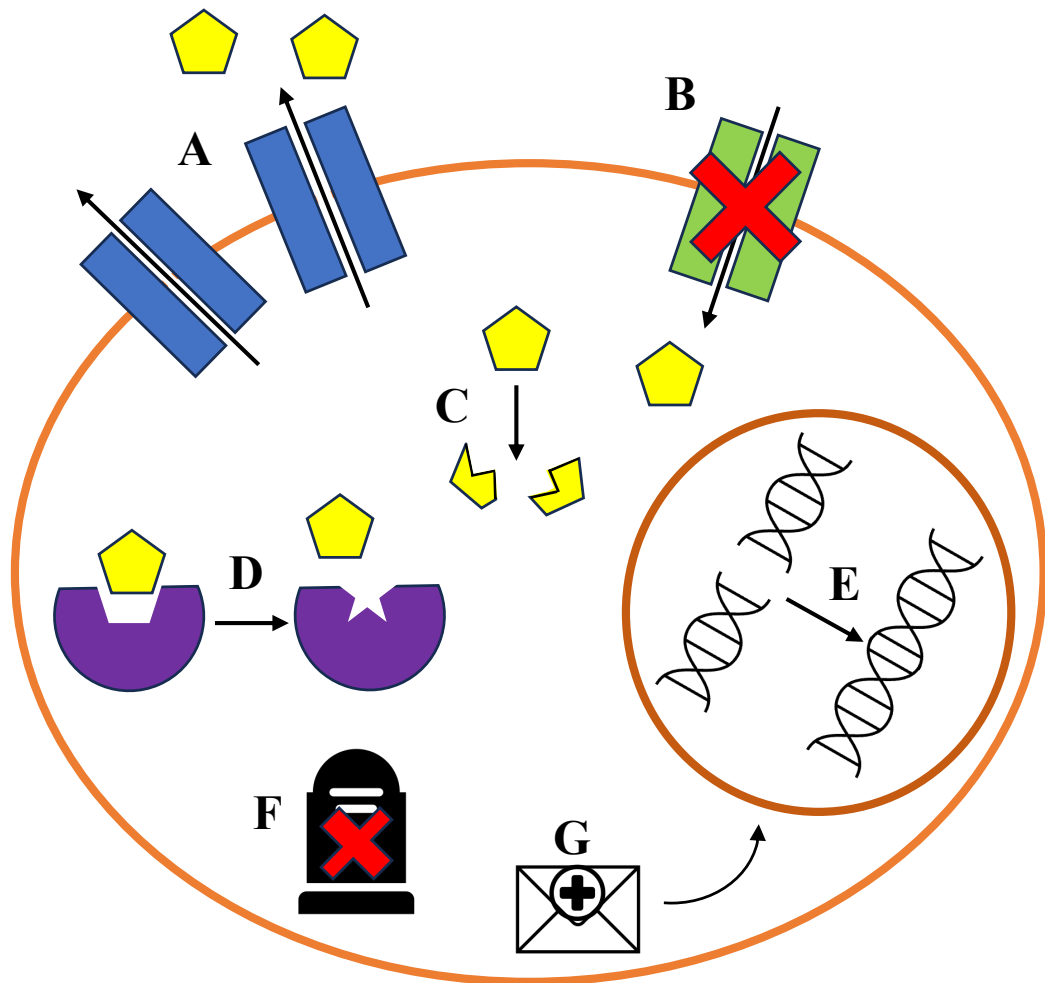


Figure 1.4: Overview of Mechanisms of Drug Resistance in Cancer Cells

Mechanisms which may convey MDR include: (A) increased drug efflux through ABC-transporters, (B) decreased drug influx through uptake transporters, (C) drug inactivation by detoxifying mechanisms, (D) modification of drug targets, (E) promoting DNA damage repair, (F) avoidance of apoptosis, and (G) increased survival signalling.

1.4.5.1: Drug Efflux Transporters

The best characterized mechanism for MDR development is the overexpression of adenosine triphosphate-binding cassette (ABC) drug efflux transporters. The ABC superfamily of transmembrane transporters consist of 48 known transporters, divided into 7 subfamilies labeled A-G, which share sequence homology and similar function (Dean et al., 2001). These are individually identified by a number, hence ABCB1 would be protein 1 of the B subfamily. These transporters use adenosine triphosphate (ATP) to remove compounds (**Table 1.10**) within the cytoplasm to the extracellular environment (Dean et al., 2001). For this work, the focus will be on 3 ABC transporters commonly involved in resistance to chemotherapy in breast cancer; namely ABCB1, ABCC1, and ABCG2.

ABCB1, alternatively known as multidrug resistance protein 1 (MDR1) or permeability-glycoprotein (P-gp), is the best characterized ABC transporter due to its ability to confer MDR (Dean et al., 2001). ABCB1 is a promiscuous transporter of hydrophobic substrates and has an important role in removing toxic metabolites from healthy cells. It is found in physiological barriers such as the blood-brain barrier, placental barrier, and intestinal barrier (Famta et al., 2021). The identification of ABCB1 in clinical samples taken from kidney, colon, breast, lung, and blood cancers is associated with a poor response to chemotherapy (Goldstein et al., 1989; Robey et al., 2010; Amiri-Kordestani et al., 2012; Robey et al., 2018). ABCC1, alternatively known as multidrug resistance-associated protein 1 (MRP1), was first identified in a small-cell lung carcinoma cell line which exhibited MDR but did not express ABCB1 (Cole et al., 1992; Dean et al., 2001). Generally, ABCC1 has a similar substrate profile to ABCB1, but additionally transports compounds conjugated to glutathione, glucuronide, or sulfate (Wang et al., 2019). ABCG2 was identified by analyzing cell lines resistant to mitoxantrone that did not overexpress ABCB1 or ABCC1, leading to its alternatively being called mitoxantrone resistance protein 1 (MXR1) or and breast cancer resistance protein (BCRP) (Allikmets et al., 1998; Doyle et al., 1998; Miyake et al., 1999; Dean et al., 2001). ABCG2 is most notable in conferring resistance to anthracycline drugs. Inhibitors of ABC transporters (**Table 1.10**) have been found to reduce MDR *in vitro* but have been largely unsuccessful in clinical trials due to toxicity (Marquette and Nabell, 2012).

Table 1.10: ABC Transporters Involved in Multidrug Resistance

List of ABC drug efflux transporters known to be involved in multidrug resistance with example small molecule substrates and inhibitors for those transporters. Figure reproduced, under creative commons fair use (**Appendices A.7 and A.8**), from Dean et al. (2001)

ABC Transporter	Substrates	Inhibitors
ABCB1	Colchicine	Verapamil
	Doxorubicin	PSC833
	VP16	GG918
	Adriamycin	V-104
	Vinblastine	Pluronic L61
	Digoxin	
	Saquinivir Paclitaxel	
ABCC1	Doxorubicin	Cyclosporin A
	Danuorubicin	V-104
	Vincristine	
	VP16	
	Colchicine	
	Etoposide Rhodamine	
ABCC2	Vinblastine	
	Sulfinpyrazone	
ABCC3	Methotrexate	
	Etoposide	
ABCC4	Nucleoside monophosphates	
ABCC5	Nucleoside monophosphates	
ABCG2	Mitoxantrone	Fumitremorgin C
	Topotecan	GF120918
	Doxorubicin	
	Danuorubicin	
	CPT-11 Rhodamine	

1.4.5.2: Drug Influx Transporters

Preventing chemotherapeutics from entering the cells is another mechanism through which MDR can be established. Solute carrier (SLC) transport proteins are responsible for actively transferring essential minerals and nutrients across the plasma membrane to overcome the concentration gradient between the cell and its environment. It has been hypothesized that alterations to these transporters which limit their ability to convey chemotherapeutics or decrease their expression could result in increased drug resistance (Gillet and Gottesman, 2010; Mansoori et al., 2017). One well described example of this is the entry of methotrexate into the cell via the reduced folate carrier (RFC) transporter. Osteosarcoma samples with reduced RFC showed poor response to methotrexate therapy, and a RFC mutation resulting in decreased transport was associated with worse prognosis in children treated with methotrexate for lymphoblastic leukemia (Guo et al., 1999; Laverdière et al., 2002). While the exact mechanism for drug uptake remains unknown for many chemotherapeutic drugs, it is reasonable to assert that alterations to drug influx transporters would alter this uptake (Longley and Johnston, 2005).

1.4.5.3: Drug Inactivation

Chemotherapy can be rendered ineffective through a reduction in concentration, providing a similar effect to enhanced efflux or decreased influx. This can be accomplished through enzymatic degradation to inactive metabolites. The degradation of 5-fluorouracil to an inactive metabolite by dihydropyrimidine dehydrogenase (DPD) is one example of this. DPD degrades more than 80% of administered 5-fluorouracil in the liver before it can reach tumour cells (Longley and Johnston, 2005; Verma et al., 2022). When overexpressed in cancer cells, DPD degrades remaining 5-fluorouracil and decreases the efficacy of treatment (Verma et al., 2022). The reverse is true in patients with reduced DPD activity who are therefore at increased risk of toxicity (Vogel et al., 2020). Alternatively, when the chemotherapeutic is delivered as a pro-drug requiring enzymatic activity to produce an active metabolite, reduction in enzyme activity can also reduce the efficacy of treatment (Housman et al., 2014). For example, tamoxifen has

weak affinity for ER but upon metabolic conversion to endoxifen by cytochrome P450s 2D6 and 3A4/5 has 100-fold more affinity for the ER (de Souza and Olopade, 2011). Reduced 2D6 expression by cancer cells would therefore render tamoxifen treatment far less effective.

In addition to enzymatic inactivation, drugs can also be modified in ways which make them more likely to be removed from the cell. Platinum-containing compounds can be covalently linked to glutathione through the action of glutathione-S-transferase enzymes (Longley and Johnston, 2005). Once linked to glutathione, the platinum-containing compounds become better substrates for ABC transporters, reducing their effectiveness due to removal (Ishikawa and Ali-Osman, 1993; Longley and Johnston, 2005).

1.4.5.4: Modification of Drug Targets

Anticancer drugs are often specific to a particular molecular target. Alterations to this target, by means of mutation or expression changes, can result in decreased or lack of efficacy by chemotherapeutics. For example, drugs like amsacrine and etoposide target TOP2 and cause it to inappropriately generate double strand DNA breaks which result in apoptosis. In a human leukemia cell line, repeated exposure to amsacrine caused mutations to TOP2 which conferred a 100-fold increase in resistance without affecting susceptibility of the mutated enzyme to etoposide (Zwelling et al., 1989). This demonstrates that while both amsacrine and etoposide target the same molecule, specific mutations can interfere with the functionality of one drug without affecting another.

Another example is the targeting of microtubules by taxanes. The taxanes exert an anticancer effect by stabilizing microtubules, preventing their depolymerization, and thereby blocking chromosome separation during cell division. Microtubules are comprised of α -tubulin and β -tubulin subunits, and there are multiple isoforms of each (Longley and Johnston, 2005; Coley, 2008; Marquette and Nabell, 2012). By altering the isoform of β -tubulin expressed to one less susceptible to paclitaxel stabilization, cancer cells can become resistant to taxanes (Kamath et al., 2005). Clinically, overexpression of

the β -tubulin III isoform has been associated with paclitaxel resistance and disease progression in breast cancer (Paradiso et al., 2005; Coley, 2008).

1.4.5.5: DNA Damage Repair

For those drugs which exert their effect by causing DNA damage, DNA damage repair mechanisms can affect resistance. Nucleotide excision repair, for example, is the major pathway by which DNA damaged caused by platinum-containing compounds is repaired (Longley and Johnston, 2005). When DNA damage associated with the addition of a bulky group added to a nucleotide is detected, such as those produced by cisplatin or oxaliplatin, the nucleotide excision repair pathway is activated to remove the damaged nucleotides and synthesize new DNA to fill the created gap (Reardon et al., 1999; Marteijn et al., 2014). Breast cancers with deficient expression of nucleotide excision repair proteins like p53, BRCA1, or BRCA2 show increased sensitivity to platinum-containing compounds, while reintroduction of their expression in cellular models increases resistance (Rajkumar-Calkins et al., 2019). Increased expression of proteins involved in nucleotide excision repair can confer MDR to any chemotherapeutic causing these kinds of bulky additions to DNA (Reardon et al., 1999; Martin et al., 2008).

In addition to repairing additions to DNA, cancer cells can also express changes in proteins responsible for DNA mismatch repair. The mismatch repair pathway normally identifies and corrects single nucleotide mismatches occurring as a result of DNA replication errors or damage (Schofield and Hsieh, 2003). Loss of the mismatch repair pathway elicits increased genomic instability, allowing for an increased rate of mutations which can result in the development of cancer (Hanahan and Weinberg, 2000; Fedier et al., 2001; Longley and Johnston, 2005; Hanahan and Weinberg, 2011). Beyond the increased likelihood of accumulating further hallmarks of cancer, loss of the mismatch repair pathway in breast cancer cells has been associated with increased resistance to cytotoxic agents like doxorubicin and mitoxantrone which target TOP2 (Fink et al., 1998b; Fedier et al., 2001; Longley and Johnston, 2005). Loss of mismatch repair is thought to increase chemotherapeutic resistance by impairing cellular capacity to detect damage, leading to avoidance of apoptosis and poor clinical outcome in breast cancer (Fink et al., 1998a; Malik et al., 2019).

1.4.5.6: Avoidance of Apoptosis and Increased Survival Signalling

Anticancer drugs operate by inducing cell death in cancer cells, predominantly through apoptosis. Apoptosis is tightly regulated by a variety of cellular factors which can be disrupted by genetic changes. As previously discussed in sections 1.3.1.1 and 1.3.1.3, sustaining proliferative signalling and resisting cell death are key hallmarks in the development of cancer (Hanahan and Weinberg, 2000; Hanahan and Weinberg, 2011). Cancer cells exposed to chemotherapeutic drugs will have increased pressure selecting for defects in these regulatory pathways. For instance, increased expression of cyclooxygenase-2 (COX2) has been associated with recurrence in both invasive breast cancer and ductal carcinoma *in situ* following surgical removal (Barnes et al., 2006; Coley, 2008). COX2 limits the ubiquitination of the protein survivin, also associated with recurrent disease, which in turn blocks the activity of caspases involved in the apoptotic process (Barnes et al., 2006). Alterations to *BRCA1*, responsible for aspects of DNA repair and activation of cell cycle checkpoint response, are another example of mutations giving rise to innate drug resistance. While *BRCA1* mutations are only present in 5-10% of breast cancers, decreased expression of the BRCA1 protein can confer a 1000-fold increase in resistance to paclitaxel (Quinn et al., 2003; Longley and Johnston, 2005). The same study simultaneously found that increased BRCA1 can also induce resistance to chemotherapeutics which generate double strand DNA breaks such as etoposide (Quinn et al., 2003). This highlights the intricate nature of MDR and how resistance to one agent may be result in sensitivity to another.

Related to changes in apoptotic signalling are the potential changes to proliferative signalling. HER2, for instance, is associated with advanced breast cancers as previously discussed due to increased proliferative signalling. HER2⁺ cancer cells have been shown to be resistant to cisplatin, doxorubicin, paclitaxel, and 5-fluoruracil (Pegram et al., 1997; Chen et al., 2000; Longley and Johnston, 2005). Given both the innate differences in resistance based on breast cancer subtype and the development of acquired resistance in response to selective pressures, continued development of new anticancer agents is needed to overcome these resistances when they occur.

1.4.6: The Role of Prostaglandins in Breast Cancer

An additional signalling pathway involved in the progression of breast cancer is comprised of the prostaglandins and their precursors. A summary of this pathway is provided in **Figure 5.1** at the conclusion of this work. While COX2 was previously discussed in **section 1.4.5.6** for its involvement in ubiquitination of survivin, the primary role of COX2 is the metabolism of arachidonic acid (AA) to prostaglandins.

AA itself is derived from two cellular sources: conversion of cellular membrane phospholipids by phospholipase A2 (PLA2) or through *de novo* lipogenesis (Vessby et al., 2002; Pavithra et al., 2018). PLA2 functions to catalyze the deacylation of glycerophospholipids, producing free fatty acids which can be used as signalling molecules by the cell (Qu et al., 2018). Increased PLA2 activity has been found in patients with breast cancer, and as such PLA2 has been suggested as a potential biomarker for breast cancer diagnosis (Qu et al., 2018). Alternative to reclaiming fatty acids from the lipid membrane, *de novo* lipogenesis is the process by which excess carbohydrates are converted to new fatty acids by the cell (Ameer et al., 2014). Human breast cancers are known to have an increased capacity for *de novo* lipogenesis and inhibitors of fatty acid synthesis like cerulenin or C75 have been demonstrated to suppress breast cancer cell growth and induce apoptosis *in vitro* and *in vivo* (Pizer et al., 2000; Ameer et al., 2014). The primary product of *de novo* lipogenesis is palmitic acid, from which more complex fatty acids are subsequently synthesized (Ameer et al., 2014; Pavithra et al., 2018). A variety of desaturase and elongase enzymes act on the synthesized fatty acids to produce more complex fatty acids used in cellular signalling, with the most biologically important being those with a n-6 or n-3 desaturation (Pavithra et al., 2018). AA is one such n-6 fatty acid which is involved in the production of active metabolites through the cyclooxygenase, lipoxygenase, and cytochrome P450 pathways (Borin et al., 2017). It is through the cyclooxygenase pathway that the prostaglandins are produced.

There are two cyclooxygenase isoforms found in humans, cyclooxygenase-1 (COX1) and COX2, which both convert AA to prostaglandin G₂ which is again converted by either cyclooxygenase isoform to prostaglandin H₂ (Simmons et al., 2004; Majumder

et al., 2018). While most somatic cells constitutively express COX1, only the stomach, kidney, nerve, reproductive, and immune cells routinely express COX2 (Majumder et al., 2018; Hashemi Goradel et al., 2019). Prostaglandin H₂ is then converted to prostaglandin E₂ (PGE₂) by prostaglandin E synthase (Ching et al., 2020). PGE₂ is of particular importance as it is the most abundant prostaglandin in cancer cells and cyclooxygenase activity is the rate-limiting step in its synthesis (Chandrasekharan and Simmons, 2004; Ching et al., 2020). Despite low basal expression in healthy breast epithelium, becoming increased only during breast remodelling at puberty and during pregnancy, COX2 is highly expressed in breast cancer where it is associated with poor clinical outcome (Simmons et al., 2004; Fornetti et al., 2014; Majumder et al., 2018; Ching et al., 2020). Accordingly, research on COX2 inhibitors has demonstrated that nonselective inhibitors of both cyclooxygenase isoforms, such as indomethacin or flurbiprofen, can reduce the frequency of mammary tumourigenesis in rats exposed to carcinogens (McCormick and Moon, 1983; McCormick et al., 1985; Regulski et al., 2016). Selective inhibitors of COX2, such as celecoxib, have been shown to be more effective at preventing cancer development than nonselective inhibitors (Harris et al., 2000; Regulski et al., 2016). Combining COX2 inhibitors with other chemotherapeutics has been of recent interest as a means to reduce adverse effects, reduce chemoresistance, and increase cancer cell sensitivity to treatment (Li et al., 2020). For instance, a combination of doxorubicin and celecoxib has been shown to overcome drug resistance in MDR breast cancer cells (Zhang et al., 2019; Li et al., 2020). By inhibiting COX2, PGE₂ production is reduced and signalling *via* this pathway can be inhibited.

Normally, PGE₂ is an inducible signalling molecule which regulates fever, kidney function, pain, mucosal integrity, blood vessel homeostasis, and inflammation in different tissues throughout the body (Finetti et al., 2020). In breast cancer, PGE₂ overexpression has been shown to increase tumour cell proliferation, survival, angiogenesis, and metastasis (Finetti et al., 2020). Once produced in a cancer cell, PGE₂ must be transported out of the cell for it to exert an autocrine or paracrine effect through binding to cell surface receptors (Reader et al., 2011). Transport of PGE₂ out of the cell occurs *via* multidrug resistance-associated protein 4 (MRP4; ABCC4), another member of the ABC transporter family (Russel et al., 2008; Reader et al., 2011). TNBC cells have been shown

to overexpress MRP4, leading to increased extracellular PGE₂ and an associated increased availability for interaction with cell membrane receptors (Kochel et al., 2016; Kochel et al., 2017). Correlated to increased MRP4 expression, TNBC cells have also been observed to express low levels of prostaglandin transporter (PGT) and 15-prostaglandin dehydrogenase (15-PGDH) which are involved in the metabolism of PGE₂ (Kochel et al., 2016; Kochel et al., 2017). PGT actively transports PGE₂ into the cell where it can be oxidized by 15-PGDH to 15-keto-prostaglandin E₂, an inactive metabolite incapable of binding PGE₂ receptors (Kochel et al., 2016; Kochel et al., 2017). Decreased expression of 15-PGDH has been associated with increased tumourigenesis and, for this reason, 15-PGDH has been categorized as a tumour suppressor in several types of cancer, including breast (Tai, 2011; Kochel et al., 2016). If PGE₂ is not transported into the cell and metabolized it is free to interact with receptors on the cell surface.

Once produced and released, PGE₂ can interact with a group of G-protein coupled receptors known as prostaglandin E₂ receptors 1 through 4 which are responsible for the activation of intracellular signalling cascades (Sugimoto and Narumiya, 2007). Prostaglandin E₂ receptor-1 (EP1), prostaglandin E₂ receptor-2 (EP2), and prostaglandin E₂ receptor-4 (EP4) are commonly upregulated in breast cancer cells as compared to normal breast tissue while prostaglandin E₂ receptor-3 (EP3) is typically downregulated in breast cancer (Reader et al., 2011). The roles of EP1 and EP3 are less well characterized than those of EP2 or EP4. EP1 stimulation has been associated with increased angiogenesis in breast cancer cells *in vitro*, while in murine models of breast cancer EP1 stimulation functions as a suppressor of metastatic potential (Timoshenko et al., 2006; Ma et al., 2010; Reader et al., 2011). EP3 has been reported as inhibitory to adenylate cyclase, decreasing cAMP production and associated signalling (Woodward et al., 2011; O'Callaghan and Houston, 2015). EP2 and EP4 have been of more interest as possible therapeutic targets in the treatment of breast cancer (Reader et al., 2011; O'Callaghan and Houston, 2015; Majumder et al., 2018; Ching et al., 2020; Finetti et al., 2020; Walker et al., 2021). Both EP2 and EP4 activate adenylate cyclase when stimulated, resulting in cAMP production and subsequent intracellular signalling (O'Callaghan and Houston, 2015; Majumder et al., 2018). EP4 can additionally activate PI3K/AKT signalling to initiate cellular responses (O'Callaghan and Houston, 2015;

Majumder et al., 2018). EP2 stimulation has been associated with angiogenesis, suppression of the immune response, and transition to a cancer stem cell-like phenotype (Finetti et al., 2020; Walker et al., 2021). EP4 stimulation has additionally been associated with tumour cell migration and metastasis (Finetti et al., 2020). Due to the tumorigenic effects of PGE₂ as mediated through the EP2 and EP4 receptors, small molecule inhibitors of those receptors have attracted interest as possible new anticancer therapies. Antagonism of EP4 with either AH23848 or ONO-AE3-208, for instance, reduced breast cancer metastasis in murine models (Ma et al., 2006). ONO-4578, a potent EP4 antagonist, has recently been shown to have immunosuppressive activity as monotherapy and in combination with nivolumab in a first-in-human study in patients with metastatic tumours (Iwasa et al., 2023). The continued development of new EP4 antagonists is an ongoing area of research, with new candidate molecules showing high specificity and increased potency in preclinical cancer models (Das et al., 2023). Research into this group of PGE₂ receptor inhibitors further illustrates the importance of continued development of new compounds to increase the options available for the treatment of breast cancers.

1.5: Natural Products in Drug Discovery and Development

Many of the medications in common use today were discovered or derived from natural sources. Plants, animals, fungi, and bacteria have all been sources of naturally occurring molecules used to treat disease. The oldest records of plants being used to treat illness come from Mesopotamian clay tablets dated to 2600 BCE and describe preparations of *Cedrus sp.* (cedar), *Cupressus sempervirens* (cypress), *Glycyrrhiza glabra* (licorice), *Commiphora sp.* (myrrh), and *Papaver somniferum* (poppy) used to treat a range of ailments (Cragg and Newman, 2005; Dias et al., 2012). Egyptian pharmaceutical records in the Ebers Papyrus (dating from 1500 BCE), early Chinese Materia Medica (from 1100 BCE), and Indian Ayurvedic medicine (from 1000 BCE) all contain descriptions of plants being used to treat illness in the ancient world (Cragg and Newman, 2005). Likewise, the ancient Greeks and Romans collected extensive knowledge on the use of medicinal plants used to compound drugs (Cragg and Newman, 2005).

Preparations like these take advantage of naturally occurring molecules and form the basis of many traditional medicines and remedies still used.

In 1985 the World Health Organization estimated that 80% of the world population relied on traditional medicines from plant sources as their primary method of fighting illness (Farnsworth et al., 1985; Cragg and Newman, 2005). Today, natural health products and herbal medicines are still commonly used by Canadians, and people throughout the world, as a supplement to what we now think of as modern pharmaceutical therapies (Rojas et al., 2022). The modern pharmaceuticals are themselves, however, often discovered or derived from natural sources. An analysis of all new medications approved by the United States Food and Drug Administration between 1981 and 2019 estimated that 33.6% of small molecule drugs developed in that time were derived from natural products (Newman and Cragg, 2020). Many of those traditional medicines have transitioned to modern pharmaceutical forms.

Perhaps the most famous example of this movement from natural product to pharmaceutical preparation is acetylsalicylic acid (**Figure 1.5**). Willow (*Salix alba*) bark was used by the ancient Sumerians and Egyptians as an analgesic and antipyretic (Desborough and Keeling, 2017). The active ingredient in willow bark was identified in 1828 as Salicin, and modified to produce the more efficacious salicylic acid in 1838 (Piria, 1838; Dias et al., 2012; Desborough and Keeling, 2017). In 1852 salicylic acid was further modified by the addition of an acetyl group, a step further refined by the Bayer company, to produce acetylsalicylic acid which is still in common use (Gerhardt, 1853; Desborough and Keeling, 2017). A similar course was followed in the development of a range of analgesics originating from the poppy, resulting in the subsequent production of morphine, codeine, and related opioids (Dias et al., 2012; Krishnamurti and Rao, 2016).

While the preceding examples have focused on medications derived from plant sources, fungi and bacteria have been of particular interest as a source for the development of antibiotics. A popular example is the discovery of penicillin by Alexander Fleming in 1928 from mold (*Penicillium sp.*) found growing in an agar plate in the absence of bacteria (Fleming, 1929; Gaynes, 2017). The antibiotic streptomycin was identified in 1944, produced by *Streptomyces griseus*, and expanded the action of antibiotics to include gram-negative as well as gram-positive bacteria (Schatz et al., 1944;

Woodruff, 2014). In 1947 chloramphenicol was identified as an antibiotic produced by *Streptomyces venezuelae* (Ehrlich et al., 1947). *Streptomyces sp.* were the source of 70-80% of all antimicrobials isolated in the 1950s and 1960s, mainly showing efficacy against bacteria and fungi (Bérdy, 2005). In the same time period the first anthracyclines, daunorubicin and doxorubicin, were described as products of *Streptomyces peucetius* and soon came to be used as chemotherapeutics against cancer (Camerino and Palamidessi, 1960; Arcamone et al., 1969; Mattioli et al., 2023).

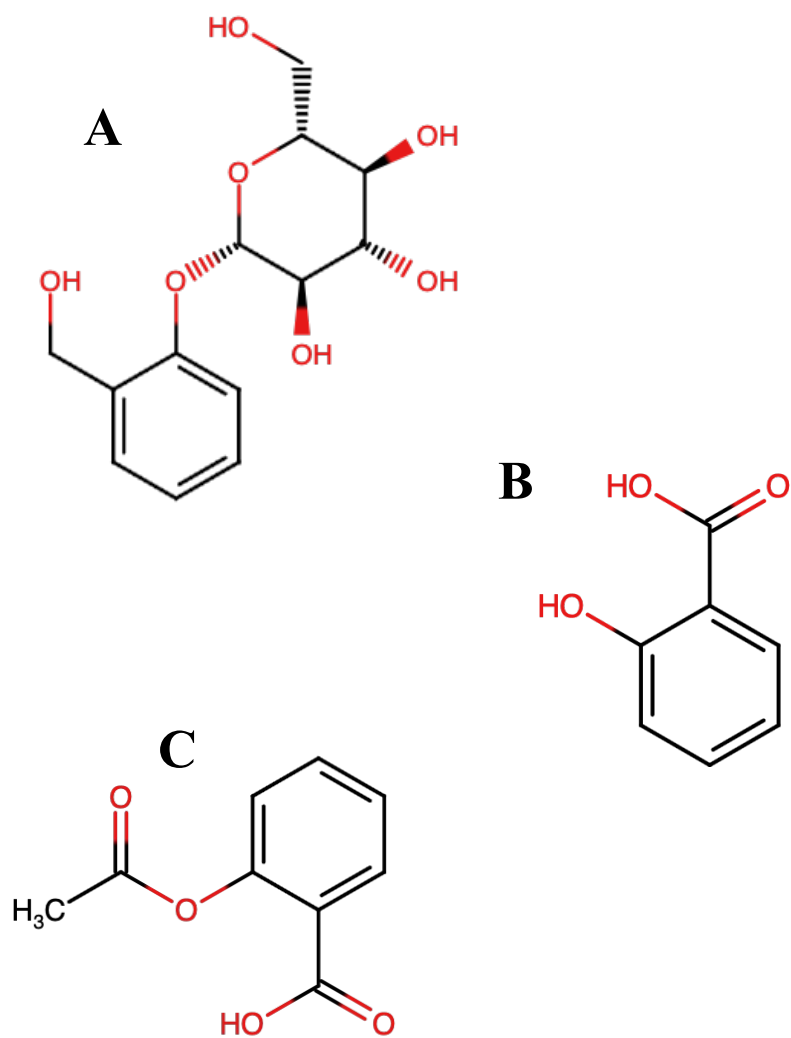


Figure 1.5: Development of Natural Products to Pharmaceutical Agents

Molecular structure of (A) salicin, a compound originally extracted from willow bark (*Salix sp.*) and subsequently developed into (B) salicylic acid and then (C) acetylsalicylic acid to improve pharmaceutical characteristics.

1.5.1: Natural Products in the Treatment of Cancer

The search for drugs which could be used in the treatment of cancer began in the early 1900s but little progress was made until the 1940s (DeVita and Chu, 2008). Early clues came from the observation that sulfur mustards, used as war gasses in the first and second world wars, caused the death of white blood cells and bone marrow in those who had been fatally exposed (Krumbhaar and Krumbhaar, 1919; DeVita and Chu, 2008). This information was successfully applied to the treatment of leukemias with nitrogen mustards, although the effect was brief and recurrence was common (Gilman, 1946; Goodman et al., 1946; DeVita and Chu, 2008).

From the early trials with nitrogen mustards in 1946 to 2019, 321 anticancer drugs have been approved by the United States Food and Drug Administration and 101 of which (31.5%) were discovered as or derived from natural products (Newman and Cragg, 2020). A few representative compounds derived from separate sources are paclitaxel, vincristine, etoposide, and doxorubicin. Paclitaxel, one of the most widely used drugs to treat breast cancer, was isolated from the bark of the Pacific yew (*Taxus brevifolia*) by the United States Department of Agriculture and National Cancer Institute (Wani et al., 1971; Cragg, 1998). It was shown to have a unique mechanism of action in stabilizing microtubules and is representative of the taxanes (Manfredi and Horwitz, 1984; Cragg, 1998). The vinca alkaloids which, in contrast to taxanes, destabilize microtubules were isolated from the Madagascar periwinkle (*Catharanthus roseus*) and are represented by vincristine (Noble et al., 1958; Noble, 1990; Moudi et al., 2013). Etoposide is a representative of the epipodophyllotoxins, derived from naturally occurring toxins produced by the American mandrake (*Podophyllum peltatum*) and modified to allow it to act as a potent TOP2 inhibitor (Meresse et al., 2004). Finally, doxorubicin, as previously discussed, represents the anthracyclines which are derived from antimicrobial molecules produced by *Streptomyces peucetius* and also act to inhibit TOP2.

1.6: Jadomycins: Source, Structure, and Diversity

Jadomycins are a group of natural compounds first described in 1991, isolated from *Streptomyces venezuelae* grown under stress conditions (Ayer et al., 1991; de Koning et al., 2020; Bonitto et al., 2021). The genus *Streptomyces* represents a group of gram-positive members of the order *Actinomycetales*, within the class *Actinobacteria* (Anderson and Wellington, 2001). The species *Streptomyces venezuelae* was originally known simply as Burkholder sample number A26 and has since been identified by the International *Streptomyces* Project (ISP) as strain number 5320, with alternative registrations in the Culture Bureau of Park, Davis and Company (PD) as strain number 04745 and with the American Tissue Culture Collection (ATCC) as number 10712 (Ehrlich et al., 1948; Shirling and Gottlieb, 1969). This species was initially isolated from a soil sample collected near Caracas, Venezuela, hence the name (Ehrlich et al., 1947; Ehrlich et al., 1948). *Streptomyces venezuelae* is morphologically described as forming grey or tan colonies prior to sporulation (**Figure 1.6A**), with smooth spores appearing grey (**Figure 1.6B, C**) in mass and individually measuring 0.4-0.8 μm in diameter and 0.7-1.6 μm in length (Ehrlich et al., 1948; Shirling and Gottlieb, 1969). When mature, vegetative hyphae are branched and approximately 150 μm in length while aerial hyphae are generally unbranched, straight or slightly curved (**Figure 1.6D**), and form chains of more than 50 spores (Ehrlich et al., 1948; Shirling and Gottlieb, 1969). A diagram of the typical *Streptomyces* life cycle is described in **Figure 1.6E** (Jones and Elliot, 2017). Species within the genus *Streptomyces* produce secondary metabolites, which are often species specific, that are used to compete with other microorganisms in their environment through inhibitory or toxic effects (Procópio et al., 2012).

Initial interest in *Streptomyces venezuelae* arose due to the discovery of chloramphenicol (**Figure 1.7A**), an antibiotic with a broad spectrum of activity (Ehrlich et al., 1947; Smadel and Jackson, 1947). By altering the culture medium and growth conditions a second group of compounds called jadomycins (a partial group of representative jadomycins are depicted in **Figure 1.7B-E**), so named after one of the co-discoverers Janice Doull, were isolated in the search for novel antibiotics (Ayer et al., 1991). The first jadomycins described, jadomycin A, was produced instead of

chloramphenicol when glucose in the growth medium was replaced with galactose and the incubation temperature raised from 28 °C to 37 °C (Ayer et al., 1991). Jadomycin B was subsequently produced following either a brief heat shock (at 42 °C), exposure to ethanol, or phage infection (Doull et al., 1993; Doull et al., 1994).

As a group, jadomycins are pigmented, angucycline-derived antibiotics which contain a pentacyclic 8*H*-benz[*b*]oxazolo[3,2-*f*]-phentathridine backbone (each of the five rings labeled A-E in **Figure 1.7B**) including a dihydropyridine (B) and oxazolone (E) ring (Ayer et al., 1991; Doull et al., 1993; Han et al., 1994). Jadomycins belong to a larger group of naturally occurring products known as angucyclines, but uniquely incorporate a nitrogen atom in ring B (Rohr and Thiericke, 1992; de Koning et al., 2020). The differentiating feature between jadomycin A and B is the addition of a 2,6-dideoxy-L-digitoxose, attached *via* a phenol to ring D (Doull et al., 1993; Doull et al., 1994). When the first jadomycins were originally isolated, *Streptomyces venezuelae* cultures were grown in a medium with the amino acid L-isoleucine as the only nitrogen source (Doull et al., 1993). As jadomycins differed from other angucyclines due to the nitrogen shared between rings B and E, it was concluded that L-isoleucine was being incorporated to form ring E with various mechanisms proposed for this process (Doull et al., 1994; Yang et al., 1996; Rix et al., 2004; Syvitski et al., 2006). Early experiments replacing the nitrogen source with each of the other 19 naturally occurring amino acids resulted in the production of a variety of different coloured products assumed to be jadomycin analogues (Doull et al., 1994).

Regardless of the mechanism underlying the incorporation of amino acids, an extensive library of over 70 jadomycin analogues have been developed through the selective use of various naturally occurring and non-naturally occurring amino acids or subsequent synthetic derivation (Rix et al., 2004; Jakeman et al., 2005a; Jakeman et al., 2005b; Borissow et al., 2007; Jakeman et al., 2009b; Dupuis et al., 2011; Dupuis et al., 2012; Fan et al., 2012; Martinez-Farina and Jakeman, 2015; Martinez-Farina et al., 2015b; Robertson et al., 2015; Forget et al., 2017; Forget et al., 2018a; Forget et al., 2018b; MacLeod et al., 2018a; MacLeod et al., 2018b; Robertson et al., 2018). This catalogue began with the characterization of jadomycins produced when the 20 naturally occurring L-amino acids were used as the lone nitrogen source in growth medium (Rix et

al., 2004; Jakeman et al., 2005a). These experiments also incorporated D-valine, D-isoleucine, *O*-methoxy-L-threonine, and *O*-methoxy-methylene-L-threonine into the jadomycin structure, proving that alternative nitrogen sources could be used as well (Jakeman et al., 2005a). The list of additional nitrogen sources used was quickly expanded (MacLeod et al., 2018a; de Koning et al., 2020; Bonitto et al., 2021). While the first two jadomycins, A and B, were named in the order of their discovery, subsequent jadomycin naming convention has been based on the incorporated group forming ring E (MacLeod et al., 2018a).

Originally, jadomycins could only be produced through bacterial fermentation, with gradual progress being made to optimize their production (Doull et al., 1994; Jakeman et al., 2006). Since 2010, several groups have sought to synthesize jadomycins without the need for bacterial fermentation, thus, opening the possibility to produce the large quantities needed for therapeutic use and allowing for the discovery of even more novel jadomycin analogues (Akagi et al., 2010; Shan et al., 2010; Tajima et al., 2012; Yang and Yu, 2013; Akagi et al., 2022; Iwasaki et al., 2023). Recently, genetic manipulation of *Streptomyces venezuelae* has been used as a means of optimizing jadomycin B production, resulting in increased yield (Qiu et al., 2024). The generation of so many different jadomycin analogues led to the question of differing biological activity. As such, the jadomycins were tested for their antimicrobial effect to determine if new antibiotics could be discovered within this chemically versatile compound.

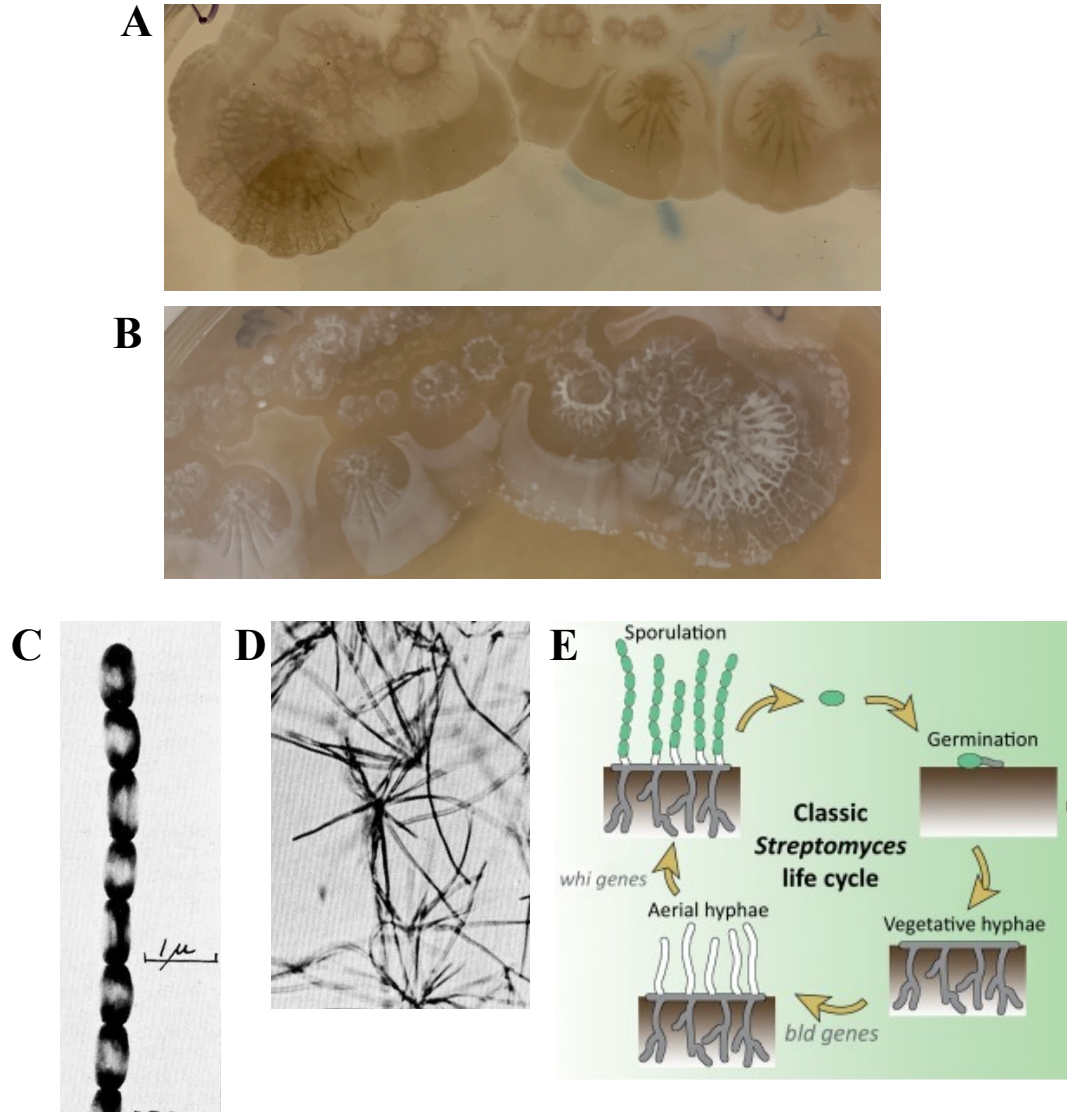


Figure 1.6: Morphology and Life Cycle of *Streptomyces venezuelae*

S. venezuelae typically forms (A) grey or tan colonies (here on MYM agar) which produce (B) grey spores upon maturation. The spores (C) appear smooth under microscopy, with (D) aerial hyphae forming spore chains. The classical *Streptomyces* life cycle (E) involves germination, growth of vegetative and aerial hyphae, and sporulation. Figure adapted, with permission and under creative commons fair use (Appendices A.7 and A.9), from Shirling and Gottlieb (1969) and Jones and Elliot (2017)

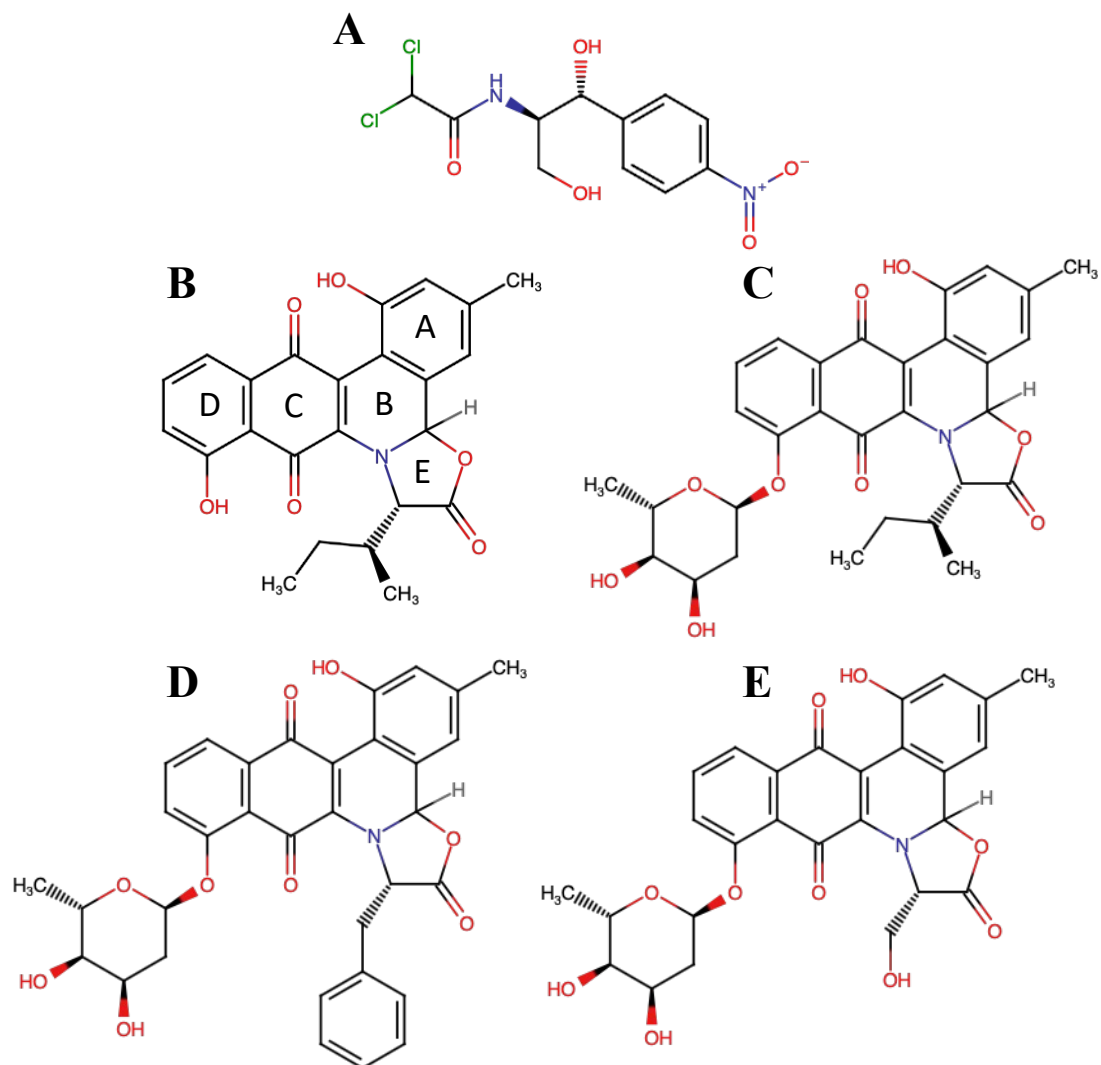


Figure 1.7: Molecular Structures of Example Jadomycin Analogues

Molecular structure of (A) chloramphenicol, (B) jadomycin A (with labeled rings), (C) jadomycin B, (D) jadomycin F, and (E) jadomycin S.

1.6.1: Antimicrobial Activity of Jadomycins

Initial screening of jadomycin A and jadomycin B for antimicrobial activity demonstrated inhibitory activity against both gram-positive and gram-negative bacteria, however, only jadomycin B inhibited the growth of yeast (Doull et al., 1994; Rix et al., 2004). As jadomycin A and B differ only in the presence or absence of a sugar attached to ring D, this was the first evidence that structural differences between the jadomycins could lead to functional differences in activity (Wang et al., 2002; Rix et al., 2004).

The first comprehensive report on antimicrobial activity demonstrated that jadomycins inhibited growth of multiple strains of *Staphylococcus aureus* (including methicillin-resistant *S. aureus*; MRSA), *Staphylococcus epidermidis*, *Pseudomonas aeruginosa*, *Enterococcus faecalis*, and *Bacillus subtilis* (Jakeman et al., 2009a). All jadomycins tested generally showed greater inhibitory effect against gram-positive bacteria. Jadomycin G and jadomycin N were the least active analogues tested in that study, noteworthy in that jadomycin G does not contain an amino acid substituent extending from the oxazolone ring E and jadomycin N instead incorporates a unique 6 member ring with 2 nitrogen atoms rather than the 5 member oxazolone (Borissow et al., 2007; Jakeman et al., 2009a). This observation represents early evidence that the substituent group on the oxazolone ring is responsible for biological activity. The most active analogues against MRSA were jadomycin B, jadomycin L (incorporating L-leucine), and jadomycin F (incorporating L-phenylalanine) with minimum inhibitory concentrations of less than 1 µg/mL (Jakeman et al., 2009a). In comparison, erythromycin was shown to have a minimum inhibitory concentration of greater than 126 µg/mL against MRSA (Jakeman et al., 2009a). Other jadomycins have shown similar activity against MRSA, but as a group their antibacterial activity has been moderate (Dupuis et al., 2011; Dupuis et al., 2012; Forget et al., 2017; Forget et al., 2018b; Robertson et al., 2018; de Koning et al., 2020).

1.6.2: Anticancer Effects of Jadomycins *in vitro*

Concurrent to the search for antimicrobial activity, jadomycins have also been tested for anticancer activity. Other angucyclines were previously known to possess antitumour activity and jadomycins are closely related to the anthracyclines, two factors which provided the initial rationale for screening for anticancer activity (Rohr and Thiericke, 1992; Krohn and Rohr, 1997; Zheng et al., 2005). Early experiments, such as the screening of jadomycins L, DNV, DNL, and 7 additional jadomycins with triazole moieties against 60 cancer cell lines by the National Cancer Institute, indicated that jadomycins had potential for further development for the treatment of cancer (Jakeman et al., 2009b; Dupuis et al., 2011; Dupuis et al., 2012). All jadomycins screened showed similar potencies against almost all cancer cells tested, with the as yet unexplained exception of leukemia cells in which jadomycins were less potent. Experiments like these prompted more detailed investigation of the effects of jadomycins on specific cell lines. A comprehensive list of reported half maximal inhibitory concentrations (IC₅₀s), the concentration at which cancer cell growth is inhibited by 50%, for jadomycin analogues which have been screened for anticancer activity is provided in **Tables 1.11** and **1.12**. The following sections describe the current knowledge, as of the time of writing, regarding the effects of jadomycins on cancer cells *in vitro*.

Table 1.11: Jadomycin IC₅₀ Values Reported in Breast Cancer Cell Lines

Comprehensive list of jadomycin IC₅₀ values reported in the literature across all breast cancer cell lines tested. Table adapted, with permission (**Appendices A.10**), from Bonitto et al. (2021). Continued on next page.

Study	Cell Type	Cell Line	Exposure Time (h)	Assay Used	Growth medium	IC ₅₀ (µM)													
						Pala	A	Abu	B	DM	DNV	DT	DV	F	G	H	Hse	L	M
Borissow <i>et al.</i> (2007)	Breast	T-47D	48	MITT	not reported	23.11	-	-	9.92	7.80	-	2.57	6.42	8.84	8.27	9.82	-	-	6.70
Fu <i>et al.</i> (2008) & Si (2020)	Breast	MCF-7	48	MITT	RPMI 1640 or MEM	-	-	-	27.2	-	-	-	-	-	-	-	-	-	-
Fan <i>et al.</i> (2012)	Breast	MCF-7	72	SRB	not reported	-	-	2.7	2.8	-	-	-	-	-	-	-	-	66.8	1.4
Issa <i>et al.</i> (2014)	Breast	MCF-7	72	MITT	DMEM	-	-	-	4.4	-	1.3	-	-	0.9	-	-	-	-	3.7
Issa <i>et al.</i> (2014)	Breast	MCF-7	48	LDH	DMEM	-	-	-	4.3	-	4.7	-	-	4.4	-	-	-	-	6.9
Hall <i>et al.</i> (2015)	Breast	MCF-7	72	MITT	DMEM	-	-	-	2.58	-	-	-	-	3.59	-	-	-	-	-
Iwasaki <i>et al.</i> (2023)	Breast	MCF-7	48	WST-8	DMEM	-	3.44	-	7.98	-	-	-	-	-	-	-	-	-	-
Issa <i>et al.</i> (2014)	Breast	MCF-7-TXL	72	MITT	DMEM	-	-	-	5.8	-	2.0	-	-	3.1	-	-	-	-	5.5
Issa <i>et al.</i> (2014)	Breast	MCF-7-TXL	48	LDH	DMEM	-	-	-	11.8	-	13.3	-	-	15.6	-	-	-	-	16.4
Issa <i>et al.</i> (2014)	Breast	MCF-7-ETP	72	MITT	DMEM	-	-	-	8.0	-	2.2	-	-	3.2	-	-	-	-	6.8
Issa <i>et al.</i> (2014)	Breast	MCF-7-ETP	48	LDH	DMEM	-	-	-	13.9	-	11.3	-	-	10.9	-	-	-	-	17.8
Issa <i>et al.</i> (2014)	Breast	MCF-7-MITX	72	MITT	DMEM	-	-	-	9.9	-	4.2	-	-	3.6	-	-	-	-	8.3
Issa <i>et al.</i> (2014)	Breast	MCF-7-MITX	48	LDH	DMEM	-	-	-	13.7	-	12.3	-	-	11.4	-	-	-	-	12.6
Hall <i>et al.</i> (2015)	Breast	BT474	72	MITT	DMEM	-	-	-	4.16	-	-	-	-	5.05	-	-	-	-	-
Hall <i>et al.</i> (2015)	Breast	SKBR3	72	MITT	DMEM	-	-	-	3.82	-	-	-	-	4.70	-	-	-	-	-
Hall <i>et al.</i> (2015)	Breast	231-CON	72	MITT	DMEM	-	-	-	1.76	-	-	-	-	3.25	-	-	-	-	-
Hall <i>et al.</i> (2017) & Goralski (2020)	Breast	231-CON	72	MITT	DMEM	-	-	-	2.77	-	-	-	-	2.97	-	-	-	-	-
Hall <i>et al.</i> (2017) & Goralski (2020)	Breast	231-TXL	72	MITT	DMEM	-	-	-	2.49	-	-	-	-	3.17	-	-	-	-	-
McKeown <i>et al.</i> (2022)	Mammary (mouse)	4T1	72	MITT	DMEM	-	-	-	10.0	-	-	-	-	-	-	-	-	-	-
McKeown <i>et al.</i> (2022)	Mammary (mouse)	4T1-TXL	72	MITT	DMEM	-	-	-	9.7	-	-	-	-	-	-	-	-	-	-

Table 1.11 (continued)

Study	Cell Type	Cell Line	Exposure Time (h)	Assay Used	Growth medium	IC ₅₀ (µM)												
						N	Nle	Orn	R-Phe	S	S-Phe/SPhG	T	T-aglycon	V	W	Y	ILEY/S1080 dalomycin T	
Borissow <i>et al.</i> (2007)	Breast	T-47D	48	MTT	not reported	8.16	-	-	5.16	2.90	7.57	4.04	-	7.44	9.03	31.07	8.47	3.19
Fu <i>et al.</i> (2008) & Si (2020)	Breast	MCF-7	48	MTT	RPMI 1640 or MEM	-	-	-	-	23.3	-	29.4	-	-	-	-	-	-
Fan <i>et al.</i> (2012)	Breast	MCF-7	72	SRB	not reported	-	8.5	4.5	-	4.4	-	0.97	-	1.9	-	-	-	-
Issa <i>et al.</i> (2014)	Breast	MCF-7	72	MTT	DMEM	-	-	-	-	1.9	2.8	2.5	-	-	19.3	-	-	-
Issa <i>et al.</i> (2014)	Breast	MCF-7	48	LDH	DMEM	-	-	-	-	4.4	5.7	4.8	-	-	42.3	-	-	-
Hall <i>et al.</i> (2015)	Breast	MCF-7	72	MTT	DMEM	-	-	-	-	3.38	-	-	-	-	-	-	-	-
Iwasaki <i>et al.</i> (2023)	Breast	MCF-7	48	WST-8	DMEM	-	-	-	-	-	-	3.53	0.75	-	-	-	-	-
Issa <i>et al.</i> (2014)	Breast	MCF-7-TXL	72	MTT	DMEM	-	-	-	-	3.6	5.2	6.1	-	-	73.3	-	-	-
Issa <i>et al.</i> (2014)	Breast	MCF-7-TXL	48	LDH	DMEM	-	-	-	-	12.0	12.3	12.3	-	-	88.9	-	-	-
Issa <i>et al.</i> (2014)	Breast	MCF-7-ETP	72	MTT	DMEM	-	-	-	-	3.6	3.5	4.8	-	-	50.2	-	-	-
Issa <i>et al.</i> (2014)	Breast	MCF-7-ETP	48	LDH	DMEM	-	-	-	-	10.7	13.3	11.4	-	-	67.0	-	-	-
Issa <i>et al.</i> (2014)	Breast	MCF-7-MITX	72	MTT	DMEM	-	-	-	-	5.2	6.5	5.6	-	-	75.1	-	-	-
Issa <i>et al.</i> (2014)	Breast	MCF-7-MITX	48	LDH	DMEM	-	-	-	-	11.3	11.4	14.8	-	-	94.2	-	-	-
Hall <i>et al.</i> (2015)	Breast	BT474	72	MTT	DMEM	-	-	-	-	3.09	-	-	-	-	-	-	-	-
Hall <i>et al.</i> (2015)	Breast	SKBR3	72	MTT	DMEM	-	-	-	-	3.08	-	-	-	-	-	-	-	-
Hall <i>et al.</i> (2015)	Breast	231-CON	72	MTT	DMEM	-	-	-	-	2.79	-	-	-	-	-	-	-	-
Hall <i>et al.</i> (2017) & Goralski (2020)	Breast	231-CON	72	MTT	DMEM	-	-	-	-	2.64	-	-	-	-	-	-	-	-
Hall <i>et al.</i> (2017) & Goralski (2020)	Breast	231-TXL	72	MTT	DMEM	-	-	-	-	2.77	-	-	-	-	-	-	-	-
McKeown <i>et al.</i> (2022)	Mammary (mouse)	4T1	72	MTT	DMEM	-	-	-	-	-	-	-	-	-	-	-	-	-
McKeown <i>et al.</i> (2022)	Mammary (mouse)	4T1-TXL	72	MTT	DMEM	-	-	-	-	-	-	-	-	-	-	-	-	-

Table 1.12: Jadomycin IC₅₀ Values Reported in All Other Cancer Cell Lines

Comprehensive list of jadomycin IC₅₀ values reported in the literature across all other cancer cell lines tested. Table adapted, with permission (Appendices A.10), from Bonitto et al. (2021). Continued on next page.

Study	Cell Type	Cell Line	Exposure Time (h)	Assay Used	Growth medium	IC ₅₀ (µM)													
						βala	A	Abu	Ala	B	DM	DT	DV	F	G	H	Hse	L	M
Iwasaki et al. (2023)	Brain	A172	48	WST-8	RPMI 1640	-	3.10	-	4.20	-	-	-	-	-	-	-	-	-	-
Fu et al. (2008) & Si (2020)	Cervix	HeLa	48	MTT	RPMI 1640 or MEM	-	-	-	-	18.2	-	-	-	-	-	-	-	-	-
Fan et al. (2012)	Colon	HCT116	72	SRB	not reported	-	-	8.3	-	3.8	-	-	-	-	-	-	-	56.8	3.8
Iwasaki et al. (2023)	Colon	HCT116	48	WST-8	RPMI 1640	-	3.64	-	-	3.77	-	-	-	-	-	-	-	-	-
Fan et al. (2012)	Epithelium	HMEC	72	SRB	not reported	-	-	3.0	-	2.3	-	-	-	-	-	-	-	62.9	2.1
Zheng et al. (2005)	Hepatic	HepG2	24	MTT	not reported	-	-	-	100.0	10.8	-	-	-	-	49.0	-	-	-	-
Iwasaki et al. (2023)	Hepatic	HepG2	48	WST-8	DMEM	-	1.72	-	-	6.21	-	-	-	-	-	-	-	-	-
Zheng et al. (2005)	Lung	H460	24	MTT	not reported	-	-	-	30.7	21.8	-	-	-	12.4	-	-	-	-	-
Fu et al. (2008) & Si (2020)	Lung	A549	48	MTT	RPMI 1640 or MEM	-	-	-	-	11.3	-	-	-	-	-	-	-	-	-
Iwasaki et al. (2023)	Lung	A549	48	WST-8	MEM	-	2.39	-	-	6.81	-	-	-	-	-	-	-	-	-
Borissow et al. (2007)	Melanoma	MDA-MB-435	48	MTT	not reported	10.66	-	-	-	6.89	2.87	1.15	3.24	6.11	3.35	20.99	-	-	3.57
Zheng et al. (2005)	Myeloma	IM-9	24	MTS	not reported	-	-	-	40.0	8.5	-	-	-	29.0	-	-	-	-	-
Zheng et al. (2005)	Myeloma	IM-9/Bcl-2	24	MTS	not reported	-	-	-	>100	>100	-	-	-	>100	-	-	-	-	-
Iwasaki et al. (2023)	Pancreas	KP-3L	48	WST-8	RPMI 1640	-	2.19	-	-	5.06	-	-	-	-	-	-	-	-	-
Iwasaki et al. (2023)	Prostate	PC3	48	WST-8	RPMI 1640	-	1.64	-	-	2.07	-	-	-	-	-	-	-	-	-
Iwasaki et al. (2023)	Stomach	MKN74	48	WST-8	RPMI 1640	-	2.58	-	-	3.91	-	-	-	-	-	-	-	-	-

Table 1.12 (continued)

Study	Cell Type	Cell Line	Exposure Time (h)	Assay Used	Growth medium	IC ₅₀ (µM)																	
						N	Nle	Om	R-Phe	S	S-Phe/SPhG	T	T-aglycon	V	W	Y	ILEY/S1080	dalomycin	T				
Iwasaki <i>et al.</i> (2023)	Brain	A172	48	WST-8	RPMI 1640	-	-	-	-	-	-	1.96	0.92	-	-	-	-	-	-	-	-	-	-
Fu <i>et al.</i> (2008) & Si (2020)	Cervix	HeLa	48	MTT	RPMI 1640 or MEM	-	-	-	-	24.5	-	26.7	-	-	-	-	-	-	-	-	-	-	-
Fan <i>et al.</i> (2012)	Colon	HCT116	72	SRB	not reported	-	14.5	5.4	-	4.6	-	1.3	-	4.4	-	-	-	-	-	-	-	-	-
Iwasaki <i>et al.</i> (2023)	Colon	HCT116	48	WST-8	RPMI 1640	-	-	-	-	-	-	5.80	4.36	-	-	-	-	-	-	-	-	-	-
Fan <i>et al.</i> (2012)	Epithelium	HMEC	72	SRB	not reported	-	9.2	10.2	-	4.3	-	1.4	-	2.0	-	-	-	-	-	-	-	-	-
Zheng <i>et al.</i> (2005)	Hepatic	HepG2	24	MTT	not reported	-	-	-	-	9.8	-	27.0	-	27.0	-	-	-	-	-	-	-	-	-
Iwasaki <i>et al.</i> (2023)	Hepatic	HepG2	48	WST-8	DMEM	-	-	-	-	-	-	3.29	1.30	-	-	-	-	-	-	-	-	-	-
Zheng <i>et al.</i> (2005)	Lung	H460	24	MTT	not reported	-	-	-	-	19.2	-	19.6	-	-	-	-	-	-	-	-	-	-	-
Fu <i>et al.</i> (2008) & Si (2020)	Lung	A549	48	MTT	RPMI 1640 or MEM	-	-	-	-	38.4	-	47.8	-	-	-	-	-	-	-	-	-	-	-
Iwasaki <i>et al.</i> (2023)	Lung	A549	48	WST-8	MEM	-	-	-	-	-	-	5.16	0.72	-	-	-	-	-	-	-	-	-	-
Borissow <i>et al.</i> (2007)	Melanoma	MDA-MB-435	48	MTT	not reported	4.01	-	-	1.57	1.06	3.50	2.82	-	3.76	7.60	10.65	10.86	-	-	-	-	-	1.34
Zheng <i>et al.</i> (2005)	Myeloma	IM-9	24	MTS	not reported	-	-	-	-	6.3	-	9.1	-	8.2	-	-	-	-	-	-	-	-	-
Zheng <i>et al.</i> (2005)	Myeloma	IM-9/Bcl-2	24	MTS	not reported	-	-	-	-	>100	-	>100	-	>100	-	-	-	-	-	-	-	-	-
Iwasaki <i>et al.</i> (2023)	Pancreas	KP-3L	48	WST-8	RPMI 1640	-	-	-	-	-	-	1.20	0.68	-	-	-	-	-	-	-	-	-	-
Iwasaki <i>et al.</i> (2023)	Prostate	PC3	48	WST-8	RPMI 1640	-	-	-	-	-	-	0.90	0.81	-	-	-	-	-	-	-	-	-	-
Iwasaki <i>et al.</i> (2023)	Stomach	MKN74	48	WST-8	RPMI 1640	-	-	-	-	-	-	0.63	1.57	-	-	-	-	-	-	-	-	-	-

1.6.2.1: Jadomycins and Liver Cancer

The first published study regarding the cytotoxic activity of jadomycins included a liver cancer cell line (Zheng et al., 2005). Jadomycins B, Ala, F, V, S, and T were screened using HepG2 cells as a model for human hepatocellular carcinoma (Zheng et al., 2005). In HepG2 cells, jadomycin S was reported as the most potent with an IC₅₀ of 9.8 μM while jadomycin Ala was the least potent (Zheng et al., 2005). Following exposure to 10 μM concentrations of each jadomycin analogue, jadomycins B and S had the greatest ability to induce apoptosis in HepG2 cells while jadomycin Ala was again the least active (Zheng et al., 2005). A single experiment reported by Fu *et al.* in a subsequent publication showed that HepG2 cells exposed to 10 μM jadomycin B for 24 h resulted in decreased histone H3 phosphorylation, a result attributed to an inhibitory effect by jadomycin B on Aurora-B kinase (ABK) activity (Fu et al., 2008). A more detailed discussion on the effects of jadomycins on ABK will follow in **section 1.6.4.3**.

A second study by Iwasaki *et al.* also tested jadomycins against 8 cancer cell lines, including HepG2 cells (Iwasaki et al., 2023). A focus within that report was the comparison of jadomycin glycosides, which feature a sugar attached to ring D and comprise the vast majority of known jadomycins, and their aglycon counterparts. HepG2 cells were more susceptible to the cytotoxic effect of jadomycins A and T-aglycon as compared to jadomycins B and T (Iwasaki et al., 2023). This is of particular interest because earlier antimicrobial studies had shown jadomycin B to have activity against a broader range of microorganisms than jadomycin A, and suggests that investigation into jadomycin aglycons could provide a new avenue for further development (Wang et al., 2002; Rix et al., 2004; Iwasaki et al., 2023).

1.6.2.2: Jadomycins and Myeloma

The same initial study reporting the effects of jadomycins on liver cancer also screened for activity against myeloma (Zheng et al., 2005). The same 6 jadomycins (B, Ala, F, V, S, and T) were tested in IM-9 and IM-9/Bcl-2 human lymphoblast cells derived from a multiple myeloma (Zheng et al., 2005). The IM-9/Bcl-2 subline of IM-9 was included because these cells are MDR. Consistent with results in HepG2 cells, jadomycin

S was reported as the most potent in IM-9 cells with an IC₅₀ of 6.3 μM and jadomycin Ala the least potent (Zheng et al., 2005). Survival of IM-9/Bcl-2 cells, which overexpress Bcl-2, was affected by all 6 jadomycins tested, however, exact IC₅₀ values were not reported as the concentration needed was >100 μM (Zheng et al., 2005). Again, jadomycins B and S had the greatest effect on apoptosis induction in IM-9 cells, however, jadomycin S was more than twice as efficacious as jadomycin B in IM-9/Bcl-2 cells (Zheng et al., 2005). A more detailed discussion on apoptosis will follow in **section 1.6.4.1**. As such, this initial study provided the first clue that jadomycins may have a role in treating MDR cancer.

1.6.2.3: Jadomycins and Lung Cancer

Human lung cancer, represented by the H460 non-small-cell lung carcinoma line, was the final cancer cell line in the original cancer screening publication (Zheng et al., 2005). Contrary to the results found for liver cancer and myeloma, jadomycin F was reported as the most potent in H460 cells with an IC₅₀ of 12.4 μM while jadomycin Ala remained the least potent (Zheng et al., 2005). The observation that jadomycin F, rather than B or S, had the greatest inhibitory effect in H460 cells suggested that chemical changes to the oxazolone ring can lead to differing biological activity. Unlike each of the previously discussed cell lines, apoptosis induction was not measured.

A second article was published in 2008 which continued the exploration of jadomycin activity against lung cancer cells (Fu et al., 2008). Jadomycin B, S, and T were assayed and it was reported that A549 human lung adenocarcinoma cells showed the most sensitivity to jadomycin B with an IC₅₀ of 11.3 μM after 24h (Fu et al., 2008; Si, 2020). Finally, exposure to 0-10 μM jadomycin B for 24 h resulted in decreased histone H3 phosphorylation in a dose-related manner, similar to that described above in HepG2 cells and again attributed to an inhibitory effect by jadomycin B on ABK activity (Fu et al., 2008).

Iwasaki *et al.* were the third group to test jadomycins in lung cancer, again using A549 cells (Iwasaki et al., 2023). As they had observed with HepG2 cells, jadomycin aglycons were more potent than their counterparts. Remarkably, the reported IC₅₀ for jadomycin T-aglycon was 0.72 μM, a 7-fold difference from the 5.16 μM concentration

needed for jadomycin T (Iwasaki et al., 2023). Replicating the experiments of Fu *et al.* in A549 cells, cytotoxicity to jadomycins B and T were tested simultaneously following 48 h exposure. Both jadomycin B and T were found to be similarly potent, at IC₅₀s of 6.81 μM and 5.16 μM respectively, to one another as opposed to the 4-fold difference previously described (Fu et al., 2008; Iwasaki et al., 2023). These differences in reported values between studies are common and may be indicative of some laboratory-specific factor involved which has yet to be determined.

1.6.2.4: Jadomycins and Cervical Cancer

Fu *et al.* conducted the first reported experiments in human cervical cancer cells using the HeLa cervical adenocarcinoma cell line. Following exposure to jadomycin B, S, or T for 24 h, HeLa cells exhibited the greatest inhibition in response to jadomycin B with an IC₅₀ of 18.2 μM (Fu et al., 2008; Si, 2020). Similar to the results observed in HepG2 liver cancer cells and A549 lung cancer cells, jadomycin B exposure also resulted in a dose-related reduction of histone H3 phosphorylation (Fu et al., 2008).

1.6.2.5: Jadomycins and Melanoma

In 2007 Borissow *et al.* tested the cytotoxic effect of 19 jadomycins in what they believed at the time were two human breast cancer cell lines (Borissow et al., 2007). One of those cell lines, MDA-MB-435, is now recognized as a misidentified derivative of the UCLA-SO-M14 male, human melanoma cell line (Rae et al., 2007; Korch et al., 2018). This error was later recognized by the original research group and in the remainder of this section will be regarded as a melanoma cell line despite the terminology used in the original publication (Borissow et al., 2007; Jakeman et al., 2009a). As such, MDA-MB-435 cells are the only melanoma cell line for which jadomycin inhibitory activity has been reported at the time of writing.

Of the jadomycins tested, jadomycin S, jadomycin DT, dalomycin T, and jadomycin *R*-Phe were the most potent with IC₅₀s ranging between 1-2 μM, while jadomycins H, ILEVS1080, βala, and Y were the least potent with IC₅₀s ranging between 10-30 μM (Borissow et al., 2007). By simultaneously testing so many jadomycins against

the same cell line an entire spectrum of activity was described which could be used to gain insight to the structure-activity relationship of the molecules. It was concluded that jadomycins with small, polar side chains could be predicted to have the greatest cytotoxic activity and further demonstrated the importance of variation in the oxazolone ring to biological activity (Borissow et al., 2007). Those jadomycins incorporating large, aromatic amino acids generally had the poorest activity, and those with non-polar amino acids were moderately active, with stereochemistry not generally a significant factor (Borissow et al., 2007).

All jadomycins tested, with the sole exception of jadomycin H, showed greater potency against MDA-MB-435 melanoma cell than they did against the simultaneously tested T-47D human breast cancer cells (Borissow et al., 2007). As MDA-MB-435 cells are more rapidly proliferative than T-47D cells it was reasoned that the mechanism by which jadomycins exert their cytotoxic effect involved interruption of the cell cycle and could be used to specifically target rapidly dividing cells while sparing more slowly replicating, healthy cells (Borissow et al., 2007).

1.6.2.6: Jadomycins and Colon Cancer

The first experiments to screen jadomycins against a colon cancer cell line were published by Fan *et al.* who used HCT116 human colon carcinoma cells (Fan et al., 2012). Interestingly, this study also selected a longer exposure time at 72 h as opposed to all previous studies which had been conducted at 24 h or 48 h of exposure. The most potent jadomycins were once again those with small, polar side chains or alkyl side chains (Fan et al., 2012). This study was also unique in being the first to include non-cancerous cells, human microvascular epithelial cells (HMEC), in their assay to determine if jadomycins had selective toxicity against cancer cells. Jadomycins showed similar toxicity to HMEC and HCT116 cells, as well as the simultaneously tested MCF-7 cells, with the sole exception of jadomycin Orn which was 2-fold more toxic in the cancer cells as compared to the HMECs (Fan et al., 2012). This observation conflicted with the previous conclusion that jadomycins were more potent in MDA-MB-435 cells as opposed to T-47D, and instead suggested that unique interactions between jadomycins and specific cellular targets could be involved.

Likewise, Iwasaki *et al.* included H116 cells in their study which allowed a comparison against the other 7 cell lines included (Iwasaki et al., 2023). In contrast to the other lines tested, there was no appreciable difference in H116 cells response to jadomycins A or T-aglycon as compared to jadomycins B or T (Iwasaki et al., 2023). This could have been the result of relatively low susceptibility of H116 cells to the jadomycins included as IC₅₀s for all 4 jadomycins ranged between 3-6 mM, among the highest values reported in that study (Iwasaki et al., 2023).

1.6.2.7: Jadomycins and Brain Cancer

The most recently published investigation into the cytotoxicity of jadomycins, at the time of writing, screened against several additional cancer types never before tested (Iwasaki et al., 2023). The first of these was brain cancer as represented by A172, a human glioblastoma cell line. Jadomycins T and T-aglycon were particularly potent in A172 cells, leading the authors to conclude that jadomycins could have a potential role in treating brain tumours which currently have limited chemotherapeutic options (Iwasaki et al., 2023). Key to the future development of jadomycins in this role will be investigations into their ability to cross the blood-brain barrier.

1.6.2.8: Jadomycins and Stomach Cancer

The MKN74 human gastric tubular adenocarcinoma cell line was used in the only published screen of jadomycins against stomach cancer (Iwasaki et al., 2023). The most remarkable result was that the IC₅₀ of jadomycin T was 0.63 μM, the lowest IC₅₀ reported for any jadomycin in the literature (Iwasaki et al., 2023). MKN74 cells were also the only cell line reported to show a greater cytotoxic response to a glycosylated jadomycin, jadomycin T, than its aglycon counterpart (Iwasaki et al., 2023). When considered together, these two factors further support differential effect of jadomycins in differing cell types and suggest that jadomycins may be more effective in types of cancer as yet uninvestigated.

1.6.2.9: Jadomycins and Pancreatic Cancer

As with the previously discussed brain and stomach cancers, Iwasaki *et al.* were the first to screen jadomycins for activity against pancreatic cancer (Iwasaki et al., 2023). KP-3L human pancreatic adenosquamous carcinoma cells exposed to jadomycins A, B, T, and T-aglycon had IC₅₀s similar to those observed in A172 and HepG2 cells (Iwasaki et al., 2023). Once again, jadomycins A and T-aglycon were the most potent.

1.6.2.10: Jadomycins and Prostate Cancer

The last of the novel cancer types in which jadomycins were tested by Iwasaki *et al.* was prostate cancer (Iwasaki et al., 2023). The PC3 human prostate adenocarcinoma cell line was used, representing advanced, highly malignant, and androgen-independent disease (Sobel and Sadar, 2005). Prostate cancer is another hormonally sensitive cancer which is easiest to treat at early stages, but treatments become more challenging with progression and loss of androgen sensitivity (Russell et al., 1998). Jadomycins A, B, T, and T-aglycon were particularly potent in PC3 cell, with IC₅₀s ranging from 0.81-2.07 μ M (Iwasaki et al., 2023). As with breast cancer, novel therapeutics discovered as natural products are being investigated for prostate cancer (Kim et al., 2014; McKeown and Hurta, 2014; McKeown et al., 2014; McKeown and Hurta, 2015). Shared features between the two cancers, namely a transition from hormone sensitivity to insensitivity and the accompanying challenges to treatment presented by this transition, could make prostate cancer another valid target for future jadomycin research.

1.6.2.11: Jadomycins and Breast Cancer

Breast cancer was among the earliest cancer types investigated when determining the cytotoxic activity of jadomycins. Recognizing that breast cancer is not a singular disease, jadomycins have been tested for cytotoxic effect in 5 different human breast cancer cell lines with different ER/PR/HER2 profiles and a single mouse mammary carcinoma cell line (Borissow et al., 2007; Fu et al., 2008; Fan et al., 2012; Issa et al., 2014; Hall et al., 2015; Hall et al., 2017; McKeown et al., 2022; Iwasaki et al., 2023). The

first of these was the T-47D, ER⁺/PR⁺/HER2⁻, human ductal carcinoma cell line which was tested alongside the MDA-MB-435 melanoma cell line as described in **section 1.6.2.5** (Borissow et al., 2007; Holliday and Speirs, 2011; Dai et al., 2017). Similar results to those discussed above for MDA-MB-435 cells were reported: jadomycins DT and S were the most potent with IC₅₀s between 2-3 μM and jadomycins βala and Y being the least potent with IC₅₀s between 20-35 μM after 48 h (Borissow et al., 2007). As with the MDA-MB-435 cells, comparing the structure-activity relationship of jadomycins based on the observed range of potencies was made possible by simultaneously testing 19 analogues against the same cell line.

The second cell line tested was the human MCF-7, ER⁺/PR⁺/HER2⁻, breast adenocarcinoma cell line. This cell line has been the most extensively investigated in the literature and represents a more prevalent, hormonally sensitive disease (Fu et al., 2008; Fan et al., 2012; Issa et al., 2014; Hall et al., 2015; Iwasaki et al., 2023). The 3 studies which used a 48 h exposure time reported very different IC₅₀ values, perhaps attributable to differing methodology in assessing cytotoxicity (Fu et al., 2008; Iwasaki et al., 2023). Nonetheless, the IC₅₀ values reported by Iwasaki *et al.* and Borissow *et al.* were in close agreement for jadomycins B and T which the studies shared across the 2 different cell lines, each showing jadomycin T to be more efficacious in ER⁺/PR⁺/HER2⁻ cells (Borissow et al., 2007; Iwasaki et al., 2023). The data available for MCF-7 cells following 72 h exposure to jadomycins is more consistent across all 3 studies, with jadomycins B, S, and F being among the most potent included (Fan et al., 2012; Issa et al., 2014; Hall et al., 2015). The variety of jadomycins tested in similar cells across 2 time points, when taken together, give greater evidence that the most potent jadomycins are those which have small, polar side chains attached to the oxazolone ring.

Issa *et al.* took their investigation of jadomycins in MCF-7 cells one step further by testing jadomycins in paclitaxel-resistant (MCF-7-TXL), etoposide-resistant (MCF-7-ETP), and mitoxantrone-resistant (MCF-7-MITX) cell lines which overexpressed ABCB1, ABCC1, and ABCG2, respectively (Issa et al., 2014). **Table 1.11** provides a comparison of all IC₅₀s found in the literature for ABC overexpressing, resistant cell lines as compared to their non-resistant controls for jadomycins and control drugs tested. Using these resistant cells it was shown that the IC₅₀s for ABC transporter substrate molecules

increased by 10-fold to 80-fold depending on the chemotherapeutic, while IC_{50} s for jadomycins in the resistant cell lines only increased by 1.5-fold to 3.8-fold with the majority of changes being approximate 2-fold (Issa et al., 2014). This result was confirmed by co-exposing control or resistant MCF-7 cells to jadomycins and inhibitors of ABC transporters. Small molecule inhibitors of ABCB1, ABCC1, or ABCG2 had minor to no effects on jadomycin toxicity while vastly increasing the toxicity of the known substrate molecules doxorubicin and mitoxantrone, providing further evidence that these transporters did not mediate resistance to jadomycins (Issa et al., 2014).

Given the observation that jadomycins were not substrates of ABC transporters, the possibility that jadomycins could inhibit ABC transporters was explored (Issa et al., 2014). Experiments using human embryonic kidney HEK293 cells transfected for overexpression of ABCB1, ABCC1, or ABCG2 were conducted where cells were allowed to accumulate fluorescent ABC substrate molecules in the presence or absence of jadomycins or positive control inhibitors (Issa et al., 2014). With only the exception of jadomycin DNV at a high concentration of 50 μ M, jadomycins did not inhibit transporter activity (Issa et al., 2014). Thus, the potential for jadomycins to act as ABC transport inhibitors was ruled out.

Three additional cell lines, along with MCF-7, were subsequently tested by our research group (Hall et al., 2015). These included the BT-474 (ER⁺/PR⁺/HER2⁺ invasive ductal carcinoma), SK-BR-3 (ER⁻/PR⁻/HER2⁺ adenocarcinoma), and MDA-MB-231 (ER⁻/PR⁻/HER2⁻ adenocarcinoma) human breast cancer cell lines which represent a range of receptor expression (Hall et al., 2015). Jadomycins B, S, and F were tested for cytotoxic effect, and all had approximately equal potency across the 4 cell lines (Hall et al., 2015). This result suggested for the first time that the cytotoxic effect of jadomycins was not dependent on the receptor status of breast cancer cells. A third study by our research group was published in 2017, this time comparing control MDA-MB-231 (231-CON) cells to paclitaxel-resistant (231-TXL) MDA-MB-231 cells which overexpressed ABCB1 (Hall et al., 2017). Similar to the results reported in 2014 regarding drug resistant MCF-7 cells, jadomycins B, S, and F showed no difference in potency in 231-TXL cells as compared to 231-CON cells despite increased resistance the ABC transporter substrates mitoxantrone and doxorubicin (Hall et al., 2017; Goralski, 2020).

The final published *in vitro* experiment looking at the anticancer effect of jadomycin B was conducted using 4T1 mouse mammary carcinoma cells and a paclitaxel-resistant (4T1-TXL) derivative line which overexpressed ABCB1a (McKeown et al., 2022). This experiment once again showed that jadomyicins were equipotent in control and drug resistant cells, providing the basis to expand experiments on jadomycin activity to an animal model.

1.6.3: Anticancer Effects of Jadomyicins *in vivo*

Only a single publication has examined the anticancer effects of jadomyicins *in vivo* (McKeown et al., 2022). A zebrafish and mouse model were used to evaluate safety and efficacy of jadomycin B, and to gain some basic understanding about jadomycin pharmacokinetics. The maximum tolerated dose of jadomycin B in zebrafish larvae was found to be 40 μ M for 120 h, approximately 10-fold to 20-fold higher than the IC₅₀ in human breast cancer cell cytotoxicity experiments (Bonitto et al., 2021; McKeown et al., 2022). Furthermore, when zebrafish larvae were xenotransplanted with 231-CON human breast cancer cells and placed in water containing jadomycin B, there was a dose-dependent reduction in cancer cell proliferation after 48 h exposure (McKeown et al., 2022).

The successes observed in zebrafish larvae provided confidence to proceed to a mouse model. A single intraperitoneal dose (6 mg/kg) of jadomycin B was administered to adult, female Balb/C mice which was rapidly absorbed with a maximum serum concentration of 3.4 ± 0.27 μ M at 15 min post injection (McKeown et al., 2022). Plasma concentration of jadomycin B declined biphasically, with an elimination half-life of 1.7 ± 0.058 h (McKeown et al., 2022). These initial pharmacokinetic analyses demonstrated that jadomycin B could be delivered safely at concentrations known to have a cytotoxic effect in cancer cells and it would remain in the plasma for an adequate length of time. When mice were injected with 4T1 cancer cells and jadomycin B (12 mg/kg every 12 h for 10 days) was administered by intraperitoneal injection, it was reported that jadomycin B significantly reduced primary tumour volume but did not significantly reduce the number of metastases after 10 days of treatment (McKeown et al., 2022). Importantly, no

behavioural or physical abnormalities occurred in mice treated with jadomycin B, which maintained healthy body weights, liver, and kidney function (McKeown et al., 2022). Although this study was a limited pilot involving a small number of animals, it justifies further exploration of the anticancer effects of jadomycins *in vivo*.

1.6.4: Proposed Jadomycin Mechanisms of Action

While the anticancer effects of jadomycins have been clearly demonstrated, the mechanism(s) by which they exert those effects remains to be fully elucidated. Several studies have attempted to answer this question of mechanism and it is likely that no single pathway will provide a complete explanation. This work continues to contribute to that body of knowledge. By better understanding the cellular target(s) with which jadomycins interact we can gain a more complete understanding of the kinds of cancer they can be most effective against. Furthermore, it is unclear if different jadomycins act on different targets, complicating the question even more. This section will summarize the current knowledge on the targets jadomycins have been shown to interact with (**Figure 1.8**).

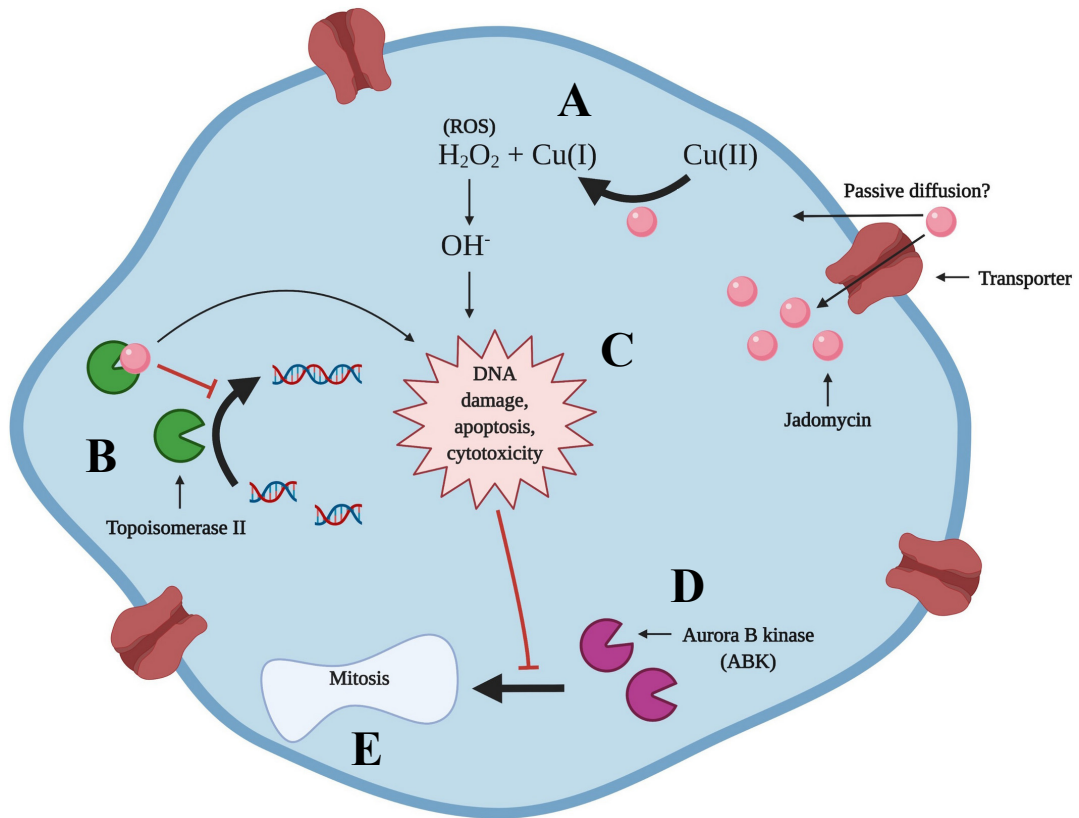


Figure 1.8: Previously Proposed Mechanisms of Action of Jadomycins in Human Breast Cancer Cells

Previous research has proposed several mechanisms of action by which jadomycins may exert their anticancer effects in human breast cancer cells. These include: (A) copper-dependent production of ROS and (B) inhibition of TOP2 leading to (C) DNA damage and apoptosis. The induced DNA damage leads to (D) inhibition of ABK, which prevents (E) cell cycle progression and mitosis. Figure adapted, with permission (Appendix A.10), from Bonitto et al. (2021)

1.6.4.1: Apoptosis Induction

The first published article examining the cytotoxic effects of jadomycins was also the first to suggest that this cytotoxicity was mediated by induction of apoptosis (Zheng et al., 2005). Apoptosis is a term used to describe programmed cell death, first proposed in 1972, a process by which damaged or unneeded cells are destroyed in a controlled manner (Kerr et al., 1972; Elmore, 2007). Apoptosis is a form of regulated cell death, reliant on tightly controlled molecular machinery, which is contrasted against accidental cell death that occurs instantaneously as the result of catastrophic damage to the cell leading to necrosis (Galluzzi et al., 2018). In necrosis, cytoplasmic contents are released into the surrounding environment which can elicit an inflammatory response (Elmore, 2007).

A wide variety of chemotherapeutics induce apoptosis in cancer cells, including doxorubicin, etoposide, mitoxantrone, paclitaxel, and vincristine (Mesner et al., 1997). Cell death through apoptosis is characterized by morphological and biochemical modifications which include cytoplasmic shrinkage, chromatin condensation (pyknosis), nuclear fragmentation (karyorrhexis), plasma membrane blebbing, protein cross-linking, and DNA fragmentation (Elmore, 2007; Galluzzi et al., 2018). Ultimately, small vesicles known as apoptotic bodies are produced which are summarily taken up by phagocytosis and degraded (Galluzzi et al., 2018).

There are two main pathways, extrinsic and intrinsic, through which apoptosis can be initiated and either of these pathways can be activated by chemotherapeutics. The extrinsic pathway initiates apoptosis in response to transmembrane receptor mediated interactions (Elmore, 2007). Here, “death receptors” like those of the tumour necrosis factor (TNF) superfamily receive extracellular signals which cause a cascade of cellular events leading to the activation of caspase-8 (Elmore, 2007; Galluzzi et al., 2018).

Alternatively, the intrinsic pathway initiates apoptosis based on intracellular signals such as growth factor withdrawal, DNA damage, endoplasmic reticulum stress, reactive oxygen species (ROS) exposure, replication stress, microtubular alterations, or mitotic defects (Elmore, 2007; Galluzzi et al., 2018). Regardless of the initiating stimulus, the signal is propagated to the mitochondria where BH3 initiator proteins are activated

(Czabotar et al., 2014). BH3 initiators inhibit activity of Bcl-2 proteins and Bcl-2 proteins in turn inhibit pro-apoptotic effectors BAX and BAK; the result of BH3 inhibition is therefore the activation of BAX and BAK leading to increased apoptosis (Czabotar et al., 2014). Caspase-8 is also capable of inhibiting Bcl-2 proteins and activation BAX and BAK effectors, linking the intrinsic and extrinsic pathways (Czabotar et al., 2014). Effectively, once Bcl-2 proteins are inhibited, BAX and BAK become activated allowing for further release of pro-apoptotic proteins like cytochrome c from the mitochondria (Czabotar et al., 2014). These pro-apoptotic proteins can then go on to activate caspase-9 (Elmore, 2007; Czabotar et al., 2014; Galluzzi et al., 2018). Caspases-8 and -9 are initiator caspases, which initiate the proteolytic cascade of subsequent effector caspases, ultimately leading to apoptotic cell death (Earnshaw et al., 1999; Czabotar et al., 2014).

The experiments of Zheng *et al.* took advantage of the morphological changes occurring during apoptosis to selectively stain the DNA in live cells, apoptotic cells, and necrotic cells allowing for determination of relative percent of the cell population in each condition (van Engeland et al., 1998; Zheng et al., 2005; Riccardi and Nicoletti, 2006). Apoptosis was most potently induced by jadomycins B and S in HepG2 cells and IM-9 cells, but did occur to a lesser degree with jadomycins Ala, F, V, and T (Zheng et al., 2005). Of particular interest was the inclusion of IM-9/Bcl-2 cells which overexpress Bcl-2. Forced overexpression of Bcl-2 has been shown to prevent apoptosis in haematopoietic cells, promoting lymphocyte accumulation and leading to the development of cancer (Vaux et al., 1988; Czabotar et al., 2014). The IM-9/Bcl-2 cells were observed to have less susceptibility to all jadomycins tested, with jadomycin S being the most potent and eliciting 66% as much apoptosis as observed in IM-9 cells at the same concentration (Zheng et al., 2005).

Similar results were reported by Fu *et al.* in A549 cells using the same technique (Fu et al., 2008). Jadomycin B at a constant concentration of 5.0 μ M elicited a time dependent induction of apoptosis, causing 48% and 71.7% of A549 cells to begin the process of apoptosis by 24h and 48h, respectively (Fu et al., 2008). These results were confirmed using Hoechst 33342 staining, a fluorescent dye which binds DNA and allowed microscopic detection of chromatin condensation (Fu et al., 2008).

The final evidence for apoptosis was described by Hall *et al.* who measured apoptosis induction by jadomycin B, S, and F in 231-CON and 231-TXL cells after 36 h exposure (Hall et al., 2017). All 3 jadomycins significantly increased the proportion of apoptotic cells as compared to control, with jadomycin S being the most potent in both cell lines (Hall et al., 2017). Co-exposure of both 231-CON and 231-TXL cells with jadomycins B, S, or F and the caspase-inhibitor Z-VAD significantly reduced the proportion of cells in the early apoptotic phase, lending further evidence to the reliance on activating apoptosis to cause cell death (Hall et al., 2017). Although these data do not explain what kind of insult jadomycins cause, the studies described make an argument that jadomycin induced cell death occurs through apoptosis. It is possible that other forms of cell death also contribute to the cytotoxic effect of jadomycins, however, this has yet to be studied.

1.6.4.2: Cell Cycle Alteration

Limited data exists on the effects of jadomycins on the cell cycle, with only a single paper directly measuring cell cycle progression (Fu et al., 2008). For cells to successfully multiply they must replicate their genetic material, grow in size, and divide into identical daughter cells. This mitotic division is regulated by the cell cycle. The cell cycle can be broken into several distinct phases informed by cellular activities involved in division (Vermeulen et al., 2003). The interphase consists of 3 distinct steps: G₁, wherein cells grow and prepare for DNA synthesis; S, where DNA replication occurs; and G₂, where DNA replication has completed and cells prepare for mitosis (Vermeulen et al., 2003). Mitosis is the final stage of the cell cycle where genetic material is separated and the cell completes division (Vermeulen et al., 2003). Outside of the cell cycle exists G₀, which represents a resting state where no active growth or division occurs (Vermeulen et al., 2003). Transition between the phases of the cell cycle is controlled by the cyclin-dependent kinases and their associated cyclins (Vermeulen et al., 2003; Schwartz and Shah, 2005). Fluctuations in the expression of these kinases drive the cell cycle forward, and small molecule inhibitors have been an area of interest for chemotherapeutic development (Schwartz and Shah, 2005; McKeown et al., 2014).

The first indication that jadomycins may affect the cell cycle was the recognition that 18 of 19 different jadomycins tested had a greater potency in the rapidly proliferating MDA-MB-435 cell line as compared to the more slowly replicating T-47D cells (Borissow et al., 2007). Rapidly dividing cells must necessarily go through the cell cycle more frequently, so it was reasoned that an effect interrupting the cell cycle could be responsible for the observed difference (Borissow et al., 2007). This logic was followed in later experiments by Fu *et al.* where jadomycin B was observed to dose dependently decrease the rate at which A549, MCF-7, and HeLa cells proliferated (Fu et al., 2008). Further analysis of the effects on cell cycle and apoptosis induction in A549 cells showed that 5 µg/mL jadomycin B elicited a non-significant cell cycle arrest in S-phase following 3, 12, 24, or 48 h incubation (Fu et al., 2008). No further investigation into the effects of jadomycins on the cell cycle have been conducted, so this remains an area in which additional data is needed.

1.6.4.3: Aurora-B Kinase Inhibition

The first mechanism of action, beyond the simple induction of apoptosis, explored to explain the cytotoxic effect of jadomycins was inhibition of ABK (Fu et al., 2008). In all mammals, including humans, there are 3 aurora kinases: aurora-A, ABK, and aurora-C (Brown et al., 2004). Each of the aurora kinases is involved in cell division, interacting with cytoskeletal components and the chromosomes (Brown et al., 2004). Aurora-A and ABK are expressed in mitotically active cells, while aurora-C is generally confined to meiosis (Willems et al., 2018). Aurora-A kinase concentrates in centrosomes and the mitotic spindles which facilitate chromosome separation, playing a key role in spindle formation (Kollareddy et al., 2008; Willems et al., 2018). ABK is localized to the centromeres of condensed chromosomes, as part of a chromosome passenger complex, and triggers spindle elongation and associated chromatid separation and cytokinesis (Kollareddy et al., 2008; Willems et al., 2018). Aurora-C kinase is generally associated with germ cells undergoing meiosis, otherwise behaving similarly to ABK (Willems et al., 2018).

Overexpression of aurora kinases is common in cancer cells, leading to genetic instability by increasing the occurrence of mitotic defects involving altered DNA content of daughter cells (Kollareddy et al., 2008). Alterations in both aurora-A and ABK have been associated a variety of primary tumour types, and have been associated with increased risk of breast cancer (Lin et al., 2006; Tchatchou et al., 2007; Kollareddy et al., 2008). As ABK is only expressed during mitosis, ABK inhibitors would have no effect on quiescent cells making them an attractive target for cancer therapy (Lin et al., 2006; Fu et al., 2008).

Virtual screening for potential inhibitors of ABK identified jadomycin B as a good fit for the ATP-binding pocket of the enzyme where it was predicted to become strongly bound, resulting in enzyme inhibition by blocking ATP access (Fu et al., 2008). ABK is an evolutionarily conserved protein, with a homologue in budding yeast called increase-in-ploidy 1 protein (Ipl1) that has a nearly identical ATP-binding pocket (Chan and Botstein, 1993; Kimura et al., 1997; Fu et al., 2008). Like ABK, Ipl1 is responsible for chromosome segregation during mitosis, and inhibition results in inhibition of cell growth (Fu et al., 2008). A temperature sensitive, mutant *Ilp1-321* gene was predicted to produce an Ipl1-321 protein more sensitive to ABK inhibitors than wild-type Ipl1. Growth of mutant *Ilp-321* yeast cells was inhibited by jadomycin B at 10 μ M, but wild-type cells required 100 μ M concentrations to show an effect (Fu et al., 2008). Jadomycins S and T were also assayed, but neither showed any inhibitory effect (Fu et al., 2008). Purified enzyme assays confirmed that jadomycin B could competitively inhibit ATP binding in human ABK in a dose dependant fashion, while jadomycins S and T again had no effect (Fu et al., 2008).

As described in **sections 1.6.2.1, 1.6.2.3, and 1.6.2.4**, jadomycin B exposure resulted in decreased phosphorylation at serine-10 of histone H3 in HepG2 liver cancer cells, A549 lung cancer cells, and HeLa cervical cancer cells (Fu et al., 2008). ABK is responsible for phosphorylating this residue so it was reasoned that the observed decrease in phosphorylation, considered in combination with the purified enzyme assay results, was indicative of ABK inhibition (Fu et al., 2008). These experiments were followed up by Issa *et al.* who measured the effect of jadomycin B on inhibition of ABK-dependant histone H3 phosphorylation at serine 10 and found that there was a dose-dependent

reduction in phosphorylation in the control MCF-7, MCF-7-TXL, and MCF-7-MITX cell lines at 10-20 μM concentrations (Issa et al., 2014). This mode of action was not entirely satisfactory, however, because the concentrations needed to achieve ABK inhibition were much higher than the $\text{IC}_{50\text{s}}$ reported in the same study and because only jadomycin B had demonstrated inhibitory effects in earlier assays (Fu et al., 2008; Issa et al., 2014).

Further support for the idea that ABK-inhibition is not a direct mechanism of action was a novel experiment included in a recent review of jadomycin activity in breast cancer (Bonitto et al., 2021). In purified enzyme assays, jadomylicins B, F, and S were only able to inhibit ABK enzyme activity at 50 μM , a concentration 10-fold higher than the observed $\text{IC}_{50\text{s}}$ for these molecules *in vitro* (Bonitto et al., 2021). It is therefore reasonable to conclude that ABK inhibition is not a mechanism by which jadomylicins exert a cytotoxic effect, but rather a consequence of other disrupted cellular processes.

1.6.4.4: DNA Cleavage

Based on the structural similarity between jadomylicins and doxorubicin, and on the proven ability of naturally derived molecules to cause DNA damage, Cottreau *et al.* conducted a series of experiments looking at the effect of jadomylicins on DNA cleavage (Eliot et al., 1984; Hansen and Hurley, 1996; Melvin et al., 2000; Cottreau et al., 2010). Jadomylicins B, L, and *S*-Phe were shown to cause DNA cleavage in acellular assays through 3 distinct mechanisms (Cottreau et al., 2010). When jadomycin B was in the presence of copper(II) ions it caused single strand DNA cleavage, however, jadomycin B or copper(II) ions alone were not sufficient to cause the same result (Cottreau et al., 2010). The authors speculated that jadomycin B may be reducing copper(II) ions in a manner that generates ROS.

In contrast, jadomycin L induced single strand DNA breaks in the absence of copper(II) ions; at concentrations exceeding 20 μM jadomycin L also generated double strand DNA breaks (Cottreau et al., 2010). The double strand breaks were theorized to have occurred due to the accumulation of single strand breaks as opposed to introducing simultaneous double strand breaks. Jadomycin *S*-Phe did not generate DNA cleavage in the presence or absence of copper(II) ions, but did elicit single strand breaks following photoactivation (Cottreau et al., 2010). Finally, jadomycin G did not cause DNA cleavage

under any attempted conditions within the study. Taken together, these experiments demonstrated that differing jadomycins can behave in very different ways based on their specific side chain. It also suggested that jadomycins could be selectively activated in tumours by of copper(II) ions or photoactivation, thereby providing a potential means to achieve selectivity in cancer cells and limit adverse effects in other tissues of the body.

A subsequent publication followed this line of inquiry and determined that DNA cleavage does not directly involve jadomycin B binding to DNA, but rather that jadomycin B acts as a source of electrons for copper(II) ion reduction to generate copper(I) which in turn reacts with hydrogen peroxide to form ROS in the form of hydroxyl radicals (Monro et al., 2011). Breast cancer cells are known to have elevated levels of copper as compared to healthy breast tissue, therefore, the authors theorized that this could be used to selectively target cancer cells with jadomycin B (Mulay et al., 1971; Monro et al., 2011). Later analysis of jadomycins DNV, DNL, and 6 triazole jadomycins revealed that each of these jadomycin analogues generate concentration dependent single strand DNA breaks in the presence of copper(II) as well, providing evidence that jadomycins other than jadomycin B could possess this attribute (Dupuis et al., 2011; Dupuis et al., 2012).

1.6.4.5: Reactive Oxygen Species Formation

The results of DNA cleavage assays and limited support for the inhibition of ABK as a primary mode of action prompted further investigation into ROS as a mechanism by which jadomycins caused cell death (Hall et al., 2015). Hydrogen peroxide, hydroxyl radical, and superoxide are collectively known as ROS and are produced as natural by-products of normal cellular activities like ATP production by the mitochondria, peroxisome activity, and conversion of AA by cyclooxygenases (Pathak et al., 2005; Snezhkina et al., 2019). Transition metal ions such as iron or copper are also known to generate ROS through decomposition of hydrogen peroxide (Liochev and Fridovich, 2002; Valko et al., 2016; Snezhkina et al., 2019). Normally, ROS generation and elimination is carefully balanced to maintain homeostasis, allowing ROS to fulfill roles in cellular signalling and cell cycle progression without reaching excess levels (He et al., 2017; Snezhkina et al., 2019). When excess ROS accumulate, oxidative stress can occur

in the form of damage to proteins, lipids and DNA which can eventually lead to carcinogenesis or cell death (He et al., 2017; Snezhkina et al., 2019). Many chemotherapeutics take advantage of this by producing high levels of ROS which causes extensive cellular damage (Mizutani et al., 2005; Yang et al., 2018).

The authors of the first report on DNA cleavage by jadomycins hypothesized that generation of ROS could be responsible for the observed activity (Cottreau et al., 2010). Experiments conducted by Hall *et al.* directly followed this line of reasoning (Hall et al., 2015). Jadomycins B, S, F, and *S*-Phe were all found to increase ROS in MCF-7 cells in a dose dependent fashion (Hall et al., 2015). When co-administered with the antioxidant *N*-acetyl cysteine, the IC₅₀s of the 4 tested jadomycins increased, demonstrating a loss of potency (Hall et al., 2015). Measuring the production of ROS and viability simultaneously revealed that MCF-7 cells exposed to jadomycins experienced a 1.4-fold to 2.6-fold increase in ROS associated with a 61% to 78% decrease in viability (Hall et al., 2015).

While the antioxidant *N*-acetyl cysteine reduced toxicity and ROS generation, it did not affect jadomycin mediated ABK inhibition (Hall et al., 2015). This suggested that inhibition of ABK by jadomycins is correlated to cytotoxicity rather than the cause of it. MCF-7 cells co-exposed to copper(II) sulfate and jadomycins B, S, F, or *S*-Phe displayed increased intracellular ROS and decreased cellular viability while copper(II) sulfate alone was not sufficient to affect viability (Hall et al., 2015). Finally, combinations of jadomycins with prooxidants resulted in increased ROS and decreased viability (Hall et al., 2015). The one caveat to these results was that very high concentrations (10-35 μ M) of jadomycins were used in the above experiments.

Further studies have also shown jadomycins can induce ROS production in breast cancer cells (Hall et al., 2017; Forget et al., 2018b). Jadomycins B, S, and F were shown to increase ROS production in 231-CON cells in a dose dependent manner (Hall et al., 2017). Again, this production occurred at 30-40 μ M concentrations, much higher than the concentrations typically needed to elicit 50% cell death (Bonitto et al., 2021). As was observed in MCF-7 cells in the prior study, jadomycins B, S, and F induced equal proportions of cells to undergo apoptosis, regardless of the presence/absence of the antioxidant *N*-acetyl cysteine, suggesting ROS was not responsible for the apoptotic effect

(Hall et al., 2017). Addition of a pro-oxidant did not affect proportion of cells in early apoptosis but did increase the number of late apoptotic cells.

The experiments described above, like those before them regarding ABK, offered the best explanation of mechanism through which jadomycins exerted their cytotoxic effect available at their time of publication. Still, there were unanswered questions which the generation of ROS did not satisfy. The most important of these was the observation that while ROS inhibition could reduce jadomycin potency, jadomycins could still attain near 100% cell death in the presence of antioxidants (Hall et al., 2015; Hall et al., 2017). This led to the conclusion that while ROS production was likely involved in jadomycin action at higher concentrations, there were ROS-independent mechanisms at lower concentrations as well.

1.6.4.6: Topoisomerase II Inhibition

The previously discussed DNA cleavage activity and structural similarity to doxorubicin prompted experiments intended to determine if jadomycins could inhibit TOP2 β (Martinez-Farina et al., 2015a). There are 6 known human topoisomerases, all of which are responsible for managing topological problems (**Figure 1.9**) arising from the double helical nature of DNA and from interactions between long, folded, and intertwined DNA and RNA (Pommier et al., 2022). During transcription, replication, chromatin remodelling, and repair, DNA can become folded and intertwined in ways which introduce stresses or interlock strands. Topoisomerases can target nuclear or mitochondrial DNA or cytoplasmic RNA to alleviate these problems (Pommier et al., 2022).

All topoisomerases function by cleaving the nucleic acid backbone and then rejoining the cleaved ends. Topoisomerase I (TOP1) and mitochondrial topoisomerase I (TOP1MT) exclusively act on double stranded DNA, but cleave only a single strand to allow rotation around the intact strand and thereby relax supercoiling (Stewart et al., 1998; Pommier et al., 2022). TOP2 exists in 2 isoforms, TOP2 α and TOP2 β , which exclusively act on double stranded DNA to generate double strand breaks allowing for both relaxation of supercoiling and decatenation, or unlinking, of interlocked loops of

DNA (Pommier et al., 2022). The main difference between TOP2 α and TOP2 β is that TOP2 α is primarily associated with the G₂ and M phases of the cell cycle and is typically absent from quiescent cells while TOP2 β is expressed in both cycling and non-cycling cells (Woessner et al., 1991; Turley et al., 1997). TOP3 is present in 2 isoforms which exclusively act on single stranded nucleic acids (Pommier et al., 2022). TOP3 α and TOP3 β allow the passage of single stranded DNA through another, however, TOP3 β is unique in having the capacity to relieve knots and linkages in RNA acting as both a DNA and RNA topoisomerase (Ahmad et al., 2016; Pommier et al., 2022).

TOP1, TOP2 α , and TOP2 β are the topoisomerases primarily involved in DNA replication, with all 3 commonly expressed in cancer cells (Turley et al., 1997). As such, they are attractive targets for chemotherapeutics as discussed in **section 1.4.4.6**. Molecules which target topoisomerases can be separated into 2 categories: topoisomerase poisons and topoisomerase catalytic inhibitors. The term “poison” was originally applied to TOP2 poisons because they result in the conversion of the TOP2 enzyme to a toxin with mutagenic and cytotoxic effects (Burden and Osheroff, 1998; Vann et al., 2021). The term “TOP2 poison” will therefore be used throughout this work to refer to this mechanism and to distinguish from compounds which catalytically inhibit the TOP2 enzyme without the generation of a cellular toxin. Many chemotherapeutics currently in use for the treatment of breast cancer, such as doxorubicin or etoposide, are TOP2 poisons (Nitiss, 2009; Delgado et al., 2018). These molecules stabilize TOP2 in a cleavage complex (**Figure 1.10**), trapping the enzyme in a state where a double strand break has been generated and preventing the repair of that break (Nitiss, 2009; Hall and Goralski, 2018; Vann et al., 2021). Once trapped, the topoisomerase cleavage complex undergoes proteolytic degradation leading to the accumulation of double strand DNA breaks and subsequent apoptotic signalling (Mao et al., 2001; Nitiss, 2009; Vann et al., 2021). Cancer cells typically have elevated TOP2 α while TOP2 β poisoning has been associated with cardiotoxicity, thus, it has been speculated that the development of TOP2 α -specific poisons could provide a safer alternative for therapy (Delgado et al., 2018). In contrast, TOP2 catalytic inhibitors block enzyme turnover and prevent enzyme activity by interfering with ATP binding but do not generate a cellular toxin (Burden and Osheroff, 1998; Delgado et al., 2018; Vann et al., 2021). In cancer therapy, TOP2

catalytic inhibitors are mainly used to prevent cardiotoxicity resulting from TOP2 β poisoning (Vavrova et al., 2013; Delgado et al., 2018). The only TOP1 targeting agents currently in clinical use are the TOP1 poisons derived from camptothecin (Delgado et al., 2018). These act similarly to TOP2 poisons, trapping TOP1 in a cleavage complex resulting in inhibition of DNA replication and generation of double strand breaks (Hsiang et al., 1989; Delgado et al., 2018).

Through the use of WaterLOGSY nuclear magnetic resonance spectroscopy jadomycin DS was found to bind recombinant human TOP2 β with a mean dissociation constant concentration of 9.4 mM, establishing for the first time that topoisomerase inhibition could provide another explanation for jadomycin induced DNA damage (Martinez-Farina et al., 2015a). This binding was noted to be much weaker than the mean dissociation constant of 5 μ M typical of etoposide and TOP2 β . In contrast, jadomycin LN was not able to bind TOP2 β , suggesting that TOP2 β binding is not a shared feature among all jadomycin analogues (Martinez-Farina et al., 2015a). Martinez-Farina *et al.* noted that jadomycin DS was also able to bind several other proteins, suggesting that certain jadomyccins can promiscuously bind many different proteins (β -phosphoglucomutase, thymidyl transferase, and bovine serum albumin) with dissociation constants between 0.5-2.0 mM and offering this as a possible explanation for the polypharmacologic nature of jadomyccins (Martinez-Farina et al., 2015a).

Hall *et al.* continued work on the interaction between jadomyccins and topoisomerases. Jadomyccins B, S, and F increased phosphorylated histone H2AX (γ H2AX), a marker of double strand DNA breaks in both 231-CON and 231-TXL cells (Hall et al., 2017). Production of γ H2AX following jadomycin S exposure was not affected by exposure to an antioxidant or prooxidant, leading to the conclusion that these double strand breaks were not associated with ROS (Hall et al., 2017). When cells were co-exposed to jadomycin S and an inhibitor of DNA repair poly(ADP-ribose) polymerases, γ H2AX expression was significantly increased (Hall et al., 2017). Furthermore, jadomyccins B, S, and F (20 μ M for 36 h) reduced expression of *TOP2A* and *TOP2B* genes in 231-CON cells while *TOP1* gene expression was also significantly decreased by jadomycin S (Hall et al., 2017). Purified protein assays demonstrated that jadomyccins B, S, and F (160-640 μ M) concentration dependently inhibited TOP2 α and

TOP2 β activity, preventing enzymatic cleavage of catenated DNA to decatenated DNA, which could indicate an accumulation of topoisomerase cleavage complexes (Hall et al., 2017). In a DNA cleavage assay, jadomycins B and F (640 μ M and 320 μ M, respectively) selectively increased the formation of linear DNA from a supercoiled precursor by TOP2 β with no effect on TOP2 α , while jadomycin S did not affect either isoform (Hall et al., 2017).

The observed effects of jadomycins on topoisomerases have predominantly been conducted using acellular enzymatic assays. It remains to be determined if those effects remain observable *in vitro* and at concentrations known to cause cytotoxic activity. Further experimentation is therefore needed to determine fully describe the role of topoisomerases as a target for jadomycins.

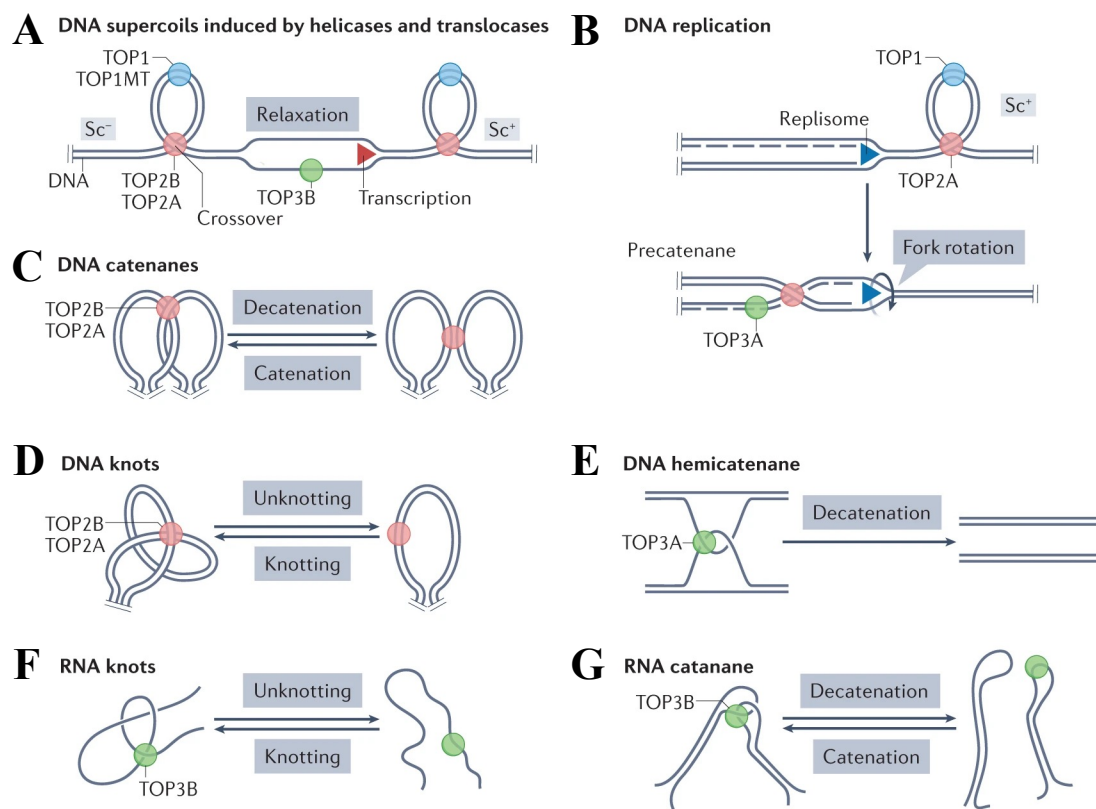


Figure 1.9: DNA and RNA Topological Problems Managed by Topoisomerases

Topoisomerases serve a vital role in resolving topological problems arising from interaction between long, folded, and intertwined DNA and RNA. These include (A) supercoiling, (B) stresses introduced during DNA replication, (C) interlinking (catenation) of double stranded DNA, (D) DNA knotting, (E) hemicatenation of a single strand of double stranded DNA, (F) RNA knotting, and (G) RNA catenation. Figure reproduced, with permission (Appendix A.11), from Pommier et al. (2022)

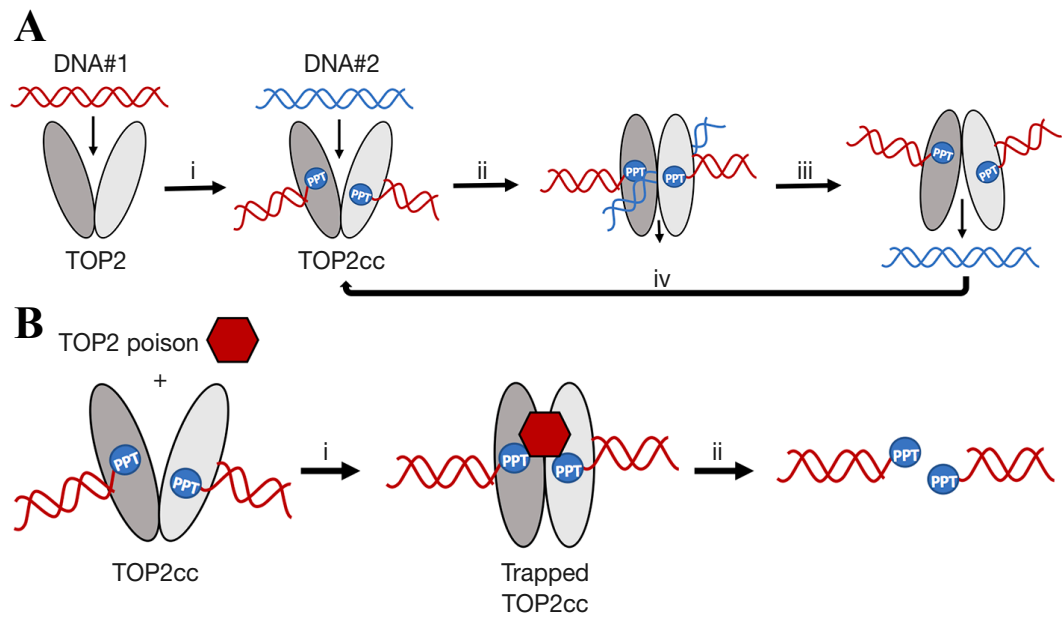


Figure 1.10: Topoisomerase II Cleavage Complex Formation

TOP2 normally (A) binds to and forms a double strand break in DNA allowing for the passage of double stranded DNA by forming a TOP2 cleavage complex (TOP2cc), then repairs the break and releases from the DNA. In the presence of a TOP2 poison (B) the TOP2cc becomes trapped, resulting in proteolytic degradation of the TOP2 enzyme and release of DNA without repairing the generated double strand break. Figure reproduced, with permission (Appendix A.12), from Hall and Goralski (2018)

1.7: Drug-Drug Combination Therapy

The use of single agent therapies for cancer treatment is no longer common practice (Carrick et al., 2009). Instead, combinations of complimentary chemotherapeutics are given to maximize efficacy and minimize adverse effects. This is especially true in the context of MDR cancers, where resistance can be mitigated by utilizing multiple drugs which act in different ways. Understanding how different drugs act in combination is important to successfully implementing them (Roell et al., 2017). When given in combination, drugs can act additively, antagonistically, or synergistically to complement or detract from their combined effect. Pharmacological synergy (or antagonism) is classically defined as 2 or more drugs working in combination to produce an effect greater (or lesser) than the expected additive effect (Greco et al., 1996; Roell et al., 2017). The effect described as synergistic can be either beneficial or detrimental: the drug combination may have enhanced anticancer effects but may have enhanced adverse effects instead or as well.

1.7.1: Mathematical Models for Determining Synergy

Unfortunately, the determination of what is synergistic is not always simple to define in biological systems. For instance, the additive effect of drugs in combination is not always the arithmetic sum of their effects (Chou, 2010; Roell et al., 2017). While the idea that if *Drug A* causes 20% inhibition and *Drug B* causes 30% inhibition of cell growth then the combination of *Drug A + B* is 50% inhibition is tempting, this cannot always be the case because if the numbers were greater (60% and 80%) then a combined inhibition beyond 100% (140%) is not possible (Chou, 2010). An alternative idea could be that if *A* and *B* retain their 20% and 30% inhibition, respectively, then the fractional product of the combination *A+B* may be 44% (Chou, 2010).

$$1 - ((1 - A) \times (1 - B)) = A + B$$

This approach may be true in simple systems, but is flawed if either drug does not follow first order kinetics or has a high or low affinity (a Michaelis constant $\neq 1$) for the active site (Michaelis and Menten, 1913; Chou, 2010; Michaelis et al., 2011).

To address this problem, mathematical reference models have been developed for the determination of synergy. The most popular models used are Loewe Additivity and Bliss Independence (Roell et al., 2017; Lederer et al., 2019). By calculating a reference value for the additive effect, any significant deviation from that value can be classified as synergy or antagonism (Roell et al., 2017). Therefore, a basic understanding of these reference models is needed to assess drug synergy.

1.7.4.1: Loewe Additivity

The first of the commonly used methods to determine synergy is the Loewe Additivity reference model (Loewe and Muischnek, 1926; Loewe, 1928). This model makes 3 fundamental assumptions which tend to hold true when a pair of drugs share the same mechanism of action: the sham combination principle, the dose equivalence principle, and the constant potency principle (Roell et al., 2017; Lederer et al., 2018; Lederer et al., 2019; Duarte and Vale, 2022).

The sham combination principle holds that a drug cannot interact with itself, where mixing discreet concentrations of *Drug A* can only result in a purely additive effect (Roell et al., 2017; Lederer et al., 2019). The second assumption, the dose equivalence principle, holds that for any concentration *a* of *Drug A* there is a corresponding concentration *b* of *Drug B* which will have the same degree of effect (Duarte and Vale, 2022). The inverse is also true where any concentration *b* will have a corresponding concentration *a*. When both principles are combined, they predict how combinations of *Drug A* and *Drug B* would be able to interact additively to produce the same effect.

The final component of the Loewe Additivity model is the constant potency principle, where concentrations of Drugs *A* and *B* that have the same effect can be used to generate a ratio which is constant for any given degree of effect (Roell et al., 2017). Taken as a group, these assumptions mean that a known degree of effect established for a pair of drugs acting independently can be plotted such that a straight line can be drawn

between them and all concentration combinations along that line can be predicted to be additive when the following equation holds true:

$$\frac{a}{a^*} + \frac{b}{b^*} = 1$$

where a is the concentration of *Drug A* tested, b is the concentration of *Drug B* tested, and a^* and b^* are concentrations of a and b known to produce the same degree of effect (Lederer et al., 2018). Deviation from this predicted result would be interpreted as synergistic if the degree of effect is less than 1, or antagonistic if the degree of effect is greater than 1. This model can be extended further to account for any number of drugs in combination (Berenbaum, 1977; Roell et al., 2017).

$$\frac{a}{a^*} + \frac{b}{b^*} + \dots + \frac{n}{n^*} = 1$$

The main limitations of the Loewe Additivity model are that it assumes that the drugs being compared have the same mechanism of action and that they have similar potency (Roell et al., 2017). A further complication is that this model requires full characterization of the dose response curves for each drug individually and in combination, which can result in complex experimental design.

1.7.4.2: Chou-Talalay Combination Index

The Chou-Talalay Combination Index is derived from the Loewe Additivity model (Berenbaum, 1977; Chou and Talalay, 1983; Chou and Talalay, 1984; Roell et al., 2017; Duarte and Vale, 2022). This method expands on that proposed by Loewe by involving the median effect equation:

$$\frac{f_a}{f_u} = \left(\frac{D}{D_m}\right)^m$$

where D is the dose, f_a is the fraction affected by the dose, f_u is the fraction unaffected by the dose, D_m is the dose required to produce a median effect, and m is a coefficient used to define the slope of the dose-effect curve (Chou and Talalay, 1984). By using the median effect equation, the Chou-Talalay Combination Index can use data collected from dose response curve experiments involving a pair of drugs individually and in combination at a single, constant ratio to determine a combination index (CI) value with the following equation:

$$CI = \frac{(D)_A}{(D_x)_A} + \frac{(D)_B}{(D_x)_B}$$

where $(D)_A$ is the dose of *Drug A* in the combination, $(D)_B$ is the dose of *Drug B* in the combination, $(D_x)_A$ is the dose of *Drug A* alone needed to achieve a f_a of $x\%$, and $(D_x)_B$ is the dose of *Drug B* alone needed to achieve a f_a of the same $x\%$ (Chou and Talalay, 1984). This simplifies the experimental design needed from that of the earlier Loewe method. This combination index calculation can be modified to simulate any value of f_a by including the ratio of the drugs and the slope, m , for the median effects plot:

$$CI = \frac{(D)_{1,2} \left[\frac{P}{P+Q} \right]}{(D_m)_1 \left[\frac{f_a}{1-f_a} \right]^{1/m_1}} + \frac{(D)_{1,2} \left[\frac{Q}{P+Q} \right]}{(D_m)_2 \left[\frac{f_a}{1-f_a} \right]^{1/m_2}}$$

where P is the concentration of *Drug A* relative to Q the concentration of *Drug B* (Zhang et al., 2016).

The combination index equation is similar to that defined by Loewe, where a value of 1 would again indicate additivity, less than 1 would indicate synergism, and greater than 1 would indicate antagonism. Like Loewe Additivity, the Chou-Talalay Combination Index assumes the drugs being compared have a similar mechanism of action (Roell et al., 2017).

In addition to the median effect equation and combination index, a dose reduction index can be calculated using the following equations:

$$(DRI)_1 = \frac{(D_m)_1 \left[\frac{f_a}{1 - f_a} \right]^{1/m_1}}{(D)_1}$$

$$(DRI)_2 = \frac{(D_m)_2 \left[\frac{f_a}{1 - f_a} \right]^{1/m_2}}{(D)_2}$$

Where the fraction affected f_a is equivalent to IC_x where x is any value from 0.05 to 0.97. Like the combination index, a dose reduction index of 1 indicates that no dose reduction takes place, and a value greater than or less than 1 would indicate the fold change in dose required to achieve the same fraction affected when the compounds are delivered at the modeled ratio. (Zhang et al., 2016).

1.7.4.3: Bliss Independence

In contrast to Loewe Additivity, the Bliss Independence model is based on the principal assumption that the sites of action by the drugs being assessed for synergistic effect are independent (Bliss, 1939; Lederer et al., 2019). The most commonly used equation for Bliss Independence is as follows:

$$E_{AB} = E_A + E_B(1 - E_A)$$

where E_{AB} is the combined effect of *Drug A* and *Drug B*, E_A is the effect of *Drug A* alone, and E_B is the effect of *Drug B* alone (Roell et al., 2017; Lederer et al., 2019; Duarte and Vale, 2022). If the actual effect measured is greater than the E_{AB} predicted, then the interaction is classified as synergism, if it is smaller than predicted it is classified as antagonism (Duarte and Vale, 2022).

This equation can be thought of as describing the probability of each of the drugs resulting in statistically independent effects, hence the name of the model. The limitations of the Bliss model include that it relies on differing sites of action of drugs being compared and it presumes that the drugs will have an exponential dose-effect response

(Duarte and Vale, 2022). It is also limited in that it can only be used to assess categorical datasets with only two possible states, for example cells being alive or dead, as opposed to continuous data like blood pressure or time.

Chapter 2: Research Rationale, General Hypothesis, and Objectives

Breast cancer is the most common cancer in Canadian women and advanced, metastatic breast cancer remains incurable (Brenner et al., 2022). 15-20% of invasive breast cancers are TNBCs, which are not susceptible to targeted therapies and require the use of cytotoxic therapies instead (Ismail-Khan and Bui, 2010; Li et al., 2017). Overexpression of drug efflux transporters is a common occurrence with prolonged breast cancer treatment, leading to development of MDR (Longley and Johnston, 2005). It is therefore important to develop novel cytotoxic therapeutics which are not susceptible to MDR so that further treatment options remain available once MDR has begun to develop. It has previously been determined that many jadomycin analogues retain their ability to reduce viability in MDR human breast cancer cells overexpressing *ABCB1*, *ABCC1*, and *ABCG2*, suggesting that they could be useful in the treatment of MDR, TNBC and justifying further research into their anticancer effects (Issa et al., 2014; Hall et al., 2017). Jadomycin B has been the most extensively studied jadomycin analogue in the search for a mechanism of action and the only jadomycin studied in animal models (Fu et al., 2008; Issa et al., 2014; Hall et al., 2015; Hall et al., 2017; Bonitto et al., 2021; McKeown et al., 2022). While several mechanisms of action have been proposed for jadomycin B, these tend to be observed at concentrations higher than those needed to observe the cytotoxic effects. Understanding the mechanism through which a molecule exerts a cytotoxic effect can be useful in determining which tumour types or subpopulations are most likely to exhibit a clinical response to that molecule. Additionally, knowledge of the mechanism through which a drug exerts an effect is useful in determining possible combination therapies which may potentiate or compliment those effects. It is therefore important to further refine our understanding of the action of jadomycin B *in vitro* to determine how it causes cancer cell death.

The purpose of this work is to expand on the current body of knowledge regarding the action of jadomycin B on human breast cancer cells *in vitro*. It was therefore hypothesized that **jadomycin B exerts a cytotoxic effect on human, multidrug resistant triple negative breast cancer cells due to low susceptibility to drug efflux mechanisms through interaction with an intracellular target**. The overall objective of

this work was to investigate the interaction of jadomycin B with previously proposed molecular targets and to develop a jadomycin-resistant human breast cancer cell line to elucidate further pharmacological mechanism(s) through which jadomycin B may exert anticancer activity. To achieve this overall objective, the following specific objectives have been investigated:

- 1) Determination of the effect of jadomycin B on topoisomerase-2
- 2) Establishment of a jadomycin-resistant human breast cancer cell line
- 3) Determination of additional mechanisms through which jadomycin B may be exerting its effect
- 4) Determination of synergistic potential of jadomycin B in combination with other small molecules rationally selected based on putative mechanisms identified by the results of objectives 1-3

Each of the above specific objectives have been achieved.

Chapter 3: Materials and Methods

The third chapter of this work will present the materials and methods used to conduct the research necessary to achieve the specific objectives outlined in the preceding chapter.

3.1: Chemical and Biological Materials

Dulbecco's modified Eagle's medium (DMEM), fetal bovine serum (FBS), penicillin and streptomycin, sodium pyruvate, trypsin, phosphate buffered saline (PBS), Super Script II Reverse Transcriptase, Random Hexamer Primer, RNase OUT, dithiothreitol (DTT), deoxynucleoside triphosphates (dNTPs), Reverse Transcriptase Buffer, and antibiotic-antimycotic solution were purchased from Thermo Fisher Scientific (Burlington, ON).

Jadomycin B, mitoxantrone, doxorubicin, thiazolyl blue methyltetrazolium bromide (MTT), SN-38, MG132, dimethyl sulfoxide (DMSO), celecoxib, ibuprofen, naproxen, bovine serum albumin (BSA), sodium carbonate (Na_2CO_3), sodium hydroxide (NaOH), copper(II) sulfate pentahydrate ($\text{CuSO}_4 \cdot 5\text{H}_2\text{O}$), potassium sodium tartrate tetrahydrate ($\text{KNaC}_4\text{H}_4\text{O}_6 \cdot 4\text{H}_2\text{O}$), Folin and Ciocalteu's phenol reagent, tris-HCl, sodium dodecyl sulfate (SDS), bromophenol blue, glycerol, β -mercaptoethanol, acrylamide, N'N' methylenebisacrylamide, ammonium persulphate, N,N,N',N'- Tetramethylethylenediamine (TMED), glycine, sodium chloride (NaCl), potassium chloride (KCl), tween-20, chloroform, methanol, apramycin sulfate, magnesium sulfate (MgSO_4), ammonium heptamolybdate tetrahydrate ($(\text{NH}_4)_6\text{Mo}_7\text{O}_{24} \cdot 4\text{H}_2\text{O}$), potassium phosphate dibasic (K_2HPO_4), potassium phosphate monobasic (KH_2PO_4), sulfuric acid (H_2SO_4), and dichloromethane were purchased from Sigma-Aldrich (Oakville, ON).

D-maltose, yeast extract, malt extract, agar, 3-(*N*-morpholino)propanesulfonic acid, *L*-isoleucine, *L*-serine, and *L*-phenylalanine were purchased from Bioshop Canada Inc. (Burlington, ON).

Ferrous sulfate ($\text{FeSO}_4 \cdot 7\text{H}_2\text{O}$), calcium chloride (CaCl_2), zinc sulfate ($\text{ZnSO}_4 \cdot 7\text{H}_2\text{O}$), manganese sulfate ($\text{MnSO}_4 \cdot 4\text{H}_2\text{O}$), boric acid (H_3BO_3), and glucose were purchased from Fisher Scientific Canada (Ottawa, ON).

Anhydrous ethanol was purchased from Commercial Alcohols (Brampton, ON).

Nitrocellulose membranes were purchased from GE Healthcare (Mississauga, ON).

MammoCult medium, proliferation supplement, heparin solution, and hydrocortisone solution were purchased from Stem Cell Technologies (Vancouver, BC).

Immunoblot blocking solution, protein ladder, and all secondary antibodies used in this study (**Table 3.1**) were purchased from LI-COR Biosciences (Lincoln, NE).

Primary antibodies for TOP1, TOP2 α , and TOP2 β (**Table 3.1**) were purchased from TopoGEN Inc. (Buena Vista, CO).

All other primary antibodies used in this study (**Table 3.1**) were purchased from Abcam Inc. (Toronto, ON).

Table 3.1: Primary and Secondary Antibodies used for Immunoblotting Assays

List of primary and secondary antibodies used in this work, with expected molecular weight of bands in Western Blot, dilution ratio used, and manufacturer product number.

1° Antibody	Molecular Weight (kDa)	Dilution Ratio	Manufacturer (Product Number)
Mouse-anti- β -actin	42	1:1000	Abcam Inc. (ab8226)
Mouse-anti-TOP1	100	1:1000	TopoGEN Inc. (TG1020-1)
Rabbit-anti-AKT (AKT1 + AKT2 + AKT3)	56	1:1000	Abcam Inc. (ab179463)
Rabbit-anti-COX2	69	1:500	Abcam Inc. (ab179800)
Rabbit-anti-EP4	40	1:500	Abcam Inc. (ab217966)
Rabbit-anti-mTOR	289	1:1000	Abcam Inc. (ab134903)
Rabbit-anti-p-AKT (AKT1 + AKT2 + AKT3 [phospho S472 + S473 + S474])	56	1:1000	Abcam Inc. (ab192623)
Rabbit-anti-PI3K p85 α	84	1:1000	Abcam Inc. (ab191606)
Rabbit-anti-p-PI3K p85 α (phospho Y607)	84	1:1000	Abcam Inc. (ab182651)
Rabbit-anti-TOP2A	170	1:1000	TopoGEN Inc. (TG1020-2a)
Rabbit-anti-TOP2B	180	1:1000	TopoGEN Inc. (TG1020-2b)
2° Antibody		Dilution Ratio	Manufacturer (Product Number)
Donkey-anti-mouse 680RD	-	1:10,000	LI-COR Biosciences (LI926-68072)
Goat-anti-rabbit 800CW	-	1:10,000	LI-COR Biosciences (LI926-3221)

3.2: Production of Jadomycins

Jadomycin B (*L*-isoleucine), jadomycin F (*L*-phenylalanine), and jadomycin S (*L*-serine) were isolated and characterized as previously described (Jakeman et al., 2006; Jakeman et al., 2009b; Dupuis et al., 2011; Issa et al., 2014; Robertson et al., 2018). These jadomycin analogues were chosen as they represent 3 categories spanning the diversity of jadomycins: jadomycins with hydrophobic aliphatic side chains (B), hydrophobic aromatic side chains (F), and hydrophilic side chains (S). *S. venezuelae* ISP 5230 bacteria were cultured on MYM agar (0.4% w/v maltose, 0.4% w/v yeast extract, 1% w/v malt extract, 1.5% w/v agar) at pH 7.0, supplemented with 50 µg/ml apramycin sulfate at 30 °C until sporulation occurred (approximately 3 weeks). Surface growth and spores were collected from a 1 cm² area of bacterial growth and used to inoculate 250 ml of liquid MYM medium (0.4% w/v maltose, 0.4% w/v yeast extract, 1% w/v malt extract) at pH 7.0 and incubated for 24 h at 30 °C in a controlled environment incubator-shaker (New Brunswick Scientific, Edison, NJ) at 250 RPM. At 24 h, bacteria were pelleted in a Sorvall Legend RT centrifuge (Mandel Scientific, Guelph, ON) at 3750 RPM (2800 x G) for 30 min and washed with mineral salts medium (MSM; 0.4 g/L magnesium sulfate, 3.77 g/L 3-(*N*-morpholino)propanesulfonic acid, 4.5 mL/L iron sulfate, 0.09 g/L sodium chloride, 0.09 g/L calcium chloride, 4.0 mg/L zinc sulfate, 0.18 mg/L copper sulfate, 0.027 mg/L manganese sulfate, 0.026 mg/L boric acid, and 0.017 mg/L ammonium heptamolybdate tetrahydrate) at pH 7.0, 3 times before resuspension in 15 mL MSM. Bacteria was added to a production medium (MSM with 33mM glucose and 50 µM 7:3 potassium phosphate dibasic:monobasic) supplemented with 60 mM amino acid (*L*-isoleucine for jadomycin B, *L*-phenylalanine for jadomycin F, or *L*-serine for jadomycin S) until absorbance at 600 nm was 0.6, as measured on a SpectraMax-plus 384 spectrophotometer (Cambridge Scientific, Watertown, MA) using a cuvette with a 1 cm path length. Production media was adjusted to pH 7.5 and 3% v/v anhydrous ethanol was added before incubation at 30 °C for 24 h in an incubator-shaker at 250 RPM, with pH readjusted to 7.5 every 24 h. Absorbance readings at 526 nm were measured every 8 h until a reading of ≥ 0.5 was recorded, at which point bacteria and debris were removed from the medium *via* suction filtration through Whatman No. 5 filter paper (Fisher

Scientific Canada) followed by 0.4 μm and 0.22 μm Millipore Durapore membrane filters (Millipore-Sigma, Oakville, ON).

Once filtered, medium was passed through a reverse-phase SiliCycle phenyl column (70 g; Quebec City, QC) using a Biotage SP1 Flash Chromatograph (Charlottesville, VA) and washed with distilled water until flow through the column was colourless (approximately 8 L). Material remaining in the column was eluted using 100% methanol and dried *in vacuo* to form a crude extract. Thin layer chromatography using normal phase silica gel plates (Silicycle) was used to separate jadomycins against known samples using dichloromethane:methanol:water (95.6:4.0:0.4) and bands were scraped off the glass backing and eluted with methanol. Samples were dried using a GeneVac EZ-Bio evaporator (SP Scientific, Warminster, PA) and stored at $-80\text{ }^{\circ}\text{C}$ for future use.

Synthesized jadomycin B was used only in the comparison against commercially produced jadomycin B (Sigma-Aldrich) reported in **section 4.1**. All other experiments involving jadomycin B were conducted using commercially available material.

3.3: Cell Lines

MCF-7 cells were kindly provided by Dr. Aik Jiang Lau (Dalhousie University, Halifax, Canada). Control MDA-MB-231 (231-CON) cells were kindly provided by Drs. David Hoskin and Anna Greenshields (Dalhousie University, Halifax, NS, Canada). Polyclonal jadomycin-resistant MDA-MB-231 cells (231-JB) and mitoxantrone resistant MDA-MB-231 cells (231-MITX) were generated in-house using previously described methods (Schneider et al., 1994; Hall et al., 2017). Briefly, increased resistance to jadomycin B or mitoxantrone was selected for by gradually increasing concentrations of jadomycin B or mitoxantrone in growth medium over 7 months until a final concentration of 3.0 μM jadomycin B or 0.015 μM mitoxantrone, respectively, was reached. Cells were not exposed to mutagens prior to selection nor clonally isolated after selection. Following selection, 231-JB and 231-MITX cells were passaged in drug-free medium and remained stably resistant to jadomycin B or mitoxantrone, respectively. To prevent reversion of resistance, 231-JB and 231-MITX cells were maintained in medium containing 3.0 μM

jadomycin B or 0.015 μM mitoxantrone, respectively. Resistant cells were cultured in drug-free medium for 1 week prior to experiments.

3.4: Cell Culture

All human breast cancer cell lines (231-CON, 231-JB, 231-MITX, and MCF-7) were cultured in 75 mm² tissue-culture flasks (Corning Inc., Corning, NY) in phenol red free DMEM supplemented with 10% FBS, 100 IU/mL penicillin and 250 $\mu\text{g}/\text{mL}$ streptomycin, and 1mM sodium pyruvate (complete medium) at 37 °C in a humidified atmosphere of 5% CO₂ (standard conditions). Cells were subcultured and/or growth medium was changed every 3-4 days up to a maximum of 35 passages. To subculture, all relevant solutions were warmed to 37 °C then the medium was removed from cells by aspiration and cells were removed using 0.25% trypsin diluted in PBS then re-suspended in complete medium and centrifuged for 6 min at 740 x G. The medium was removed by aspiration and the remaining cell pellet was resuspended and washed in PBS before being centrifuged again. PBS was removed by aspiration and the pellet was resuspended in 5 mL fresh complete medium before being counted using a TC20 Automated Cell Counter (Bio-Rad Laboratories, Mississauga, ON) and reseeded into a new flask for continued culture or multi-well plate (Corning Inc.) for experimentation.

3.5: MTT Viability Assays

Thiazolyl blue methyltetrazolium bromide (MTT) assays were used to evaluate relative anticancer activity of jadomylicins B, S, and F (0.2-25 μM) and the ABC transporter substrates mitoxantrone (0.004-50 μM), doxorubicin (0.08-15 μM), and SN-38 (0.08-20 μM) in 231-CON, 231-JB, and 231-MITX cells as previously described (Issa et al., 2014). Jadomycin B (0.2-25 μM) and mitoxantrone (0.5-10 μM) were evaluated in MCF-7 cells. Briefly, cells were seeded in 96-well plates (Corning Inc.) at 5000 cells/well in 100 μL of complete medium and allowed to adhere for 24 h under standard conditions, then exposed to the above concentrations for 48 or 72 h. Following incubation, 20 μL of MTT solution (5 mg/mL) in PBS was added to medium and incubated for 2 h at 37 °C in

the dark. Medium and MTT solution were aspirated and formazan containing cells were solubilized in 100 μ L of DMSO. Optical density of formazan was measured at 550 nm using a BioTek Synergy HT plate reader using Gen5 v2.01 software (Agilent Technologies, Mississauga, ON) and mean readings from blank wells were subtracted from all test and control well measurements. Cell viability was calculated as the absorbance of each well divided by the average absorbance of the vehicle control wells multiplied by 100.

$$\% \text{ Cell Viability} = \frac{\text{mean absorbance in test wells}}{\text{mean absorbance in control wells}} \times 100$$

The IC₅₀ was calculated from the log₁₀ concentration versus normalized response curves using the following equation:

$$y = \frac{100}{(1 + 10^{(\log_{10} IC_{50} - x) \times \text{hill slope}})}$$

where y is the measured absorbance at 550 nm and x is the drug concentration. Fold-resistance values for 231-JB and 231-MITX cells were obtained by dividing the IC₅₀ values by the mean IC₅₀ value calculated for 231-CON cells (Limtrakul et al., 2007).

3.6: Jadomycin B Aging and Evaluation of Potency and Chemical Stability

To verify that jadomycin B remained stably potent at experimental conditions, a series of aging experiments were conducted. Jadomycin B (1 mg/mL) dissolved in DMSO or vehicle alone was aliquoted to individual treatment volumes, sealed with parafilm, and then stored at -80 °C. Samples were retrieved from storage at -80 °C and allowed to age, at either 25 °C or 37 °C, in the dark for 0-90 days such that all timepoints in a replicate could be tested simultaneously.

Cellular viability (as described in **section 3.5**) and absorption spectra were measured for each of the aged samples to determine changes in potency or colour.

Cellular viability was assayed at jadomycin B concentrations ranging from 0.1-10 μM for 72h. Absorption spectra was measured by diluting jadomycin B to 100 μM in DMSO in a 96-well UV-Star optically clear microplates (Greiner Bio-One Inc., Monroe, NC) using a BioTek Synergy HT plate reader using Gen5 v2.01 software (Agilent Technologies, Mississauga, ON) and absorbance readings were taken at 1 nm intervals between 200-700 nm.

3.7: Combination Index and Drug Reduction Index Calculation

Synergy was assessed between jadomycin B (0.1-10 μM), known TOP2 poisons doxorubicin (0.08-15 μM) and mitoxantrone (0.004-5.0 μM), known TOP1 poison SN-38 (0.16-20 μM), and proteasome inhibitor MG132 (0.06-1.8 μM) using the Chou-Talalay method to calculate combination index values and drug reduction index values as described in **section 1.7.4.2**. Briefly, combination index represents the fold change in potency of drugs used in combination while drug reduction index represents the fold change in dose needed to attain a similar degree of potency. Comparisons were designed as previously described (Zhang et al., 2016). Briefly, MTT assays were used to measure cellular viability (**section 3.5**) in 231-CON cells for each agent alone and constant-ratio combinations of each pair of agents included in the analysis: jadomycin B:doxorubicin (1:1.5), jadomycin B:mitoxantrone (10:1), jadomycin B:SN-38 (1:1), jadomycin B:MG132 (1:0.18), doxorubicin:mitoxantrone (15:1), doxorubicin:SN-38 (1.5:1), doxorubicin:MG132 (8:1), mitoxantrone:SN-38 (1:10), mitoxantrone:MG132 (1:1), and SN-38:MG132 (8:1). Combination index and dose reduction index values were then used to interpolate effect size at all fractions of effect between 0.05 and 0.97 at intervals of 0.05 (equivalent to $\text{IC}_5 - \text{IC}_{97}$ in the context of the MTT assays used). CompuSyn was used to perform the median effect, combination index, and dose reduction index calculations described in **section 1.7.4.2**. As combination index represents fold change in potency and dose reduction index represents fold change in dose needed to attain a given degree of potency, changes of 0.1 (10%) or greater were considered significant. All comparisons were analyzed using CompuSyn software v1.0 (ComboSyn Inc., Paramus, NJ).

3.8: Flow Cytometry and Cell Cycle Analysis

Flow cytometric analysis was used to characterize cell cycle progression in 231-CON cells exposed to jadomycin B (1.0 μ M), mitoxantrone (0.01 μ M), or vehicle control for 48 hours. Cells were cultured as above, then synchronized to G₀ by culturing them for 24 hours in a defined medium consisting of DMEM supplemented with 100 IU/mL penicillin and 250 μ g/mL streptomycin, and 1mM sodium pyruvate at standard conditions before exposure began. Cells were centrifuged for 6 min at 740 x G, washed in 5 mL ice cold PBS, centrifuged again, and resuspended in 0.5 mL ice cold PBS. Cells were then fixed by adding 4.5 mL ice cold 70% ethanol dropwise while vortexing. Cells were incubated at 4 °C for 24 hours to complete fixation. Fixed cells were centrifuged at 1000 x G for 5 min and resuspended in 300 μ L staining solution consisting of 0.1 % (v/v) Triton-X in PBS, 2 μ L/mL of RNase A, and 20 μ L/mL of propidium iodide (at a concentration of 1mg/mL in PBS) and incubated for 30 minutes at room temperature, in the dark. Following incubation, fluorescence was measured at 488 nm excitation and a 585/42 nm emission filter using a FACSCanto II flow cytometer (BD Biosciences, Mississauga, ON) equipped with BD CellQuest version 3.3 software (BD Biosciences). A minimum of 10000 cells were collected for flow cytometric analysis per sample, and each sample was measured in triplicate. Cell counts were gated on the live cell population plotted on FSC-H versus SSC-H and linked to plots for propidium iodide. Data were analyzed using ModFit LT software version 3.0 (Verity Software House, Topsham, ME).

3.9: *In Vivo* Complex of Enzyme Assay

Accumulation of topoisomerase cleavage complexes was quantified using *in vivo* complex of enzyme (ICE) assays (TopoGEN Inc.) as per manufacturer instructions. To collect DNA-enzyme cleavage complexes, 231-CON cells were seeded on 100 mm tissue culture dishes (Falcon, Mississauga, ON) in complete medium and cultured at standard conditions until 80-95% confluence was reached. Cells were then exposed to jadomycin B (50 μ M), epotoside (80 μ M), camptothecin (80 μ M), or vehicle control (DMSO) for 60 min to allow cleavage complexes to form. TopoGEN cell lysis solution was used to

prepare samples and DNA was eluted using 70% ethanol and collected *via* spooling on a micropipette tip. The DNA sample was washed using TopoGEN wash solution and resuspended using TopoGEN DNA resuspension solution with a proprietary fixative added. Once resuspended, DNA samples were mechanically sheared by pipetting to reduce viscosity.

DNA samples were quantified using a BioTek Synergy HT plate reader using Gen5 v2.01 software (Agilent Technologies) in a UV transparent microplate (Corning Inc.) with pathlength correction. DNA samples diluted to an equivalent concentration (1 $\mu\text{g}/100 \mu\text{L}$) were loaded into wells of a dot blot apparatus (Bio-Rad Laboratories) containing a nitrocellulose membrane pre-soaked in 25 mM sodium phosphate for 30 min. A light vacuum (-14 kPa) was applied to the apparatus to facilitate sample filtration through the membrane. Membranes were then washed for 15 min in tris-buffered saline (TBS)-Tween (0.1% v/v) at room temperature and then placed in LI-COR blocking solution for 30 min. After blocking, membranes were again washed in TBS-Tween (0.1% v/v) for 10 min before incubation in a 1:1000 dilution of primary antibody (**Table 3.1**) for 2 h at room temperature, followed by washing three times with TBS-Tween (0.1 % v/v) for a total of 30 min and incubation in a 1:10,000 dilution of secondary antibody (**Table 3.1**) for 1 h at room temperature, in the dark. After incubation with secondary antibodies membranes were again washed three times with TBS-Tween (0.1 % v/v) for a total of 30 min and then visualized. For visualization and quantification, membranes were scanned at 800 nm using a LI-COR Odyssey CLx Imager (Mandel Scientific) and analyzed using Image Studio v5.2 software (Mandel Scientific) to measure pixel intensity.

3.10: RNA Isolation, Reverse Transcription, and Quantitative Real-Time Polymerase Chain Reaction

Total RNA was isolated from lysates of 231-CON, 231-JB, and 231-MITX cells using the Aurum Total RNA Mini Kit (Bio-Rad Laboratories) as per manufacturer instructions. Cells were seeded in 6-well plates (Corning Inc.) at 200,000 cells/well in 2 mL of drug-free complete medium and allowed to adhere under standard conditions. Cells were then either allowed to grow for 48 h and collected to generate control samples or

exposed in triplicate for 48 h with either DMSO vehicle control, or jadomycin B (2.5-5.0 μM). Triplicate well lysates were pooled to generate a single sample. RNA samples were quantified using a BioTek Synergy HT plate reader using Gen5 v2.01 software (Agilent Technologies) in a UV transparent microplate (Corning Inc.) with pathlength correction. Isolated RNA (0.5 μg) was reverse transcribed to complementary DNA using Super Script II Reverse Transcriptase and a TProfessional Basic 96 Thermocycler (Montreal Biotech Inc., Kirkland, QC). Complementary DNA was amplified by quantitative polymerase chain reaction (PCR) using 125 nM gene-specific primers (**Table 3.2**) in a total volume of 20 μL using Sso Advanced Universal SYBER Green Supermix (Bio-Rad Laboratories), and a Step One Plus real-time PCR thermocycler (Applied Biosystems, Foster City, CA) using StepOne Software v2.1 (Applied Biosystems) in duplicate for each primer set. Gene expression was normalized using the average of three housekeeping genes (*glyceraldehyde phosphate dehydrogenase* [*GAPDH*], *β -actin*, and *peptidylprolyl isomerase A* [*PPIA*, alternatively known as *cyclophilin A*]) via the $\Delta\Delta\text{C}_t$ method (Livak and Schmittgen, 2001).

Table 3.2: PCR Primers Used in this Work

List of PCR primers used to determine expression of relevant genes in 231-CON, 231-JB, and 231-MITX cells.

Gene	PCR Forward Primer (5'-3')	PCR Reverse Primer (5'-3')
<i>β-actin</i>	GGACTTCGAGCAAGAGATGG	AGCACTGTGTTGGCGTACAG
<i>ABCB1</i>	AGGCCAACATACATGCCTTC	CCTTCTCTGGCTTTGTCCAG
<i>ABCC1</i>	AGGTGGACCTGTTTCGTGAC	TCCACCAGAAGGTGATCCTC
<i>ABCG2</i>	TTATCCGTGGTGTGTCTGGA	TTCCTGAGGCCAATAAGGTG
<i>GAPDH</i>	GAGTCAACGGATTTGGTCGT	TTGATTTTGGAGGGATCTCG
<i>PPIA</i>	ACCGCCGAGGAAAACCGTGT	CTGTCTTTGGGACCTTGCTGCA
<i>PTGER4</i>	TGCTCTTCTTCAGCCTGTCC	GAGCTACCGAGACCCATGTT
<i>PTGS1</i>	GCACAGGAGCCTGCACTC	GTCACACTGGTAGCGGTCAA
<i>PTGS2</i>	CTGATGATTGCCCGACTCCC	CGCAGTTTACGCTGTCTAGC

3.11: RT² Profiler PCR Array

Total RNA was collected and converted to cDNA as in **section 3.10** from 231-CON and 231-JB cells which were not exposed to any small molecule intervention. Human Cancer Drug Targets RT² Profiler PCR Arrays (Qiagen Inc., Mississauga, ON) were conducted as per manufacturer instructions using a Step One Plus real-time PCR thermocycler using StepOne Software v2.1 (Applied Biosystems).

3.12: Immunoblot Analysis

231-CON and 231-JB cells were seeded in 6-well plates (Corning Inc.) at 200,000 cells per well and left to adhere overnight in complete medium at standard conditions. Cells were then either collected to generate control samples or exposed in duplicate for 48 h with either drug-free medium, DMSO vehicle control, or jadomycin B (2.5-5.0 μ M). Duplicate wells were pooled to generate a single sample and lysed using RIPA Buffer (Santa Cruz Biotechnologies Inc, Dallas, TX) as per manufacturer instructions. Protein content in lysate was measured using the Lowry Assay (Lowry et al., 1951). Immunoblotting was conducted as previously described (McKeown et al., 2014). Briefly, 25 μ g protein samples were prepared in a standard Laemmli buffer consisting of 50 mM Tris-HCl (pH 6.8), 2% SDS, 0.1% bromophenol blue, 10% glycerol, and 100 mM β -mercaptoethanol then boiled for 3 min (Laemmli, 1970). Electrophoresis through 12.5 % SDS-PAGE gels was conducted in duplicate for each sample and these were transferred to nitrocellulose membranes. Membranes were incubated in LI-COR blocking solution (Mandel Scientific) overnight at 4 °C and then incubated in a 1:500 or 1:1000 dilution of primary antibody (**Table 3.1**) for 1 h at room temperature, followed by washing three times with TBS-Tween (0.1 % v/v) for a total of 30 min and incubation in a 1:10,000 dilution of secondary antibody (**Table 3.1**) for 1.25 h at room temperature, in the dark. After incubation with secondary antibodies membranes were again washed three times with TBS-Tween (0.1 % v/v) for a total of 30 min and then visualized. For visualization and quantification, membranes were scanned at 700 nm and 800 nm using a LI-COR Odyssey CLx Imager (Mandel Scientific) and analyzed using Image Studio v5.2 software

(Mandel Scientific) to measure pixel intensity. Pixel intensity of each band was normalized to the intensity of the respective β -actin band and these ratios were expressed as a fold change versus either unexposed 231-CON cells or vehicle control 231-CON cells.

3.13: PGE₂ ELISA

Levels of PGE₂ in cell culture medium were measured using a colorimetric PGE₂ ELISA Kit (Abcam Inc.) as per manufacturer instructions. Briefly, 231-CON cells were seeded into 6-well plates (Corning Inc.) at 400,000 cells per well and left to adhere overnight in complete medium at standard conditions. Cells were exposed to jadomycin B (2.5 or 5.0 μ M) or vehicle control (DMSO) in complete medium for 6, 24, 48, or 72 h, then the medium was collected and a total of 3 unique samples were immediately assayed in duplicate. Optical density of each sample was read at 405 nm and compared against a standard curve comprised of known PGE₂ concentrations. Optical density of non-specific binding controls were subtracted from the average optical density of duplicate test or standard readings. Each standard concentration of PGE₂ was calculated as a percentage of the maximum binding in blank wells containing no PGE₂, then the standards were plotted on a logarithmic scale and a line of best fit was calculated. Unknown concentrations of PGE₂ were interpolated using this line of best fit.

3.14: Cellular Lipid Profile Analysis

Cellular lipid profile analysis was conducted as previously described (Hall et al., 2020). Briefly, 231-CON cells were cultured in jadomycin B (2.5 or 5.0 μ M) or DMSO vehicle control for 24 or 48 hours in complete medium under standard conditions, then fixed in 12 mL 2:1 chloroform:methanol with 0.01 mg internal standard tricosanoic acid (23:0) before lysis by sonication. Lipids were extracted using a modified Floch method (Budge et al., 2004) and extracted lipids were converted to methyl esters using 0.5 N sulfuric acid in methanol at 100 °C for 1 hour (Hilditch and Williams, 1964). Fatty acid analysis was performed on recovered samples (0.10 mg/mL) using splitless injection (250

°C injector temperature) on a gas chromatograph (Bruker Ltd., Milton, ON) with DB-23 column (Agilent Technologies) and flame ionization detector (GCFID). The temperature program used involved an initial temperature of 60 °C for 0.5 minutes, increased to 150 °C at 45 °C/minute, then the temperature was held for 2 minutes before being increased at 5.1 °C/minute to a final temperature of 220 °C and held for 5.77 minutes, yielding a total run time of 24 minutes. FID was set to 270 °C. Samples were analyzed in triplicate and fatty acids profiles are reported as mass percent of total fatty acid identified.

3.15: Calculation of Lipogenesis Indices and Estimated Desaturase Enzyme Activity

Using the cellular lipid data collected as described in **section 3.14** it was possible to use ratios of fatty acids to estimate the effects of a drug exposure on lipogenesis without directly measuring enzymatic activity. An indication of the relative rate of *de novo* lipogenesis can be estimated using the following equation:

$$de\ novo\ lipogenesis = \frac{16:0}{18:2n-6}$$

where 16:0 (palmitic acid) is the fatty acid preferentially generated by mammalian fatty acid synthase and 18:2n-6 (linoleic acid) cannot be synthesized by human cells (Hudgins et al., 1996; Cedernaes et al., 2013; Drąg et al., 2017). To determine if the observed changes in percent of total for a particular fatty acid are a result of a shift between n-3 and n-6 fatty acids, the following equation:

$$n-3/n-6\ ratio = \frac{(18:3n-3 + 20:3n-3 + 20:5n-3 + 22:5n-3 + 22:6n-3)}{(18:2n-6 + 18:3n-6 + 20:2n-6 + 20:3n-6 + 20:4n-6 + 22:2n-6 + 22:4n-6)}$$

can be used to estimate any broad shift between the two groups (Jurczyszyn et al., 2015).

To estimate the relative activity of the $\Delta 5$ desaturase ($\Delta 5D$) and $\Delta 6$ desaturase ($\Delta 6D$) enzymes the following equations were used (Cedernaes et al., 2013; Jurczyszyn et al., 2015; Drąg et al., 2017; Pavithra et al., 2018):

$$\Delta 5 \text{ desaturase } (\Delta 5D) = \frac{20:4n-6}{20:3n-6}$$

$$\Delta 6 \text{ desaturase } (\Delta 6D) = \frac{20:3n-6}{18:2n-6}$$

3.16: Purified COX2 Enzyme Activity Assay

A fluorometric COX2 Inhibitor Screening Kit (Sigma-Aldrich) was used to evaluate relative inhibitory potential of the COX2 enzyme by jadomycin B (0-20 μM), celecoxib (0-0.2 μM), or a combination of the two. The assay functions by detecting prostaglandin G_2 , a conversion product of AA produced by the COX2 enzyme. Assays were conducted as per manufacturer instructions. Briefly, a reaction mixture consisting of supplied COX Assay Buffer (77.99% v/v), COX Probe (1% v/v), COX cofactor (0.01% v/v), and human recombinant COX2 enzyme (1% v/v) was added to each well of an opaque 96-well plate (Corning Inc.). Jadomycin B, celecoxib, a combination of the two, DMSO vehicle control, or assay buffer was added to each well (10% v/v), then AA (5% v/v) in NaOH (5% v/v) was added and fluorescence was immediately read at 535 nm excitation (using a 530/25 filter) and 587 nm emission (using a 590/20 filter), kinetically, at 25 °C for 5 min at 20 second intervals using a BioTek Synergy HT plate reader using Gen5 v2.01 software (Agilent Technologies). For samples involving a pre-incubation of jadomycin B with the COX2 enzyme, the reaction mixture and jadomycin B were incubated for 30 min at 25 °C in the dark prior to adding AA. Relative fluorescence units (RFU) were plotted against time and a slope was calculated from the line of best fit for the linear range of each sample, as determined by an R^2 value ≥ 0.99 using GraphPad Prism 9 (GraphPad Software, Boston, MA). Each sample was separately measured in triplicate. Relative percent inhibition was calculated using the following equation:

$$\% \text{ Relative Inhibition} = \frac{\text{Slope of Enzyme Control} - \text{Slope of Sample}}{\text{Slope of Enzyme Control}} \times 100\%$$

3.17: Synergy Score Calculation

MTT assays were conducted as described above using combinations of jadomycin B (0-5.0 μM) and celecoxib (0-60 μM), ibuprofen (0-1600 μM), naproxen (0-1500 μM), or vehicle control (DMSO) in 231-CON, 231-JB, or MCF-7 cells. Purified COX2 enzyme activity assays were conducted as above using combinations of jadomycin B (0-20 μM) and celecoxib (0-0.2 μM). The expected drug combination responses were calculated based on the Bliss reference model with LL4 curve fitting using the web-based application SynergyFinder 3.0 (Ianevski et al., 2022). Synergy scores represent fold change from expected effect if the two molecules act additively. Scores < 10 but > -10 denote synergy. Deviations between observed and expected responses with positive (> 10) and negative (< -10) values denote synergy and antagonism respectively.

3.18: Molecular Docking of Molecules of Interest to the COX2 Active Site *In Silico*

Molecular docking was modeled *in silico* using Molsoft ICM-Pro 3.9 (Molsoft, San Diego, CA). Jadomycins B, S, and F, celecoxib, ibuprofen, naproxen, rofecoxib, flufenamic acid, tolfenamic acid, meclofenamic acid, mefenamic acid, salicylic acid, and AA were modeled for docking at the active site of the COX2 enzyme. Reported Score and RTCNNscore were calculated in Molsoft as previously described (Schapira et al., 1999; Totrov and Abagyan, 1999). Score refers to simulated binding energy between the ligand and receptor, where a lower (more negative) Score would indicate greater propensity for binding. RTCNNscore differs from Score in that it represents an adjusted Score determined by a proprietary neural network trained to recognize native-like complexes.

3.19: Cell Spheroid Formation

Two cell spheroid assays were conducted and MCF-7 cells were chosen for these assays due to increased spheroid formation efficiency (Wang et al., 2014). In the first, MCF-7 cells were grown in ultra-low adherent cell culture plates (Corning Inc.) in MammoCult medium supplemented with 10% proliferation supplement, 4 $\mu\text{g}/\text{mL}$

heparin, 0.48 $\mu\text{g}/\text{mL}$ hydrocortisone, and 1% antibiotic-antimycotic solution (spheroid medium) for 2 hours, then exposed to either jadomycin B (0.05-1.5 μM) or vehicle control (DMSO) for 7 days. Each concentration was assayed in triplicate. In the second assay, MCF-7 cells were pre-exposed to either 2.5 or 5.0 μM jadomycin B or vehicle control (DMSO) for 48 h prior to transfer to ultra-low adherent cell culture plates in spheroid medium, then allowed to grow for 7 days in the absence of additional exposure. Each concentration was assayed in triplicate.

Following culture, spheroids were photographed using a Nikon Eclipse TS 100 phase contrast microscope (Nikon, Melville, NY) and spheroids larger than 100 μm were counted. The viability of cells in spheroids was determined using an acid phosphatase assay.

3.20: Acid Phosphatase Assay for Spheroid Viability

Viability of MCF-7 cells in spheroids was measured following exposure to jadomycin B or vehicle control (DMSO) using an acid phosphatase assay as previously described (Greenshields et al., 2015). This assay was chosen because the acid phosphatase buffer lyses the cells prior to analysis, allowing determination of total phosphatase activity of cells in the entire spheroid population as opposed to MTT assays which would only indicate viability of cells on the exterior layer of the spheroid. Spheroids were washed with PBS and resuspended in 1 mL acid phosphatase assay solution (0.1 M sodium acetate at pH 5.5, 0.1% (v/v) Triton-X, and 4 mg/mL phosphatase substrate) and incubated for 2 hours at 37 °C in the dark. The reaction was stopped by adding 25 μL 1 N NaOH. Optical density was measured at 405 nm and mean readings from blank wells were subtracted from all test and control well measurements. Measurements were taken in triplicate as described in **section 3.19**. Acid phosphatase activity was calculated as the absorbance of each well divided by the average absorbance of the vehicle control wells multiplied by 100 and used as a relative indicator of cellular viability.

$$\% \text{ Acid Phosphatase Activity} = \frac{\text{mean absorbance in test wells}}{\text{mean absorbance in control wells}} \times 100$$

3.21: Statistical Analysis

For each experiment individual exposures were performed in duplicate, triplicate, or quadruplicate as described above. All data are expressed as mean \pm standard deviation. An unpaired t-test was used for statistical comparisons involving 2 groups, a one-way ANOVA was used for multiple comparisons in experiments with 1 independent variable, and a two-way ANOVA was used for multiple comparisons with 2 independent variables. A Bonferroni test was used for *post-hoc* analysis of significant ANOVA results. A difference in mean values between groups was considered to be significant when $P \leq 0.05$. All statistical tests were conducted using GraphPad Prism 9 (GraphPad Software).

Chapter 4: Results

The fourth chapter reviews the results collected over the course of this work, describing those results in the order previously described in Chapter 3.

4.1: Comparison of Potency Between Jadomycin B Produced Commercially and Synthesized Locally

The jadomycin analogues used in previous studies by our research group were synthesized locally (Issa et al., 2014; Hall et al., 2015; Hall et al., 2017; McKeown et al., 2022). However, in 2019 a commercial source (Sigma-Aldrich) of jadomycin B became available, which was advantageous to use as it could be acquired in greater quantities and at a faster rate, but at a similar cost to local production. This made cellular assays easier to complete and had the potential to facilitate future work in animal models once the commercial source was established to be equivalent.

To determine if there was any significant difference in jadomycin B potency when procured from a commercial source as compared to locally synthesized material, MTT assays were conducted following 72 h exposure of 231-CON cells to jadomycin B from each source and used to determine IC_{50} values (**Table 4.1** and **Figure B.1**). No significant difference in potency was observed between jadomycin B obtained from the 2 sources. Accordingly, commercially obtained jadomycin B was used in subsequent experimentation.

Table 4.1: Comparison of IC₅₀s after 72 h Exposure to Synthesized or Commercial Jadomycin B in 231-CON cells

231-CON cells were exposed to jadomycin B. (0.21-25 μ M) for 72 h. Calculated IC₅₀ values for jadomycin B synthesized by our research group or purchased commercially are not significantly different (unpaired t-test, P=0.34, n=3). IC₅₀s were calculated using dose response curves generated from datapoints representing the mean value of triplicate assays, each consisting of a mean of quadruplicate technical replicates and expressed as % viability of unexposed controls.

Jadomycin B Source	IC₅₀ μM (95% CI)	SD
Laboratory Synthesis	0.9127 (0.1423-1.683)	0.3101
Commercially Purchased (Sigma-Aldrich)	0.6957 (0.3287-1.063)	0.1478

4.2: Determination of Jadomycin B Cytotoxic Effect Stability Following Long-Term Storage at 25 °C and 37 °C

Prior to beginning this work the long-term stability of jadomycin B was unknown. To determine jadomycin B stability and suitability for prolonged exposure times and at temperatures relevant to *in vitro* and *in vivo* assays, samples of jadomycin B were aged for up to 90 days. No significant difference in jadomycin B potency was observed following storage for up to 60 days at 25 °C in the dark, or following storage for up to 30 days at 37 °C in the dark (**Figures 4.1, B.2, and B.3**) as measured by MTT viability assays in 231-CON cells after 72 h exposure to jadomycin B. While jadomycin B potency remained stable following prolonged storage, a colour change did occur after 8 or more days (**Figures 4.2 and 4.3**) as determined by absorbance spectra readings. As 100 µM jadomycin B demonstrated measurable absorbance readings at 550 nm, a wavelength used to conduct the preceding MTT assays, the absorbance of several concentrations of jadomycin B was measured following dilution in cell culture medium, DMSO, or PBS (**Figure B.4**). At all concentrations lower than 12.5 µM, regardless of diluent, jadomycin B did not significantly affect absorbance as compared to diluent alone. At greater concentrations the measured change, while statistically significant, was not large enough to meaningfully alter results at any concentration tested. As the greatest concentration of jadomycin B used experimentally was less than 20 µM it was determined that jadomycin B did not meaningfully interfere with absorbance at 550 nm.

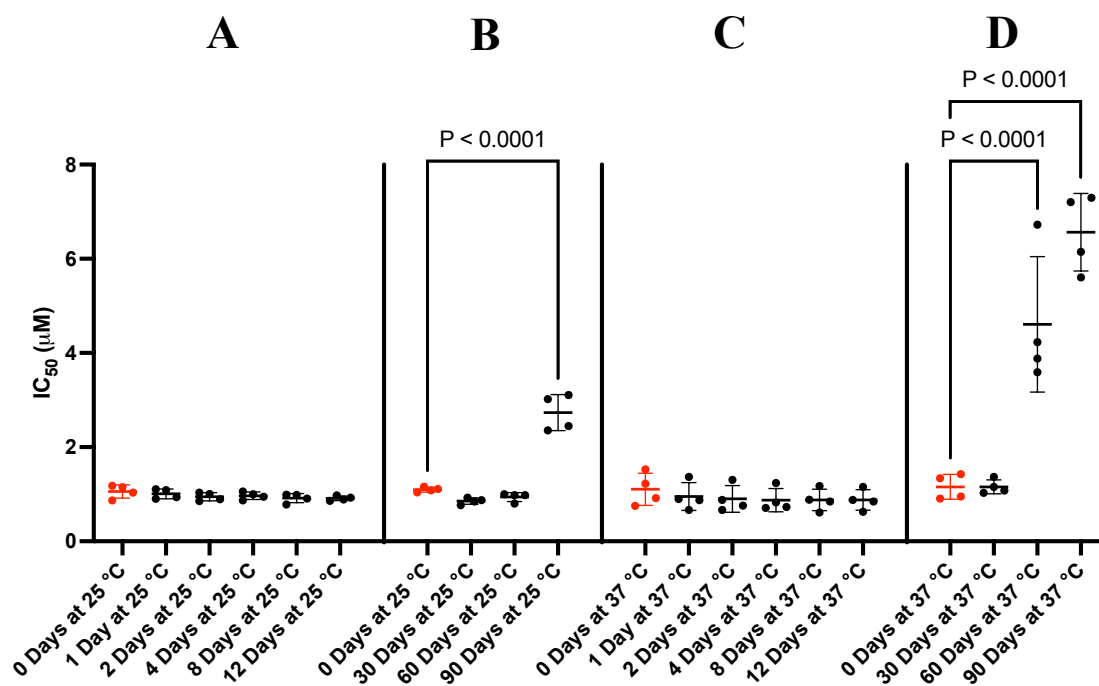


Figure 4.1: Change in Jadomycin B Potency Following Aging

231-CON cells were exposed to aged samples of jadomycin B (0.1-4.0 µM) for 72 h (n=4, where each replicate consisted of the mean of quadruplicate technical replicates). Calculated IC₅₀ values were determined from dose response curves (**Figures B.2 and B.3**) for jadomycin B following aging for up to 12 days (**A and C**) or up to 90 days (**B and D**) at either 25 °C (**A and B**) or 37 °C (**C and D**). Significant difference from control (0 days aged, highlighted in red) is indicated by reported p-values ($P \leq 0.05$) as determined by one-way ANOVA, followed by Bonferroni's multiple comparison test. Error bars are \pm standard deviation.

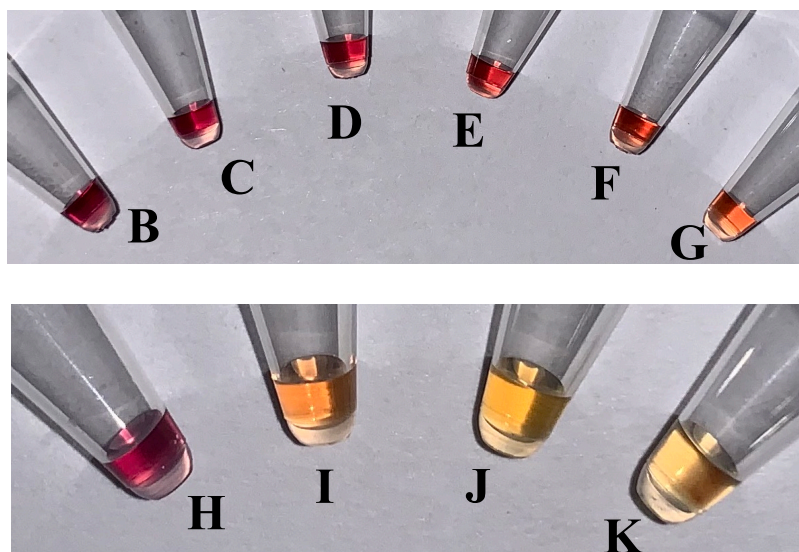
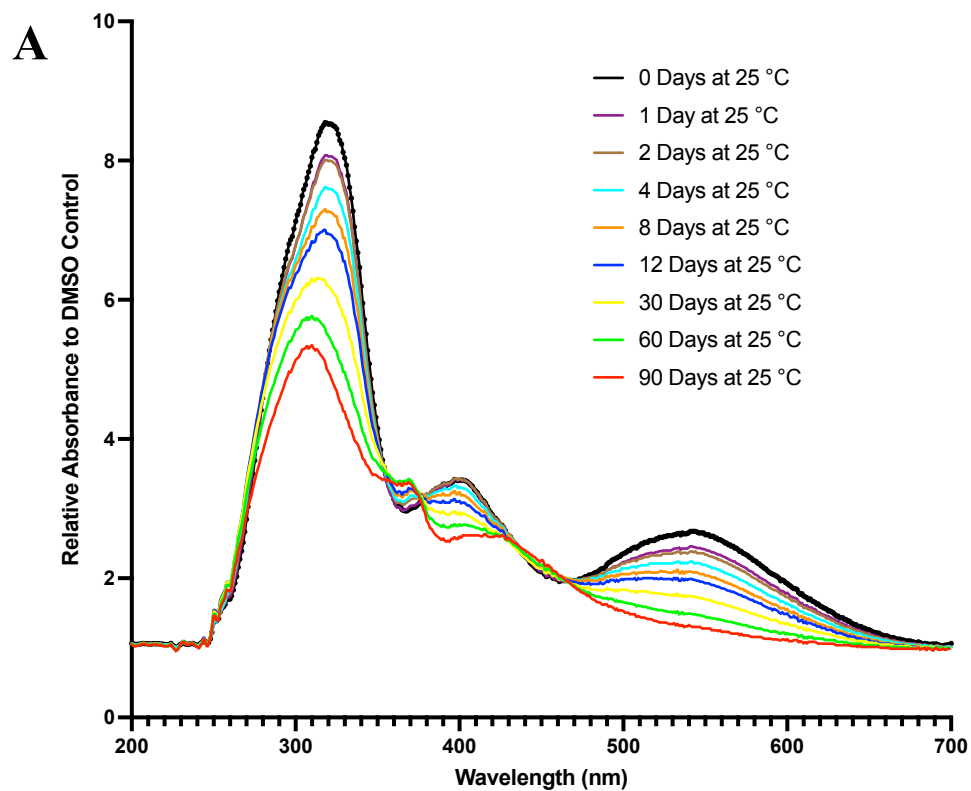


Figure 4.2: Jadomycin B Changes Colour Following Aging at 25 °C

Absorption Spectra (A) measured at 1nm intervals between 200-700 nm and representative photographs of jadomycin B samples following aging at 25 °C for 0 (B), 1 (C), 2 (D), 4 (E), 8 (F), 12 (G), 30 (I), 60 (J), or 90 (K) days. Each datapoint represents the mean value of duplicate measurements.

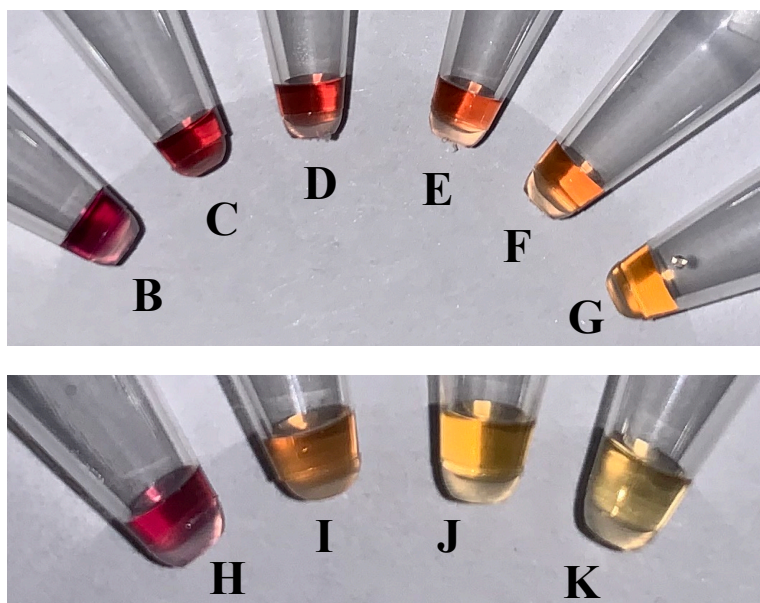
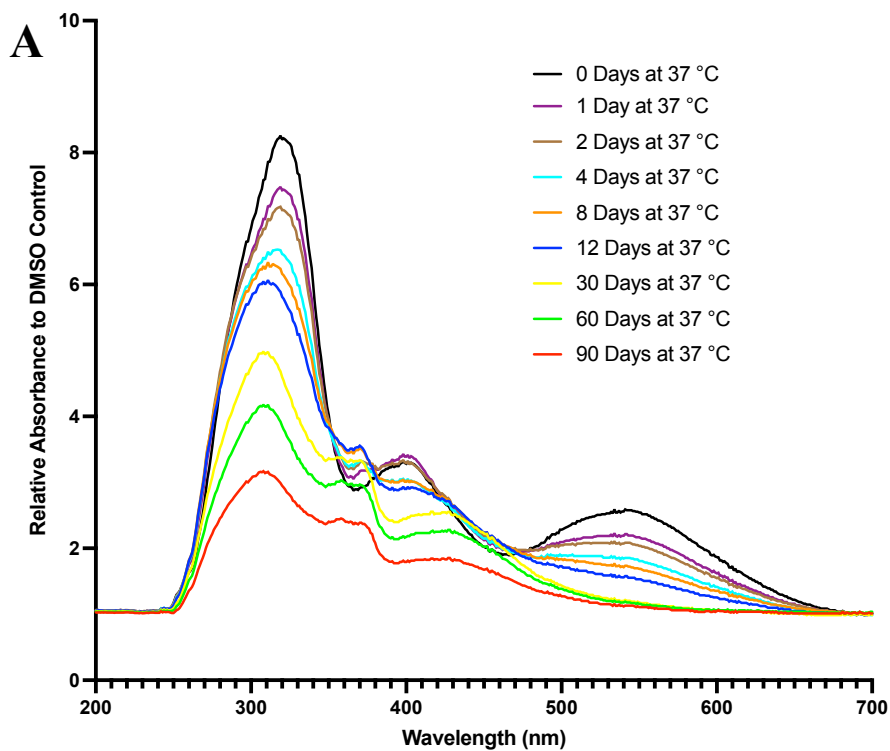


Figure 4.3: Jadomycin B Changes Colour Following Aging at 37 °C

Absorption Spectra (A) measured at 1nm intervals between 200-700 nm and representative photographs of jadomycin B samples following aging at 37 °C for 0 (B, H), 1 (C), 2 (D), 4 (E), 8 (F), 12 (G), 30 (I), 60 (J), or 90 (K) days. Each datapoint represents the mean value of duplicate measurements.

4.3: Effect of Jadomycin B on Accumulation of Cells in Phases of the Cell Cycle

Previous work by Hall et al., suggested that jadomycin B was acting as a TOP2 poison as defined in **section 1.6.4.6** (Hall et al., 2017). Thus, the initial goal of this work was to validate or reject this proposed mechanism through additional experimentation. If jadomycin B is acting as a TOP2 poisoning agent, we would expect that both would have a similar effect on the cell cycle. Anthracyclines like doxorubicin and mitoxantrone have been previously reported to cause an arrest at the G₂/M phase of the cell cycle (Bar-On et al., 2007; Khan et al., 2010). 231-CON cells were exposed to either jadomycin B (1.0 μM), mitoxantrone (0.01 μM), or vehicle control (DMSO) for 48 h and distribution of cells in the G₀/G₁, S, and G₂/M phase of the cell cycle were measured (**Figure 4.4**). Vehicle control cells had a distribution of 51.4 ± 2.5 % of cells in the G₀/G₁ phase, 39.0 ± 1.8 % of cells in the S phase, and 9.6 ± 3.2 % of cells in the G₂/M phase. Mitoxantrone exposed cells exhibited the expected change in distribution with a significant decrease to 24.5 ± 9.3 % of cells in the G₀/G₁ phase and 24.5 ± 4.5 % of cells in the S phase, and a significant increase to 51.0 ± 13.9 % of cells in the G₂/M phase. Following jadomycin B exposure, a small but significant increase to 47.9 ± 1.5 % of cells in the S phase was observed. This change accompanied a small but significant decrease to 44.3 ± 2.8 % of cells in the G₀/G₁ phase and a no significant change to the proportion of cells in the G₂/M phase at 7.9 ± 2.6 %.

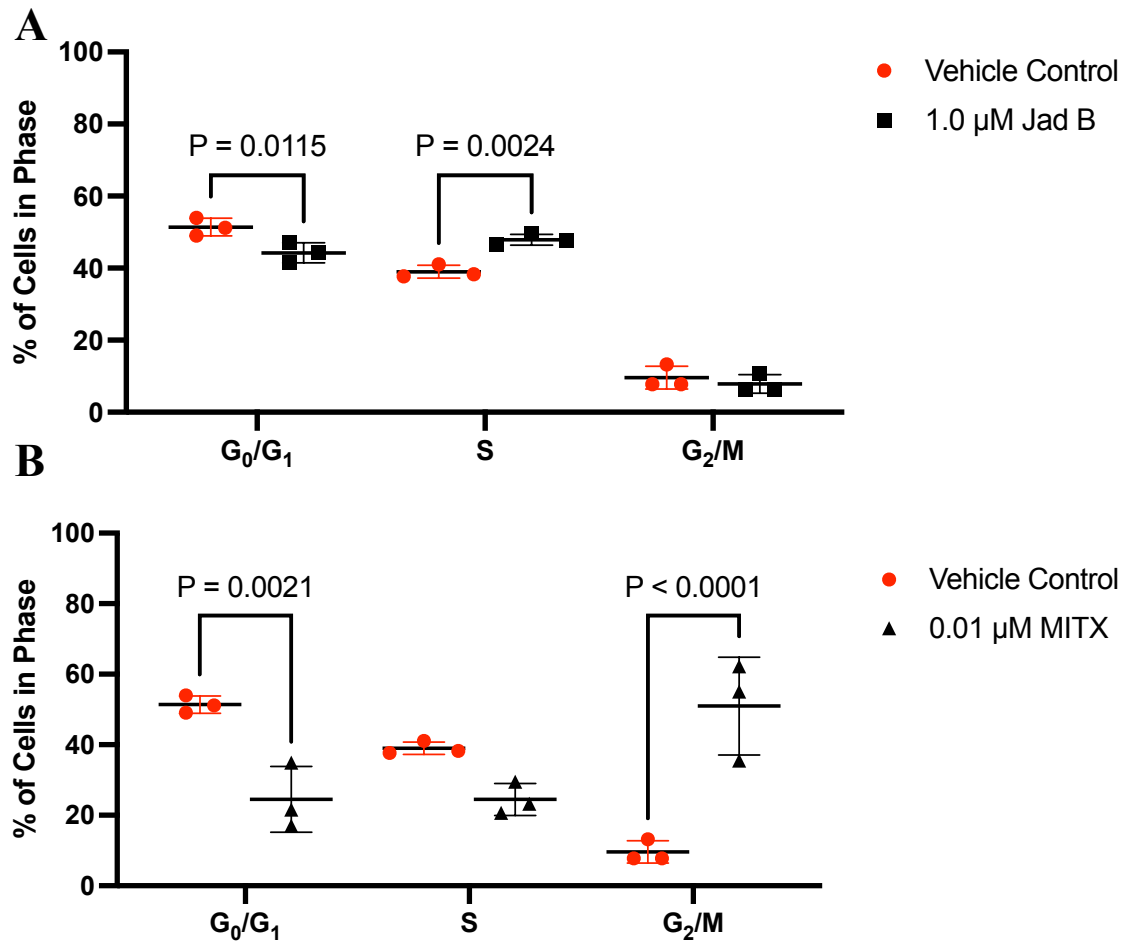


Figure 4.4: Alterations in Cell Cycle Distribution Following Jadomycin B or Mitoxantrone Exposure

Cell cycle analysis of 231-CON cells exposed to (A) jadomycin B (1.0 μM) or (B) mitoxantrone (0.01 μM) as compared to vehicle control (DMSO) for 48 h (n = 3, where each replicate consisted of a minimum of 10000 cells collected). Significant difference from vehicle control (highlighted in red) is indicated by reported p-value ($P \leq 0.05$) as determined by two-way ANOVA, followed by Bonferroni's multiple comparison test. Error bars are mean \pm standard deviation.

4.4: TOP2 Cleavage Complex Accumulation in the Presence of Jadomycin B

As with changes to the cell cycle, if jadomycin B is acting as a TOP2 poisoning agent then it would be expected to cause an accumulation of TOP2 cleavage complexes. Preliminary data shows that jadomycin B did not cause a comparable increase in cleavage complex formation for TOP2 α nor TOP2 β as compared to the positive control etoposide (**Figure 4.5**), and in the case of TOP2 α the assay did not meet the 3-fold threshold for a positive response with the etoposide control as defined by the manufacturer. To verify that jadomycin B was not causing the formation of TOP1 cleavage complexes, preliminary data was also collected which showed no apparent change as compared to the positive control camptothecin (**Figure 4.6**). As the preliminary data did not provide compelling evidence that jadomycin B was acting as a TOP2 poison, additional synergy experiments were conducted to assess interaction in other ways.

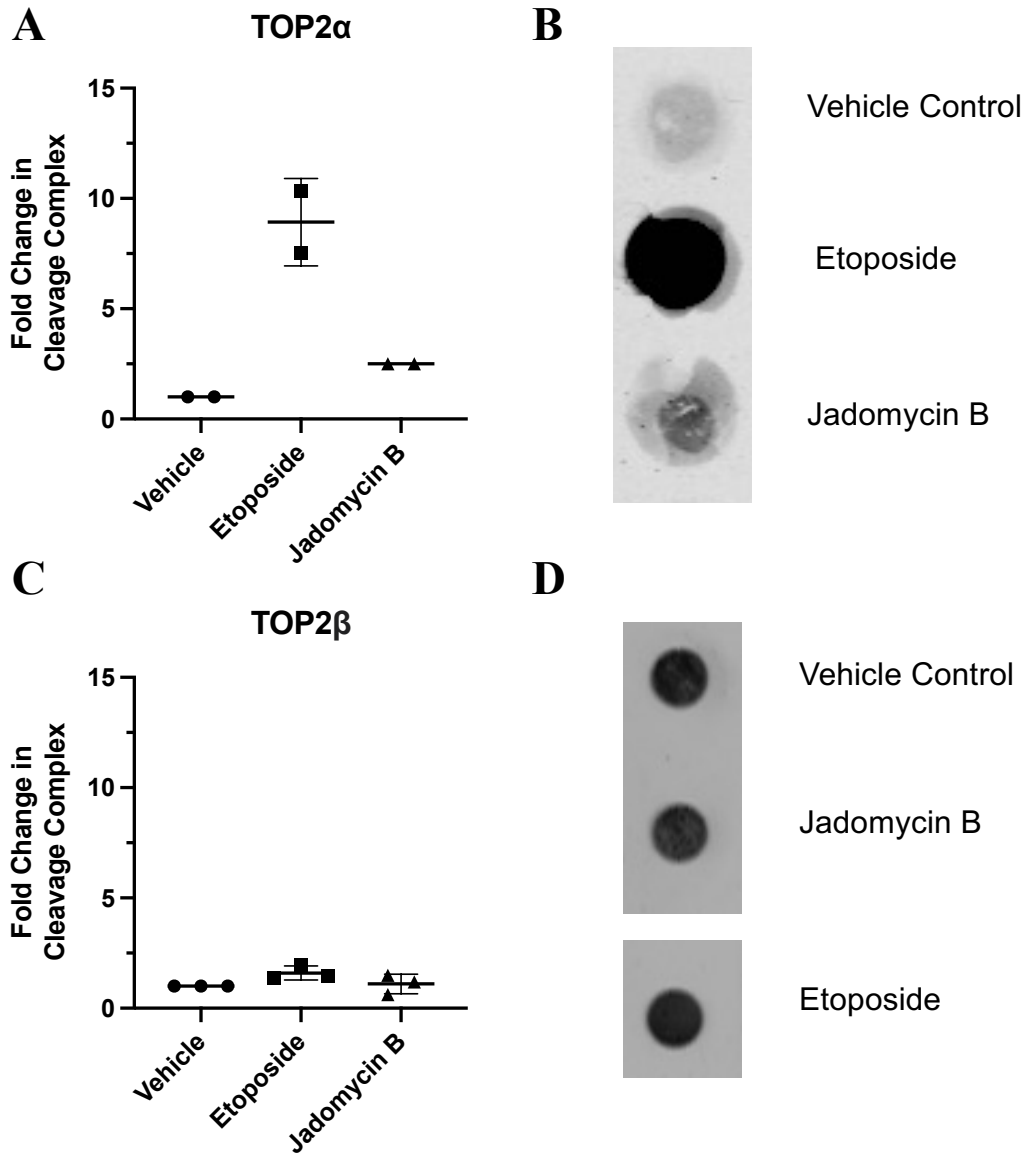


Figure 4.5: Jadomycin B Does Not Cause Accumulation of TOP2 Cleavage Complexes

Preliminary data from ICE assays showing fold change in accumulation of (A) TOP2 α or (C) TOP2 β protein bound to DNA in 231-CON cells as compared vehicle control (DMSO) exposed cells following exposure to etoposide (80 μ M) or jadomycin B (50 μ M) for 60 min. Representative dot blots are shown for (B) TOP2 α and (D) TOP2 β where each datapoint consisted of 2 independent replications and error bars represent \pm standard deviation. No statistical tests were conducted on these data.

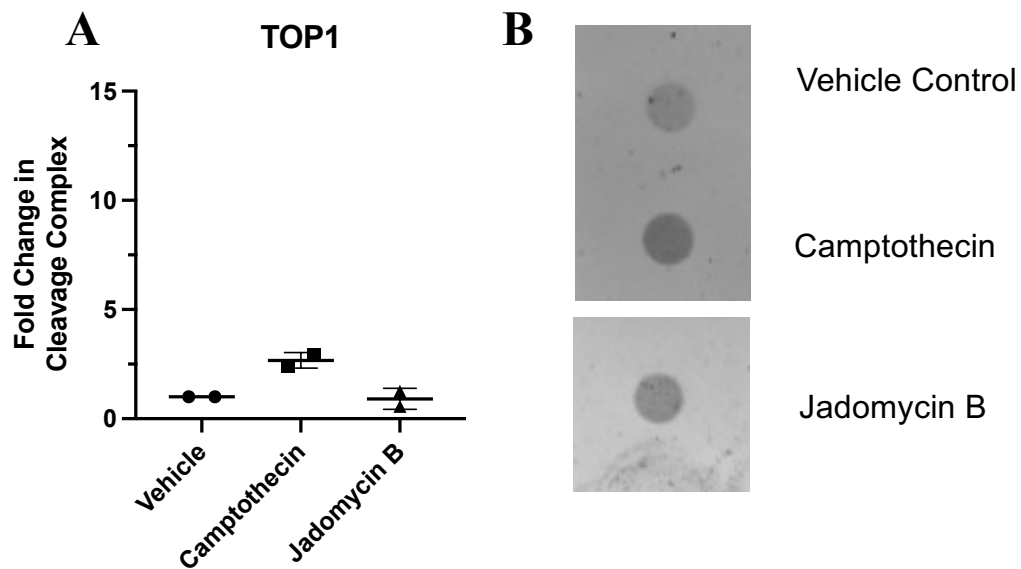


Figure 4.6: Jadomycin B Does Not Cause Accumulation of TOP1 Cleavage Complexes

Preliminary data from ICE assays showing (A) fold change in accumulation of TOP1 protein bound to DNA in 231-CON cells as compared vehicle control (DMSO) exposed cells following exposure to camptothecin (80 μ M) or jadomycin B (50 μ M) for 60 min. The dot blot shown (B) is representative of 2 independent replications and error bars represent \pm standard deviation. No statistical tests were conducted on these data.

4.5: Synergy Between Jadomycin B and Topoisomerase Poisons

The third approach utilized to determine if jadomycin B acts as a TOP2 poison was to compare the synergistic activity of each combination of jadomycin B, doxorubicin, mitoxantrone, SN-38, and MG132. SN-38 was included as an example TOP1 poison to determine if jadomycin B may target that enzyme, while MG132 was included due to known antagonistic activity with TOP2 poisons. The rationale for this approach was that if jadomycin B behaves similarly to both doxorubicin and mitoxantrone in each combination, then that would provide evidence of a shared mechanism of action. **Table 4.2** presents median effect parameters for single drugs or combinations tested for synergy, and the calculated combination index and drug reduction index values for those combinations. Separately calculated dose response curves for the MTT data entered into CompuSyn are presented in **Figures B.5** and **B.6**.

Using the median effect parameters calculated in **Table 4.2**, combination index values (**Table 4.3**) and dose reduction index values (**Tables C.1, C.2, C.3, C.4, C.5, C.6, C.7, C.8, C.9, and C.10**) were generated for effect sizes ranging between 0.05 and 0.97 at intervals of 0.05. This range is equivalent to determining predicted combination index and dose reduction index values for IC_5 - IC_{97} and can be used to evaluate how each pair of drugs works in combination throughout that range.

While the entire range of effect sizes was calculated, it is often more helpful to focus on a range of effects similar to those of the desired outcome, for instance the effective killing of 50% or more of a cancer cell population (Zhang et al., 2016). Considering drug combinations which caused between 55-90% loss in cellular viability (f_a of 0.55-0.9 in **Table 4.3**) combinations involving jadomycin B can be compared against those involving doxorubicin or mitoxantrone. All combinatorial permutations of jadomycin B, doxorubicin, and mitoxantrone were similar, demonstrating additive or weakly synergistic effects. Jadomycin B, doxorubicin, and mitoxantrone all also behaved synergistically in combinations with the TOP1 poison SN-38, although mitoxantrone and SN-38 showed the greatest degree of synergy with combination index values ranging from 0.2-0.3 as compared to the range of 0.5-0.9 for both jadomycin B and doxorubicin. Jadomycin B, doxorubicin, and mitoxantrone differed when in combination with the

proteasome inhibitor MG132, where jadomycin B acted additively (combination index values ranging from 0.8-1.2) while doxorubicin and mitoxantrone both demonstrated antagonism (combination index values ranging from 1.2-2.3). MG132 is a proteasome inhibitor which is predicted to act antagonistically with TOP2 poisons due to inhibition of proteasomal degradation of the topoisomerase cleavage complex which would allow for DNA repair and thereby prevent double stranded breaks in the DNA (Lee et al., 2016; Destanovic et al., 2018). When averaged across the entire range of simulated f_a values (0.05-0.97), jadomycin B acted synergistically with SN-38 and MG132, but additively with the TOP2 poisons, while doxorubicin and mitoxantrone acted additively with each other, synergistically with SN-38, and antagonistically with MG132.

Using the simulated dose reduction index values and the median effect curve for each drug used individually, a series of isobiograms were generated plotting the concentration of each individual drug and each combination needed to produce a f_a of 0.9, 0.75, and 0.5 (**Figure 4.7** and **4.8**). As the combination index and dose reduction index are different methods of presenting the same information, these isobiograms provide an easier method to visualize the changes in combination index described above.

Table 4.2: Calculated Median Effect Parameters for Combinations of Drugs against 231-CON Cell Viability

Median effects parameters for jadomycin B (test compound), doxorubicin (TOP2 poison), mitoxantrone (TOP2 poison), SN-38 (TOP1 poison), and MG132 (proteasome inhibitor) alone and in combination in 231-CON cells as calculated by CompuSyn using individual datapoints presented in **Figures B.5** and **B.6**.

Drug or Combination	Calculated Median Effect Parameters		
	Slope of Median Effect Plot (m)	Median Effect Dose (Dm) in μM	Linear Correlation Coefficient (r)
Jadomycin B	1.65 ± 0.27	1.38	0.95
Doxorubicin	0.65 ± 0.03	1.33	0.99
Mitoxantrone	0.76 ± 0.07	0.34	0.97
SN-38	0.95 ± 0.08	3.77	0.98
MG132	2.58 ± 0.36	0.39	0.96
Jadomycin B + Doxorubicin	1.12 ± 0.18	1.16	0.95
Jadomycin B + Mitoxantrone	1.41 ± 0.13	1.01	0.98
Jadomycin B + SN-38	1.25 ± 0.10	1.25	0.99
Jadomycin B + MG132	1.42 ± 0.22	0.76	0.95
Doxorubicin + Mitoxantrone	0.71 ± 0.07	1.25	0.98
Doxorubicin + SN-38	0.58 ± 0.04	0.8	0.99
Doxorubicin + MG132	1.12 ± 0.06	1.45	0.99
Mitoxantrone + SN-38	0.90 ± 0.20	0.56	0.9
Mitoxantrone + MG132	1.14 ± 0.09	0.53	0.98
SN-38 + MG132	1.93 ± 0.21	1.41	0.97

Table 4.3: Interpolated Combination Index Values for Drugs Tested Against 231-CON Viability

Interpolated combination index values, describing fold-change in potency of drugs when used in combination in 231-CON cells, as calculated from mean effect parameters described in **Table 4.2** using CompuSyn Software. The fraction affected (f_a) is equivalent to IC_{50} in this usage as cellular viability, measured by MTT assay, was the effect measured. f_a s greater than 50% (0.50) are most relevant to the anticancer effect of a compound because the goal of chemotherapeutics is to kill a larger proportion of the cancerous cells. Continued on next page.

Fraction Affected (f_a)	Combination Index Value for Drug Combinations			
	Jadomycin B + Doxorubicin	Jadomycin B + Mitoxantrone	Jadomycin B + SN-38	Jadomycin B + MG132
0.05	3.54	2.07	0.60	0.46
0.1	2.29	1.54	0.58	0.52
0.15	1.78	1.32	0.58	0.56
0.2	1.48	1.19	0.58	0.59
0.25	1.29	1.11	0.58	0.62
0.3	1.16	1.06	0.59	0.65
0.35	1.05	1.01	0.60	0.68
0.4	0.97	0.98	0.60	0.71
0.45	0.91	0.95	0.61	0.73
0.5	0.56	0.93	0.62	0.76
0.55	0.81	0.92	0.63	0.79
0.6	0.78	0.90	0.64	0.82
0.65	0.75	0.89	0.65	0.86
0.7	0.73	0.89	0.67	0.89
0.75	0.72	0.88	0.69	0.94
0.8	0.71	0.88	0.71	0.99
0.85	0.72	0.89	0.74	1.07
0.9	0.76	0.91	0.79	1.18
0.95	0.86	0.95	0.88	1.38
0.97	0.96	0.99	0.96	1.55
Average	1.14	1.06	0.67	0.84
Average (0.55-0.90)	0.75	0.90	0.69	0.94

Table 4.3 (continued)

Fraction Affected (f_a)	Combination Index Value for Drug Combinations					
	Doxorubicin + Mitoxantrone	Doxorubicin + SN-38	Doxorubicin + MG132	Mitoxantrone + SN-38	Mitoxantrone + MG132	SN-38 + MG132
0.05	1.43	0.22	6.39	0.38	3.00	1.87
0.1	1.33	0.26	4.05	0.35	2.29	1.37
0.15	1.28	0.29	3.09	0.33	1.97	1.16
0.2	1.24	0.31	2.54	0.32	1.79	1.03
0.25	1.21	0.34	2.19	0.31	1.67	0.95
0.3	1.19	0.36	1.93	0.31	1.59	0.87
0.35	1.17	0.38	1.74	0.30	1.54	0.84
0.4	1.14	0.40	1.59	0.29	1.50	0.80
0.45	1.13	0.42	1.48	0.29	1.48	0.77
0.5	1.11	0.45	1.39	0.29	1.47	0.74
0.55	1.09	0.47	1.31	0.28	1.48	0.72
0.6	1.08	0.50	1.26	0.28	1.50	0.70
0.65	1.06	0.53	1.22	0.27	1.53	0.68
0.7	1.04	0.57	1.20	0.27	1.58	0.67
0.75	1.03	0.62	1.21	0.27	1.66	0.66
0.8	1.01	0.68	1.24	0.26	1.78	0.65
0.85	0.99	0.77	1.32	0.26	1.97	0.64
0.9	0.96	0.91	1.50	0.25	2.30	0.65
0.95	0.92	1.22	1.99	0.25	3.10	0.67
0.97	0.90	1.54	2.52	0.25	3.91	0.69
Average	1.12	0.56	2.06	0.29	1.96	0.86
Average (0.55-0.90)	1.03	0.63	1.28	0.27	1.73	0.67

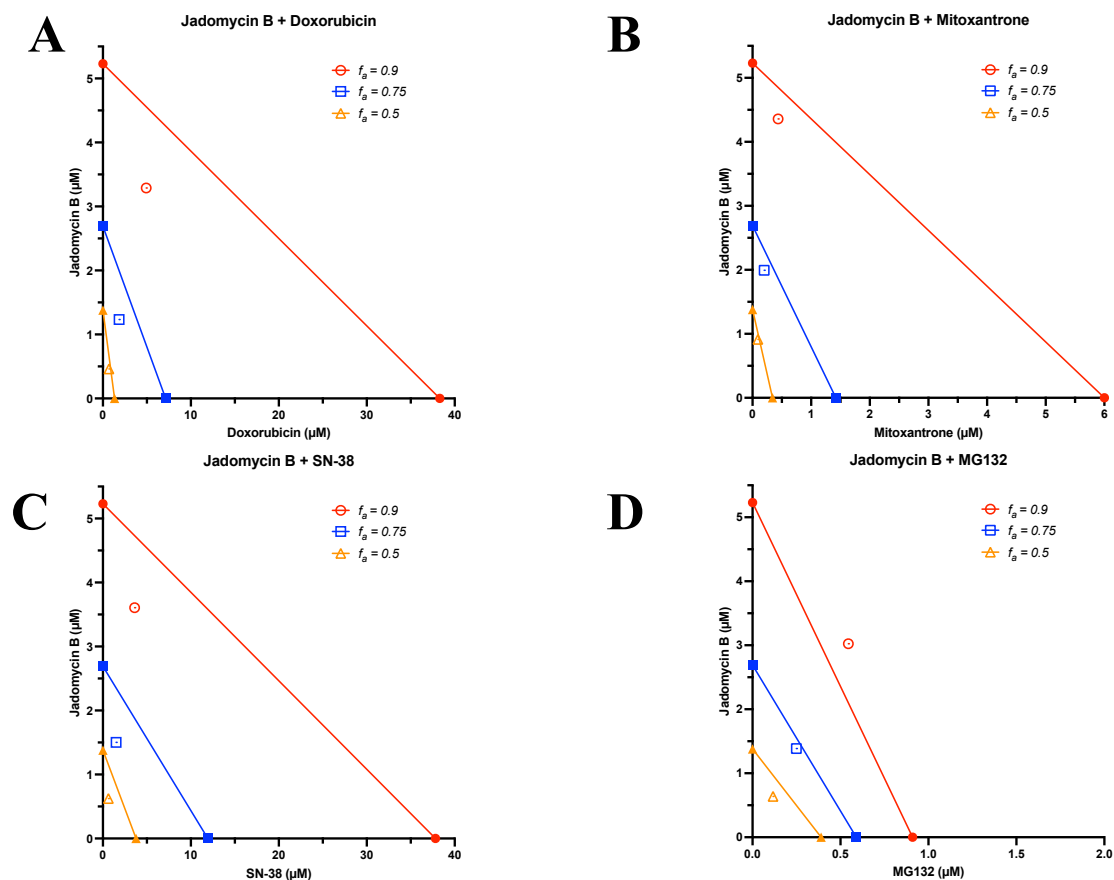


Figure 4.7: Isobiograms Representing Dose Reduction or Increase Needed When Drugs are Used in Combination with Jadomycin B

Isobiograms plotting the concentration of drug needed to achieve a fraction affected (f_a) = 0.9 (red, equivalent to IC_{90}), 0.75 (blue, equivalent to IC_{75}), or 0.5 (orange, equivalent to IC_{50}) for each possible combination of jadomycin B with (A) doxorubicin, (B) mitoxantrone, (C) SN-38, or (D) MG132 in 231-CON cells. The two concentrations corresponding to each drug used alone (filled shapes) are connected by a line representing the theoretical continuum of concentrations which should act together to produce the associated f_a . The concentration combination interpolated (open shapes) from experimental measurements presented in **Table 4.2** show predicted concentrations required to achieve the same f_a . If that point is left of the line, the drugs are acting synergistically, if on the line additively, and if right of the line antagonistically.

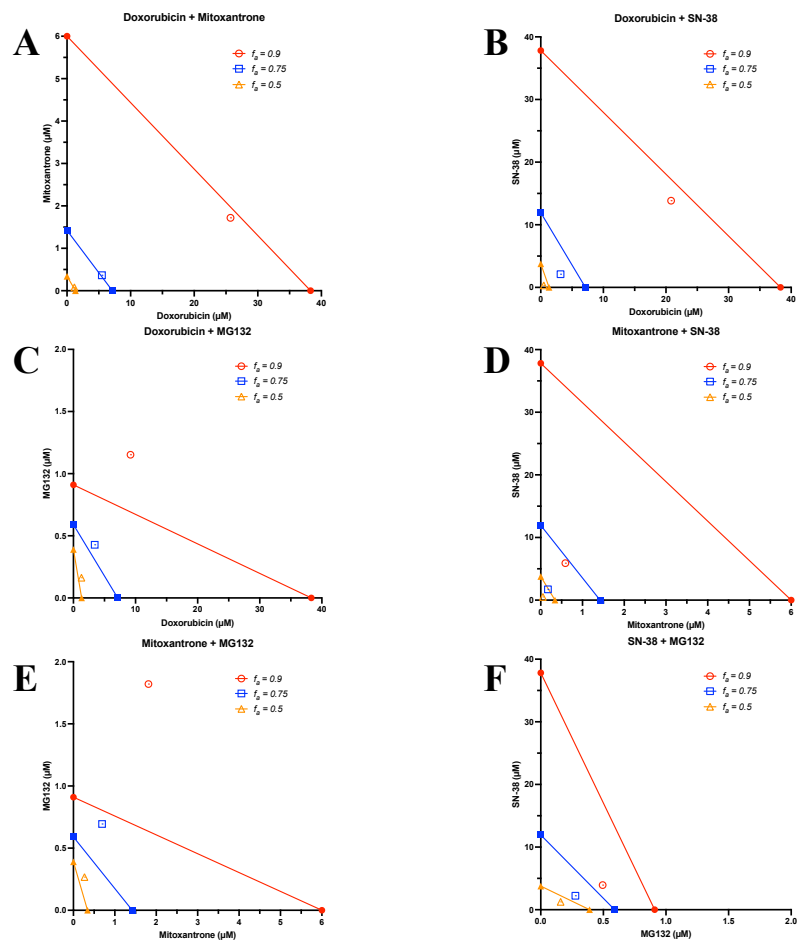


Figure 4.8: Isobiograms Representing Dose Reduction or Increase Needed For All Other Drugs Combinations

Isobiograms plotting the concentration of drug needed to achieve a fraction affected (f_a) = 0.9 (red, equivalent to IC_{90}), 0.75 (blue, equivalent to IC_{75}), or 0.5 (orange, equivalent to IC_{50}) for each possible combination of (A) doxorubicin and mitoxantrone, (B) doxorubicin and SN-38, (C) doxorubicin and MG132, (D) mitoxantrone and SN-38, (E) mitoxantrone and MG132, and (F) SN-38 and MG132 in 231-CON cells. The two concentrations corresponding to each drug used alone (filled shapes) are connected by a line representing the theoretical continuum of concentrations which should act together to produce the associated f_a . The concentration combination interpolated (open shapes) from experimental measurements presented in **Table 4.2** show predicted concentrations required to achieve the same f_a . If that point is left of the line, the drugs are acting synergistically, if on the line additively, and if right of the line antagonistically.

4.6: Assessment of Resistance in 231-JB and 231-MITX Cells

The results described in **sections 4.3, 4.4, and 4.5** demonstrate that jadomycin B does not emulate doxorubicin or mitoxantrone. These differences suggest a different primary mechanism of action is responsible for the cytotoxic effect of jadomycin B and prompted the development of jadomycin resistant cells. Once established, the resistant cells could be used to explore genetic changes to these cells associated with altered jadomycin B potency. This approach allowed assessment of potential jadomycin B targets in the cell. Jadomycin B resistant 231-JB cells and mitoxantrone resistant 231-MITX cells were successfully established from 231-CON cells. Calculated IC_{50} values are presented in **Table 4.4** and **Figure 4.9** with corresponding dose response curves presented in **Figures 4.10** and **4.11**.

The 231-JB cells exhibited a low degree of resistance to jadomycin B at approximately 3-fold the IC_{50} exhibited by 231-CON cells. Furthermore, 231-JB cells demonstrated a similar degree of resistance to jadomyocins S and F while the potency of MITX, DOX, and SN-38 was not significantly changed. In contrast, 231-MITX cells exhibited approximately a 16-fold increase in the IC_{50} of mitoxantrone, while potency of jadomyocins B, S, and F was reduced to a lesser extent. MCF-7 cells were exposed only to jadomycin B or mitoxantrone, which had a similar degree of potency as in 231-CON cells.

Table 4.4: The Cytotoxic Effects of Control Drugs and Jadomycins in Drug Sensitive and Drug Resistant Cells

IC₅₀ values with 95% confidence intervals were calculated from dose response curves for 231-CON and 231-JB cells presented in **Figures 4.9** and **4.10**. Each IC₅₀ was determined from quadruplicate assays, each consisting of quadruplicate technical replicates. Significant difference (*, P ≤ 0.05) was determined by one-way ANOVA followed by Bonferroni's multiple comparison test. Individual values are plotted in **Figures 4.11**.

Cytotoxic Drug	231-CON				231-JB			
	IC ₅₀ μM (95% CI)	SD	Fold-Resistance		IC ₅₀ μM (95% CI)	SD	Fold-Resistance	
Doxyrubicin	1.224 (0.7247-1.723)	0.3138	N/A		0.8728 (0.5144-1.231)	0.2253	0.7131	
Jadomycin B	2.833 (2.344-3.322)	0.3072	N/A		9.029 (5.818-12.24)*	2.017	3.187	
Jadomycin F	3.812 (3.627-3.996)	0.1161	N/A		12.01 (9.684-14.34)*	1.462	3.151	
Jadomycin S	2.080 (1.874-2.286)	0.1293	N/A		7.053 (2.838-11.27)*	2.649	3.391	
Mitoxantrone	0.4158 (0.1910-0.6407)	0.1413	N/A		0.7539 (-0.3003-1.808)	0.6625	1.813	
SN-38	2.824 (2.144-3.505)	0.548	N/A		4.298 (0.6499-7.946)	2.293	1.522	

Cytotoxic Drug	231-MITX				MCF7			
	IC ₅₀ μM (95% CI)	SD	Fold-Resistance		IC ₅₀ μM (95% CI)	SD	Fold-Resistance	
Doxyrubicin	2.138 (1.590-2.686)*	0.3443	1.747		-	-	-	
Jadomycin B	5.893 (4.940-6.845)*	0.5986	2.080		2.150 (1.915-2.384)	0.1473	N/A	
Jadomycin F	7.487 (5.667-9.306)*	1.143	1.964		-	-	-	
Jadomycin S	3.012 (1.712-4.312)	0.8169	1.448		-	-	-	
Mitoxantrone	6.549 (4.748-8.350)*	1.450	15.75		2.788 (0.7056-4.870)	1.309	N/A	
SN-38	5.154 (4.103-6.206)	0.423	1.825		-	-	-	

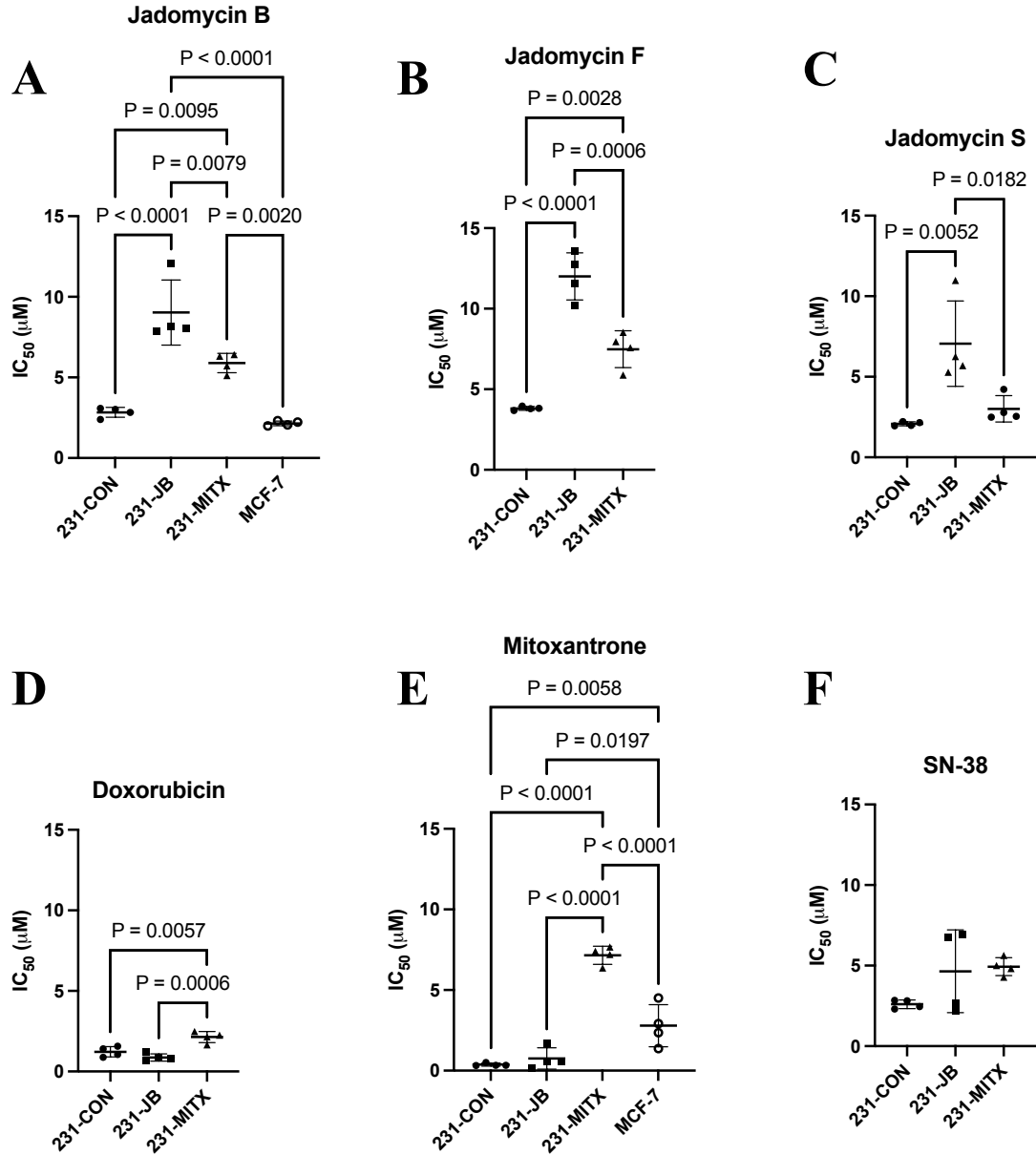


Figure 4.9: IC₅₀ Plots for Data Reported in Table 4.4

Dose response curves (Figures 4.10 and 4.11) were used to calculate IC₅₀ values (Table 4.4) in 231-CON, 231-JB, 231-MITX, and MCF-7 cells for (A) jadomycin B, (B) jadomycin S, (C) jadomycin F, (D) mitoxantrone, (E) doxorubicin, and (F) SN-38. Significant difference between values is indicated by reported p-values ($P \leq 0.05$) as determined by one-way ANOVA followed by Bonferroni's multiple comparison test. Error bars are mean \pm standard deviation.

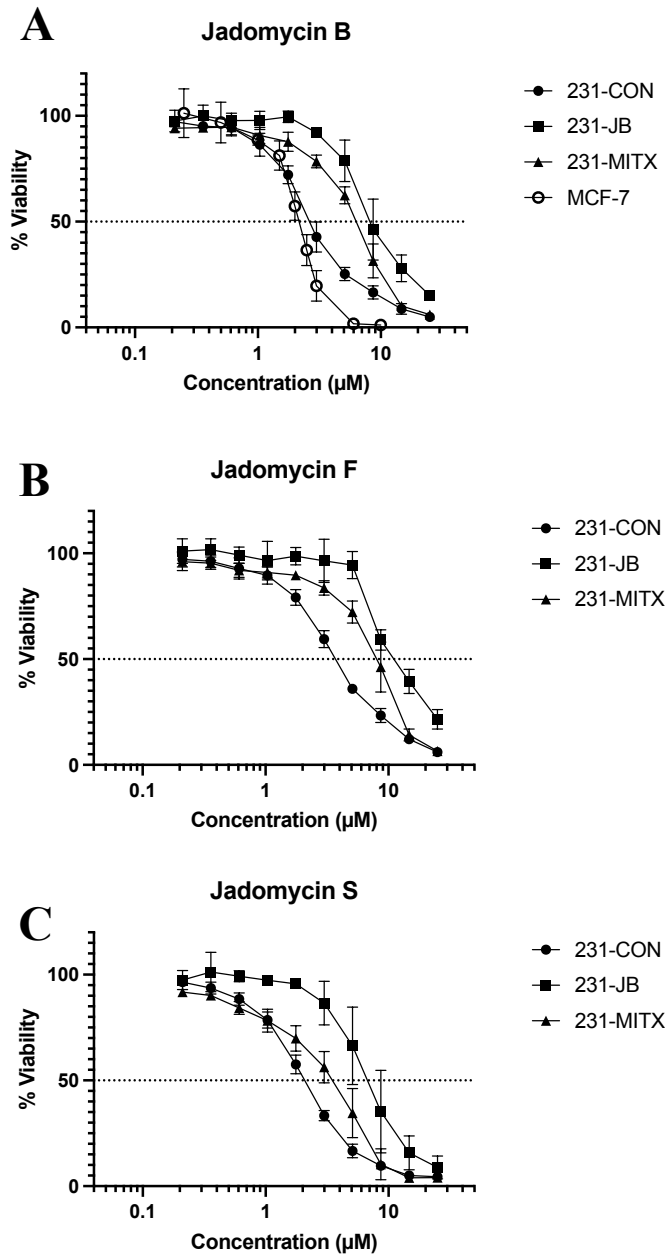


Figure 4.10: Dose Response Curves for Jadomycin IC₅₀ Values Reported in Table 4.4

Dose response curves for 231-CON, 231-JB, 231-MITX, and MCF-7 cells exposed to (A) jadomycin B, (B) S, or (C) F (0.21-25 μM) for 48 h. Datapoints represent the mean value of quadruplicate assays, each consisting of a mean of quadruplicate technical replicates and expressed as % viability of unexposed controls.

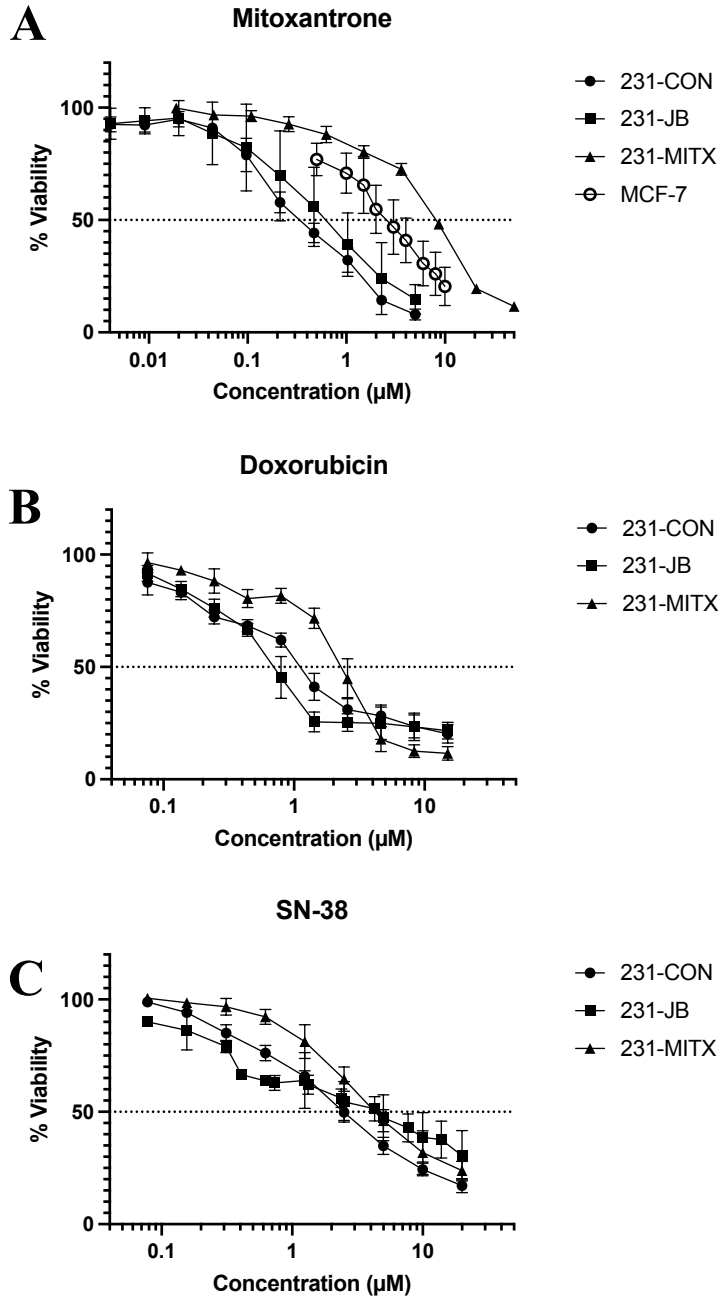


Figure 4.11: Dose Response Curves for Other IC₅₀ Values Reported in Table 4.4

Dose response curves for 231-CON, 231-JB, 231-MITX, and MCF-7 cells exposed to (A) mitoxantrone (0.004-50 μM), (B) doxorubicin (0.07-15 μM), or (C) SN-38 (0.07-20 μM) for 48 h. Datapoints represent the mean value of quadruplicate assays, each consisting of a mean of quadruplicate technical replicates and expressed as % viability of unexposed controls.

4.7: Changes in *TOP2* mRNA Expression in 231-JB and 231-MITX Cells

With jadomycin-resistant 231-JB cells developed, it was possible to determine if a change in TOP2 mRNA expression is associated with decreased jadomycin B potency. RNA was collected from 231-CON, 231-JB, and 231-MITX cells for measurement of *TOP2 α* and *TOP2 β* expression by reverse transcription qPCR (**Figure 4.12A, B**). No significant difference was observed in mRNA expression of either TOP2 isoform in 231-JB cells as compared to 231-CON. Conversely, in 231-MITX cells *TOP2 α* mRNA expression was reduced to approximately 29% that of 231-CON cells, and *TOP2 β* expression was reduced to approximately 28%.

To comprehensively verify that jadomycin B resistance was not associated with a change in mRNA expression of topoisomerases, *TOP1* was also assayed (**Figure 4.12C**). No significant difference in expression was observed between 231-CON and 231-JB or 231-MITX cells.

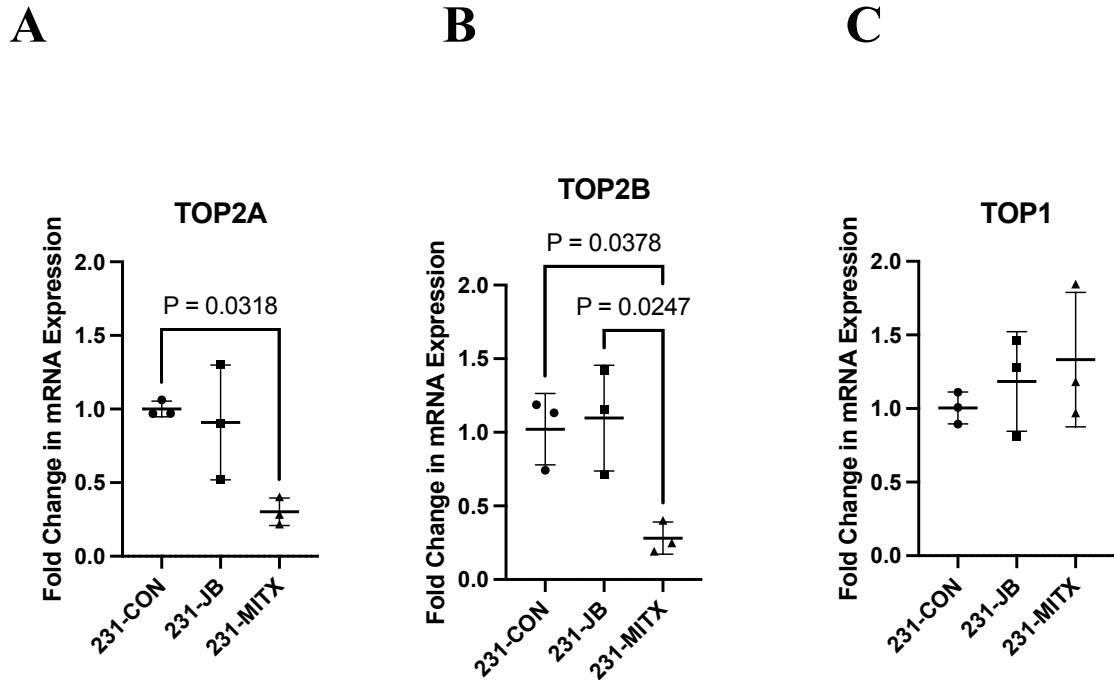


Figure 4.12: *TOP2* mRNA Expression Does Not Significantly Change in 231-JB Cells

Reverse transcription qPCR was used to measure mRNA expression of (A) *TOP2A*, (B) *TOP2B*, and (C) *TOP1* in 231-CON, 231-JB, and 231-MITX cells not exposed to any drug. Datapoints represent the mean value of triplicate assays, each consisting of a mean of duplicate technical replicates and expressed as fold change in mRNA expression as compared to 231-CON cells. Significant difference is indicated by reported p-value ($P \leq 0.05$) as determined by one-way ANOVA, followed by Bonferroni's multiple comparison test. Error bars are mean \pm standard deviation.

4.8: Association of Resistance and Increased mRNA Expression of ABC Transporters

To validate that resistance to mitoxantrone was mediated by increased expression of ABCG2 (BCRP) the mRNA expression of *ABCB1*, *ABCC1*, and *ABCG2* were measured using reverse transcription qPCR. In 231-MITX cells *ABCG2* expression was increased approximately 10-fold as compared to 231-CON cells, while 231-JB cells showed no significant change (**Figure 4.13C**). RNA expression of *ABCB1* was not significantly changed in either 231-JB nor 231-MITX cells, and expression of *ABCC1* in 231-MITX cells was increased to 2-fold that measured in 231-CON and 231-JB cells (**Figure 4.13A, B**).

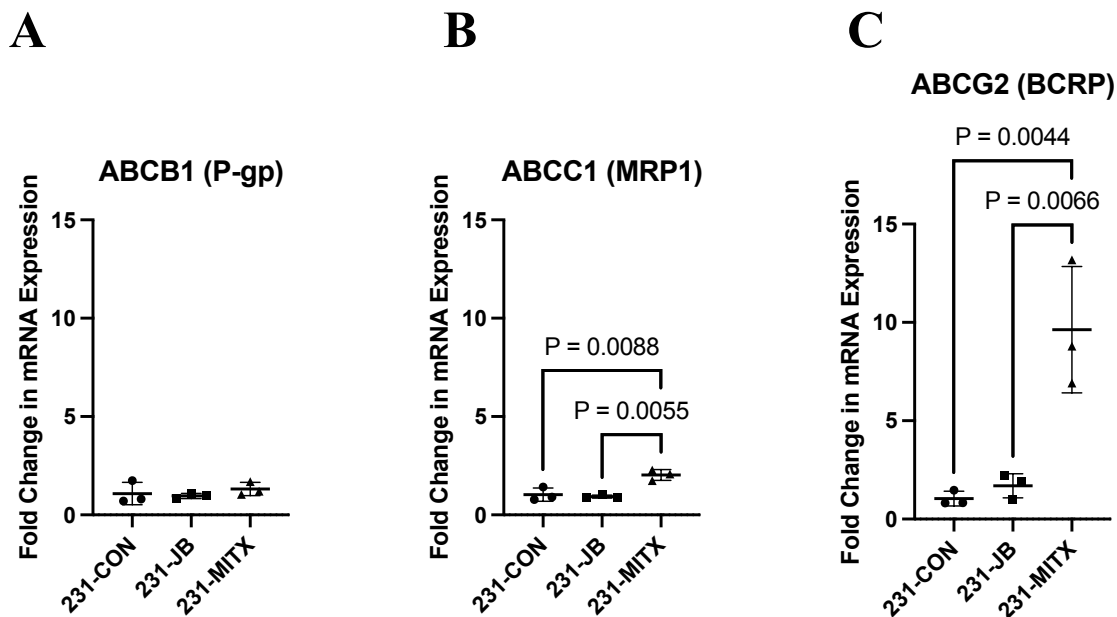


Figure 4.13: Resistance to mitoxantrone, but not to jadomycin B, is associated with increased mRNA expression of *ABCG2*

Reverse transcription qPCR was used to measure mRNA expression of (A) *ABCB1*, (B) *ABCC1*, and (C) *ABCG2* in 231-CON, 231-JB, and 231-MITX cells not exposed to any drug. Datapoints represent the mean value of triplicate assays, each consisting of a mean of duplicate technical replicates and expressed as fold change in mRNA expression as compared to 231-CON cells. Significant difference is indicated by reported p-value ($P \leq 0.05$) as determined by one-way ANOVA, followed by Bonferroni's multiple comparison test. Error bars are mean \pm standard deviation.

4.9: Changes in mRNA Expression of Human Cancer Drug Targets in 231-JB Cells

To identify potential genes of interest in 231-JB cells which may elucidate the mechanism of action by which jadomycin B exerts its cytotoxic effect an 84-gene Human Cancer Drug Targets RT² Profiler PCR Array was used to compare expression in 231-CON and 231-JB cells. Included in this array were genes commonly dysregulated during carcinogenesis, such as those involved in apoptosis, DNA repair, and signalling. Of the 84 genes included in the array the greatest change, at approximately 22-fold, was found to occur in *PTGS2* which codes for COX2 (**Table C.11**). Of additional interest was the decrease in *telomerase reverse transcriptase (TERT)*, approximately 0.33-fold, which is known to be inhibited by polyunsaturated fatty acids and downregulated in correlation with *PTGS2* overexpression (Eitsuka et al., 2005). To confirm the change in *PTGS2*, mRNA expression of *PTGS1*, *PTGS2*, and *EP4* were quantified (**Figure 4.14**). *PTGS2* exhibited approximately a 38-fold increase in expression in 231-JB cells as compared to 231-CON cells, while no significant change was observed in 231-MITX cells. *PTGS1* expression, coding for COX1, in 231-JB cells was significantly decreased by 6-fold from that observed in 231-CON cells, while increasing to approximately 4-fold in 231-MITX cells. mRNA expression of *EP4* was not significantly changed in drug resistant cells.

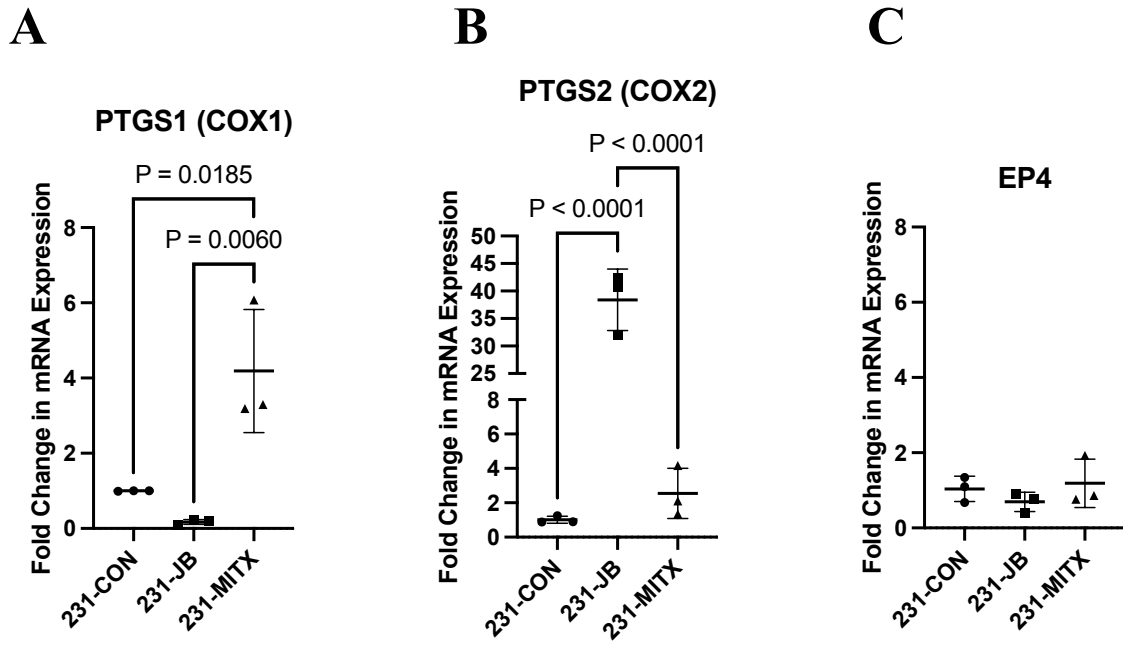


Figure 4.14: Expression of *COX2* mRNA is increased in 231-JB cells

Reverse transcription qPCR was used to measure mRNA expression of (A) *PTGS1*, (B) *PTGS2*, and (C) *EP4* in 231-CON, 231-JB, and 231-MITX cells not exposed to any drug. Datapoints represent the mean value of triplicate assays, each consisting of a mean of duplicate technical replicates and expressed as fold change in mRNA expression as compared to 231-CON cells. Significant difference is indicated by reported p-value ($P \leq 0.05$) as determined by one-way ANOVA, followed by Bonferroni's multiple comparison test. Error bars are mean \pm standard deviation.

4.10: COX2 Protein Expression in 231-JB Cells

Increases in RNA expression are not always correlated with a corresponding increase in protein expression (Maier et al., 2009). Protein expression of COX2 and EP4 were therefore quantified in 231-CON and 231-JB cells. COX2 protein was increased by 25-fold in 231-JB cells, while no significant change was observed in EP4 protein expression (**Figure 4.15**).

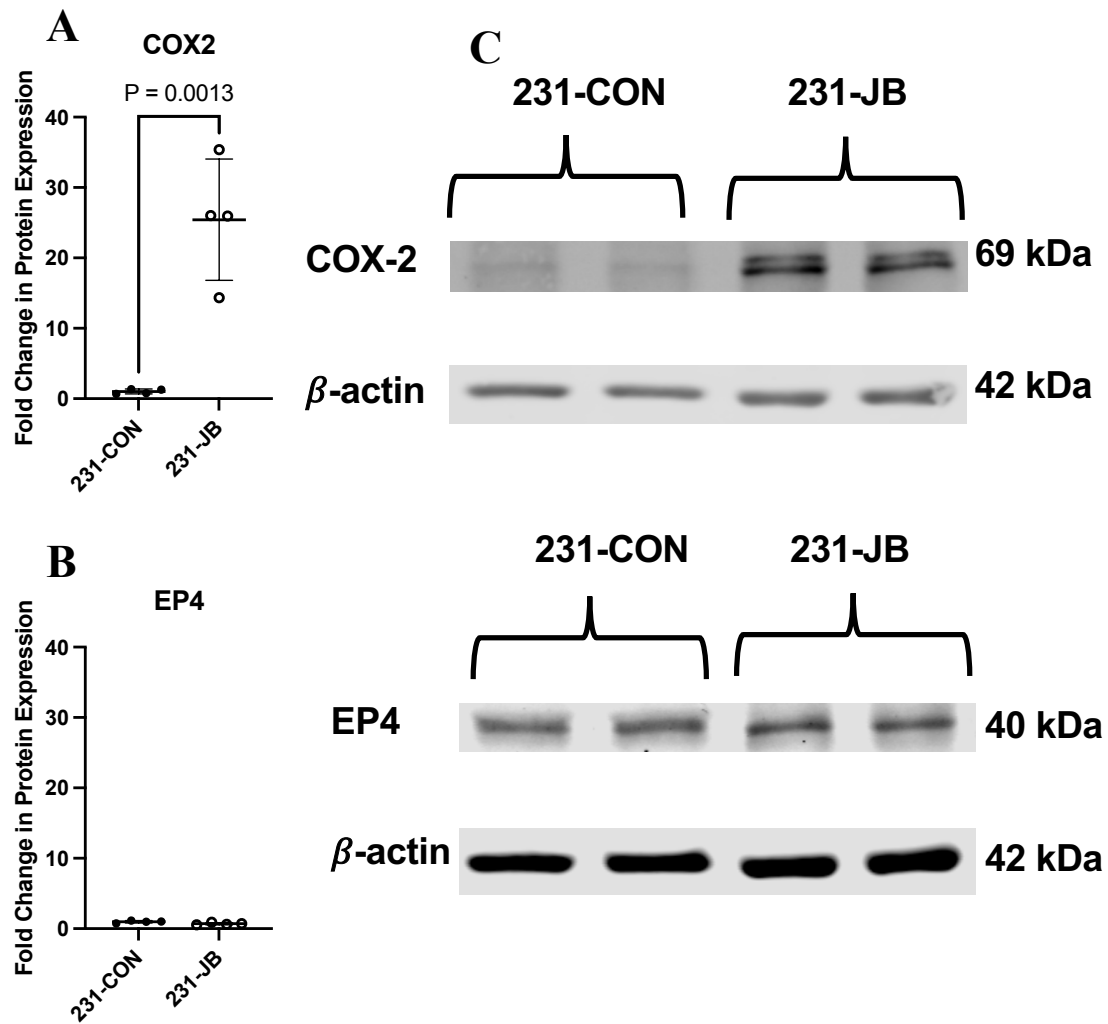


Figure 4.15: Expression of COX2 Protein is Increased in 231-JB cells

Protein expression of (A) COX2 and (B) EP4 in 231-CON and 231-JB cells not exposed to any drug was measured by Western blot. Representative blots (C) are shown.

Datapoints represent the mean value of quadruplicate assays, each consisting of a mean of duplicate technical replicates and expressed as fold change in protein expression as compared to 231-CON cells. Significant difference is indicated by reported p-value ($P \leq 0.05$) as determined by unpaired t-test. Error bars are mean \pm standard deviation.

4.11: EP4 Protein Expression in 231-CON Cells Following Transient Jadomycin B Exposure

COX2 is the rate limiting enzyme in the production of PGE₂. In turn, the EP4 receptor is commonly associated with modifications to PGE₂ signalling in cancer. It is therefore important to fully characterize the acute effect of jadomycin B on EP4. While EP4 protein expression was unchanged in 231-JB cells, there was a significant decrease in EP4 expression following exposure of 231-CON cells to jadomycin B (2.5 μM and 5.0 μM) for 24 or 48 hours (**Figure 4.16**). After 24 hours exposure to 5.0 μM jadomycin B, EP4 protein expression was decreased to 48% that observed in vehicle control. This reduction in EP4 persisted at 48 hours exposure where it was decreased to 63% of vehicle control.

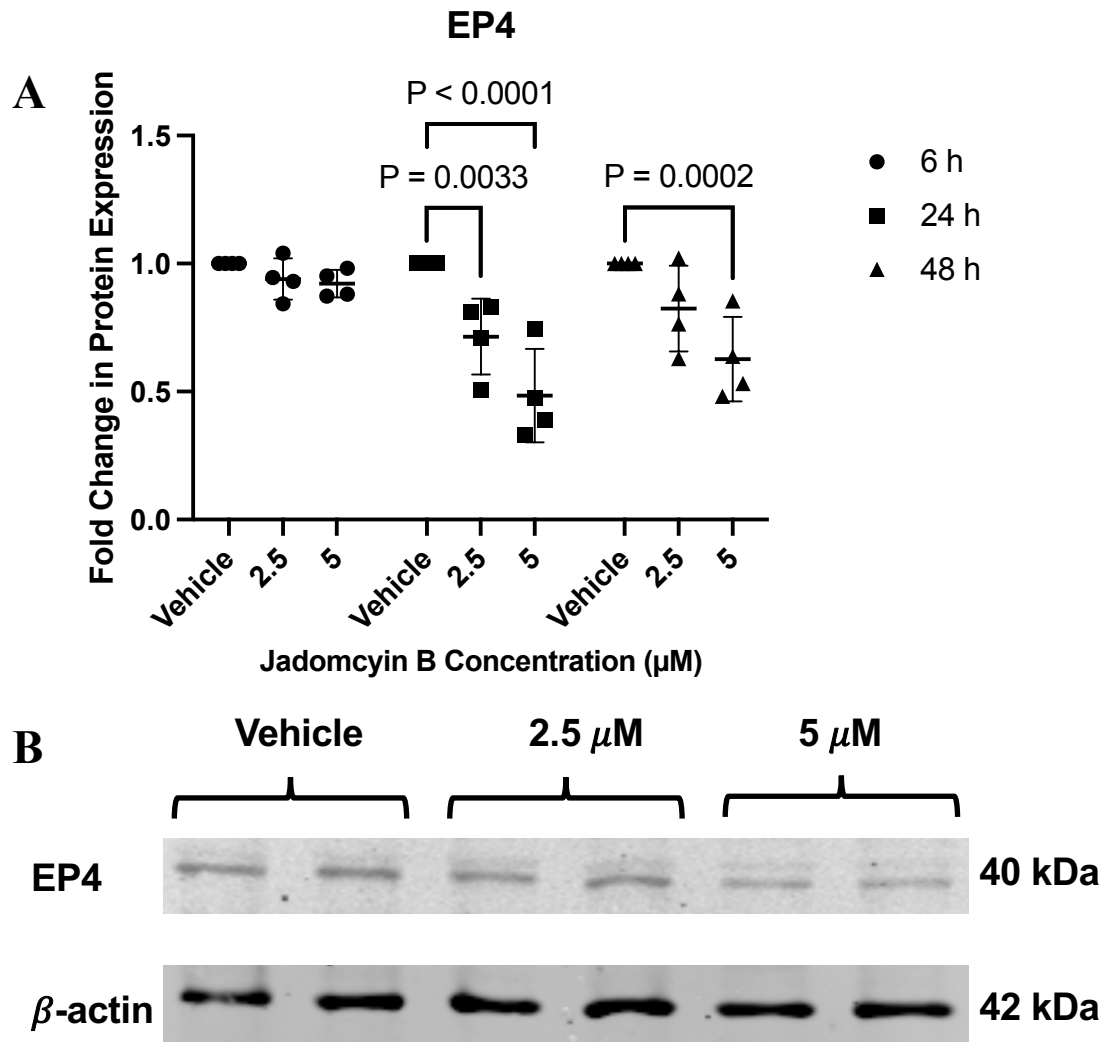


Figure 4.16: Expression of EP4 Protein Decreases with Jadomycin B

Protein expression of EP4 (**A**) decreases in 231-CON cells exposed to jadomycin B for 6, 24, or 48 h as measured by Western blot. Representative blots for 48 h data (**B**) are shown. Datapoints represent the mean value of quadruplicate assays, each consisting of a mean of duplicate technical replicates and expressed as fold change in protein expression as compared to vehicle (DMSO) exposed cells. Significant difference is indicated by reported p-value ($P \leq 0.05$) as determined by two-way ANOVA, followed by Bonferroni's multiple comparison test. Error bars are mean \pm standard deviation.

4.12: Concentrations of PGE₂ in 231-CON Growth Medium Following Exposure to Jadomycin B

As increases in the RNA and protein expression of COX2 were observed to be associated with jadomycin resistance, and decreased protein expression of the PGE₂ receptor EP4 was associated with acute exposure to jadomycin B, the next logical step was to assay the level of PGE₂ produced by 231-CON cells in the presence of jadomycin B. In cells exposed to vehicle control (DMSO) PGE₂ levels in growth medium increased to 177%, 239%, and 312% of the 6 h baseline after 24, 48, and 72 h, respectively (**Figure 4.17**). Following exposure to jadomycin B at 2.5 or 5.0 μ M there was no significant increase from 6 h levels at any timepoint tested.

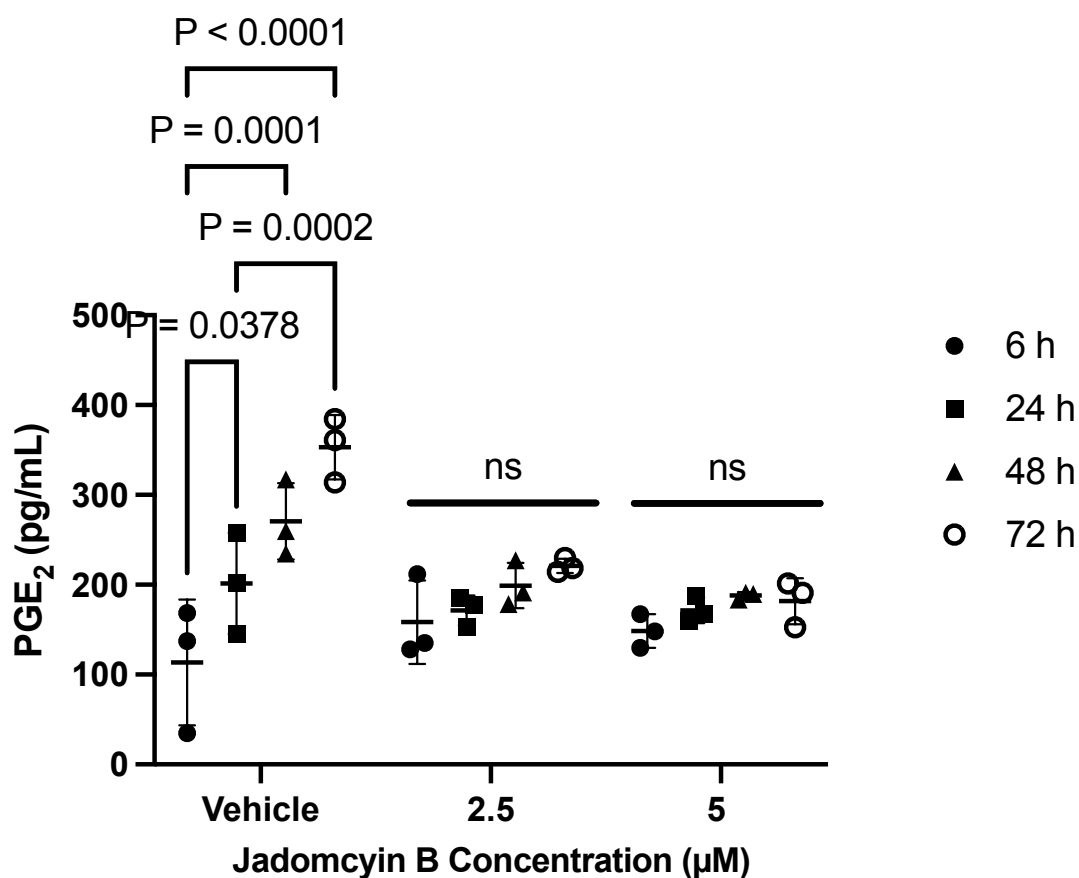


Figure 4.17: Growth Medium Concentration of PGE₂ with Jadomycin B

Concentration of PGE₂ measured in growth medium of 231-CON cells exposed to 2.5 or 5 µM jadomycin B or vehicle control (DMSO) for 6, 24, 48, or 72 h as measured by ELISA. Datapoints represent the mean value of triplicate assays, each consisting of a mean of duplicate technical replicates and expressed as concentration of PGE₂ in pg/mL. Significant difference is indicated by reported p-value ($P \leq 0.05$) as determined by two-way ANOVA, followed by Bonferroni's multiple comparison test. Error bars are mean \pm standard deviation.

4.13: Alterations to Cellular Lipid Profiles Following Jadomycin B Exposure

COX2 is the enzyme responsible for the conversion of AA (the fatty acid 20:4n-6) to prostaglandins. AA is itself derived from the metabolism of cellular fatty acids. **Figure 4.18** presents a summary of the biosynthetic pathways of the n-6 and n-3 fatty acids (Vessby et al., 2002; Pavithra et al., 2018). Having established that jadomycin B can affect levels of PGE₂ in medium, it was next important to determine if jadomycin B could affect the proportions of fatty acids in the cell.

To understand the effect of jadomycin B on fatty acid concentrations within the cell, 231-CON cells were exposed to jadomycin B (2.5 or 5.0 μM) or vehicle control (DMSO) for 24 or 48 hours and analyzed using gas chromatography to determine percent total fatty acid content of the cell for each identifiable fatty acid. Representative GCFID chromatograms (**Figures 4.19** and **4.20**) and analysis of percent fatty acid content data derived from those (**Figure 4.21** and **4.22**) show relative changes to the fatty acid content of cells. No significant change was observed in any of the n-6 fatty acids following 24 h exposure to jadomycin B, however, there was a significant increase in the levels of dihomo-γ-linolenic acid (20:3n-6; 150%), AA (20:4n-6; 134%), adrenic acid (22:4n-6; 195%), and 22:5n-6 (166%) following 48 h exposure to 5.0 μM jadomycin B as compared to vehicle control. Similarly, significant increases in n-3 fatty acids were observed in α-linolenic acid (18:3n-3; 162%), docosapentaenoic acid (22:5n-3; 168%), and docosahexaenoic acid (22:6n-3; 147%) following 48 h exposure to 5.0 μM jadomycin B. The remaining fatty acids measured are presented in **Figure B.7** for the sake of completion, but were not further analyzed as they are beyond the scope of this work.

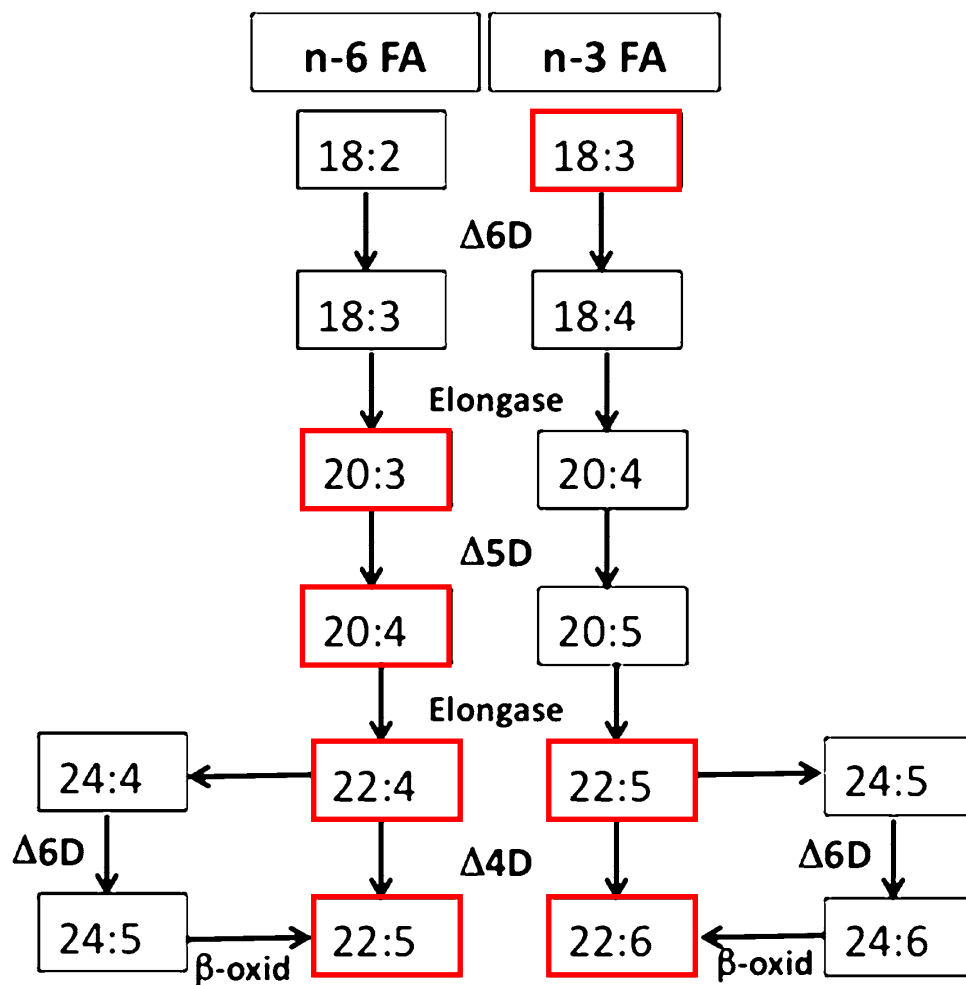
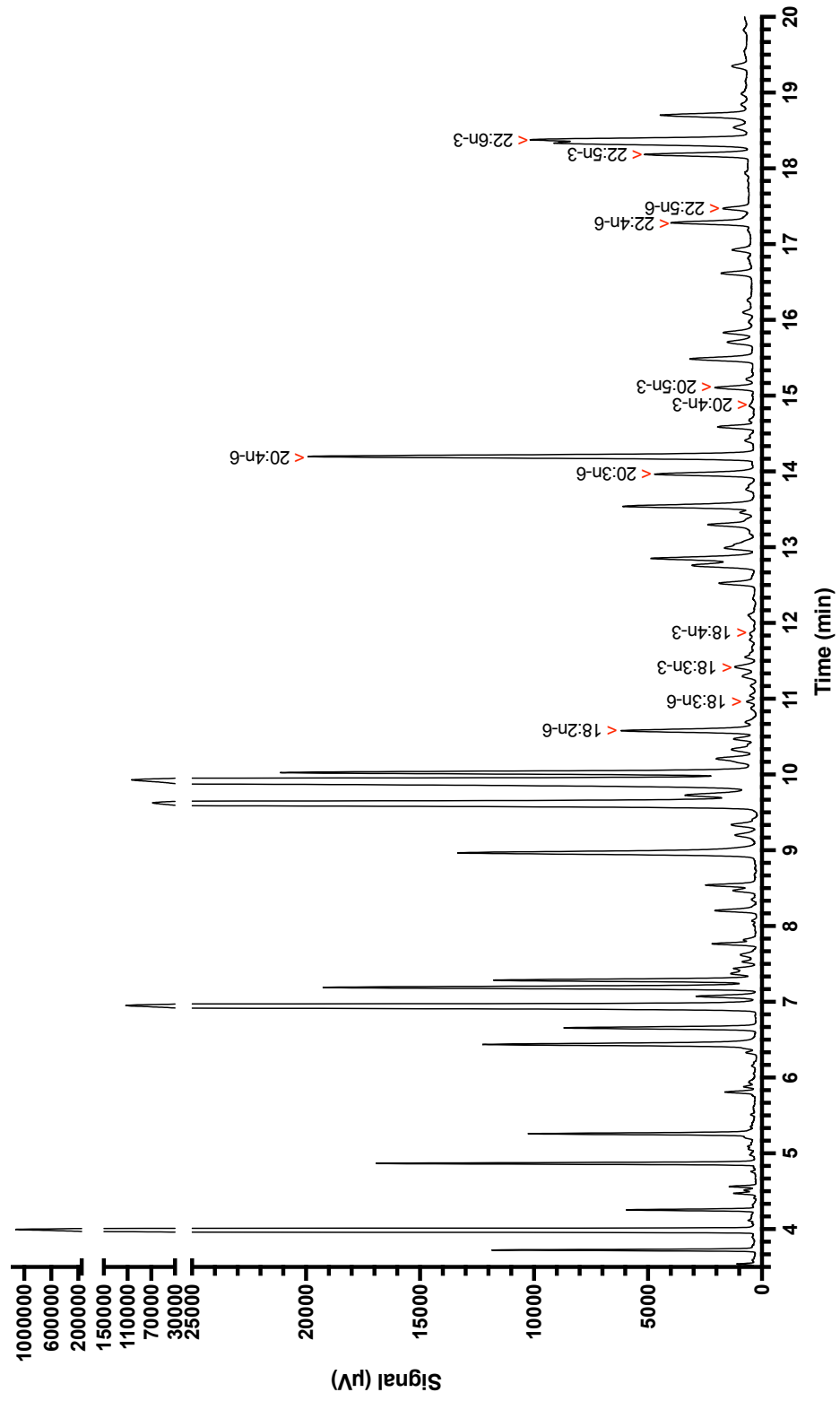


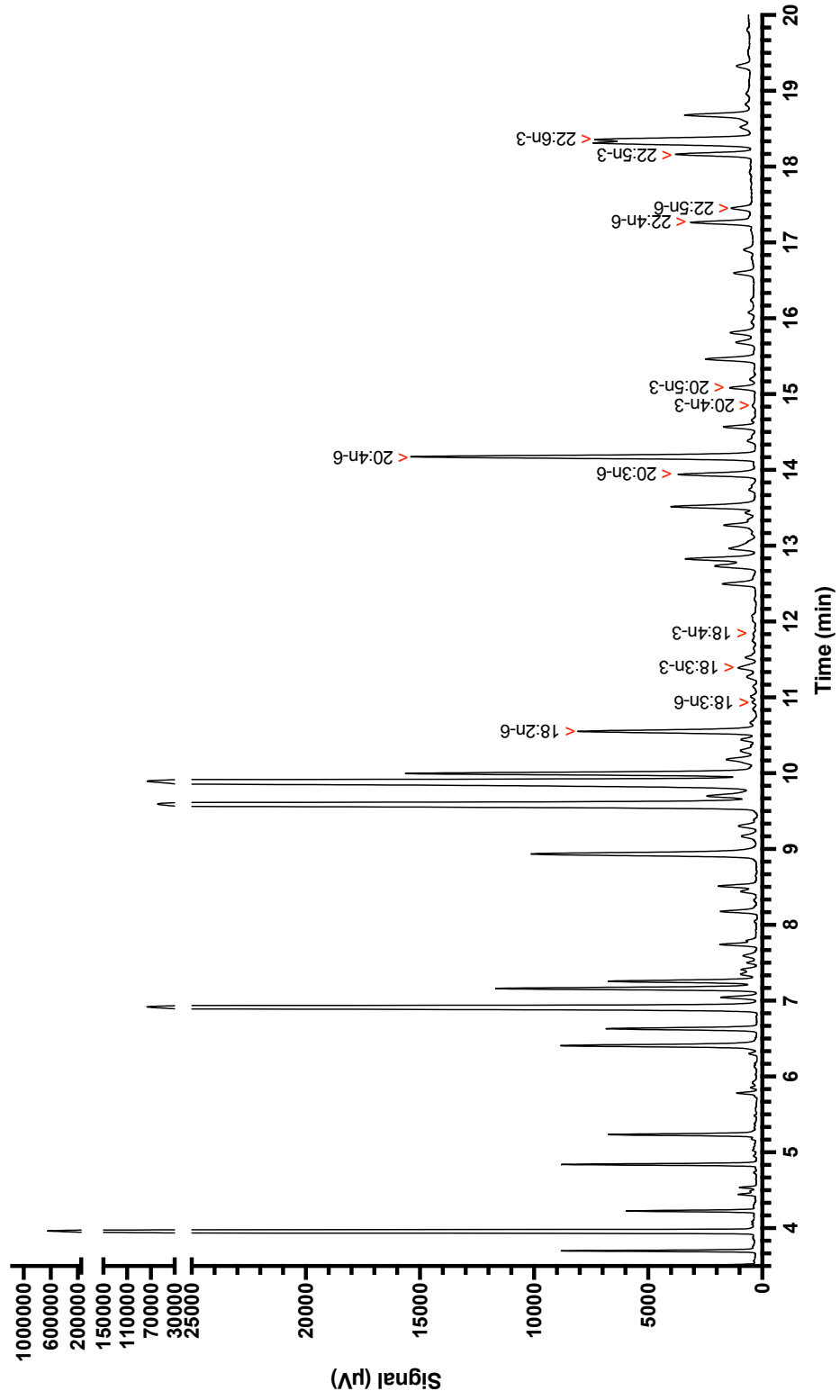
Figure 4.18: Biosynthesis of n-6 and n-3 Fatty Acids

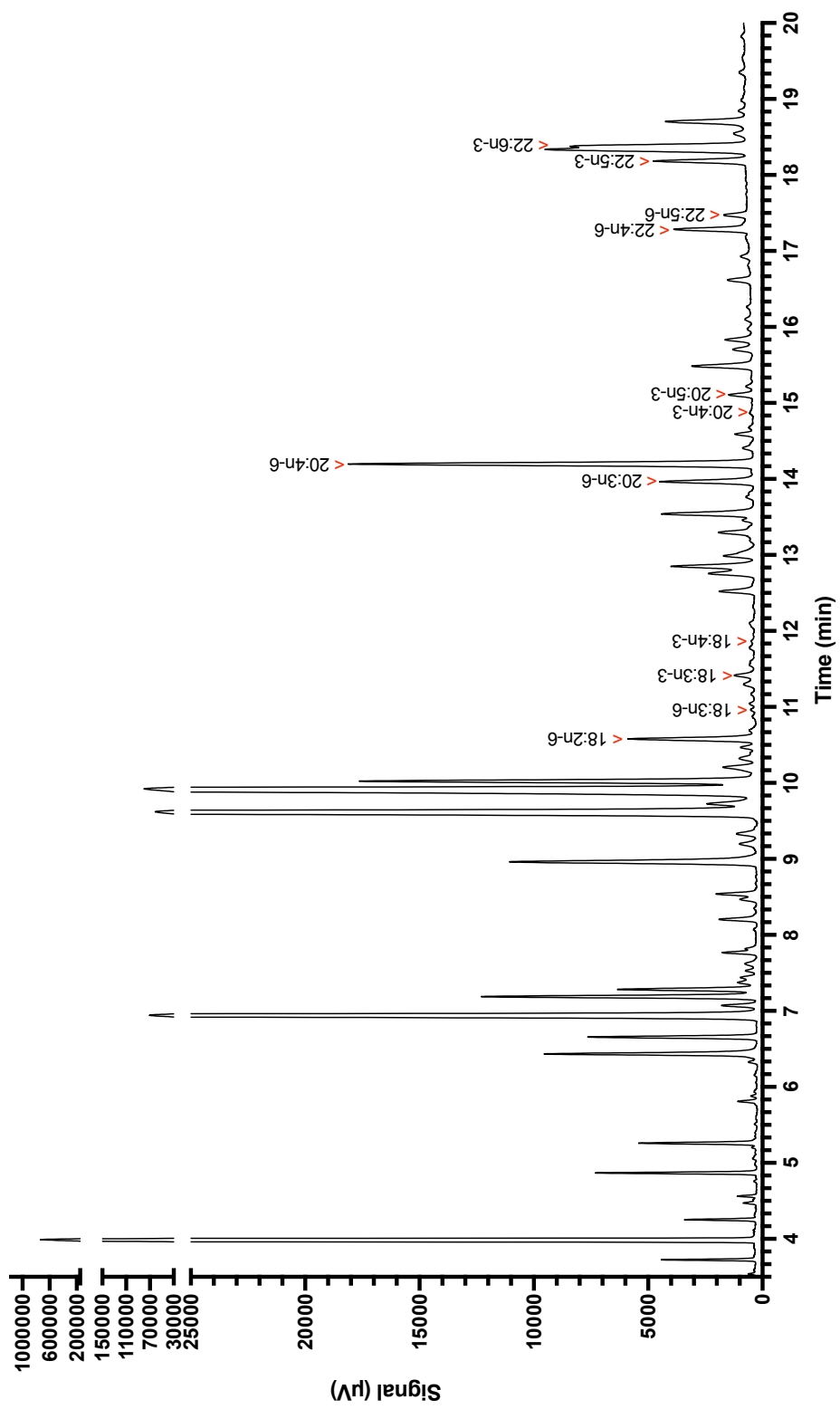
Biosynthetic pathway of n-3 and n-6 fatty acids, with enzymes responsible for each step. The fatty acids with significant change following exposure to jadomycin B in 231-CON cells are highlighted in red. Figure adapted, with permission (**Appendix A.13**), from Pavithra et al. (2018).

A



B



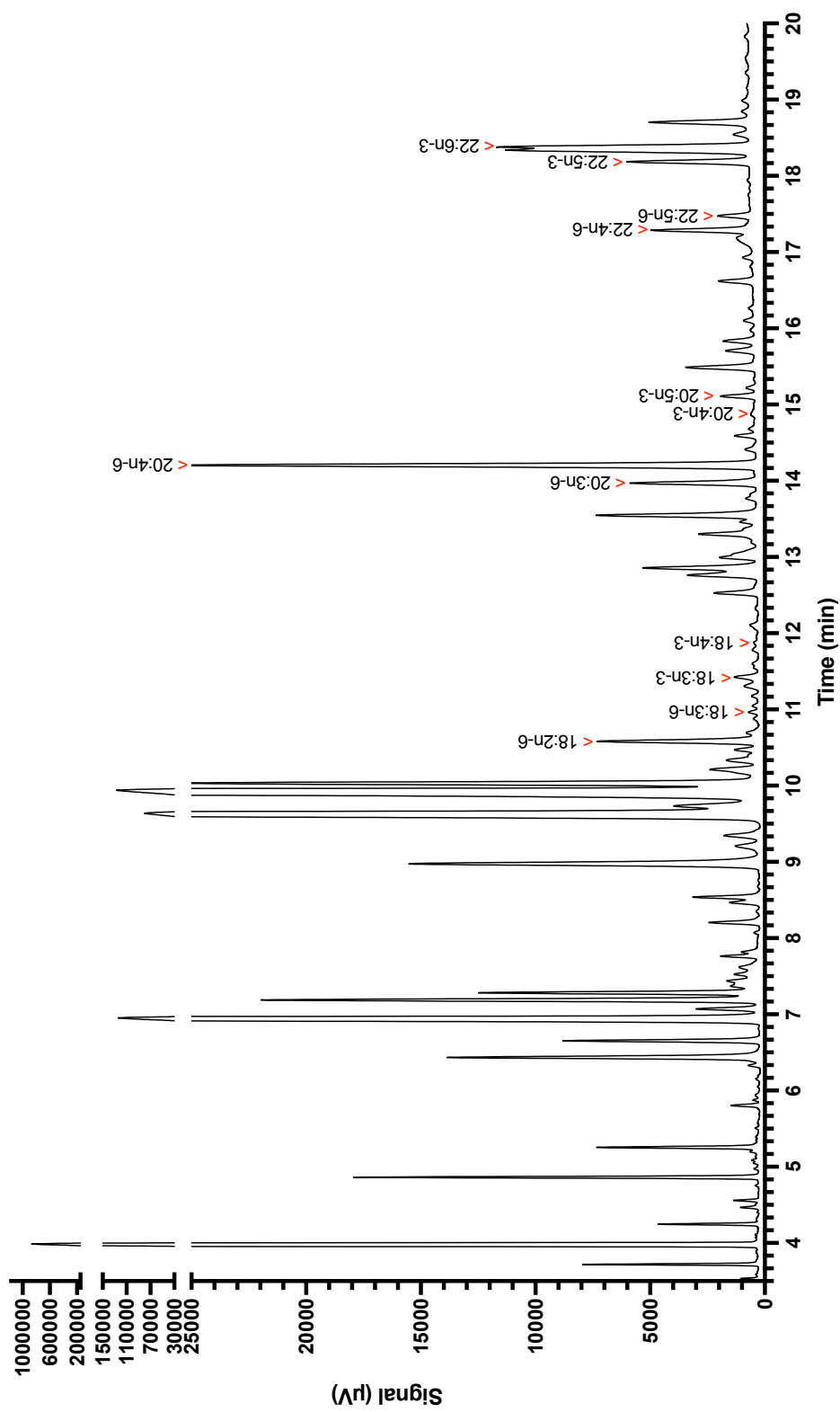


C

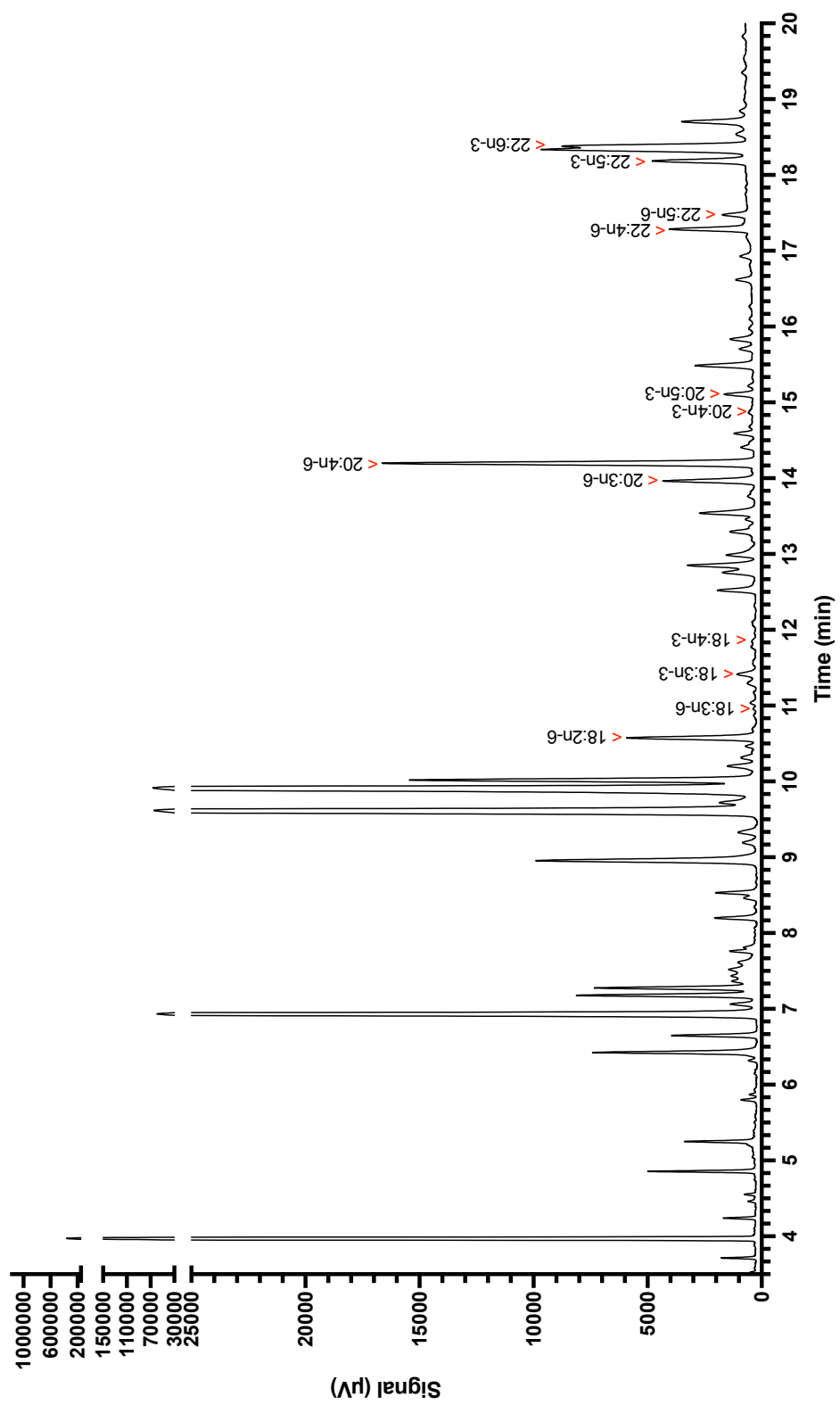
Figure 4.19: Representative GFCID Chromatograms For 24 h Fatty Acid Analysis

Representative chromatograms depicting a single replicate of each sample analyzed by GCFID. 231-CON cells were exposed to DMSO vehicle control (**A**), 2.5 μ M jadomycin B (**B**), or 5 μ M jadomycin B (**C**) for 24 h. Only those fatty acids assessed in **Figures 4.21** and **4.22** are indicated. (Figures on previous pages)

A



B



C

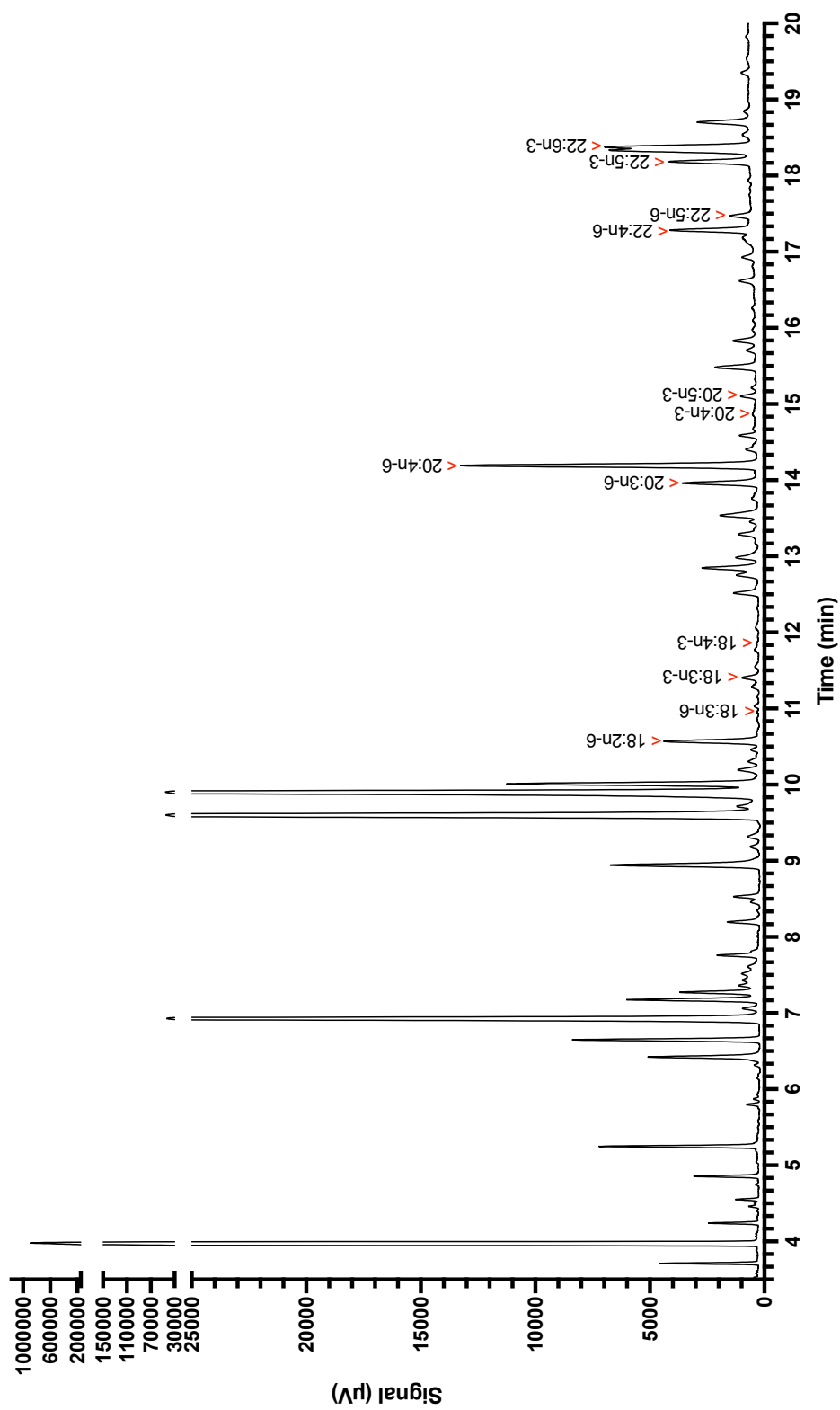


Figure 4.20: Representative GFCID Chromatograms For 48 h Fatty Acid Analysis

Representative chromatograms depicting a single replicate of each sample analyzed by GCFID. 231-CON cells were exposed to DMSO vehicle control (**A**), 2.5 μ M jadomycin B (**B**), or 5 μ M jadomycin B (**C**) for 48 h. Only those fatty acids assessed in **Figures 4.21** and **4.22** are indicated. (Figures on previous pages)

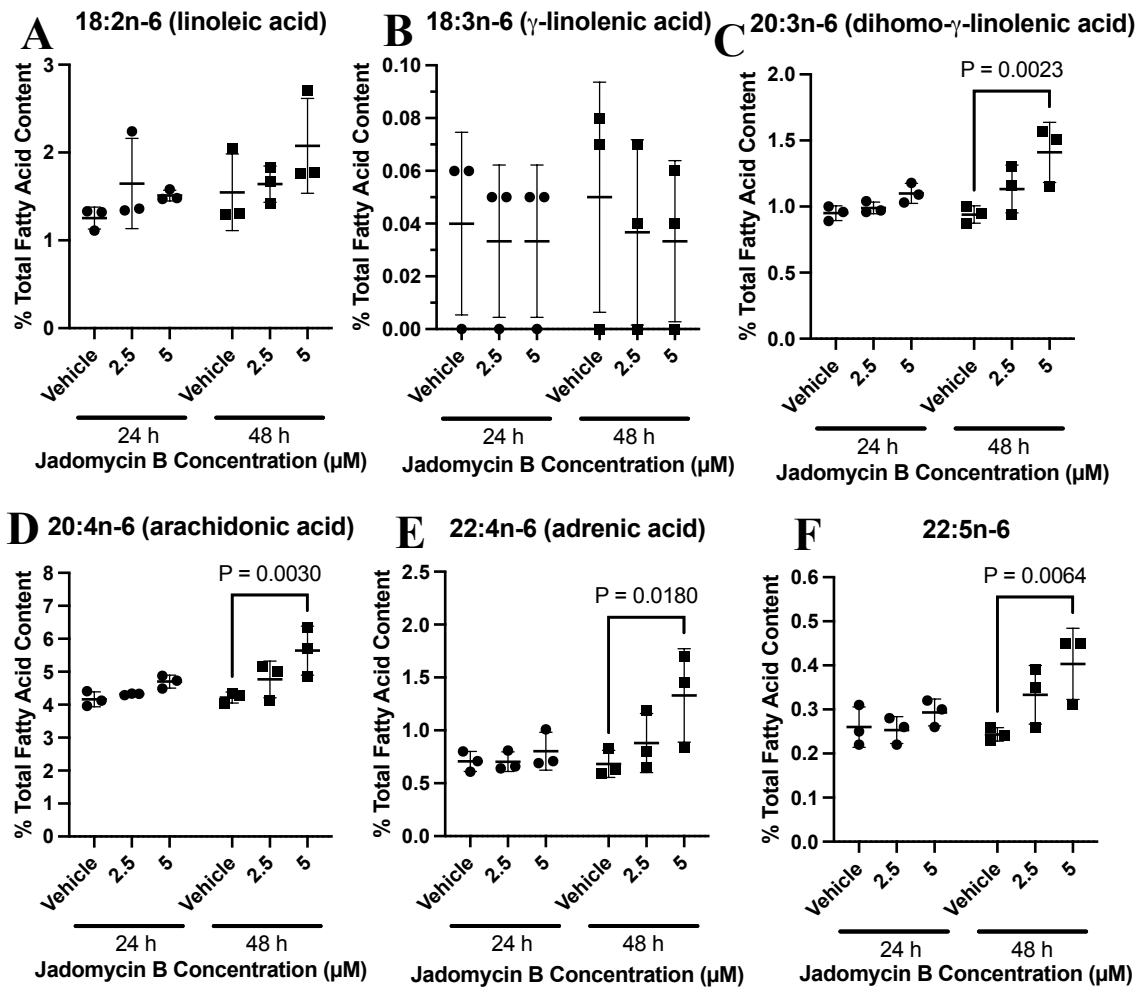


Figure 4.21: Changes in Cellular Levels of n-6 Fatty Acids Following Exposure to Jadomycin B

Levels of n-6 fatty acids in 231-CON cells exposed to jadomycin B (2.5 or 5 μ M) for 24 or 48 h as measured by GCFID. Fatty acids analyzed include (A) 18:2n-6 (linoleic acid), (B) 18:3n-6 (γ -linolenic acid), (C) 20:3n-6 (dihomo- γ -linolenic acid), (D) 20:4n-6 (arachidonic acid), (E) 22:4n-6 (adrenic acid), and (F) 22:5n-6. Datapoints represent the mean value of triplicate assays, expressed as percent of total cellular fatty acid content and compared to vehicle (DMSO) exposed cells. Significant difference is indicated by reported p-value ($P \leq 0.05$) as determined by two-way ANOVA, followed by Bonferroni's multiple comparison test. Error bars are mean \pm standard deviation.

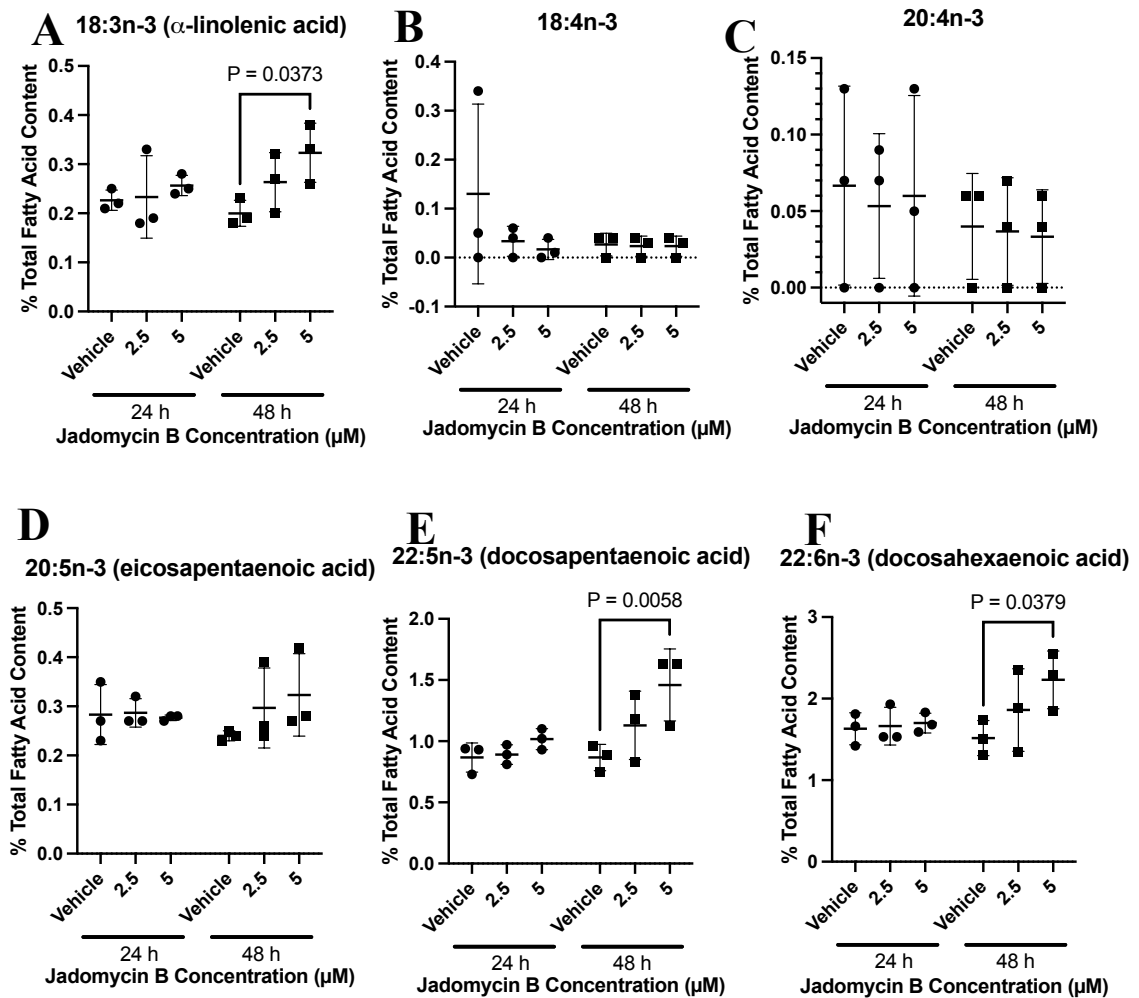


Figure 4.22: Changes in Cellular Levels of n-3 Fatty Acids Following Exposure to Jadomycin B

Levels of n-3 fatty acids in 231-CON cells exposed to jadomycin B (2.5 or 5 μ M) for 24 or 48 h as measured by GCFID. Fatty acids analyzed include (A) 18:3n-3 (α -linolenic acid), (B) 18:4n-3, (C) 20:4n-3, (D) 20:5n-3 (eicosapentaenoic acid), (E) 22:5n-3 (docosapentaenoic acid), and (F) 22:6n-3 (docosahexaenoic acid). Datapoints represent the mean value of triplicate assays, expressed as percent of total cellular fatty acid content and compared to vehicle (DMSO) exposed cells. Significant difference is indicated by reported p-value ($P \leq 0.05$) as determined by two-way ANOVA, followed by Bonferroni's multiple comparison test. Error bars are mean \pm standard deviation.

4.14: Lipogenesis Assessment by Calculation of Enzyme Indices

Using the cellular lipid profiles established by GC/FID, lipid ratios (**Figure 4.23**) and enzyme indices (**Figure 4.24**) can be calculated to gain insight into various aspects of lipogenesis. One possibility is that the differences in n-3 and n-6 fatty acids observed have occurred due to overall changes in *de novo* lipogenesis. Using the ratio of total 16:0 over 18:2n-6, it was determined that no significant change in *de novo* lipogenesis was observed at any concentration or time point tested. Additionally, the ratio of total n-3 fatty acids over total n-6 fatty acids was calculated to determine if a jadomycin B caused the cellular composition of fatty acids to skew in favour of one or the other. No significant difference in the ratio of n-3 to n-6 fatty acids was observed in any of the experimental conditions tested.

There are two major enzymes involved in the conversion of n-6 fatty acids leading to the biosynthesis of AA: $\Delta 5D$ and $\Delta 6D$ (Pavithra et al., 2018). Using established enzyme activity indices, an estimation of the activity of these two enzymes can be calculated. While there was no significant change in the estimated activity of $\Delta 6D$, there was a small but significant decrease in the estimated activity of $\Delta 5D$ following 48 h exposure to jadomycin B to 89% of that calculated for the vehicle control.

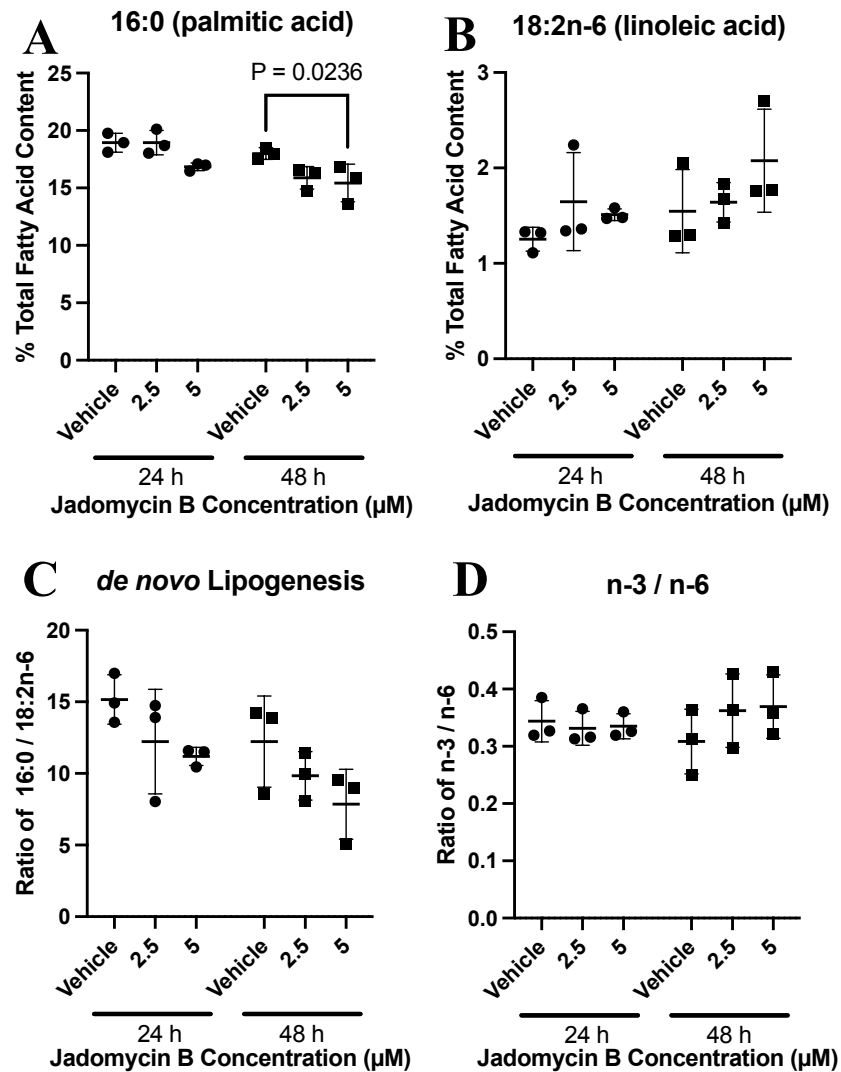


Figure 4.23: Calculations of Lipogenesis

Lipid ratios were used to calculate indicators of lipogenesis and distribution in 231-CON cells. Using the ratio of (A) 16:0 (palmitic acid) to (B) 18:2n-6 (linoleic acid) an estimation of (C) *de novo* lipogenesis can be generated. Similarly, using the ratio of total n-3 fatty acids (Figures 4.22 and B.7) to total n-6 fatty acids (Figures 4.21 and B.7) an estimation of (D) the shift between n-3 and n-6 fatty acids can be generated. Fatty acid datapoints for a single sample were treated as paired. Significant difference is indicated by reported p-value ($P \leq 0.05$) as determined by two-way ANOVA, followed by Bonferroni's multiple comparison test. Error bars are mean \pm standard deviation.

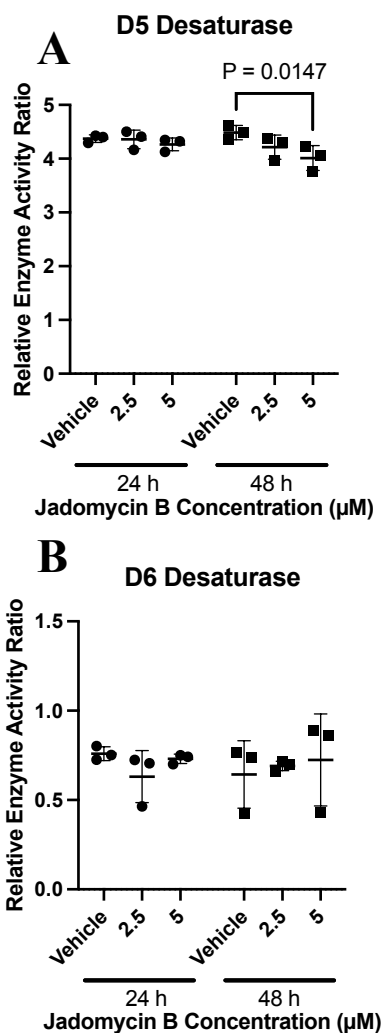


Figure 4.24: Estimation of Desaturase Activity

Estimations of (A) $\Delta 5\text{D}$ and (B) $\Delta 6\text{D}$ activity in 231-CON cells can be calculated using the ratio of 20:4n-6 over 20:3n-6 and 20:3n-6 over 18:2n-6 (**Figure 4.21**), respectively. Fatty acid datapoints for a single sample were treated as paired. Significant difference is indicated by reported p-value ($P \leq 0.05$) as determined by two-way ANOVA, followed by Bonferroni's multiple comparison test. Error bars are mean \pm standard deviation.

4.15: Assessment of Synergy Between Jadomycin B and Celecoxib in COX2 Enzyme Activity Assays

Given that changes to PGE2 and AA have been observed, it became important to determine how jadomycin B was eliciting those effects. One possibility was a direct effect on the COX2 enzyme. Using a purified COX2 enzyme, jadomycin B (0, 1, 2.5, 5, 10, and 20 μM) and celecoxib (0, 0.05, 0.1, 0.15, and 0.2 μM) were assayed for their effect on enzyme activity (**Figure 4.25**). Celecoxib is a known COX2 inhibitor and increasing concentrations of celecoxib resulted in increasing degrees of enzyme inhibition as expected. Jadomycin B alone invoked no significant change in enzyme activity at any concentration included, and pre-incubation of jadomycin B with the COX2 enzyme for 30 min had no additional effect (**Figure B.8**). In combination, jadomycin B and celecoxib acted synergistically to significantly increase the degree of inhibition of COX2 enzyme beyond the effect of celecoxib alone (**Figure 4.26, Table C.12**). At 0.15 μM and 0.2 μM celecoxib, all tested combinations with jadomycin B resulted in a greater than 12% increase in COX2 inhibition than celecoxib alone.

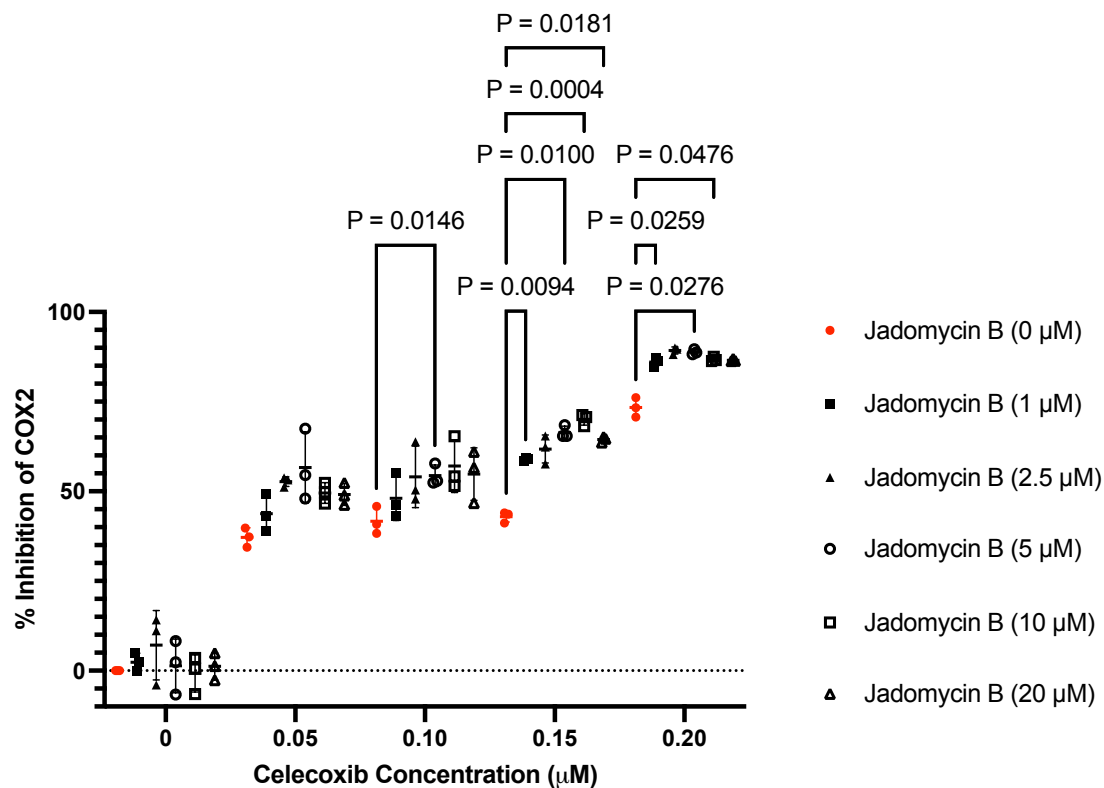


Figure 4.25: Jadomycin B Enhances Inhibition of COX2 by Celecoxib

Percent inhibition of purified COX2 enzyme activity in the presence of jadomycin B (0-20 μM), celecoxib (0-0.2 μM), or combinations of both. Datapoints represent the mean value of triplicate assays. Significant difference from celecoxib used alone (0 μM jadomycin B, highlighted in red) is indicated by reported p-value ($P \leq 0.05$) as determined by two-way ANOVA, followed by Bonferroni's multiple comparison test. Error bars are mean \pm standard deviation.

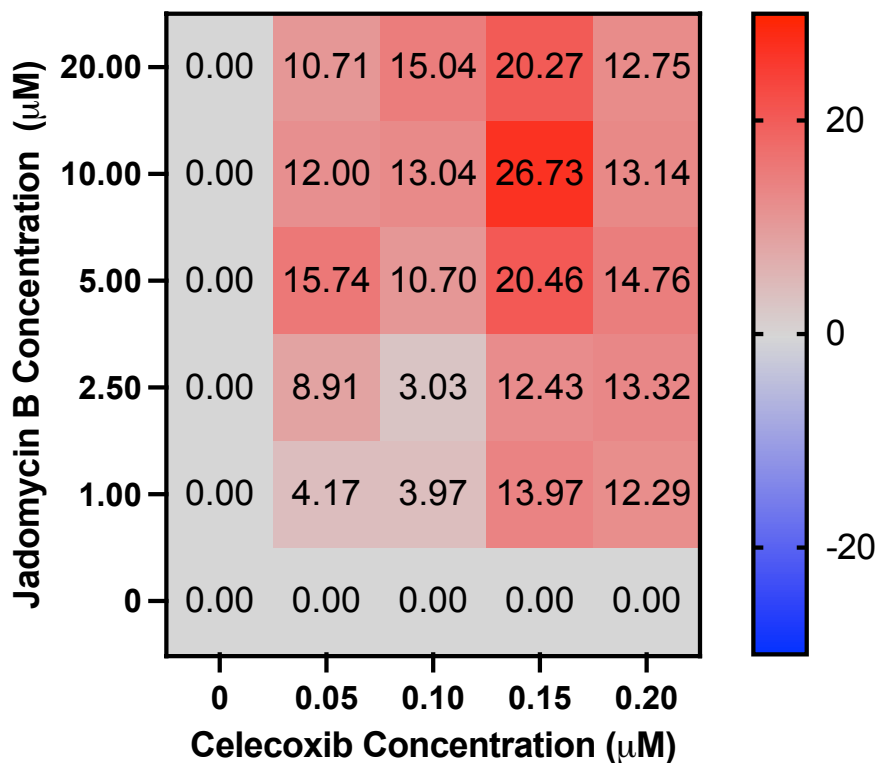


Figure 4.26: Jadomycin B and Celecoxib Act Synergistically to Inhibit COX2

Synergy scores were calculated using SynergyFinder 3.0 to determine if jadomycin B and celecoxib act synergistically in combination in a purified enzyme assay. Synergy scores represent fold change from expected effect if the two molecules were acting additively, therefore, scores > 10 denote synergy, < -10 denote antagonism, and < 10 but > -10 denote additivity. Scores were calculated from triplicate assays. Tabular results ± standard deviation are reported in **Table C.12**.

4.16: *in silico* Modeling of Jadomycin B Binding to the Active Site of COX2

The lack of direct effect of jadomycin B on enzyme activity of COX2 in purified assays combined with the observed synergistic activity between jadomycin B and celecoxib in subsequent experiments prompted the *in silico* analysis of jadomycin B binding at the active site of the COX2 enzyme. As jadomylicins naturally occur as a diastereomeric mixture (**Figure 4.27**), with 3a*S* being the predominant form of jadomycin B at a 3:2 ratio as compared to the 3a*R* form, both were modeled (Doull et al., 1994). The natural ligand, AA, and all of the included known COX2 inhibitors had negative Scores and RTCNNscores corresponding to favourable binding energy at the active site of COX2 (**Figure 4.28**). In contrast, jadomylicins B, F, and S were predicted to have positive Scores and near positive RTCNNscores, indicating that they are unlikely to bind at that site. When Score or RTCNNscore was plotted against the molecular area associated with that molecule there was a clear separation of the jadomylicins from the other molecules modeled. This model assessed only the active site of the COX2 enzyme and is consistent with the results of the purified enzyme assay in showing that an interaction with the active site is unlikely. As such, allosteric modulation may be responsible from the effect observed in **section 4.15**.

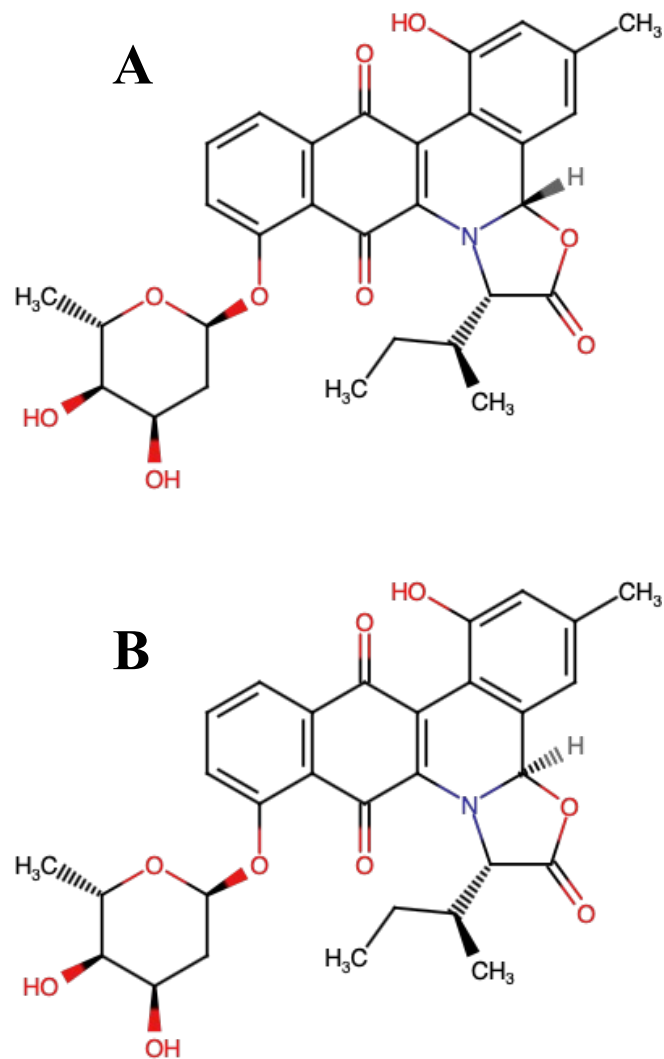


Figure 4.27: Jadomyicins Occur in a Diastereomeric Mixture of 3a*S* and 3a*R* forms

Molecular structure showing the (A) 3a*S* and (B) 3a*R* stereometric forms of jadomycin B.

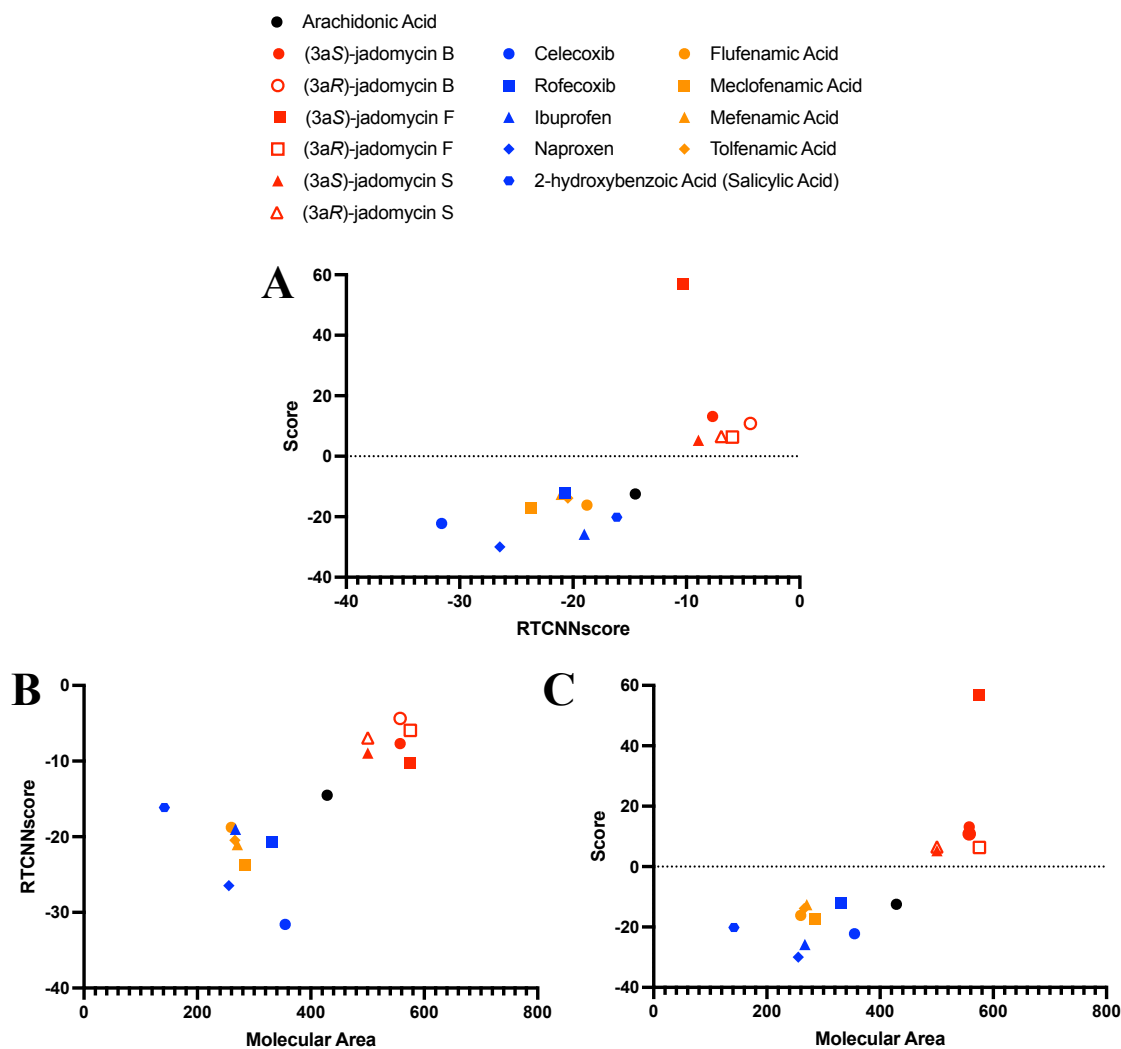


Figure 4.28: Molecular Docking of Arachidonic Acid, Jadomycin B, and Known Inhibitors of COX2

Molecular Docking was modeled using Molsoft ICM Pro 3.9 to determine if jadomycin B displayed favourable binding to the active site of the COX2 enzyme. Results showing (A) RTCNNscore vs Score, (B) molecular area vs RTCNNscore, and (C) molecular area vs Score. The natural ligand for the COX2 active site, arachidonic acid, is represented in black. Jadomycons are presented in red, common COX2 inhibitors used medicinally are in blue, and additional COX2 inhibitors in orange.

4.17: Determination of Synergistic Reduction of Cellular Viability with Jadomycin B and COX2 Inhibitors

Given the observed synergistic interaction between jadomycin B and celecoxib in purified enzyme assays, interaction between jadomycin B and known COX2 inhibitors was assessed for cytotoxic synergy (**Tables C.13, C.14, C.15, C.16, C.17, C.18, and C.19**). Celecoxib (0-60 μM), ibuprofen (0-1600 μM), and naproxen (0-1500 μM) were tested in combination with jadomycin B (0-5.0 μM) for 48 h in 231-CON and 231-JB cells (**Figures 4.29, 4.30, B.9, and B.10**). Synergy was observed between jadomycin B and ibuprofen or naproxen in both cell lines with the greatest synergy scores observed ranging from 37.85 ± 10.84 to 49.71 ± 14.34 , however, the concentrations of ibuprofen or naproxen needed were not physiologically achievable. In contrast, synergy scores for combinations of jadomycin B and celecoxib peaked at 18.87 ± 9.26 for 231-CON cells and 22.49 ± 8.10 for 231-JB cells. While this was sufficient to conclude synergy had occurred in 231-JB cells, the scores for 231-CON cells were still in the additive effect range. As with ibuprofen and naproxen, the concentrations of celecoxib needed to observe these synergy scores were not physiologically attainable. Subsequently, a greater number of concentrations of jadomycin B (0-2.2 μM) and a wider range of celecoxib (0-45 μM) concentrations (including physiologically attainable concentrations) were tested in combination and found to be synergistic in both 231-CON and 231-JB cells (**Figure 4.31, B.11, and B.12**). The greatest synergy scores in 231-CON cells were observed at concentrations of jadomycin B between 0.55 and 1.07 μM and celecoxib between 5.03 and 26.72 μM . In 231-JB cells, the required jadomycin B concentration was increased to between 0.80 and 1.57 μM .

To verify that the synergistic effect was not unique to TNBC cells, MCF-7 cells were exposed to combinations of jadomycin B (0-3 μM) and celecoxib (0-30 μM) as well (**Figures 4.32 and B.13**). The maximum synergy score observed was 40.50 ± 15.84 , similar to those observed in 231-CON and 231-JB cells.

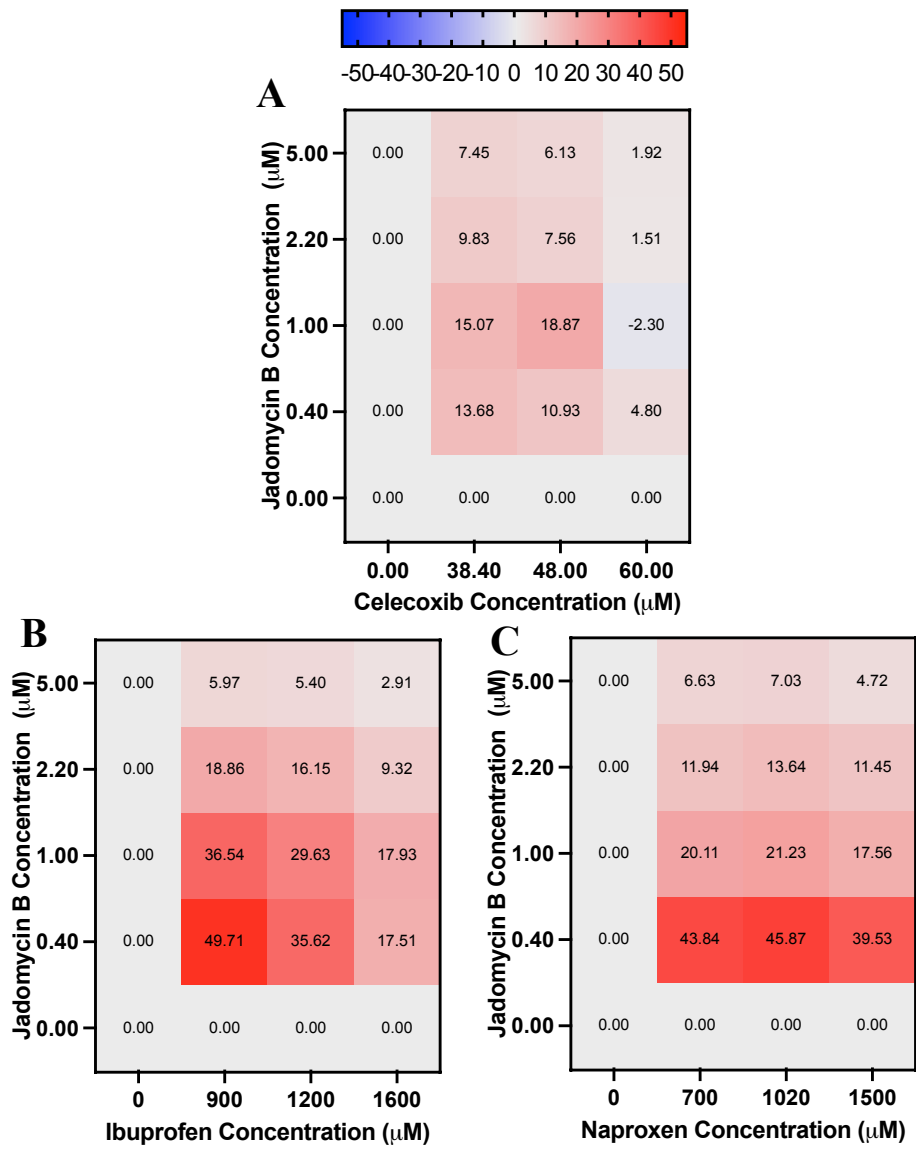


Figure 4.29: Synergy Scores for Jadomycin B and Celecoxib, Ibuprofen, or Naproxen in 231-CON Cells

Synergy scores were calculated using SynergyFinder 3.0 to determine if jadomycin B (0-5 μM) and (A) celecoxib (0-60 μM), (B) ibuprofen (0-1600 μM), or (C) naproxen (0-1500 μM) act in combination to elicit synergistic changes in cellular viability in 231-CON cells. Synergy scores represent fold change from expected effect if the two molecules were acting additively, therefore, scores > 10 denote synergy, < -10 denote antagonism, and < 10 but > -10 denote additivity. Scores were calculated from triplicate assays. Tabular results \pm standard deviation are reported in **Tables C.13, C.14, and C.15.**

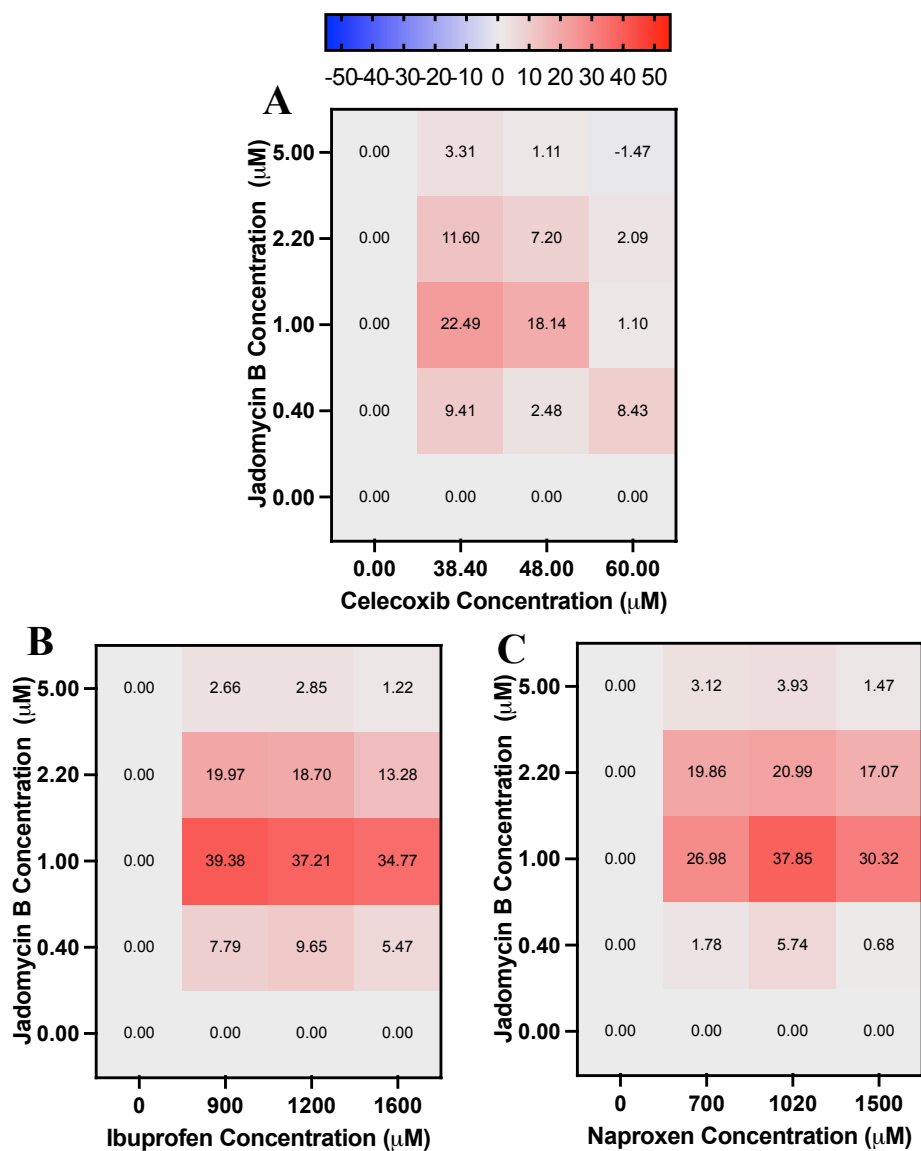


Figure 4.30: Synergy Scores for Jadomycin B and Celecoxib, Ibuprofen, or Naproxen in 231-JB Cells

Synergy scores were calculated using SynergyFinder 3.0 to determine if jadomycin B (0-5 μM) and (A) celecoxib (0-60 μM), (B) ibuprofen (0-1600 μM), or (C) naproxen (0-1500 μM) act in combination to elicit synergistic changes in cellular viability in 231-JB cells. Synergy scores represent fold change from expected effect if the two molecules were acting additively, therefore, scores > 10 denote synergy, < -10 denote antagonism, and < 10 but > -10 denote additivity. Scores were calculated from triplicate assays. Tabular results \pm standard deviation are reported in **Tables C.16, C.17, and C.18**.

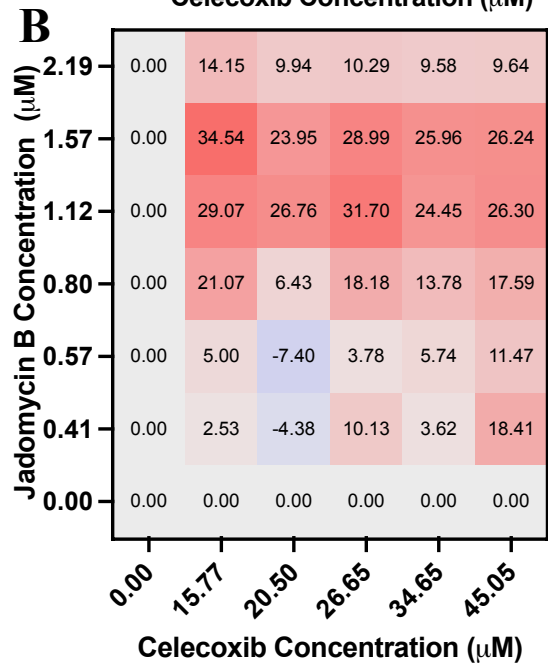
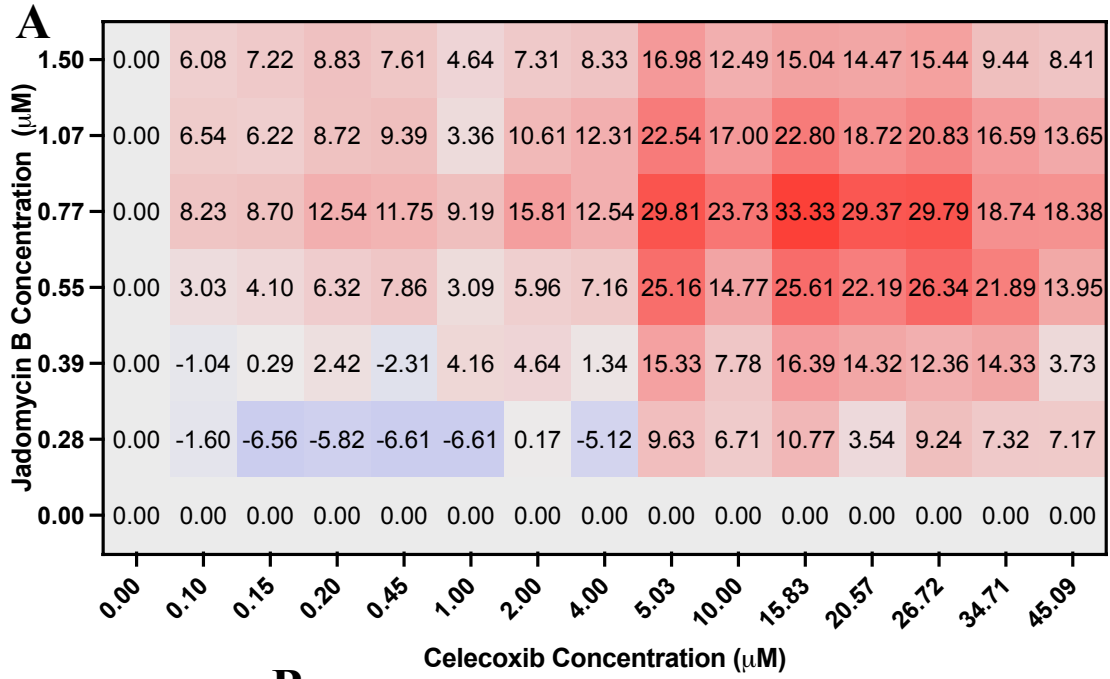
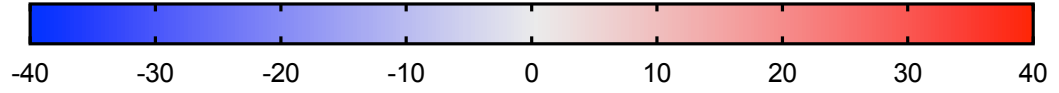


Figure 4.31: Synergy Scores for Jadomycin B and Celecoxib Across an Expanded Range of Concentrations in 231-CON and 231-JB Cells

Synergy scores were calculated using SynergyFinder 3.0 to determine if jadomycin B (0-2.2 μ M) and celecoxib (0-45 μ M) act in combination to elicit synergistic changes in cellular viability in (A) 231-CON or (B) 231-JB cells. Synergy scores represent fold change from expected effect if the two molecules were acting additively, therefore, scores > 10 denote synergy, < -10 denote antagonism, and < 10 but > -10 denote additivity. Scores were calculated from triplicate assays. Tabular results \pm standard deviation are reported in **Tables C.13**, and **C.16**. (Figures on previous page)

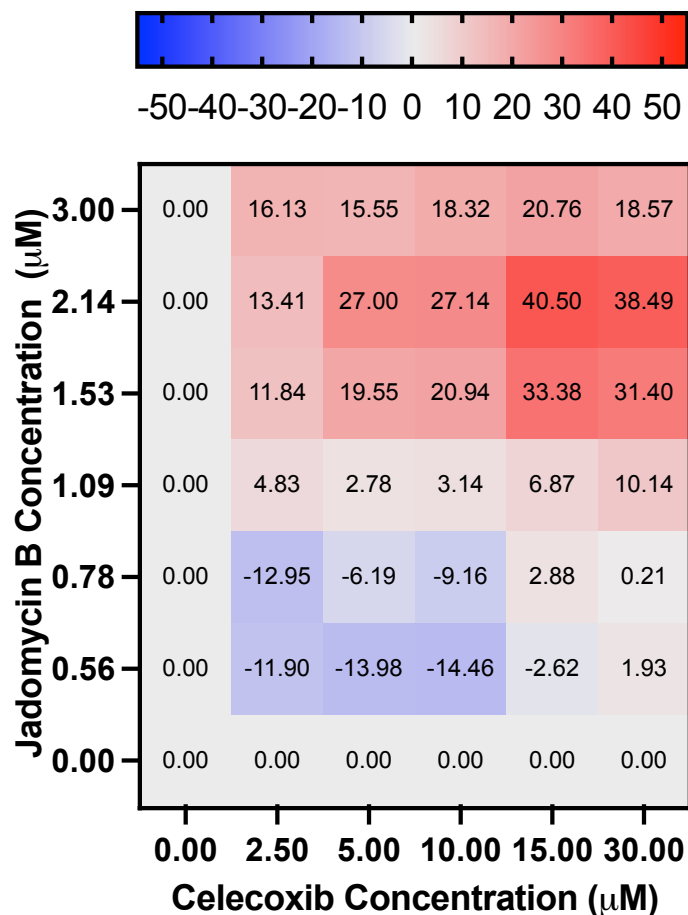


Figure 4.32: Synergy Scores for Jadomycin B and Celecoxib in MCF-7 Cells

Synergy scores were calculated using SynergyFinder 3.0 to determine if jadomycin B (0-3 μM) and celecoxib (0-30 μM) act in combination to elicit synergistic changes in cellular viability in MCF-7 cells. Synergy scores represent fold change from expected effect if the two molecules were acting additively, therefore, scores > 10 denote synergy, < -10 denote antagonism, and < 10 but > -10 denote additivity. Scores were calculated from triplicate assays. Tabular results ± standard deviation are reported in **Table C.19**.

4.18: Cell Spheroid Formation and Viability Assessment

Cancer cells, even within a single individual, do not necessarily represent a homogenous group of similar cells. This remains true within cultured cell lines, where MCF-7 and 231-CON cells are known to diversify into populations consisting of different sub-types (Fillmore and Kuperwasser, 2008). Among those are cells with stem cell-like properties which allow for increased tumorigenic capacity (Fillmore and Kuperwasser, 2008). It is possible that jadomycin B may be targeting a subset of cancer cells with stem cell-like properties. COX2 is known to control cancer cell stemness, thus, as a functional indicator of COX2 inhibition the effect of jadomycin B exposure on the formation of cell spheroids was assessed (Kundu et al., 2014; Walker et al., 2021). As jadomycin B toxicity has primarily been assessed in cells grown as a monolayer, cell spheroid assays could also help to determine the effects of jadomycin B as an intermediary to future *in vivo* studies. MCF-7 cells are known to display increased spheroid formation efficiency and, thus, were chosen as the cellular model for these assays (Wang et al., 2014). When MCF-7 cells were allowed to form spheroids in the presence of jadomycin B (0.05-1.50 μM), significantly fewer spheroids were formed in a dose-dependent manner at concentrations greater than 0.25 μM (**Figures 4.33** and **4.34**). Cellular viability of these spheroids as measured by alkaline phosphatase assay was also significantly reduced. However, the reduction in cell viability did not appear to be concentration-dependent over the range of concentrations tested.

Having established that cytotoxic effects could still be observed in spheroids directly exposed to jadomycin B, it was next determined that preexposure of MCF-7 cells in a monolayer with jadomycin B could affect subsequent spheroid formation (**Figures 4.35** and **4.36**). Following 48 h exposure to jadomycin B (2.5 or 5.0 μM), MCF-7 cells were allowed to form spheroids in drug free medium. Significantly fewer spheroids formed at both concentrations tested, however, there was a corresponding decrease in cellular viability.

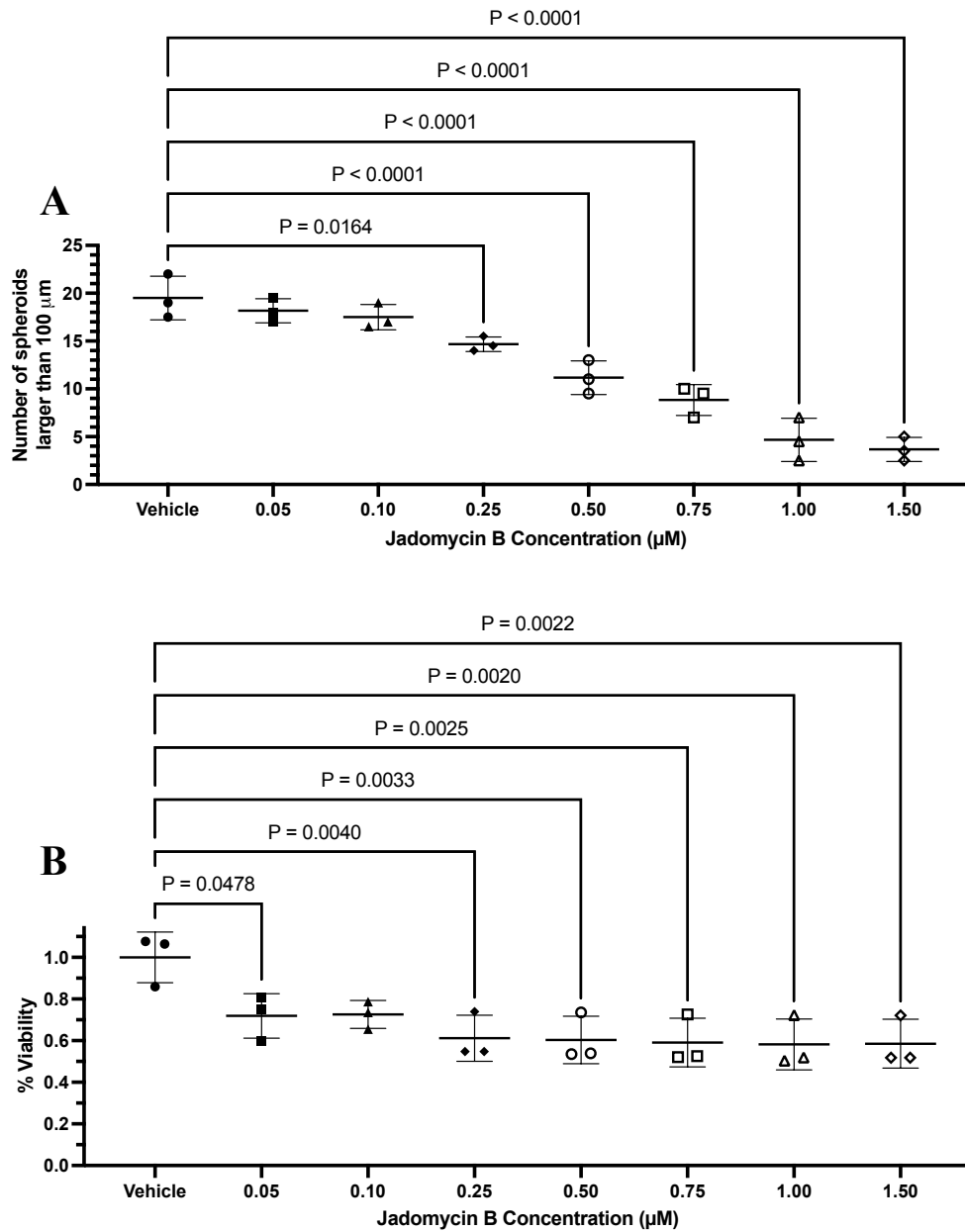
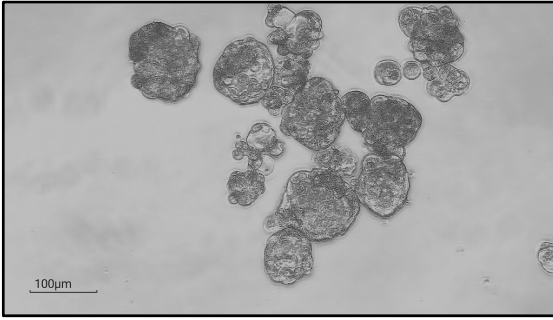


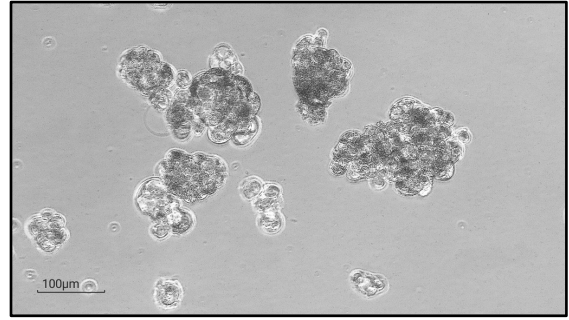
Figure 4.33: Effects of Jadomycin B on Spheroid Formation and Viability

Effects of jadomycin B (0.05-1.50 μM) exposure for 7 days on (A) the formation of spheroids > 100 μm in diameter and (B) the viability of the cells within those spheroids in MCF-7 cells. Datapoints represent the mean value of triplicate assays, each consisting of duplicate technical replicates. Significant difference from vehicle control is indicated by reported p-value ($P \leq 0.05$) as determined by one-way ANOVA, followed by Bonferroni's multiple comparison test. Error bars are mean \pm standard deviation.

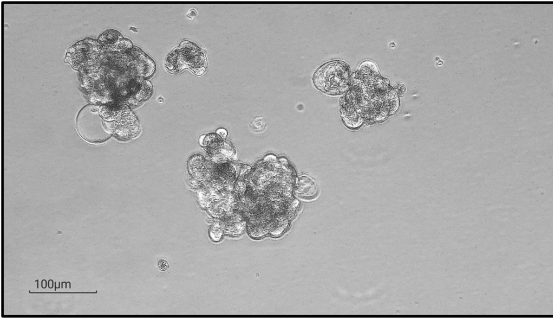
Vehicle



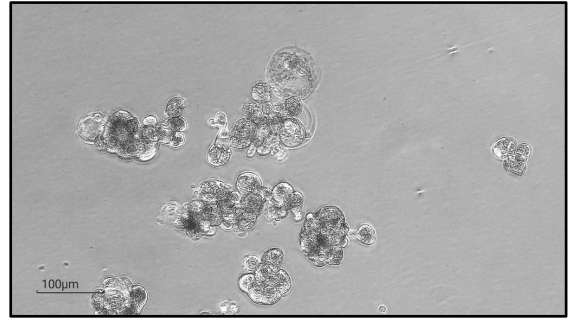
0.05 µM



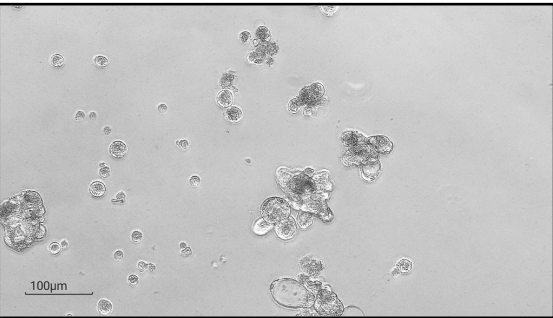
0.10 µM



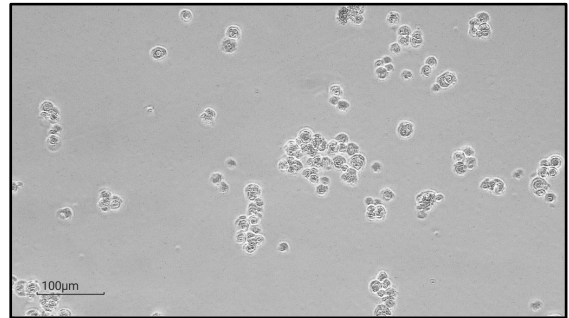
0.25 µM



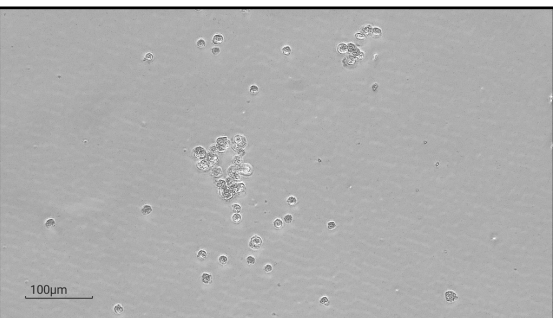
0.50 µM



0.75 µM



1.00 µM



1.50 µM

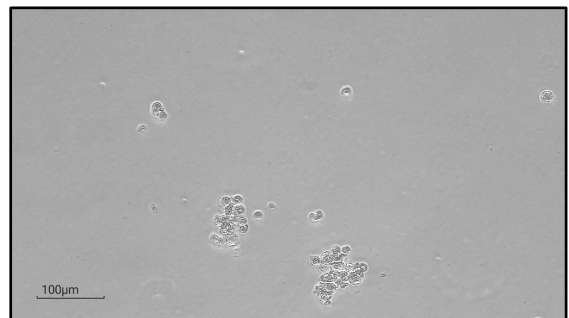


Figure 4.34: Representative Microscopic Images of Cell Spheroids Following Exposure to Jadomycin B

Representative images from a single replicate of the cell spheroid assay showing formation of spheroids greater than 100 μm (scale bar included) following 7 days exposure to vehicle control (DMSO) or jadomycin B (0.05-1.50 μM) in MCF-7 cells as presented in **Figure 4.33**. (Images on previous page)

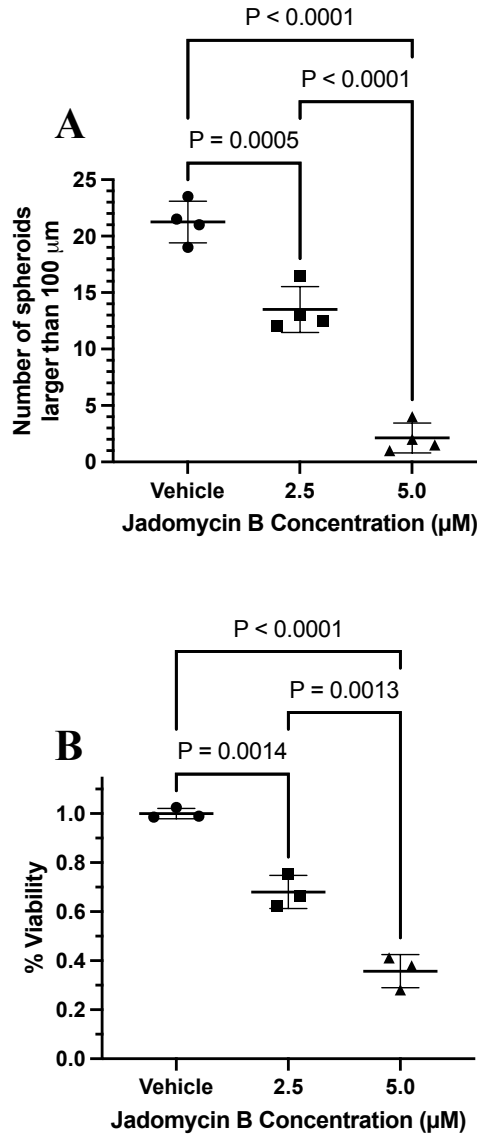
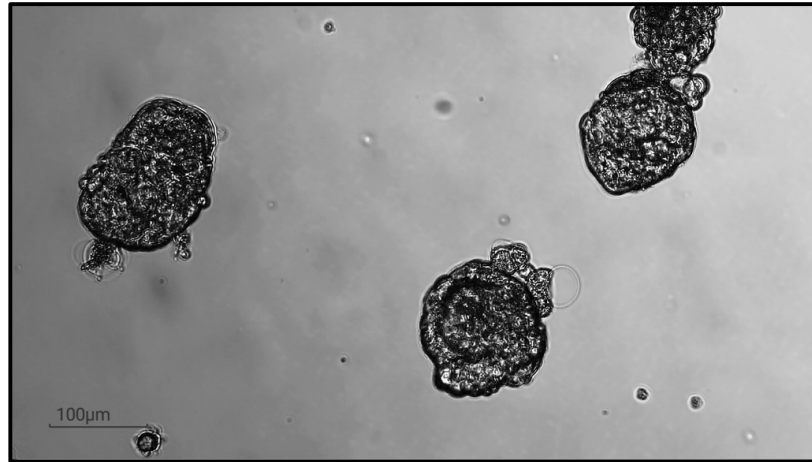


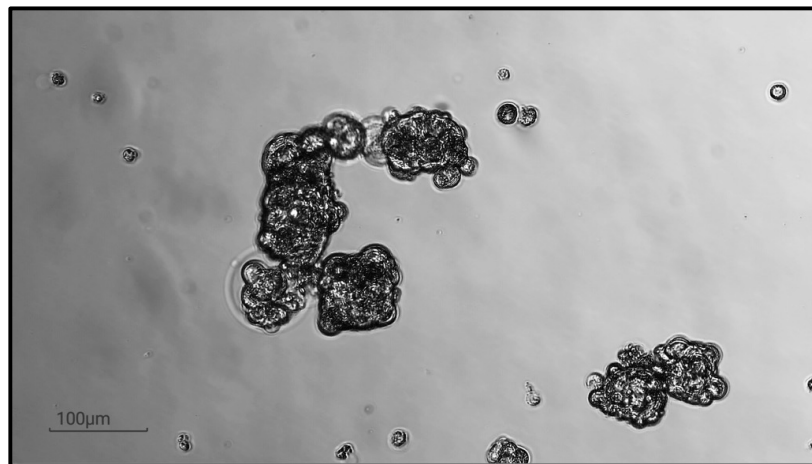
Figure 4.35: Effects of Jadomycin B Preexposure on Spheroid Formation and Viability

Effects of jadomycin B (2.5-5.0 μM) preexposure for 48 h followed by 7 days incubation in drug free medium on (A) the formation of spheroids > 100 μm in diameter and (B) the viability of the cells within those spheroids in MCF-7 cells. Datapoints represent the mean value of triplicate assays, each consisting of duplicate technical replicates. Significant difference from vehicle control is indicated by reported p-value ($P \leq 0.05$) as determined by one-way ANOVA, followed by Bonferroni's multiple comparison test. Error bars are mean \pm standard deviation.

Vehicle



2.5 μM



5.0 μM

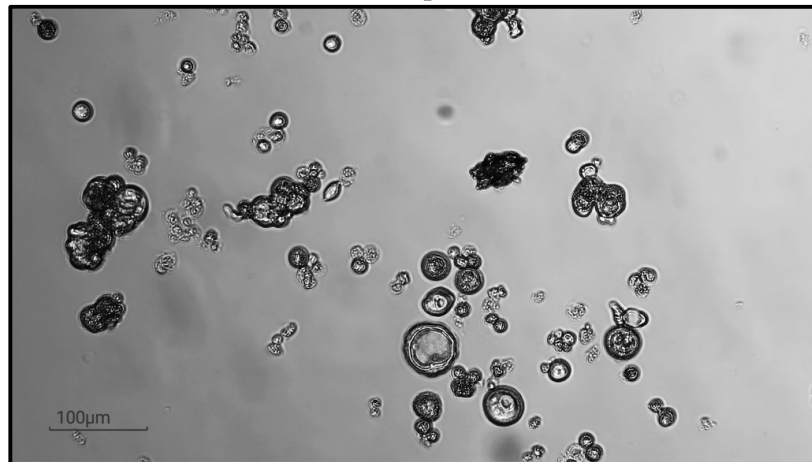


Figure 4.36: Representative Microscopic Images of Cell Spheroids Following Preexposure to Jadomycin B

Representative images from a single replicate of the cell spheroid assay showing formation of spheroids greater than 100 μm (scale bar included) following preexposure for 48 h with vehicle control (DMSO) or jadomycin B (2.5-5.0 μM) and subsequent incubation in drug free medium for 7 days in MCF-7 cells as presented in **Figure 4.35**. (Images on previous page)

4.19: Measurement of PI3K Signalling

The final experimental data collected was intended as a preliminary investigation of the cellular signalling pathway(s) involved in conveying the observed changes in the COX2 pathway to those cellular processes involved in cancer cell progression and transformation. The PI3K/AKT signalling pathway is involved in mediating the COX2 dependent upregulation of hepatocyte growth factor, leading to increased breast cancer cell growth and invasion, and the COX2/EP4 associated formation of stem-like breast cancer cells (Majumder et al., 2016; Kuang et al., 2017). For this reason, PI3K/AKT signalling pathway was elected as the initial pathway to be investigated for alterations in response to jadomycin B exposure.

No significant change was found in the protein expression of p-PI3K, total PI3K, or the ratio between p-PI3K/PI3K (**Figure 4.37**). A statistically significant increase (2.5-fold) in p-AKT was observed following 24 h exposure of 231-CON cells to 5.0 μ M jadomycin B with no significant change observed in total AKT (**Figure 4.38**). This resulted in a significant change in the ratio of p-AKT/AKT (2.6-fold) at the same time point and concentration. Finally, no significant change was observed in the protein expression of mTOR in response to jadomycin B (2.5 or 5.0 μ M) exposure in 231-CON cells at either 6 or 24 h (**Figure 4.39**).

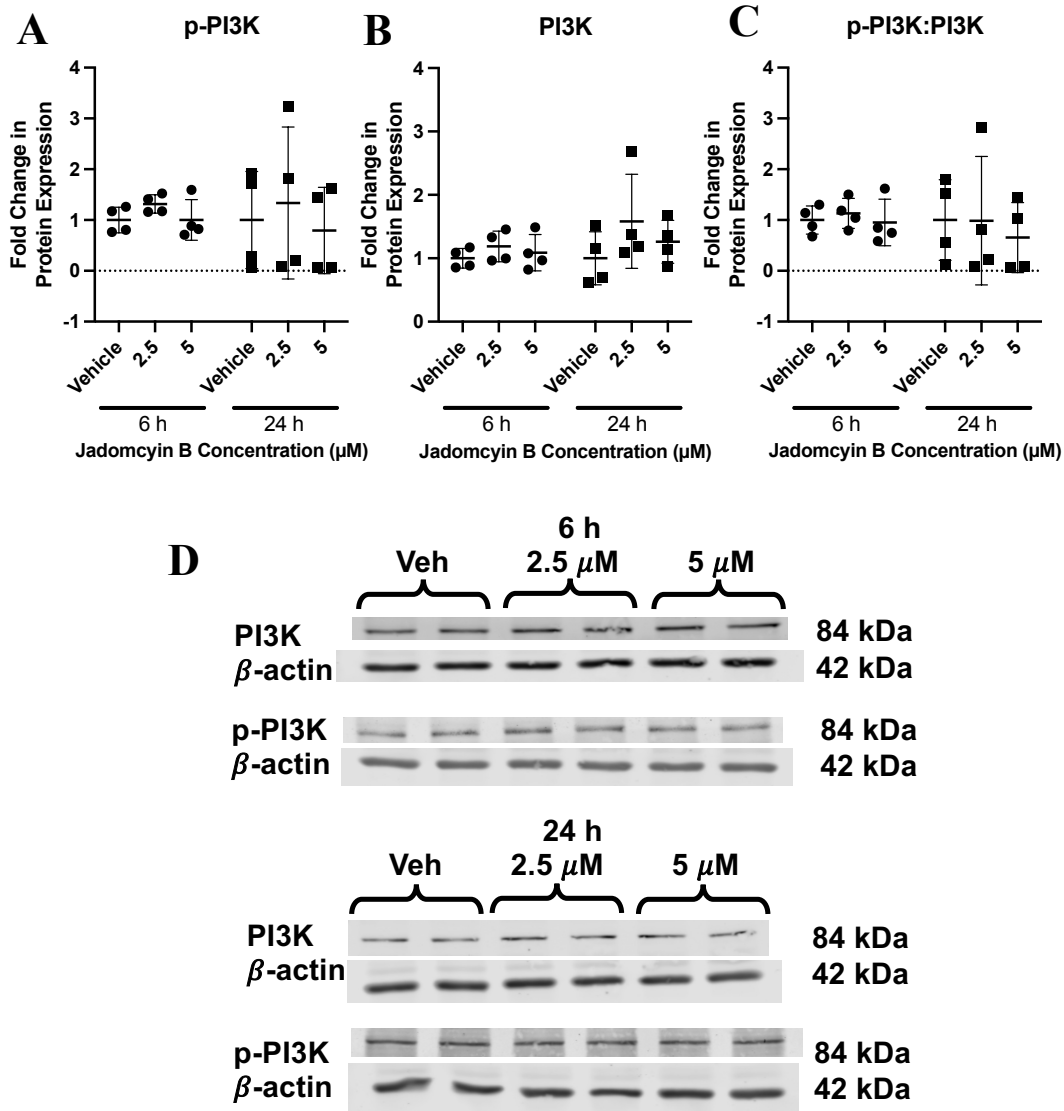


Figure 4.37: Expression of PI3K Protein with Jadomycin B

Protein expression of (A) p-PI3K, (B) PI3K, and (C) the ratio of p-PI3K:PI3K in 231-CON cells exposed to jadomycin B for 6 or 24 h as measured by Western blot.

Representative blots (D) are shown. Datapoints represent the mean value of quadruplicate assays, each consisting of a mean of duplicate technical replicates and expressed as fold change in protein expression as compared to vehicle (DMSO) exposed cells. Significant difference is indicated by reported p-value ($P \leq 0.05$) as determined by two-way ANOVA, followed by Bonferroni's multiple comparison test. Error bars are mean \pm standard deviation.

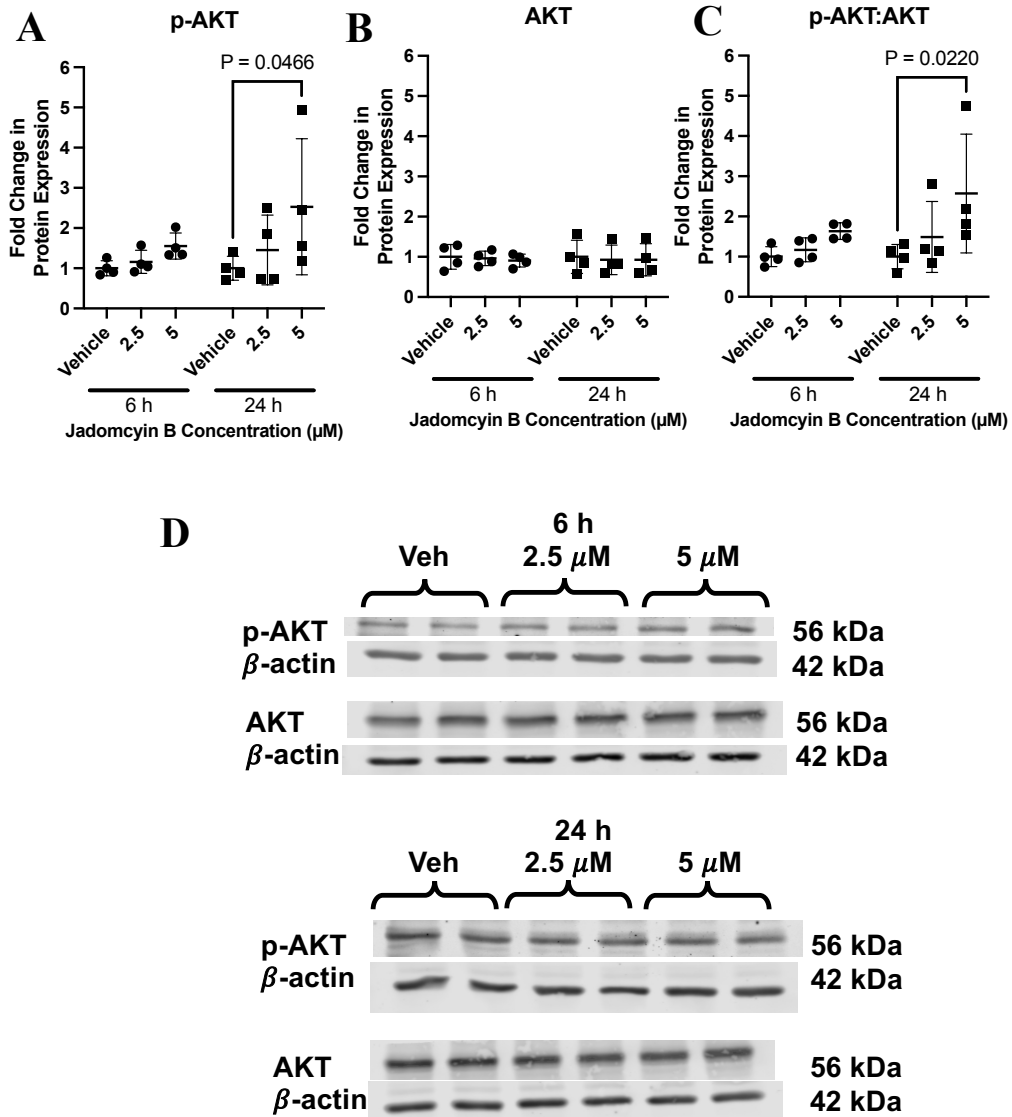


Figure 4.38: Expression of AKT Protein with Jadomycin B

Protein expression of (A) p-AKT, (B) AKT, and (C) the ratio of p-AKT:AKT in 231-CON cells exposed to jadomycin B for 6 or 24 h as measured by Western blot.

Representative blots (D) are shown. Datapoints represent the mean value of quadruplicate assays, each consisting of a mean of duplicate technical replicates and expressed as fold change in protein expression as compared to vehicle (DMSO) exposed cells. Significant difference is indicated by reported p-value ($P \leq 0.05$) as determined by two-way ANOVA, followed by Bonferroni's multiple comparison test. Error bars are mean \pm standard deviation.

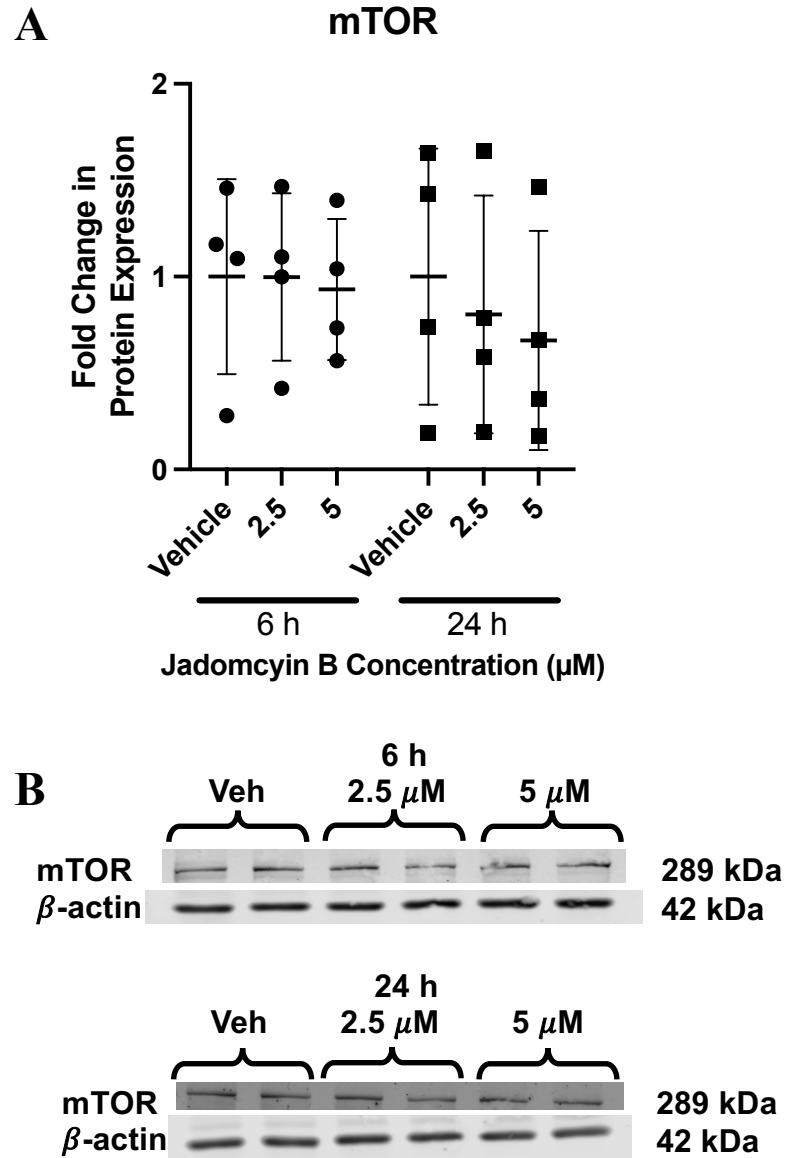


Figure 4.39: Expression of mTOR Protein with Jadomycin B

Protein expression of (A) mTOR in 231-CON cells exposed to jadomycin B for 6 or 24 h as measured by Western blot. Representative blots (D) are shown. Datapoints represent the mean value of quadruplicate assays, each consisting of a mean of duplicate technical replicates and expressed as fold change in protein expression as compared to vehicle (DMSO) exposed cells. Significant difference is indicated by reported p-value ($P \leq 0.05$) as determined by two-way ANOVA, followed by Bonferroni's multiple comparison test. Error bars are mean \pm standard deviation.

Chapter 5: Discussion

A general discussion of the results presented in this work (**Figure 5.1**) is the principal subject of this fifth chapter, divided as they relate to the specific objects outlined in **Chapter 2**. Those discussions are followed by an examination of known limitations and possible future directions. Finally, a general conclusion for this work is provided.

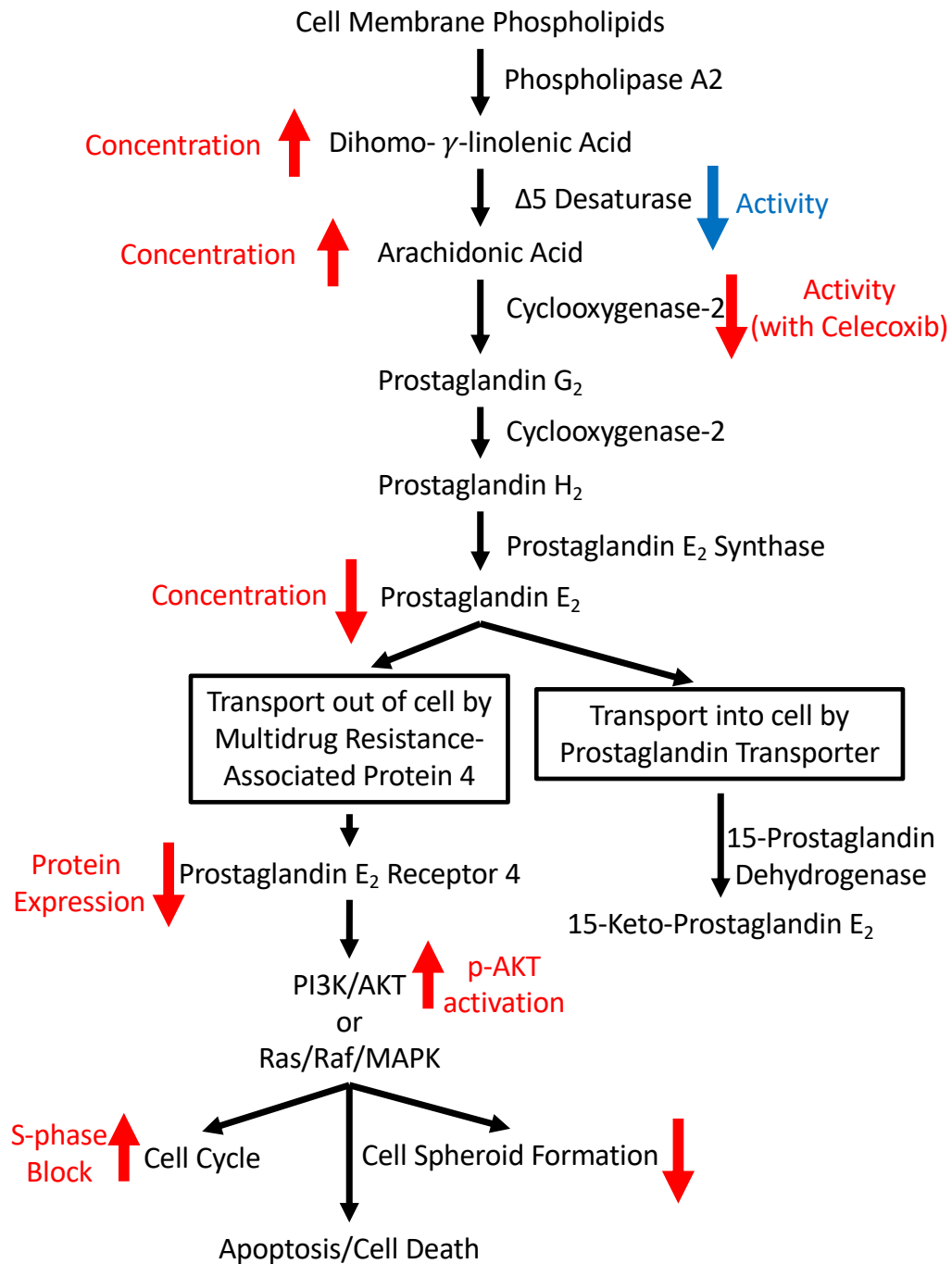


Figure 5.1: Summary of Novel Observations on the COX2 Related Activity of Jadomycin B Described in this Work

Novel observations on the effects of jadomycin B on COX2 related signalling described in this work. Red arrows and text indicate directly observed effects while blue arrows and text indicate inferred changes from enzyme activity indices.

5.1: Characterization of the Similarity of Jadomycin B Obtained from Multiple Sources and Initial Stability Assessment

At the time of this writing, all published research into the pharmacology of jadomycin B, and indeed all jadomycins, has been conducted using material locally synthesised by the research group involved. For the first time, this work presents a comparison of commercially and locally produced material and demonstrates equivalent cytotoxic potency between them. Comparing jadomycin B produced by individual research groups and manufacturers is an important component in determining the applicability of the results from one study to the next and in allowing progression from discovery to optimization (Hughes et al., 2011). In this work, the IC_{50} for 231-CON cells exposed to jadomycin B for 72 h was determined to be $0.91 \pm 0.31 \mu\text{M}$ for locally synthesized jadomycin B and $0.70 \pm 0.15 \mu\text{M}$ for commercially purchased jadomycin B (Table 4.1). These values are comparable to the $1.76 \pm 0.33 \mu\text{M}$ and $2.77 \pm 0.49 \mu\text{M}$ values determined previously in our laboratory using locally synthesized jadomycin B (Hall et al., 2015; Hall et al., 2017). Furthermore, the effects of prolonged storage on the cytotoxic and physical properties of jadomycin B have never before been described. This work has uniquely demonstrated that jadomycin B remains stable at both 25 and 37 °C for up to 4 days, with a colour change occurring after 8 days but no significant change in cytotoxic effect until 60 days. While the observed change in colour was examined in commercially produced jadomycin B, our research group has previously noted that similar colour changes occurred in locally synthesized material as well (Jakeman, 2021). In the context of this work, the longest exposure period for cellular exposure to jadomycin B was 7 days while 48 h exposures were more routinely utilized. While it is possible that jadomycin B is metabolized or otherwise degraded by cellular processes in this time, it is now known that prolonged environmental exposure to human body temperature (37 °C) alone is not sufficient to decrease jadomycin B efficacy over the timeframes and dosage intervals commonly assayed in pre-clinical research.

5.2: Jadomycin B Behaves Differently as Compared to Established TOP2 Poisons

Having established that the source of jadomycin B used and the exposure times selected were appropriate and comparable to previous studies, the first specific goal of this work was the *determination of the effect of jadomycin B on topoisomerase-2* given the previous studies finding initial evidence of TOP2 involvement in the jadomycin mechanism of action (Martinez-Farina et al., 2015a; Hall et al., 2017). If jadomycin B is acting as a TOP2 poison it would be reasonable to expect jadomycin B to have similar cell cycle effects as known TOP2 poisoning molecules. As previously described, doxorubicin and mitoxantrone are known to elicit a cell cycle arrest characterized by the accumulation of cells in the G₂/M phase (Bar-On et al., 2007; Khan et al., 2010). When used as a positive control in the present study, mitoxantrone was observed to elicit the same result (**Figure 4.4B**). The only previous study to explore the effect of jadomycin B on the cell cycle reported that A549 human lung adenocarcinoma cells did not undergo any significant change in number of cells accumulated at any change of the cell cycle, with a nonsignificant trend toward an elevated number of cells in the S phase (Fu et al., 2008). The small but statistically significant increase in proportion of cells found in the S phase in the present study (**Figure 4.4A**) corroborates these results and demonstrates that jadomycin B behaves differently from mitoxantrone at the concentration assayed.

The next experiment intended to investigate the involvement of TOP2 in the cytotoxic effects of jadomycin B involved the accumulation of TOP2 cleavage complexes. Previously, it was demonstrated that jadomycin DS binds to recombinant human TOP2 β but that jadomycin LN could not (Martinez-Farina et al., 2015a). This led to subsequent experiments demonstrating that jadomyccins B, F, and S could cause a reduction in *TOP2A* and *TOP2B* gene expression while only jadomycin S reduced *TOP1* gene expression (Hall et al., 2017). Additionally, jadomyccins B, F, and S all inhibited TOP2 α and TOP2 β protein activity in a dose dependent manner, with jadomycin B and F selectively increasing DNA cleavage by TOP2 β (Hall et al., 2017). In the present work, when the accumulation of TOP2 cleavage complexes were measured directly, preliminary data showed that jadomycin B did not cause an appreciable increase in cleavage complex formation for TOP2 α , TOP2 β , nor TOP1 (**Figures 4.5 and 4.6**). This again demonstrates

a divergence from the expected action of a topoisomerase poison. One explanation for this seeming incongruence of data may be the concentrations of jadomycin used. Focusing on jadomycin B, the cytotoxic effects measured in the experiments described in this work range from $0.70 \pm 0.15 \mu\text{M}$ at 72 h to $2.83 \pm 0.31 \mu\text{M}$ at 48 h (**Tables 4.1 and 4.4**) while $20 \mu\text{M}$ jadomycin B for 36 h was required to observe the inhibitory effect on *TOP2A* and *TOP2B* gene expression and $160 \mu\text{M}$ jadomycin B was the lowest concentration to significantly prevent conversion of catenated DNA to decatenated DNA as previously described (Hall et al., 2017). It is therefore reasonable to conclude that while jadomycin B can interact with TOP2, it does so at concentrations greater than those required to elicit the cytotoxic effect in breast cancer cells.

A second possible explanation is that, at high concentrations, jadomycin B is acting as a TOP2 catalytic inhibitor rather than as a TOP2 poison. Both TOP2 poisons and TOP2 catalytic inhibitors act to inhibit TOP2 activity; the distinction between them comes from the point at which that inhibition occurs and the generation of a toxic form of the enzyme. If TOP2 is inhibited while bound to DNA and a double strand break is generated, converting the enzyme into a cellular toxin, then the responsible molecule is deemed a TOP2 poison (Jensen and Sehested, 1997; Burden and Osheroff, 1998; Vann et al., 2021). If no double strand break is generated, then the molecule is classified as a TOP2 catalytic inhibitor (Jensen and Sehested, 1997). The previous report that jadomyccins B, F, and S could inhibit TOP2 activity did not distinguish between catalytic inhibition and poisoning, thus, measurement of cleavage complex accumulation was intended to make that distinction (Hall et al., 2017). The observation that TOP2 cleavage complexes do not accumulate in the present work suggests that the previously observed inhibition may have been catalytic in nature. A third possible explanation is also offered by the proposal that jadomyccins may be capable of promiscuously binding many different proteins at high concentrations (Martinez-Farina et al., 2015a). At high concentrations jadomyccins may be binding TOP2 in addition to other undescribed target(s) which are responsible for their cytotoxic effect at lower concentrations. This suggests that additional, yet to be discovered, targets susceptible to low concentrations of jadomyccins need to be investigated.

The third experiment intended to determine if the cellular response to jadomycin B was similar to that invoked by known TOP2 poisons involved a comparison of several drug combinations which were then assessed for synergy (**Table 4.3**). Doxorubicin and mitoxantrone are both known to poison TOP2 and, therefore, would be expected to act additively given that they share a mechanism of action (Gewirtz, 1999). This is what was observed, with an average combination index value across all calculated effect sizes of 1.12 and an average combination index value of 1.03 in the 50-90% range of effect sizes. If jadomycin B acts as a TOP2 poison, it too should act additively with doxorubicin and mitoxantrone. Conversely, catalytic inhibitors of TOP2 are known to antagonize the effect of TOP2 poisons because they act at a point in enzymatic activity where no double strand DNA breaks are present and thereby prevent the formation of those DNA double strand breaks (Jensen and Sehested, 1997). If jadomycin B were acting as a catalytic inhibitor of TOP2 then an antagonistic response would be expected. The third possibility, that jadomycin B acts on some other cellular target, could result in additivity, synergy, or antagonism. When either doxorubicin or mitoxantrone were combined with jadomycin B a similar slightly synergistic or additive response was observed, with average combination index values of 0.75 and 0.90 respectively in the 50-90% effect sizes. While the synergy assays alone do not prove or disprove TOP2 poisoning activity, they do make catalytic inhibition of TOP2 a less likely explanation for the previously observed interactions.

SN-38 is a known TOP1 poison which has previously been shown to act synergistically with doxorubicin in human breast cancer cells (Wu et al., 2020). This synergy can be explained in that SN-38 and doxorubicin act on separate cellular targets leading to different cytotoxic pathways. It is therefore reasonable to conclude that SN-38 will act synergistically with all TOP2 poisons, however, SN-38 may also act synergistically with molecules causing cytotoxicity *via* other cellular targets. When SN-38 was combined with jadomycin B, doxorubicin, or mitoxantrone, all 3 combinations were found to be synergistic with the average combination index values ranging from 0.27 to 0.69 in the 50-90% effect range. This similarity in response may indicate that jadomycin B is acting on the same target as doxorubicin and mitoxantrone due to the

shared profile of mutual additivity and synergy with SN-38. Alternatively, it may demonstrate that jadomycin B is targeting an unrelated pathway.

Adding combinations of MG132 would help to define this interaction as MG132 is a proteasome inhibitor which is expected to act antagonistically with TOP2 poisons (Lee et al., 2016; Destanovic et al., 2018). By inhibiting proteasomal activity the topoisomerase cleavage complex will not be degraded; a step necessary to the generation of DNA double strand breaks produced by TOP2 poisons. Combinations of MG132 with either doxorubicin or mitoxantrone resulted in the expected antagonistic combination index values. In contrast, the combination of jadomycin B and MG132 was additive which again suggested a difference in mechanism of action. Taken together, the drug synergy data presented do not definitively demonstrate that jadomycin B exerts its primary cytotoxic effect through interaction with TOP2, although some interaction with the enzyme is suggested.

Combining the results from the cell cycle, cleavage complex, and synergy experiments presents a broad comparison between jadomycin B and known TOP2 poisons. In the cell cycle and cleavage complex assays jadomycin B behaves dissimilarly to mitoxantrone and etoposide. In the synergy experiments, jadomycin shows some similarity to mitoxantrone and doxorubicin but a contrasting response when in combination with MG132. While previous reports on the interaction between jadomycin B and topoisomerase are compelling, the observed differences in this work suggest that TOP2 inhibition is not the primary mechanism of action of jadomycin B and some other process or processes may be involved.

5.3: Resistance to Jadomycin B is Differentially Mediated as Compared to Mitoxantrone Resistance

To determine what other processes may be involved in the cytotoxic effect of jadomycin B, the *establishment of a jadomycin-resistant human breast cancer cell line* became the second specific goal of this work. IC₅₀ values after 48 h exposure were determined in 231-CON cells, for the first time, to use as a control for the determination of the degree of resistance gained in 231-JB or 231-MITX cells (**Table 4.4**). The 15.8-

fold increase in resistance to mitoxantrone observed in 231-MITX cells is comparable to the approximately 8-fold increase in resistance to mitoxantrone previously reported for 231-TXL cells (Hall et al., 2017; Goralski, 2020). In comparison, 231-JB cells demonstrated a lesser degree of resistance to jadomycin B at approximately 3-fold. It should be noted, however, that cell lines established from post-chemotherapy patients typically have a 2- to 5-fold increase in resistance, suggesting that a 3-fold increase is within the clinically relevant range (McDermott et al., 2014). Interestingly, this 3-fold degree of resistance remained consistent in the 231-JB cells when exposed to each of the jadomycins tested (B, F, and S), suggesting that the mechanism through which resistance is conveyed is dependent upon the unchanged jadomycin backbone as opposed to the amino acid substituent group. This was a unique observation and demonstrates for the first time that resistance to one jadomycin conveys resistance to others. Additionally, while 231-JB cells showed cross resistance to jadomycins F and S, there was no significant increase in resistance to mitoxantrone, doxorubicin, nor SN-38. The 231-MITX cells, in contrast, expressed only a 2-fold increase in resistance to jadomycins B or F despite their 15.8-fold increase in resistance to mitoxantrone. While this suggests that a high degree of resistance to mitoxantrone may be sufficient to convey a clinically relevant degree of resistance to jadomycin B, there is a disparity in the extent of resistance attained by the two cell lines. This again is an important observation as it demonstrates that jadomycin B resistance is not expected to occur to the same degree as mitoxantrone resistance with the over expression of ABCG2 that has been associated with resistance to other breast cancer treatments.

Having established that differences in resistance are exhibited by 231-JB and 231-MITX cells, it was important to characterize possible ways in which that resistance arose. If jadomycin B cytotoxicity were dependent on interaction with TOP2 it would be reasonable to assume that 231-JB cells may have decreased TOP2 expression, preventing enzyme poisoning. High concentrations of jadomycins B, F, and S (20 μ M for 36 h) and mitoxantrone (1 μ M for 36 h) have previously been shown to decrease expression of *TOP2A* and *TOP2B* genes in 231-CON cells so it was important to determine if a similar change is occurring in conjunction with established jadomycin resistance (Hall et al., 2017). While 231-MITX cells exhibited the expected decrease in gene expression of

TOP2A and *TOP2B*, with no effect on *TOP1*, 231-JB cells showed no significant change (**Figure 4.12**). As with the previously discussed data on cell cycle, cleavage complex formation, and synergy, this lack of effect on topoisomerase gene expression provides greater evidence that jadomycin B is acting on some other target or targets at the low concentrations known to induce cytotoxicity.

It has been well established that resistance to mitoxantrone can be mediated by increased expression of the BCRP drug efflux transporter coded for by the *ABCG2* gene (Allikmets et al., 1998; Doyle et al., 1998; Miyake et al., 1999; Dean et al., 2001). Indeed, previous work by our group has demonstrated that MCF-7-TXL, MCF-7-ETP, and MCF-7-MITX cells which respectively overexpress *ABCB1*, *ABCC1*, and *ABCG2* remain susceptible to jadomycin B as do 231-TXL cells which overexpress *ABCB1* (Issa et al., 2014; Hall et al., 2017). As expected, 231-MITX cells were shown to overexpress *ABCG2* while 231-JB cells showed no significant change in *ABCB1*, *ABCC1*, nor *ABCG2* (**Figure 4.13**). From this, it can be concluded that 231-MITX cells are exhibiting resistance to mitoxantrone in the previously identified manner and confirms that this mechanism of resistance does not convey cross resistance to jadomyccins (Issa et al., 2014). By corroborating previous research showing that jadomyccins B, F, and S are not susceptible to a common form of multidrug resistance developed through increased drug efflux transporter expression, this work confirms the continued interest in jadomyccins as a potential anticancer drug. These results are novel in that they demonstrate that 231-JB cells fundamentally differ from 231-MITX cells in the how resistance is achieved and therefore represent a unique jadomycin resistant human breast cancer cell line.

5.4: Jadomycin B Resistance is Correlated to Increased COX2 Expression

With the establishment of the 231-JB cell line, a *determination of additional mechanisms through which jadomycin B may be exerting its effect* could be conducted. Using a drug resistant cancer cell line is an established approach for determination of the mechanism through which cytotoxicity is effected (McDermott et al., 2014). By looking at the genetic changes present in 231-JB cells, insight can be gained into the pathway(s) with which jadomycin B is interacting. A human cancer drug target array was used to

screen for changes in gene expression in 231-JB cells as compared to 231-CON cells (**Table C.11**). This screen matched the previously discussed result that *TOP2A* and *TOP2B* gene expression were unchanged in 231-JB cells. Importantly, the largest change identified was a 22-fold increase in expression of *PTGS2* which codes for the COX2 protein. The increase in expression of both the *PTGS2* gene (**Figure 4.14**) and COX2 protein (**Figure 4.15**) were therefore verified in 231-JB cells.

Cyclooxygenase is an enzyme with two isoforms in humans, COX1 and COX2, respectively coded for by the *PTGS1* and *PTGS2* genes. COX2 is highly expressed in a variety of cancers, including breast cancer, where it is associated with poor clinical outcome (Simmons et al., 2004; Majumder et al., 2018; Ching et al., 2020). While most somatic cells express COX1 in a constitutive manner, only the stomach, kidney, nerve, reproductive, and immune cells routinely express COX2 (Majumder et al., 2018; Hashemi Goradel et al., 2019). As only *PTGS2* was included in the cancer drug target array, it was therefore important to determine if jadomycin B resistance was associated with a change in *PTGS1* expression as well. While 231-JB cells exhibited a significant reduction in *PTGS1* expression by about 6-fold, the comparatively large 38-fold increase in *PTGS2* expression represented the more compelling target for further examination. In response to lipopolysaccharide, which is used to induce inflammation, astrocytes have been shown to increase COX2 and PGE₂ production while simultaneously decreasing COX1 expression (Font-Nieves et al., 2012). The similar profile of increased *PTGS2* and decreased *PTGS1* in 231-JB cells could therefore represent a similar increase in inflammation or disruption of the signalling pathway governed by COX2 and PGE₂.

The COX1 and COX2 enzymes convert AA to prostaglandin G₂ which is again converted by either cyclooxygenase to prostaglandin H₂, from whence it is converted by various prostaglandin synthases to other prostaglandins (Simmons et al., 2004; Majumder et al., 2018). Of particular importance is PGE₂ as this is the most abundant prostaglandin in cancer (Ching et al., 2020). The generation of PGE₂ is regulated by prostaglandin E synthase. Regardless of the endpoint prostaglandin being produced, cyclooxygenase activity is recognized as the rate-limiting step (Chandrasekharan and Simmons, 2004; Ching et al., 2020). The PGE₂ pathway has been identified as being of particular

importance in breast cancer due to its tumour promoting effects and role in the development of a cancer stem cell phenotype (Kundu et al., 2014; Walker et al., 2021).

Once produced and released, PGE₂ can bind to any member of a group of G-protein coupled receptors responsible for the activation of intracellular signalling cascades; these are known as prostaglandin E₂ receptors 1 through 4 (EP1-4) (Sugimoto and Narumiya, 2007; Reader et al., 2011). In the context of breast cancer, EP1, EP2, and EP4 are commonly upregulated as compared to their expression in normal breast tissue, whereas EP3 is typically downregulated in breast cancer (Reader et al., 2011). The evidence for involvement of EP1 in breast cancer is limited and a consensus on its role in breast cancer has yet to be reached (Reader et al., 2011). In 231-CON cells EP1 stimulation has been associated with increased angiogenesis, while there is strong evidence in murine models of breast cancer demonstrating EP1 stimulation functions as a suppressor of metastatic potential (Timoshenko et al., 2006; Ma et al., 2010; Reader et al., 2011). Due to the anti-metastatic effects of EP1 signalling, it is now believed that EP1 acts in opposition to EP2 and EP4 signalling. EP4 is commonly upregulated in many cancers included those of the breast (Majumder et al., 2018; Ching et al., 2020). When activated, EP4 initiates intracellular signalling to promote cell survival, proliferation, and the acquisition of cancer stem cell-like characteristics (Kundu et al., 2014; Majumder et al., 2015; Xu et al., 2018; Ching et al., 2020). EP4 activation has also been associated with increased breast cancer cell invasion and metastasis through EGFR transactivation, which can be blocked by EP4 antagonists in murine models of breast cancer (Ma et al., 2006; Tönisen et al., 2017). As such, EP4 was chosen as the initial PGE₂ receptor for investigation.

In 231-JB cells, there was no significant change in *EP4* gene expression nor EP4 protein expression. However, acute exposure of 231-CON cells to jadomycin B for 24 and 48 h has been shown for the first time to result in a significant decrease in EP4 protein (**Figure 4.16**). EP4 has been proposed as a promising therapeutic target in breast cancer and the reduction in EP4 protein expression may contribute to the observed effects of jadomycin B on human breast cancer cells (Majumder et al., 2018; Ching et al., 2020). EP4, therefore, is a potential target of jadomycin B activity. If EP4 expression is reduced following transient exposure, prolonged exposure may result in selection toward

increased PGE₂ production *via* increased COX2 expression leading to jadomycin resistance. Another possibility is that jadomycin B may have increased toxicity against a subset of cells with greater EP4 expression. Breast cancer stem cells are known to have upregulated EP4 expression, so disruption of either EP4 or signalling by PGE₂ may disproportionately affect those cells (Kundu et al., 2014).

5.5: Jadomycin B Abolishes PGE₂ Accumulation and Alters Cellular Lipid Profiles

Connecting COX2 and EP4 is PGE₂ as the signal conducting molecule. The novel observation that PGE₂ concentration in the growth medium remained unchanged from baseline levels following jadomycin B exposure (**Figure 4.17**) demonstrates that jadomycin B is acting on the metabolic pathway responsible for PGE₂ production. One possibility was that jadomycin B interacted with COX2 in an inhibitory manner. If this were the case, an increase in AA would be expected as has previously been suggested to occur with cyclooxygenase inhibitors in Alzheimer's disease (Sagi et al., 2003). Measurement of the cellular lipid profiles of cells exposed to jadomycin B revealed that AA and its precursor dihomo- γ -linolenic acid were significantly increased as compared to vehicle exposed cells (**Figure 4.21**) by approximately 2-fold and 1.5-fold, respectively. AA is not, however, the only substrate of COX2. Dihomo- γ -linolenic acid, eicosapentaenoic acid (20:5n-3), and adrenic acid (22:4n-6) are all also oxidized by COX2 (Smith and Malkowski, 2019). As concentrations of dihomo- γ -linolenic acid and adrenic acid were significantly increased following jadomycin B exposure, it is reasonable to conclude that inhibition of COX2 activity may have been responsible. Like AA, dihomo- γ -linolenic acid is also necessary to produce a prostaglandin, prostaglandin E₁, which is thought to have anti-inflammatory as opposed to pro-inflammatory effects (Levin et al., 2002). A change in COX2 activity could, therefore, explain the accumulation of both n-3 and n-6 fatty acids in addition to the diminished production of PGE₂.

Biosynthesis of AA was another aspect of PGE₂ production potentially affected by jadomycin B exposure. To address this possibility, lipogenic indices were calculated from the cellular fatty acid composition data (**Figure 4.23**). No significant changes were

observed in the ratio of n-3 to n-6 fatty acids, suggesting that any changes observed in the percent total of AA and dihomo- γ -linolenic acid are the result of changes within the biosynthetic pathway rather than a shift between n-3 and n-6 fatty acid groups. Similarly, the same conclusion is supported by the observation that there was no significant change in *de novo* lipogenesis. In fact, the only significant change was a decrease in $\Delta 5D$ activity (**Figure 4.24**) which was minor at only a 0.89-fold change. The absence of significant difference in lipogenesis, therefore, further supports that jadomycin B is acting on COX2 to prevent PGE₂ biosynthesis from AA.

5.6: Celecoxib and Jadomycin B Act Synergistically to Inhibit COX2 Activity and Result in an Enhanced Cytotoxic Effect

Having identified COX2 as a likely target of jadomycin B, *determination of synergistic potential of jadomycin B in combination with other small molecules rationally selected based on putative mechanisms identified by the results of objectives 1-3* became the final specific objective of this work. Non-steroidal anti-inflammatory drugs (NSAIDs) are a group of related small molecules which target cyclooxygenase enzymes and inhibit the synthesis of prostaglandins (Simmons et al., 2004). Certain NSAIDs, for example celecoxib and rofecoxib, are more selective for COX2 while others, for example ibuprofen and naproxen, will inhibit COX1 and COX2 non-specifically (Simmons et al., 2004). The primary reason for this difference in specificity is the more accessible active site on the COX2 enzyme allowing for greater substrate conformational freedom (Vecchio et al., 2012). If jadomycin B is acting to inhibit the synthesis of PGE₂ then it is reasonable to expect some synergistic interaction with NSAIDs may occur (**Figures 4.25 and 4.26**). Additionally, there has been considerable interest in implementing COX2 inhibitors in breast cancer therapy as chemosensitizers which this result would support (Hashemi Goradel et al., 2019).

Surprisingly, when purified COX2 was exposed to jadomycin B alone there was no significant inhibitory effect on the enzyme. In contrast, celecoxib alone had a dose-dependent inhibitory effect. Without further investigation, this could have suggested that jadomycin B does not act on COX2 but rather exerts an effect elsewhere in the pathway

leading to reduced signal transduction by EP4. When COX2 was co-exposed to jadomycin B and celecoxib, however, there was a synergistic inhibitory effect which leads to the conclusion that jadomycin B is acting on the COX2 enzyme at an alternative site to celecoxib. This novel finding demonstrates that jadomycin B can modify the activity of a purified COX2 enzyme, but only in the presence of a COX2 inhibitor.

COX2 is a structural homodimer which functions as a conformational heterodimer consisting of an allosteric and catalytic pair (Smith and Malkowski, 2019). Celecoxib, like other NSAIDs, inhibits COX2 by binding to the active site of the catalytic subunit and thereby blocking AA access (Smith and Malkowski, 2019). As previously discussed, several other fatty acids are COX2 substrates in addition to AA and accumulation of those substrates has an inhibitory effect similar to NSAIDs. Molecular docking of substrates to the active site of COX2 was modeled *in silico* (**Figure 4.28**) and revealed that jadomycins do not have a favourable binding affinity at this active site. In combination, these results suggest that jadomycin B does act directly on the COX2 enzyme but not at the active site on the catalytic subunit. Jadomycin B may therefore be acting at an allosteric site to modify COX2 activity in conjunction with celecoxib in purified enzyme assays. The lack of inhibitory effect of jadomycin B alone in purified enzyme assays may suggest that the cytotoxic effect observed *in vitro* is the result of a similar allosteric interaction with COX2 in combination with endogenous fatty acids, which are absent from these purified assays, acting as COX2 inhibitors.

Nonsubstrate fatty acids can alter the activity of COX2. When bound to the allosteric site of COX2, palmitic acid can enhance the oxygenation of AA at the catalytic site by 2-fold, however, palmitic acid itself is unable to bind the catalytic site (Smith and Malkowski, 2019). While adrenic acid and docosahexaenoic acid are known to bind the catalytic site of COX2 and thus are capable of competitive inhibition, when bound to the allosteric site they also have an inhibitory effect on AA oxygenation by COX2 (Yuan et al., 2009; Smith and Malkowski, 2019). In this way, endogenous fatty acids are capable of modulating COX2 activity as both direct inhibitors and allosteric inhibitors.

Other endogenous molecules can also bind the allosteric site of COX2. Assessment of the affinity of AA and the endocannabinoid 2-arachidonoylglycerol for the allosteric and catalytic sites of COX2 found that when AA is bound to the allosteric site,

the catalytic efficiency of COX2 in oxygenation of 2-arachidonoylglycerol was decreased (Mitchener et al., 2015). AA bound to the allosteric site had no effect on AA at the catalytic site (Mitchener et al., 2015). Conversely, when 2-arachidonoylglycerol was bound to the allosteric site there was increased catalytic efficiency for AA oxygenation at the active site (Mitchener et al., 2015).

An alternative possibility is exemplified by cyclosporine A. Cyclosporine A has been shown to bind an allosteric site on COX2, resulting in increased COX2 activity (Groenendyk et al., 2018). When modelled, cyclosporine A was found to bind a unique site which is not involved in the interaction of COX2 with any other known ligand (Groenendyk et al., 2018). For this reason, future research is needed to determine if jadomycin B is binding an as-yet undescribed site in a similar manner to cyclosporine A but resulting in an inhibitory effect through modification of ligand binding at the active site.

Given that synergistic activity was observed in purified enzyme assays, the next logical step was to confirm synergy *in vitro* using 231-CON and 231-JB cells. While jadomycin B acted synergistically with ibuprofen and naproxen *in vitro* (**Figures 4.29** and **4.30**), the concentrations of the NSAIDs needed to achieve this effect were much greater than those concentrations achieved with typical oral dosing. Peak plasma concentration for a single 600 mg oral dose of ibuprofen is 51.3 ± 1.9 mg/L and for a single 500 mg oral dose of naproxen is 64.05 mg/L in healthy, adult volunteers (Janssen and Venema, 1985; Davies and Anderson, 1997). These typical concentrations would equate to approximately 250 μ M and 280 μ M, respectively, one third of the concentration used to show synergy in this work. Despite this, the novel observation that jadomycin B can act synergistically with NSAIDs *in vitro* in 231-CON cells confirms earlier results from the purified enzyme assay and demonstrates that disruption of COX2 activity enhances cytotoxic effect. Furthermore, the ability of jadomycin B and NSAIDs to act synergistically is preserved in 231-JB cells, albeit at greater jadomycin B concentrations, demonstrating that an increased concentration is needed to overcome the increased COX2 expression.

While the initially tested concentrations of celecoxib were also outside the typical range following oral dosing in humans, subsequent experiments were conducted at lower, physiologically attainable concentrations (**Figure 4.31**). In healthy volunteers given either

a single 400 mg or 800 mg oral dose of celecoxib, peak plasma concentrations were 0.97 mg/L or 2.93 mg/L, respectively (Davies et al., 2000). These concentrations equate to 2.5 μ M or 7.7 μ M, within the 0.10 μ M to 45.09 μ M concentration range used in the present work. While jadomycin B has not been trialed in humans, a single study has demonstrated that a peak concentration of 3.4 ± 0.27 μ M jadomycin B is attainable following a single intraperitoneal injection of 6 mg/kg in mice (McKeown et al., 2022). Thus, the concentrations determined to synergistically increase cytotoxicity in the present work are feasible to attain in preclinical mouse studies.

5.7: Formation of Cell Spheroids is Inhibited by Jadomycin B Exposure

As an intermediary to progressing from cellular breast cancer models to animal models, it is important to validate the effects of jadomycin B in a model similar to tumours in actual disease. To that end, cell spheroids more closely simulate the environment within a tumour, representing a mass of cells with a hypoxic core that does not have immediate access to the nutrient containing medium. MCF-7 cells were chosen for cell spheroid assays due to increased spheroid formation efficiency (Wang et al., 2014). Before moving to spheroid assays, synergy between jadomycin B and celecoxib was verified to occur in MCF-7 cells (**Figure 4.32**) at similar concentrations to 231-CON cells.

Cancer stem cells represent a small subpopulation of cancer cells which are capable of extreme proliferation and self-renewal (Reya et al., 2001; Lytle et al., 2018). Although relatively scarce within tumours, these cancer stem cells are less susceptible to anticancer therapies and therefore drive resistance and disease recurrence (Adams and Strasser, 2008; Baumann et al., 2008; Najafi et al., 2019). COX2 and EP4 are known to stimulate the formation of stem-cell like breast cancer cells via the PI3K/AKT signalling pathway (Majumder et al., 2016). Additionally, increased PGE₂ is associated with a stem cell like phenotype (Kundu et al., 2014; Walker et al., 2021). This link between COX2 and cancer stem cells may explain the effects of jadomycin B in the cell spheroid assays.

When cultured in the presence of jadomycin B, spheroid formation was inhibited in a dose dependent manner, but viability of those spheroids which did form was similar

across all concentrations tested (**Figure 4.33**). This suggests that jadomycin B may be affecting cancer cell stemness separately from the cytotoxic effects alone. With regard to cancer stem cell characteristics, increased *EP4* gene expression has been associated with cells that more readily form spheroids and EP4 antagonists have been demonstrated to inhibit the stem cell phenotype (Kundu et al., 2014). In the present work, the observation that pre-exposure to jadomycin B resulted in a dose dependent decrease in both cell spheroid formation and viability (**Figure 4.35**) further supports the conclusion that jadomycin B affects cancer cell stemness.

5.8: Jadomycin B Induces Minor Changes to PI3K/AKT Intracellular Signalling

It has previously been shown that MCF-7 cells exposed to EP4 agonists increase intracellular signalling *via* PI3K/AKT, extracellular signal-regulated kinase (ERK), and nuclear factor kappa-light-chain-enhancer of activated B cells (NF κ B) to mediate their effects (Majumder et al., 2018). Additionally, the PI3K/AKT and p38 mitogen-activated protein kinase (MAPK) pathways are the predominant signaling pathways mediating COX2 upregulation by human growth factor in human breast cancer cells (Kuang et al., 2017). As such, a rational starting point for the exploration of intracellular signalling after EP4 activation was the characterization of changes occurring in the PI3K/AKT pathway. No significant difference was observed in PI3K protein expression and a 2.5-fold increase in p-AKT protein expression was observed after 24 h exposure to 5.0 μ M jadomycin B (**Figures 4.37** and **4.38**). This was opposite to the expected effect as increased activation of AKT is typically tumourigenic. From these results it appears that a low degree of PI3K/AKT activation may be associated with jadomycin-related cellular effects, however, further investigation confirming these results is needed.

One possibility is that the timeframes included in the present work did not capture a larger, transient alteration in PI3K/AKT expression and increased rebound signalling occurs at the later time points measured. If this were the case, reduction in PI3K/AKT signalling may occur at an earlier timepoint resulting in observed changes to cellular viability and stem cell-like characteristics by the 6 h and 24 h timepoints assayed. Further experiments could also be conducted to differentiate between changes to basal PI3K/AKT

signalling in the presence of jadomycin B alone and compared to cells in which an inflammatory response has been stimulated. The lipopolysaccharide endotoxin produced by *Escherichia coli* has been shown to stimulate COX2 activity which should amplify signalling through the PGE₂ receptors (Sekhon-Loodu et al., 2015). If jadomycin B is modulating this pathway, the exaggerated signalling stimulated by lipopolysaccharide would allow observation of that response. Another alternative is that modulation by jadomycin B is predominantly conveyed by the Ras/Raf/MAPK signalling pathway. PGE₂ has been reported to block apoptosis through the Ras/Raf/ERK pathway in leukemia and TNBC cell lines (Yeo et al., 2012; Huang et al., 2017).

In either case, additional research is needed to elucidate the intracellular signalling pathway(s) involved in the cytotoxic effect of jadomycin B as changes to cell spheroid formation were detected and have previously been associated with changes to PI3K/AKT signalling. Another possible discrepancy could be the difference in cellular model used, as MCF-7 cells were used for cell spheroid assays while PI3K/AKT expression was measured in 231-CON cells. Repeating these experiments in the MCF-7 cell line will therefore be important.

5.9: Limitations and Future Directions

While care and consideration were taken in the design of all experiments conducted as part of this work certain limitations exist and could be improved upon. Consideration of these limitations is important to rationally design future experiments and more completely describe the potential role of jadomycin B in the treatment of breast cancer.

The first major limitation of this study was found in the topoisomerase cleavage complex assays. These assays show minimal interaction between jadomycin B and TOP2 α , however this was the only isoform for which a lack of interaction can be confidently concluded as the positive controls failed to reach the manufacturer recommended minimum of a 3-fold accumulation in topoisomerase cleavage complex for TOP1 and TOP2 β . An alternative future approach which could be used to rule out interaction between jadomycin B and the topoisomerases could be the use of small

interfering RNA to individually silence *TOP2A*, *TOP2B*, or *TOP1*. Alternatively, the use of clustered regularly interspaced short palindromic repeats (CRISPR) and CRISPR-associated protein 9 (Cas9) could be used to silence *TOP2A*, *TOP2B*, or *TOP1* in a more specific manner (Boettcher and McManus, 2015). By eliminating expression of individual topoisomerases and repeating cytotoxicity assays it would be possible to determine the degree of involvement of each topoisomerase in the activity of jadomycin B.

With regard to cytotoxicity assays, MTT assays were used throughout this work as the primary means by which to measure cellular viability. For cells in the log phase of growth the amount of formazan product produced is proportional to the number of metabolically active, viable cells. However, if cellular metabolism is altered due to cell culture conditions or the effects of small molecules then the amount of formazan produced can be decreased, giving the false impression of reduced viability (Riss et al., 2013). This has been partially mediated through the use of lactate dehydrogenase (LDH) assays by previous members of our lab (Issa et al., 2014). LDH assays measure the LDH released from cells when the membrane is damaged, providing an alternative method for determining cellular toxicity. It has been shown that MTT and LDH assays provide similar measure of IC_{50} when a given cell line is exposed to a given jadomycin (Issa et al., 2014). For this reason, the use of MTT assays is sufficient to provide an accurate assessment of cellular viability. Additional measures of cellular viability may, however, be considered for future experiments to validate these results.

Additional validation may also be required for the 231-JB cells described in this work. As discussed in **section 5.3**, the low degree of resistance to jadomycin B in 231-JB cells is both a benefit and a limitation. Patient-derived cells showing resistance following clinical exposure to anticancer drugs typically exhibit a 2- to 5-fold increase in tolerance while artificially selected resistant cell lines can represent anywhere from 2- to several thousand-fold increases in resistance (McDermott et al., 2014). It has therefore been proposed that resistant cell lines be divided into two classifications: those representing clinically relevant degrees of resistance and those representing high-level laboratory selected resistance (McDermott et al., 2014). The high-level laboratory lines are more typically used for mechanistic studies while the clinically relevant lines are generally used for translational studies. Continued culture of 231-JB cells to select for a greater degree of

resistance could reveal more subtle changes to additional genes of interest and thereby lend greater clarity to the mechanism of action of jadomycin B. The 231-JB cell line established in this work, however, was sufficient to identify the large increase in *COX2* expression and therefore increased resistance was not necessary to achieve that goal.

Of specific interest is that the 231-JB cell line overexpresses *COX2* without a correlated increase in ABC transporter expression. ABC transporter and *COX2* overexpression is typically linked in cancer (Paweł et al., 2008; Szczuraszek et al., 2009; Zeliha et al., 2020). The 231-JB cells represent a possible model for investigating the molecular mechanisms underlying that linkage because of their unusual disconnection between *COX2* and ABC transporter expression. Determining the way(s) in which 231-JB cells differ from other MDR cells which have simultaneous upregulation of *COX2* and ABC transporters may offer insight into the different ways in which MDR can develop. For this purpose, 231-JB cells could be used to study the role of *COX2* in multidrug resistance in a role completely apart from functional studies of jadomycin B activity.

Additional studies could be conducted on a broader scope of ABC transporters. MRP4 is another ABC transporter capable of removing a variety of endogenous and exogenous compounds from cells (Russel et al., 2008). One function of the transporter is the removal of eicosanoids, such as PGE_2 , which can allow ABCC4 to play an important role in cellular signalling (Russel et al., 2008; Kochel et al., 2017). This has been shown to occur in TNBC cells, contributing to increased metastatic activity through increased PGE_2 in the tumour microenvironment (Kochel et al., 2017). If 231-JB cells have increased expression of ABCC4, the associated increase in PGE_2 release into the medium could be an additional mechanism involved in resistance and further support jadomycin B as targeting *COX2* related signalling. For this reason, comparative measurement of PGE_2 levels in 231-CON and 231-JB cells would be informative as to the relative rate of production and release. The present work is limited to only an examination of those ABC transporters most typically involved in multidrug resistance. The additional analysis of the ABCC4 transporter would allow any remaining doubt regarding transport of jadomycin B itself to be dispelled should 231-JB cells not have increased expression.

The studies involving fatty acid analysis were likewise limited in that they measured only proportional fatty acid content relative to total cellular lipids. This was the

result of limited material availability, instrument access, and cost. While this provided a starting point for assessment of the effect of jadomycin B on cellular lipids, it would be beneficial to repeat these experiments with larger samples such that precise quantities of each fatty acid could be measured. In doing so, the changes in fatty acids observed could be assessed for clinical relevance. Additionally, the fatty acid analysis in this work was limited to 231-CON cells exposed to jadomycin B alone. It would be interesting to determine the combined effect of jadomycin B and celecoxib, or a variety of artificially added endogenous COX2 substrates/inhibitors, within the synergistic and physiologically attainable range of concentrations to determine if functional consequences of that synergy persist at the lipid level.

Cellular fatty acid levels can be affected by more than just COX2 activity. Changes to $\Delta 5D$, $\Delta 6D$, and PLA2 are known to alter lipid levels through synthetic and metabolic activities. While desaturase activity can be estimated by looking at the ratio between product and substrate fatty acids, an important future direction will be direct measurement of $\Delta 5D$ expression and activity to confirm if jadomycin B is having an effect on that enzyme. Similarly, PLA2 is an important enzyme in AA synthesis and has not been explored in the present work (Balsinde et al., 2002). An additional observation made in **section 4.9** was that *TERT* expression was decreased in the cancer drug target array. While this lead was not followed in the present work, *TERT* is known to be inhibited by polyunsaturated fatty acids and downregulated in correlation with *PTGS2* overexpression (Eitsuka et al., 2005). *TERT* functions to maintain telomeres and is highly active in over 90% of breast cancer tumours (Yang et al., 2023). Polyunsaturated fatty acids have been shown to inhibit telomerase activity, with oleic acid (18:1n-9) being the most potent inhibitor tested (Oda et al., 2002; Eitsuka et al., 2005). A necessary future direction is the exploration of the effects of jadomycin B on alternative fatty acids, *TERT*, and telomerase activity to determine if the DNA damage previously ascribed to TOP2 interaction is resultant from this interaction.

Downstream of AA and PGE₂, this work has been limited to a discussion of EP4 only. There are 3 other PGE₂ receptors, with EP2 also playing an important role in signal transduction and cancer stem cell-like activity (Walker et al., 2021). Further investigation of EP2 would be helpful in assessing if other receptors are involved and what their role(s)

may be. The minor alteration to the PI3K/AKT pathway discussed in **section 5.8** could suggest alternative intracellular signalling pathway(s) are involved such as Ras/Raf/MAPK or NFκB. While EP2 signalling is also typically conveyed through PI3K/AKT, a more complete description of this group of receptors is needed.

Finally, the scope of this work has been limited to *in vitro* models of breast cancer, however, it is important to expand that scope to include *in vivo* models. Zebrafish larvae have been exposed to jadomycin B to determine a maximum tolerated concentration, and it was shown that xenotransplanted 231-CON breast cancer cells were killed at jadomycin B concentrations which did not harm the larvae (McKeown et al., 2022). More fully characterizing the toxicity of jadomycin B in developing zebrafish would be beneficial in determining translatability to higher animal models. Another member of our lab group is currently undertaking this project and has established fluorescent breast cancer cell lines to assay the anti-metastatic effects of jadomycin B in zebrafish. Determining how jadomycin B, alone or in combination with celecoxib, can affect metastasis in zebrafish will help to guide the development of subsequent mouse studies. Similarly, CRISPR-Cas9 knockout screening could be conducted in zebrafish to further identify genes associated with jadomycin B sensitivity or resistance.

5.10: Conclusion

Jadomycins are natural products which continue to demonstrate promising anticancer activity. This work has shown for the first time that jadomycin B interacts with COX2-related signalling in human breast cancer cells. By establishing a jadomycin resistant human breast cancer cell line, COX2 was identified as a potential target through which jadomycin B exerts its anticancer effect. Following exposure of nonresistant cells to jadomycin B, EP4 expression was shown to be decreased and accumulation of PGE₂ in the medium was abolished. Decreased PGE₂ production was also correlated to increased levels of AA, its metabolic precursor. This demonstrates that jadomycin B is interfering with the conversion of AA by COX2. While jadomycin B does not inhibit the COX2 active site directly, molecular docking models and purified enzyme assays provide compelling evidence that jadomycin B does act allosterically in conjunction with COX2

inhibitors to exert its effect. When breast cancer cells are concomitantly exposed to jadomycin B and celecoxib they act synergistically with respect to anticancer activity. Finally, jadomycin B was shown to decrease cancer cell stemness through decreased capacity to form cell spheroids.

This work represents a novel and significant increase in the accumulated knowledge regarding the anticancer effects of jadomycins. By establishing the role of COX2 in its anticancer effect, jadomycin B has shown increased promise as a potential treatment for breast cancer. While future studies are still needed to describe the effects of jadomycin B in animal models, the work presented here will help justify the future development of jadomycin B as a chemotherapeutic drug.

References

- [ACS] American College of Surgeons (2017) *AJCC Cancer Staging Manual*. American College of Surgeons, Chicago, Illinois.
- [CCS] Canadian Cancer Statistics Advisory Committee in collaboration with the Canadian Cancer Society Statistics Canada and the Public Health Agency of Canada (2021) *Canadian Cancer Statistics 2021*. Canadian Cancer Society, Toronto, ON.
- [CCS] Canadian Cancer Statistics Advisory Committee in collaboration with the Canadian Cancer Society Statistics Canada and the Public Health Agency of Canada (2022) *Canadian Cancer Statistics: A 2022 Special Report on Cancer Prevalence*. Canadian Cancer Society, Toronto, ON.
- [EBCTCG] Early Breast Cancer Trialists' Collaborative Group (2018) Long-term outcomes for neoadjuvant versus adjuvant chemotherapy in early breast cancer: meta-analysis of individual patient data from ten randomised trials. *Lancet Oncol* **19**:27-39.
- [UICC] Union for International Cancer Control (2017) *TNM Classification of Malignant Tumours*. John Wiley & Sons, Incorporated, Oxford, UK.
- Adams JM and Strasser A (2008) Is tumor growth sustained by rare cancer stem cells or dominant clones? *Cancer Res* **68**:4018-4021.
- Adams S, Gatti-Mays ME, Kalinsky K, Korde LA, Sharon E, Amiri-Kordestani L, Bear H, McArthur HL, Frank E, Perlmutter J, Page DB, Vincent B, Hayes JF, Gulley JL, Litton JK, Hortobagyi GN, Chia S, Krop I, White J, Sparano J, Disis ML and Mittendorf EA (2019) Current landscape of immunotherapy in breast cancer: a review. *JAMA Oncology* **5**:1205-1214.
- Adem C, Reynolds C, Ingle JN and Nascimento AG (2004) Primary breast sarcoma: clinicopathologic series from the Mayo Clinic and review of the literature. *Br J Cancer* **91**:237-241.
- Ahmad M, Xue Y, Lee SK, Martindale JL, Shen W, Li W, Zou S, Ciaramella M, Debat H, Nadal M, Leng F, Zhang H, Wang Q, Siaw GE, Niu H, Pommier Y, Gorospe M, Hsieh TS, Tse-Dinh YC, Xu D and Wang W (2016) RNA topoisomerase is prevalent in all domains of life and associates with polyribosomes in animals. *Nucleic Acids Res* **44**:6335-6349.

- Akagi Y, Mori Y, Sato Y, Iwasaki E and Komatsu T (2022) Total synthesis of jadomycins A, B, and l-digitoxosyl-phenanthroviridin. *Tetrahedron Lett* **101**:153919.
- Akagi Y, Yamada S-i, Etomi N, Kumamoto T, Nakanishi W and Ishikawa T (2010) Synthetic studies on jadomycins: synthesis of dimethyljadomycin A. *Tetrahedron Lett* **51**:1338-1340.
- Allikmets R, Schriml LM, Hutchinson A, Romano-Spica V and Dean M (1998) A human placenta-specific ATP-binding cassette gene (ABCP) on chromosome 4q22 that is involved in multidrug resistance. *Cancer Res* **58**:5337-5339.
- Alluri P and Newman LA (2014) Basal-like and triple-negative breast cancers: searching for positives among many negatives. *Surg Oncol Clin N Am* **23**:567-577.
- Ameer F, Scandiuzzi L, Hasnain S, Kalbacher H and Zaidi N (2014) De novo lipogenesis in health and disease. *Metabolism* **63**:895-902.
- Amiri-Kordestani L, Basseville A, Kurdziel K, Fojo AT and Bates SE (2012) Targeting MDR in breast and lung cancer: discriminating its potential importance from the failure of drug resistance reversal studies. *Drug Resist Updat* **15**:50-61.
- An KC (2016) Selective estrogen receptor modulators. *Asian Spine J* **10**:787-791.
- Anderson AS and Wellington EM (2001) The taxonomy of *Streptomyces* and related genera. *Int J Syst Evol Microbiol* **51**:797-814.
- Anderson WF, Althuis MD, Brinton LA and Devesa SS (2004) Is male breast cancer similar or different than female breast cancer? *Breast Cancer Res Treat* **83**:77-86.
- Andes D and Craig WA (2002) Animal model pharmacokinetics and pharmacodynamics: a critical review. *Int J Antimicrob Agents* **19**:261-268.
- André F, O'Regan R, Ozguroglu M, Toi M, Xu B, Jerusalem G, Masuda N, Wilks S, Arena F, Isaacs C, Yap YS, Papai Z, Lang I, Armstrong A, Lerzo G, White M, Shen K, Litton J, Chen D, Zhang Y, Ali S, Taran T and Gianni L (2014) Everolimus for women with trastuzumab-resistant, HER2-positive, advanced breast cancer (BOLERO-3): a randomised, double-blind, placebo-controlled phase 3 trial. *Lancet Oncol* **15**:580-591.
- Arcamone F, Cassinelli G, Fantini G, Grein A, Orezzi P, Pol C and Spalla C (1969) Adriamycin, 14-hydroxydaimomycin, a new antitumor antibiotic from *S. Peucetius* var. *caesius*. *Biotechnol Bioeng* **11**:1101-1110.

- Aslakson CJ and Miller FR (1992) Selective events in the metastatic process defined by analysis of the sequential dissemination of subpopulations of a mouse mammary tumor. *Cancer Res* **52**:1399-1405.
- Ayer SW, McInnes AG, Thibault P, Walter JA, Doull JL, Parnell T and Vining LC (1991) Jadomycin, a novel 8H-benz[b]oxazolo[3,2-f]phenanthridine antibiotic from from streptomyces venezuelae ISP5230. *Tetrahedron Lett* **32**:6301-6304.
- Balsinde J, Winstead MV and Dennis EA (2002) Phospholipase A2 regulation of arachidonic acid mobilization. *FEBS Lett* **531**:2-6.
- Bar-On O, Shapira Ma and Hershko DD (2007) Differential effects of doxorubicin treatment on cell cycle arrest and Skp2 expression in breast cancer cells. *Anticancer Drugs* **18**:1113-1121.
- Barnes N, Haywood P, Flint P, Knox WF and Bundred NJ (2006) Survivin expression in in situ and invasive breast cancer relates to COX-2 expression and DCIS recurrence. *Br J Cancer* **94**:253-258.
- Baselga J, Bradbury I, Eidtmann H, Di Cosimo S, de Azambuja E, Aura C, Gómez H, Dinh P, Fauria K, Van Dooren V, Aktan G, Goldhirsch A, Chang T-W, Horváth Z, Coccia-Portugal M, Domont J, Tseng L-M, Kunz G, Sohn JH, Semiglazov V, Lerzo G, Palacova M, Probachai V, Puzstai L, Untch M, Gelber RD and Piccart-Gebhart M (2012) Lapatinib with trastuzumab for HER2-positive early breast cancer (NeoALTTO): a randomised, open-label, multicentre, phase 3 trial. *Lancet* **379**:633-640.
- Bauer KR, Brown M, Cress RD, Parise CA and Caggiano V (2007) Descriptive analysis of estrogen receptor (ER)-negative, progesterone receptor (PR)-negative, and HER2-negative invasive breast cancer, the so-called triple-negative phenotype: a population-based study from the California cancer Registry. *Cancer* **109**:1721-1728.
- Baumann M, Krause M and Hill R (2008) Exploring the role of cancer stem cells in radioresistance. *Nat Rev Cancer* **8**:545-554.
- Baylin SB and Jones PA (2016) Epigenetic determinants of cancer. *Cold Spring Harb Perspect Biol* **8**:a019505.
- Bazira PJ, Ellis H and Mahadevan V (2022) Anatomy and physiology of the breast. *Surgery (Oxf)* **40**:79-83.
- Bennink HJTC (2004) Are all estrogens the same? *Maturitas* **47**:269-275.

- Bérdy J (2005) Bioactive microbial metabolites. *J Antibiot* **58**:1-26.
- Berenbaum MC (1977) Synergy, additivism and antagonism in immunosuppression. A critical review. *Clin Exp Immunol* **28**:1-18.
- Berx G and van Roy F (2009) Involvement of members of the cadherin superfamily in cancer. *Cold Spring Harb Perspect Biol* **1**:a003129.
- Binder M, Roberts C, Spencer N, Antoine D and Cartwright C (2014) On the antiquity of cancer: evidence for metastatic carcinoma in a young man from ancient Nubia (c. 1200 BC). *PLoS One* **9**:e90924.
- Birkhauser M (1996) Chemistry, physiology, and pharmacology of sex steroids. *J Cardiovasc Pharmacol* **28**:S1-S13.
- Blackadar CB (2016) Historical review of the causes of cancer. *World J Clin Oncol* **7**:54-86.
- Blasco MA (2005) Telomeres and human disease: ageing, cancer and beyond. *Nat Rev Genet* **6**:611-622.
- Bliss CI (1939) The toxicity of poisons applied jointly. *Ann App Biol* **26**:585-615.
- Boettcher M and McManus MT (2015) Choosing the right tool for the job: RNAi, TALEN, or CRISPR. *Mol Cell* **58**:575-585.
- Bonitto EP, McKeown BT and Goralski KB (2021) Jadomycins: a potential chemotherapy for multi-drug resistant metastatic breast cancer. *Pharmacol Res Perspect* **9**:e00886.
- Bonnetterre J, Dieras V, Tubiana-Hulin M, Bougnoux P, Bonnetterre ME, Delozier T, Mayer F, Culine S, Dohoulou N and Bendahmane B (2004) Phase II multicentre randomised study of docetaxel plus epirubicin vs 5-fluorouracil plus epirubicin and cyclophosphamide in metastatic breast cancer. *Br J Cancer* **91**:1466-1471.
- Borin TF, Angara K, Rashid MH, Achyut BR and Arbab AS (2017) Arachidonic Acid Metabolite as a Novel Therapeutic Target in Breast Cancer Metastasis. *Int J Mol Sci* **18**.
- Borissow CN, Graham CL, Syvitski RT, Reid TR, Blay J and Jakeman DL (2007) Stereochemical integrity of oxazolone ring-containing jadomycins. *Chembiochem* **8**:1198-1203.

- Borowsky AD (2011) Choosing a mouse model: experimental biology in context--the utility and limitations of mouse models of breast cancer. *Cold Spring Harb Perspect Biol* **3**:a009670.
- Bray F, Laversanne M, Weiderpass E and Soerjomataram I (2021) The ever-increasing importance of cancer as a leading cause of premature death worldwide. *Cancer* **127**:3029-3030.
- Breasted JH (1930) *The Edwin Smith Surgical Papyrus*. The University of Chicago Press, Chicago, Illinois.
- Brenner DR, Poirier A, Woods RR, Ellison LF, Billette JM, Demers AA, Zhang SX, Yao C, Finley C, Fitzgerald N, Saint-Jacques N, Shack L, Turner D and Holmes E (2022) Projected estimates of cancer in Canada in 2022. *CMAJ* **194**:E601-E607.
- Briske-Anderson MJ, Finley JW and Newman SM (1997) The influence of culture time and passage number on the morphological and physiological development of Caco-2 cells. *Proc Soc Exp Biol Med* **214**:248-257.
- Brown JR, Koretke KK, Birkeland ML, Sanseau P and Patrick DR (2004) Evolutionary relationships of Aurora kinases: implications for model organism studies and the development of anti-cancer drugs. *BMC Evol Biol* **4**:39.
- Budge SM, Cooper MH and Iverson SJ (2004) Demonstration of the deposition and modification of dietary fatty acids in pinniped blubber using radiolabelled precursors. *Physiol Biochem Zool* **77**:682-687.
- Burden DA and Osheroff N (1998) Mechanism of action of eukaryotic topoisomerase II and drugs targeted to the enzyme. *Biochim Biophys Acta* **1400**:139-154.
- Burrows HJ (1935) Pathological conditions induced by oestrogenic compounds in the coagulating gland and prostate of the mouse. *Am J Cancer* **23**:490-512.
- Cailleau R, Young R, Olivé M and Reeves WJ, Jr. (1974) Breast tumor cell lines from pleural effusions. *J Natl Cancer Inst* **53**:661-674.
- Camerino B and Palamidessi G (1960) Derivati della parazina II. Sulfonamidopir. *Gazz Chim Ital* **90**:1802-1815.
- Carmeliet P (2005) VEGF as a key mediator of angiogenesis in cancer. *Oncology* **69 Suppl 3**:4-10.

- Carrel A and Burrows MT (1911) Cultivation in vitro of malignant tumors. *J Exp Med* **13**:571-575.
- Carrick S, Parker S, Thornton CE, Ghersi D, Simes J and Wilcken N (2009) Single agent versus combination chemotherapy for metastatic breast cancer. *Cochrane Database Syst Rev* **2009**:Cd003372.
- Cedernaes J, Alsjö J, Västermark A, Risérus U and Schiöth HB (2013) Adipose tissue stearoyl-CoA desaturase 1 index is increased and linoleic acid is decreased in obesity-prone rats fed a high-fat diet. *Lipids Health Dis* **12**:2.
- Chan CS and Botstein D (1993) Isolation and characterization of chromosome-gain and increase-in-ploidy mutants in yeast. *Genetics* **135**:677-691.
- Chandrasekharan NV and Simmons DL (2004) The cyclooxygenases. *Genome Biol* **5**:241.
- Chang-Liu CM and Woloschak GE (1997) Effect of passage number on cellular response to DNA-damaging agents: cell survival and gene expression. *Cancer Lett* **113**:77-86.
- Chavez KJ, Garimella SV and Lipkowitz S (2010) Triple negative breast cancer cell lines: one tool in the search for better treatment of triple negative breast cancer. *Breast Dis* **32**:35-48.
- Chen X, Yeung TK and Wang Z (2000) Enhanced drug resistance in cells coexpressing ErbB2 with EGF receptor or ErbB3. *Biochem Biophys Res Commun* **277**:757-763.
- Ching MM, Reader J and Fulton AM (2020) Eicosanoids in cancer: prostaglandin E₂ receptor 4 in cancer therapeutics and immunotherapy. *Front Pharmacol* **11**:819.
- Chou T-C (2010) Drug combination studies and their synergy quantification using the Chou-Talalay Method. *Cancer Res* **70**:440-446.
- Chou T-C and Talalay P (1983) Analysis of combined drug effects: a new look at a very old problem. *Trends Pharmacol Sci* **4**:450-454.
- Chou T-C and Talalay P (1984) Quantitative analysis of dose-effect relationships: the combined effects of multiple drugs or enzyme inhibitors. *Adv Enzyme Regul* **22**:27-55.
- Chumsri S, Howes T, Bao T, Sabnis G and Brodie A (2011) Aromatase, aromatase inhibitors, and breast cancer. *J Steroid Biochem Mol Biol* **125**:13-22.

- Clough KB, Acosta-Marín V, Nos C, Alran S, Rouanet P, Garbay JR, Giard S, Verhaeghe JL, Houvenaeghel G, Flipo B, Dauplat J, Dorangeon PH, Classe JM, Rouzier R and Bonnier P (2015) Rates of neoadjuvant chemotherapy and oncoplastic surgery for breast cancer surgery: a French national survey. *Ann Surg Oncol* **22**:3504-3511.
- Cole SPC, Bhardwaj G, Gerlach JH, Mackie JE, Grant CE, Almquist KC, Stewart AJ, Kurz EU, Duncan AMV and Deeley RG (1992) Overexpression of a transporter gene in a multidrug-resistant human lung cancer cell line. *Science* **258**:1650-1654.
- Coley HM (2008) Mechanisms and strategies to overcome chemotherapy resistance in metastatic breast cancer. *Cancer Treat Rev* **34**:378-390.
- Coley WB (1894) Treatment of inoperable malignant tumors with the toxins of erysipelas and the bacillus prodigiosus. *Am J Med Sci* **108**:50.
- Comşa Ş, Cîmpean AM and Raica M (2015) The story of MCF-7 breast cancer cell line: 40 years of experience in research. *Anticancer Res* **35**:3147-3154.
- Cottreau KM, Spencer C, Wentzell JR, Graham CL, Borissow CN, Jakeman DL and McFarland SA (2010) Diverse DNA-cleaving capacities of the jadomycins through precursor-directed biosynthesis. *Org Lett* **12**:1172-1175.
- Cragg GM (1998) Paclitaxel (Taxol): a success story with valuable lessons for natural product drug discovery and development. *Med Res Rev* **18**:315-331.
- Cragg GM and Newman DJ (2005) Biodiversity: a continuing source of novel drug leads. *Pure Appl Chem* **77**:7-24.
- Czabotar PE, Lessene G, Strasser A and Adams JM (2014) Control of apoptosis by the BCL-2 protein family: implications for physiology and therapy. *Nat Rev Mol Cell Biol* **15**:49-63.
- Dai X, Cheng H, Bai Z and Li J (2017) Breast cancer cell line classification and its relevance with breast tumor subtyping. *J Cancer* **8**:3131-3141.
- Das D, Qiao D, Liu Z, Xie L, Li Y, Wang J, Jia J, Cao Y and Hong J (2023) Discovery of novel, selective prostaglandin EP4 receptor antagonists with efficacy in cancer models. *ACS Med Chem Lett* **14**:727-736.
- David H (1988) Rudolf Virchow and modern aspects of tumor pathology. *Pathol Res Pract* **183**:356-364.

- Davies C, Godwin J, Gray R, Clarke M, Cutter D, Darby S, McGale P, Pan HC, Taylor C, Wang YC, Dowsett M, Ingle J and Peto R (2011) Relevance of breast cancer hormone receptors and other factors to the efficacy of adjuvant tamoxifen: patient-level meta-analysis of randomised trials. *Lancet* **378**:771-784.
- Davies NM and Anderson KE (1997) Clinical pharmacokinetics of naproxen. *Clin Pharmacokinet* **32**:268-293.
- Davies NM, McLachlan AJ, Day RO and Williams KM (2000) Clinical pharmacokinetics and pharmacodynamics of celecoxib. *Clin Pharmacokinet* **38**:225-242.
- de Koning CB, Ngwira KJ and Rousseau AL (2020) Biosynthesis, synthetic studies, and biological activities of the jadomycin alkaloids and related analogues. *Alkaloids Chem Biol* **84**:125-199.
- de Oliveira C, Weir S, Rangrej J, Krahn MD, Mittmann N, Hoch JS, Chan KKW and Peacock S (2018) The economic burden of cancer care in Canada: a population-based cost study. *CMAJ Open* **6**:E1-E10.
- de Sousa GF, Wlodarczyk SR and Monteiro G (2014) Carboplatin: molecular mechanisms of action associated with chemoresistance. *Braz J Pharm Sci* **50**:693-701.
- de Souza JA and Olopade OI (2011) CYP2D6 genotyping and tamoxifen: an unfinished story in the quest for personalized medicine. *Semin Oncol* **38**:263-273.
- Dean M, Rzhetsky A and Allikmets R (2001) The human ATP-binding cassette (ABC) transporter superfamily. *Genome Res* **11**:1156-1166.
- Delgado JL, Hsieh CM, Chan NL and Hiasa H (2018) Topoisomerases as anticancer targets. *Biochem J* **475**:373-398.
- Desborough MJR and Keeling DM (2017) The aspirin story – from willow to wonder drug. *Br J Haematol* **177**:674-683.
- Desta Z, Ward BA, Soukhova NV and Flockhart DA (2004) Comprehensive evaluation of tamoxifen sequential biotransformation by the human cytochrome P450 system in vitro: prominent roles for CYP3A and CYP2D6. *J Pharmacol Exp Ther* **310**:1062.
- Destanovic E, Boos J and Lanvers-Kaminsky C (2018) Preclinical evaluation of combined topoisomerase and proteasome inhibition against pediatric malignancies. *Anticancer Res* **38**:3977.

- DeVita VT, Jr. and Chu E (2008) A history of cancer chemotherapy. *Cancer Res* **68**:8643-8653.
- Dexter DL, Kowalski HM, Blazar BA, Fligel Z, Vogel R and Heppner GH (1978) Heterogeneity of tumor cells from a single mouse mammary tumor. *Cancer Res* **38**:3174-3181.
- Diamandopoulos GT (1996) Cancer: an historical perspective. *Anticancer Res* **16**:1595-1602.
- Dias DA, Urban S and Roessner U (2012) A historical overview of natural products in drug discovery. *Metabolites* **2**:303-336.
- Disis ML and Stanton SE (2018) Immunotherapy in breast cancer: an introduction. *Breast* **37**:196-199.
- Disis MLN, Guthrie KA, Liu Y, Coveler AL, Higgins DM, Childs JS, Dang Y and Salazar LG (2023) Safety and outcomes of a plasmid DNA vaccine encoding the ERBB2 intracellular domain in patients with advanced-stage ERBB2-positive breast cancer: a phase 1 nonrandomized clinical trial. *JAMA Oncol* **9**:71-78.
- do Nascimento RG and Otoni KM (2020) Histological and molecular classification of breast cancer: what do we know? *Mastology* **30**:e20200024.
- Doull JL, Ayer SW, Singh AK and Thibault P (1993) Production of a novel polyketide antibiotic, jadomycin B, by *Streptomyces venezuelae* following heat shock. *J Antibiot (Tokyo)* **46**:869-871.
- Doull JL, Singh AK, Hoare M and Ayer SW (1994) Conditions for the production of jadomycin B by *Streptomyces venezuelae* ISP5230: effects of heat shock, ethanol treatment and phage infection. *J Ind Microbiol* **13**:120-125.
- Doyle LA, Yang W, Abruzzo LV, Krogmann T, Gao Y, Rishi AK and Ross DD (1998) A multidrug resistance transporter from human MCF-7 breast cancer cells. *Proc Natl Acad Sci U S A* **95**:15665-15670.
- Drąg J, Goździalska A, Knapik-Czajka M, Gawędzka A, Gawlik K and Jaśkiewicz J (2017) Effect of high carbohydrate diet on elongase and desaturase activity and accompanying gene expression in rat's liver. *Genes Nutr* **12**:2.
- Dragun AE, Huang B, Tucker TC and Spanos WJ (2012) Increasing mastectomy rates among all age groups for early stage breast cancer: a 10-year study of surgical choice. *Breast* **18**:318-325.

- Duarte D and Vale N (2022) Evaluation of synergism in drug combinations and reference models for future orientations in oncology. *Curr Res Pharmacol Drug Discov* **3**:100110.
- Dunnwald LK, Rossing MA and Li CI (2007) Hormone receptor status, tumor characteristics, and prognosis: a prospective cohort of breast cancer patients. *Breast Cancer Res* **9**:R6.
- Dupuis SN, Robertson AW, Veinot T, Monro SMA, Douglas SE, Syvitski RT, Goralski KB, McFarland SA and Jakeman DL (2012) Synthetic diversification of natural products: semi-synthesis and evaluation of triazole jadomycins. *Chem Sci* **3**:1640-1644.
- Dupuis SN, Veinot T, Monro SMA, Douglas SE, Syvitski RT, Goralski KB, McFarland SA and Jakeman DL (2011) Jadomycins derived from the assimilation and incorporation of norvaline and norleucine. *J Nat Prod* **74**:2420-2424.
- Earnshaw WC, Martins LM and Kaufmann SH (1999) Mammalian caspases: structure, activation, substrates, and functions during apoptosis. *Annu Rev Biochem* **68**:383-424.
- Ehrlich J, Bartz QR, Smith RM, Joslyn DA and Burkholder PR (1947) Chloromycetin, a new antibiotic from a soil actinomycete. *Science* **106**:417.
- Ehrlich J, Gottlieb D, Burkholder PR, Anderson LE and Pridham TG (1948) *Streptomyces venezuelae*, n. sp., the source of chloromycetin. *J Bacteriol* **56**:467-477.
- Eitsuka T, Nakagawa K, Suzuki T and Miyazawa T (2005) Polyunsaturated fatty acids inhibit telomerase activity in DLD-1 human colorectal adenocarcinoma cells: a dual mechanism approach. *Biochim Biophys Acta Mol Cell Biol Lipids* **1737**:1-10.
- Eliot H, Gianni L and Myers C (1984) Oxidative destruction of DNA by the adriamycin-iron complex. *Biochemistry* **23**:928-936.
- Elmore S (2007) Apoptosis: a review of programmed cell death. *Toxicol Pathol* **35**:495-516.
- Elston CW and Ellis IO (1991) Pathological prognostic factors in breast cancer. I. The value of histological grade in breast cancer: experience from a large study with long-term follow-up. *Histopathology* **19**:403-410.

- Emens LA, Kok M and Ojalvo LS (2016) Targeting the programmed cell death-1 pathway in breast and ovarian cancer. *Curr Opin Obstet Gynecol* **28**:142-147.
- Eroles P, Bosch A, Alejandro Pérez-Fidalgo J and Lluch A (2012) Molecular biology in breast cancer: Intrinsic subtypes and signaling pathways. *Cancer Treat Rev* **38**:698-707.
- Esquenet M, Swinnen JV, Heyns W and Verhoeven G (1997) LNCaP prostatic adenocarcinoma cells derived from low and high passage numbers display divergent responses not only to androgens but also to retinoids. *J Steroid Biochem Mol Biol* **62**:391-399.
- Famta P, Shah S, Chatterjee E, Singh H, Dey B, Guru SK, Singh SB and Srivastava S (2021) Exploring new horizons in overcoming P-glycoprotein-mediated multidrug-resistant breast cancer via nanoscale drug delivery platforms. *Curr Res Pharmacol Drug Discov* **2**:100054.
- Fan K, Zhang X, Liu H, Han H, Luo Y, Wang Q, Geng M and Yang K (2012) Evaluation of the cytotoxic activity of new jadomycin derivatives reveals the potential to improve its selectivity against tumor cells. *J Antibiot (Tokyo)* **65**:449-452.
- Farnsworth NR, Akerele O, Bingel AS, Soejarto DD and Guo Z (1985) Medicinal plants in therapy. *Bull World Health Organ* **63**:965-981.
- Fedier A, Schwarz VA, Walt H, Carpini RD, Haller U and Fink D (2001) Resistance to topoisomerase poisons due to loss of DNA mismatch repair. *Int J Cancer* **93**:571-576.
- Fillmore CM and Kuperwasser C (2008) Human breast cancer cell lines contain stem-like cells that self-renew, give rise to phenotypically diverse progeny and survive chemotherapy. *Breast Cancer Res* **10**:R25.
- Finetti F, Travelli C, Ercoli J, Colombo G, Buoso E and Trabalzini L (2020) Prostaglandin E2 and cancer: insight into tumor progression and immunity. *Biology (Basel)* **9**:434.
- Fink D, Aebi S and Howell SB (1998a) The role of DNA mismatch repair in drug resistance. *Clin Cancer Res* **4**:1-6.
- Fink D, Nebel S, Norris PS, Aebi S, Kim HK, Haas M and Howell SB (1998b) The effect of different chemotherapeutic agents on the enrichment of DNA mismatch repair-deficient tumour cells. *Br J Cancer* **77**:703-708.

- Fisusi FA and Akala EO (2019) Drug combinations in breast cancer therapy. *Pharm Nanotechnol* **7**:3-23.
- Fitzpatrick JM and de Wit R (2014) Taxane mechanisms of action: potential implications for treatment sequencing in metastatic castration-resistant prostate cancer. *Eur Urol* **65**:1198-1204.
- Fleming A (1929) On the antibacterial action of cultures of a penicillium, with special reference to their use in the isolation of B. influenzae. *Br J Exp Pathol* **10**:226-236.
- Font-Nieves M, Sans-Fons MG, Gorina R, Bonfill-Teixidor E, Salas-Pédomo A, Márquez-Kisinousky L, Santalucia T and Planas AM (2012) Induction of COX-2 enzyme and down-regulation of COX-1 expression by lipopolysaccharide (LPS) control prostaglandin E2 production in astrocytes. *J Biol Chem* **287**:6454-6468.
- Forget SM, Martinez-Farina CF and Jakeman DL (2018a) Correction: Jadomycins, put a bigger ring in it: isolation of seven- to ten-membered ring analogues. *Chem Commun (Camb)* **54**:3544-3545.
- Forget SM, Robertson AW, Hall SR, MacLeod JM, Overy DP, Kerr RG, Goralski KB and Jakeman DL (2018b) Isolation of a jadomycin incorporating l-ornithine, analysis of antimicrobial activity and jadomycin reactive oxygen species (ROS) generation in MDA-MB-231 breast cancer cells. *J Antibiot (Tokyo)* **71**:722-730.
- Forget SM, Robertson AW, Overy DP, Kerr RG and Jakeman DL (2017) Furan and lactam jadomycin biosynthetic congeners isolated from *Streptomyces venezuelae* ISP5230 cultured with Nε-trifluoroacetyl-l-lysine. *J Nat Prod* **80**:1860-1866.
- Fornetti J, Jindal S, Middleton KA, Borges VF and Schedin P (2014) Physiological COX-2 expression in breast epithelium associates with COX-2 levels in ductal carcinoma in situ and invasive breast cancer in young women. *Am J Pathol* **184**:1219-1229.
- Fu DH, Jiang W, Zheng JT, Zhao GY, Li Y, Yi H, Li ZR, Jiang JD, Yang KQ, Wang Y and Si SY (2008) Jadomycin B, an Aurora-B kinase inhibitor discovered through virtual screening. *Mol Cancer Ther* **7**:2386-2393.
- Gallucci BB (1985) Selected concepts of cancer as a disease: from 1900 to oncogenes. *Oncol Nurs Forum* **12**:69-78.

Galluzzi L, Vitale I, Aaronson SA, Abrams JM, Adam D, Agostinis P, Alnemri ES, Altucci L, Amelio I, Andrews DW, Annicchiarico-Petruzzelli M, Antonov AV, Arama E, Baehrecke EH, Barlev NA, Bazan NG, Bernassola F, Bertrand MJM, Bianchi K, Blagosklonny MV, Blomgren K, Borner C, Boya P, Brenner C, Campanella M, Candi E, Carmona-Gutierrez D, Cecconi F, Chan FKM, Chandel NS, Cheng EH, Chipuk JE, Cidlowski JA, Ciechanover A, Cohen GM, Conrad M, Cubillos-Ruiz JR, Czabotar PE, D'Angiolella V, Dawson TM, Dawson VL, De Laurenzi V, De Maria R, Debatin K-M, DeBerardinis RJ, Deshmukh M, Di Daniele N, Di Virgilio F, Dixit VM, Dixon SJ, Duckett CS, Dynlacht BD, El-Deiry WS, Elrod JW, Fimia GM, Fulda S, García-Sáez AJ, Garg AD, Garrido C, Gavathiotis E, Golstein P, Gottlieb E, Green DR, Greene LA, Gronemeyer H, Gross A, Hajnoczky G, Hardwick JM, Harris IS, Hengartner MO, Hetz C, Ichijo H, Jäättelä M, Joseph B, Jost PJ, Juin PP, Kaiser WJ, Karin M, Kaufmann T, Kepp O, Kimchi A, Kitsis RN, Klionsky DJ, Knight RA, Kumar S, Lee SW, Lemasters JJ, Levine B, Linkermann A, Lipton SA, Lockshin RA, López-Otín C, Lowe SW, Luedde T, Lugli E, MacFarlane M, Madeo F, Malewicz M, Malorni W, Manic G, et al. (2018) Molecular mechanisms of cell death: recommendations of the Nomenclature Committee on Cell Death 2018. *Cell Death Differ* **25**:486-541.

Gaynes R (2017) The discovery of penicillin—new insights after more than 75 years of clinical use. *Emerg Infect Dis* **23**:849-853.

Gerhardt CH (1853) Untersuchungen über die wasserfreien organischen Säuren. *Justus Liebigs Ann Chem* **87**:149-179.

Gewirtz D (1999) A critical evaluation of the mechanisms of action proposed for the antitumor effects of the anthracycline antibiotics adriamycin and daunorubicin. *Biochem Pharmacol* **57**:727-741.

Giaquinto AN, Sung H, Miller KD, Kramer JL, Newman LA, Minihan A, Jemal A and Siegel RL (2022) Breast cancer statistics, 2022. *CA Cancer J Clin* **72**:524-541.

Gillet J-P and Gottesman MM (2010) Mechanisms of multidrug resistance in cancer, in *Multi-Drug Resistance in Cancer* (Zhou J ed) pp 47-76, Humana Press, Totowa, NJ.

Gilman A (1946) Therapeutic applications of chemical warfare agents. *Fed Proc* **5**:285-292.

Giuliano AE, Connolly JL, Edge SB, Mittendorf EA, Rugo HS, Solin LJ, Weaver DL, Winchester DJ and Hortobagyi GN (2017) Breast cancer—major changes in the American Joint Committee on Cancer eighth edition cancer staging manual. *CA Cancer J Clin* **67**:290-303.

- Goldhirsch A, Wood WC, Coates AS, Gelber RD, Thürlimann B and Senn HJ (2011) Strategies for subtypes--dealing with the diversity of breast cancer: highlights of the St. Gallen International Expert Consensus on the Primary Therapy of Early Breast Cancer 2011. *Ann Oncol* **22**:1736-1747.
- Goldstein LJ, Galski H, Fojo A, Willingham M, Lai SL, Gazdar A, Pirker R, Green A, Crist W, Brodeur GM, Lieber M, Cossman J, Gottesman MM and Pastan I (1989) Expression of a multidrug resistance gene in human cancers. *J Natl Cancer Inst* **81**:116-124.
- Goodman LS, Wintrobe MM, Dameshek W, Goodman MJ, Gilman A and McLennan MT (1946) Nitrogen mustard therapy; use of methyl-bis (beta-chloroethyl) amine hydrochloride and tris (beta-chloroethyl) amine hydrochloride for Hodgkin's disease, lymphosarcoma, leukemia and certain allied and miscellaneous disorders. *J Am Med Assoc* **132**:126-132.
- Goralski KB (2020) *Personal Communication*
- Greco WR, Faessel H and Levasseur L (1996) The search for cytotoxic synergy between anticancer agents: a case of Dorothy and the ruby slippers? *J Natl Cancer Inst* **88**:699-700.
- Greenshields AL, Doucette CD, Sutton KM, Madera L, Annan H, Yaffe PB, Knickle AF, Dong Z and Hoskin DW (2015) Piperine inhibits the growth and motility of triple-negative breast cancer cells. *Cancer Lett* **357**:129-140.
- Grivennikov SI, Greten FR and Karin M (2010) Immunity, inflammation, and cancer. *Cell* **140**:883-899.
- Groenendyk J, Paskevicius T, Urta H, Viricel C, Wang K, Barakat K, Hetz C, Kurgan L, Agellon LB and Michalak M (2018) Cyclosporine A binding to COX-2 reveals a novel signaling pathway that activates the IRE1 α unfolded protein response sensor. *Sci Rep* **8**:16678.
- Gunther EJ, Belka GK, Wertheim GBW, Wang J, Hartman JL, Boxer RB and Chodosh LA (2002) A novel doxycycline-inducible system for the transgenic analysis of mammary gland biology. *FASEB J* **16**:283-292.
- Guo W, Healey JH, Meyers PA, Ladanyi M, Huvos AG, Bertino JR and Gorlick R (1999) Mechanisms of methotrexate resistance in osteosarcoma. *Clin Cancer Res* **5**:621-627.
- Hajdu SI (2011a) A note from history: landmarks in history of cancer, part 1. *Cancer* **117**:1097-1102.

- Hajdu SI (2011b) A note from history: landmarks in history of cancer, part 2. *Cancer* **117**:2811-2820.
- Hajdu SI (2012a) A note from history: landmarks in history of cancer, part 3. *Cancer* **118**:1155-1168.
- Hajdu SI (2012b) A note from history: landmarks in history of cancer, part 4. *Cancer* **118**:4914-4928.
- Hajdu SI and Darvishian F (2013) A note from history: landmarks in history of cancer, part 5. *Cancer* **119**:1450-1466.
- Hajdu SI and Vadmal M (2013) A note from history: Landmarks in history of cancer, Part 6. *Cancer* **119**:4058-4082.
- Hajdu SI, Vadmal M and Tang P (2015) A note from history: Landmarks in history of cancer, part 7. *Cancer* **121**:2480-2513.
- Hall JM, Lee MK, Newman B, Morrow JE, Anderson LA, Huey B and King MC (1990) Linkage of early-onset familial breast cancer to chromosome 17q21. *Science* **250**:1684-1689.
- Hall SR, Blundon HL, Ladda MA, Robertson AW, Martinez-Farina CF, Jakeman DL and Goralski KB (2015) Jadomycin breast cancer cytotoxicity is mediated by a copper-dependent, reactive oxygen species-inducing mechanism. *Pharmacol Res Perspect* **3**:e00110.
- Hall SR and Goralski KB (2018) ZATT, TDP2, and SUMO2: breaking the tie that binds TOP2 to DNA. *Transl Cancer Res* **7**:S439-S444.
- Hall SR, Reid A-J, Eng J, McKeown BT, St-Onge M and Goralski KB (2020) A lipid-based oral supplement protects skin cells in culture from ultraviolet light and activates antioxidant and anti-inflammatory mechanisms. *Journal of Natural Health Product Research* **2**:1-14.
- Hall SR, Toulany J, Bennett LG, Martinez-Farina CF, Robertson AW, Jakeman DL and Goralski KB (2017) Jadomycins inhibit type II topoisomerases and promote DNA damage and apoptosis in multidrug-resistant triple-negative breast cancer cells. *J Pharmacol Exp Ther* **363**:196-210.
- Halsted WS (1907) The results of radical operations for the cure of carcinoma of the breast. *Ann Surg* **46**:1-19.

- Han L, Yang K, Ramalingam E, Mosher RH and Vining LC (1994) Cloning and characterization of polyketide synthase genes for jadomycin B biosynthesis in *Streptomyces venezuelae* ISP5230. *Microbiology (Reading)* **140** (Pt 12):3379-3389.
- Hanahan D (2022) Hallmarks of cancer: new dimensions. *Cancer Discov* **12**:31-46.
- Hanahan D and Weinberg RA (2000) The hallmarks of cancer. *Cell* **100**:57-70.
- Hanahan D and Weinberg RA (2011) Hallmarks of cancer: the next generation. *Cell* **144**:646-674.
- Hansen MR and Hurley LH (1996) Pluramycins. Old drugs having modern friends in structural biology. *Acc Chem Res* **29**:249-258.
- Harris RE, Alshafie GA, Abou-Issa H and Seibert K (2000) Chemoprevention of breast cancer in rats by celecoxib, a cyclooxygenase 2 inhibitor. *Cancer Research* **60**:2101-2103.
- Harrison RG (1908) Embryonic transplantation and development of the nervous system. *Anat Rec* **2**:385-410.
- Harvey HA, Lipton A, Max DT, Pearlman HG, Diaz-Perches R and de la Garza J (1985) Medical castration produced by the GnRH analogue leuprolide to treat metastatic breast cancer. *J Clin Oncol* **3**:1068-1072.
- Hasan TN, B LG, Masoodi TA, Shafi G, Alshatwi AA and Sivashanmugham P (2011) Affinity of estrogens for human progesterone receptor A and B monomers and risk of breast cancer: a comparative molecular modeling study. *Adv Appl Bioinform Chem* **4**:29-36.
- Hashemi Goradel N, Najafi M, Salehi E, Farhood B and Mortezaee K (2019) Cyclooxygenase-2 in cancer: a review. *J Cell Physiol* **234**:5683-5699.
- He L, He T, Farrar S, Ji L, Liu T and Ma X (2017) Antioxidants maintain cellular redox homeostasis by elimination of reactive oxygen species. *Cell Physiol Biochem* **44**:532-553.
- Heppner GH, Miller FR and Shekhar PM (2000) Nontransgenic models of breast cancer. *Breast Cancer Res* **2**:331-334.
- Hilditch TP and Williams PN (1964) *The chemical constitution of natural fats*. Chapman & Hall, London, UK.

- Holliday DL and Speirs V (2011) Choosing the right cell line for breast cancer research. *Breast Cancer Res* **13**:215.
- Housman G, Byler S, Heerboth S, Lapinska K, Longacre M, Snyder N and Sarkar S (2014) Drug resistance in cancer: an overview. *Cancers (Basel)* **6**:1769-1792.
- Hsiang YH, Lihou MG and Liu LF (1989) Arrest of replication forks by drug-stabilized topoisomerase I-DNA cleavable complexes as a mechanism of cell killing by camptothecin. *Cancer Res* **49**:5077-5082.
- Hu XF, Veroni M, de Luise M, Wakeling A, Sutherland R, Watts CKW and Zalcberg JR (1993) Circumvention of tamoxifen resistance by the pure anti-estrogen ICI 182, 780. *Int J Cancer* **55**:873-876.
- Huang J, Luo Q, Xiao Y, Li H, Kong L and Ren G (2017) The implication from RAS/RAF/ERK signaling pathway increased activation in epirubicin treated triple negative breast cancer. *Oncotarget* **8**:108249-108260.
- Hudgins LC, Hellerstein M, Seidman C, Neese R, Diakun J and Hirsch J (1996) Human fatty acid synthesis is stimulated by a eucaloric low fat, high carbohydrate diet. *J Clin Invest* **97**:2081-2091.
- Hughes JP, Rees S, Kalindjian SB and Philpott KL (2011) Principles of early drug discovery. *Br J Pharmacol* **162**:1239-1249.
- Hurvitz SA, Andre F, Jiang Z, Shao Z, Mano MS, Neciosup SP, Tseng LM, Zhang Q, Shen K, Liu D, Dreosti LM, Burris HA, Toi M, Buyse ME, Cabaribere D, Lindsay MA, Rao S, Pacaud LB, Taran T and Slamon D (2015) Combination of everolimus with trastuzumab plus paclitaxel as first-line treatment for patients with HER2-positive advanced breast cancer (BOLERO-1): a phase 3, randomised, double-blind, multicentre trial. *Lancet Oncol* **16**:816-829.
- Ianevski A, Giri AK and Aittokallio T (2022) SynergyFinder 3.0: an interactive analysis and consensus interpretation of multi-drug synergies across multiple samples. *Nucleic Acids Res* **50**:W739-W743.
- Inwald EC, Klinkhammer-Schalke M, Hofstädter F, Zeman F, Koller M, Gerstenhauer M and Ortmann O (2013) Ki-67 is a prognostic parameter in breast cancer patients: results of a large population-based cohort of a cancer registry. *Breast Cancer Res Treat* **139**:539-552.

- Ishikawa T and Ali-Osman F (1993) Glutathione-associated cis-diamminedichloroplatinum(II) metabolism and ATP-dependent efflux from leukemia cells. Molecular characterization of glutathione-platinum complex and its biological significance. *J Biol Chem* **268**:20116-20125.
- Ismail-Khan R and Bui MM (2010) A review of triple-negative breast cancer. *Cancer Control* **17**:173-176.
- Issa ME, Hall SR, Dupuis SN, Graham CL, Jakeman DL and Goralski KB (2014) Jadomycins are cytotoxic to ABCB1-, ABCC1-, and ABCG2-overexpressing MCF7 breast cancer cells. *Anticancer Drugs* **25**:255-269.
- Iwasa S, Koyama T, Nishino M, Kondo S, Sudo K, Yonemori K, Yoshida T, Tamura K, Shimizu T, Fujiwara Y, Kitano S, Shimomura A, Sato J, Yokoyama F, Iida H, Kondo M and Yamamoto N (2023) First-in-human study of ONO-4578, an antagonist of prostaglandin E(2) receptor 4, alone and with nivolumab in solid tumors. *Cancer Sci* **114**:211-220.
- Iwasaki E, Shimizu Y, Akagi Y and Komatsu T (2023) Synthesis and in vitro cytotoxicity evaluation of jadomycins. *Chem Pharm Bull (Tokyo)* **71**:730-733.
- Jakeman DL (2021) *Personal Communication*
- Jakeman DL, Bandi S, Graham CL, Reid TR, Wentzell JR and Douglas SE (2009a) Antimicrobial activities of jadomycin B and structurally related analogues. *Antimicrob Agents Chemother* **53**:1245-1247.
- Jakeman DL, Dupuis SN and Graham CL (2009b) Isolation and characterization of jadomycin L from *Streptomyces venezuelae* ISP5230 for solid tumor efficacy studies. *Pure Appl Chem* **81**:1041-1049.
- Jakeman DL, Farrell S, Young W, Doucet RJ and Timmons SC (2005a) Novel jadomycins: incorporation of non-natural and natural amino acids. *Bioorg Med Chem Lett* **15**:1447-1449.
- Jakeman DL, Graham CL and Reid TR (2005b) Novel and expanded jadomycins incorporating non-proteogenic amino acids. *Bioorg Med Chem Lett* **15**:5280-5283.
- Jakeman DL, Graham CL, Young W and Vining LC (2006) Culture conditions improving the production of jadomycin B. *J Ind Microbiol Biotechnol* **33**:767-772.
- Janssen GM and Venema JF (1985) Ibuprofen: plasma concentrations in man. *J Int Med Res* **13**:68-73.

- Jensen PB and Sehested M (1997) DNA topoisomerase II rescue by catalytic inhibitors: a new strategy to improve the antitumor selectivity of etoposide. *Biochem Pharmacol* **54**:755-759.
- Jhan JR and Andrechek ER (2017) Triple-negative breast cancer and the potential for targeted therapy. *Pharmacogenomics* **18**:1595-1609.
- Johnston SJ and Cheung KL (2010) Fulvestrant - a novel endocrine therapy for breast cancer. *Curr Med Chem* **17**:902-914.
- Jones SE and Elliot MA (2017) *Streptomyces* exploration: competition, volatile communication and new bacterial behaviours. *Trends Microbiol* **25**:522-531.
- Jordan VC (2003) Tamoxifen: a most unlikely pioneering medicine. *Nat Rev Drug Discov* **2**:205-213.
- Jurczyszyn A, Czepiel J, Gdula-Argasińska J, Paško P, Czapkiewicz A, Librowski T, Perucki W, Butrym A, Castillo JJ and Skotnicki AB (2015) Plasma fatty acid profile in multiple myeloma patients. *Leuk Res* **39**:400-405.
- Kamath K, Wilson L, Cabral F and Jordan MA (2005) BetaIII-tubulin induces paclitaxel resistance in association with reduced effects on microtubule dynamic instability. *J Biol Chem* **280**:12902-12907.
- Karpozilos A and Pavlidis N (2004) The treatment of cancer in Greek antiquity. *Eur J Cancer* **40**:2033-2040.
- Kerr JF, Wyllie AH and Currie AR (1972) Apoptosis: a basic biological phenomenon with wide-ranging implications in tissue kinetics. *Br J Cancer* **26**:239-257.
- Khan Shahper N, Lal Sunil K, Kumar P and Khan Asad U (2010) Effect of mitoxantrone on proliferation dynamics and cell-cycle progression. *Biosci Rep* **30**:375-381.
- Kim J, McKeown B, Patel K, Catalli A, Kulka M, Neto C and Hurta R (2014) Proanthocyanidins from the American cranberry (*Vaccinium macrocarpon*) induce cell cycle alterations in DU145 human prostate cancer cells in vitro by affecting the expression of cell cycle-associated proteins. *Funct Foods Health Dis* **4**:130-146.
- Kimura M, Kotani S, Hattori T, Sumi N, Yoshioka T, Todokoro K and Okano Y (1997) Cell cycle-dependent expression and spindle pole localization of a novel human protein kinase, Aik, related to Aurora of *Drosophila* and Yeast Ipl1. *J Biol Chem* **272**:13766-13771.

- Kirienko NV, Mani K and Fay DS (2010) Cancer models in *Caenorhabditis elegans*. *Dev Dyn* **239**:1413-1448.
- Klijn JGM, Setyono-Han B and Foekens JA (2000) Progesterone antagonists and progesterone receptor modulators in the treatment of breast cancer. *Steroids* **65**:825-830.
- Kochel TJ, Goloubeva OG and Fulton AM (2016) Upregulation of cyclooxygenase-2/prostaglandin E2 (COX-2/PGE2) pathway member multiple drug resistance-associated protein 4 (MRP4) and downregulation of prostaglandin transporter (PGT) and 15-prostaglandin dehydrogenase (15-PGDH) in triple-negative breast cancer. *Breast Cancer (Auckl)* **10**:61-70.
- Kochel TJ, Reader JC, Ma X, Kundu N and Fulton AM (2017) Multiple drug resistance-associated protein (MRP4) exports prostaglandin E2 (PGE2) and contributes to metastasis in basal/triple negative breast cancer. *Oncotarget* **8**:6540-6554.
- Kollareddy M, Dzubak P, Zheleva D and Hajduch M (2008) Aurora kinases: structure, functions and their association with cancer. *Biomed Pap Med Fac Univ Palacky Olomouc Czech Repub* **152**:27-33.
- Kontomanolis EN, Koutras A, Syllaios A, Schizas D, Mastoraki A, Garmpis N, Diakosavvas M, Angelou K, Tsatsaris G, Pagkalos A, Ntounis T and Fasoulakis Z (2020) Role of oncogenes and tumor-suppressor genes in carcinogenesis: a review. *Anticancer Res* **40**:6009-6015.
- Korch C, Hall EM, Dirks WG, Ewing M, Faries M, Varella-Garcia M, Robinson S, Storts D, Turner JA, Wang Y, Burnett EC, Healy L, Kniss D, Neve RM, Nims RW, Reid YA, Robinson WA and Capes-Davis A (2018) Authentication of M14 melanoma cell line proves misidentification of MDA-MB-435 breast cancer cell line. *Int J Cancer* **142**:561-572.
- Koster KL, Huober J and Joerger M (2022) New antibody-drug conjugates (ADCs) in breast cancer-an overview of ADCs recently approved and in later stages of development. *Explor Target Antitumor Ther* **3**:27-36.
- Krishnamurti C and Rao SC (2016) The isolation of morphine by Serturmer. *Indian J Anaesth* **60**:861-862.
- Krishnamurti U and Silverman JF (2014) HER2 in breast cancer: a review and update. *Adv Anat Pathol* **21**:100-107.

- Krohn K and Rohr J (1997) Angucyclines: total syntheses, new structures, and biosynthetic studies of an emerging new class of antibiotics, in *Bioorganic Chemistry Deoxysugars, Polyketides and Related Classes: Synthesis, Biosynthesis, Enzymes* (Rohr J ed) pp 127-195, Springer Berlin Heidelberg, Berlin, Heidelberg.
- Krumbhaar EB and Krumbhaar HD (1919) The blood and bone marrow in yellow cross gas (mustard gas) poisoning: changes produced in the bone marrow of fatal cases. *J Med Res* **40**:497-508.493.
- Kuang W, Deng Q, Deng C, Li W, Shu S and Zhou M (2017) Hepatocyte growth factor induces breast cancer cell invasion via the PI3K/Akt and p38 MAPK signaling pathways to up-regulate the expression of COX2. *Am J Transl Res* **9**:3816-3826.
- Kundu N, Ma X, Kochel T, Goloubeva O, Staats P, Thompson K, Martin S, Reader J, Take Y, Collin P and Fulton A (2014) Prostaglandin E receptor EP4 is a therapeutic target in breast cancer cells with stem-like properties. *Breast Cancer Res Treat* **143**:19-31.
- Lacassagne A (1936) Hormonal pathogenesis of adenocarcinoma of the breast. *Am J Cancer* **27**:217-228.
- Laemmli UK (1970) Cleavage of structural proteins during the assembly of the head of bacteriophage T4. *Nature* **227**:680-685.
- Lam SH, Chua HL, Gong Z, Lam TJ and Sin YM (2004) Development and maturation of the immune system in zebrafish, *Danio rerio*: a gene expression profiling, in situ hybridization and immunological study. *Dev Comp Immunol* **28**:9-28.
- Lasfargues EY and Ozzello L (1958) Cultivation of human breast carcinomas. *J Natl Cancer Inst* **21**:1131-1147.
- Laverdière C, Chiasson S, Costea I, Moghrabi A and Krajcinovic M (2002) Polymorphism G80A in the reduced folate carrier gene and its relationship to methotrexate plasma levels and outcome of childhood acute lymphoblastic leukemia. *Blood* **100**:3832-3834.
- Lederer S, Dijkstra TMH and Heskes T (2018) Additive dose response models: explicit formulation and the Loewe Additivity consistency condition. *Front Pharmacol* **9**:31.
- Lederer S, Dijkstra TMH and Heskes T (2019) Additive dose response models: defining synergy. *Front Pharmacol* **10**:1384.

- Lee AV, Oesterreich S and Davidson NE (2015) MCF-7 cells—changing the course of breast cancer research and care for 45 years. *J Nat Cancer Inst* **107**:djv073.
- Lee EY and Muller WJ (2010) Oncogenes and tumor suppressor genes. *Cold Spring Harb Perspect Biol* **2**:a003236.
- Lee KC, Bramley RL, Cowell IG, Jackson GH and Austin CA (2016) Proteasomal inhibition potentiates drugs targeting DNA topoisomerase II. *Biochem Pharmacol* **103**:29-39.
- Levin G, Duffin KL, Obukowicz MG, Hummert SL, Fujiwara H, Needleman P and Raz A (2002) Differential metabolism of dihomo-gamma-linolenic acid and arachidonic acid by cyclo-oxygenase-1 and cyclo-oxygenase-2: implications for cellular synthesis of prostaglandin E1 and prostaglandin E2. *Biochem J* **365**:489-496.
- Li CI, Anderson BO, Daling JR and Moe RE (2003) Trends in incidence rates of invasive lobular and ductal breast carcinoma. *JAMA* **289**:1421-1424.
- Li CI, Uribe DJ and Daling JR (2005) Clinical characteristics of different histologic types of breast cancer. *Br J Cancer* **93**:1046-1052.
- Li S, Jiang M, Wang L and Yu S (2020) Combined chemotherapy with cyclooxygenase-2 (COX-2) inhibitors in treating human cancers: Recent advancement. *Biomed Pharmacother* **129**:110389.
- Li X, Yang J, Peng L, Sahin AA, Huo L, Ward KC, O'Regan R, Torres MA and Meisel JL (2017) Triple-negative breast cancer has worse overall survival and cause-specific survival than non-triple-negative breast cancer. *Breast Cancer Res Treat* **161**:279-287.
- Li Z, Wei H, Li S, Wu P and Mao X (2022) The role of progesterone receptors in breast cancer. *Drug Des Devel Ther* **16**:305-314.
- Lim HK, Lee H, Moon A, Kang K-T and Jung J (2018) Exploring protocol for breast cancer xenograft model using endothelial colony-forming cells. *Transl Cancer Res* **7**:1228-1234.
- Limtrakul P, Chearwae W, Shukla S, Phisalpong C and Ambudkar SV (2007) Modulation of function of three ABC drug transporters, P-glycoprotein (ABCB1), mitoxantrone resistance protein (ABCG2) and multidrug resistance protein 1 (ABCC1) by tetrahydrocurcumin, a major metabolite of curcumin. *Mol Cell Biochem* **296**:85-95.

- Lin YS, Su LJ, Yu CT, Wong FH, Yeh HH, Chen SL, Wu JC, Lin WJ, Shiue YL, Liu HS, Hsu SL, Lai JM and Huang CY (2006) Gene expression profiles of the aurora family kinases. *Gene Expr* **13**:15-26.
- Liochev SI and Fridovich I (2002) The Haber-Weiss cycle—70 years later: an alternative view. *Redox Rep* **7**:55-57.
- Liu H, Zang C, Fenner MH, Possinger K and Elstner E (2003) PPARgamma ligands and ATRA inhibit the invasion of human breast cancer cells in vitro. *Breast Cancer Res Treat* **79**:63-74.
- Livak KJ and Schmittgen TD (2001) Analysis of relative gene expression data using real-time quantitative PCR and the 2(-Delta Delta C(T)) Method. *Methods* **25**:402-408.
- Loewe S (1928) Die quantitativen Probleme der Pharmakologie. *Ergebnisse der Physiologie* **27**:47-187.
- Loewe S and Muischnek H (1926) Über Kombinationswirkungen. *Naunyn-Schmiedebergs Arch Exp Pathol Pharmacol* **114**:313-326.
- Longley D and Johnston P (2005) Molecular mechanisms of drug resistance. *J Pathol* **205**:275-292.
- Longley DB, Harkin DP and Johnston PG (2003) 5-Fluorouracil: mechanisms of action and clinical strategies. *Nat Rev Cancer* **3**:330-338.
- Losee JR and Ebeling AH (1914) The cultivation of human sarcomatous tissue in vitro. *J Exp Med* **20**:140-148.
- Lowry OH, Rosebrough NJ, Farr AL and Randall RJ (1951) Protein measurement with the Folin phenol reagent. *J Biol Chem* **193**:265-275.
- Lytle NK, Barber AG and Reya T (2018) Stem cell fate in cancer growth, progression and therapy resistance. *Nat Rev Cancer* **18**:669-680.
- Ma X, Kundu N, Ioffe OB, Goloubeva O, Konger R, Baquet C, Gimotty P, Reader J and Fulton AM (2010) Prostaglandin E receptor EP1 suppresses breast cancer metastasis and is linked to survival differences and cancer disparities. *Mol Cancer Res* **8**:1310-1318.
- Ma X, Kundu N, Rifat S, Walser T and Fulton AM (2006) Prostaglandin E receptor EP4 antagonism inhibits breast cancer metastasis. *Cancer Res* **66**:2923-2927.

- MacLeod JM, Forget SM and Jakeman DL (2018a) The expansive library of jadomycins. *Can J Chem* **96**:495-501.
- MacLeod JM, Forget SM, Martinez-Farina CF and Jakeman DL (2018b) Isolation of a post-PKS C–C branching jadomycin from *S. venezuelae* ISP5230 in the presence of 8-aminooctanoic acid. *Can J Chem* **96**:760-764.
- Maier T, Güell M and Serrano L (2009) Correlation of mRNA and protein in complex biological samples. *FEBS Lett* **583**:3966-3973.
- Majumder M, Landman E, Liu L, Hess D and Lala PK (2015) COX-2 elevates oncogenic miR-526b in breast cancer by EP4 activation. *Mol Cancer Res* **13**:1022-1033.
- Majumder M, Nandi P, Omar A, Ugwuagbo KC and Lala PK (2018) EP4 as a therapeutic target for aggressive human breast cancer. *Int J Mol Sci* **19**:1019.
- Majumder M, Xin X, Liu L, Tutunea-Fatan E, Rodriguez-Torres M, Vincent K, Postovit LM, Hess D and Lala PK (2016) COX-2 induces breast cancer stem cells via EP4/PI3K/AKT/NOTCH/WNT axis. *Stem Cells* **34**:2290-2305.
- Malik SS, Masood N, Asif M, Ahmed P, Shah ZU and Khan JS (2019) Expressional analysis of MLH1 and MSH2 in breast cancer. *Curr Probl Cancer* **43**:97-105.
- Manfredi JJ and Horwitz SB (1984) Taxol: an antimetabolic agent with a new mechanism of action. *Pharmacol Ther* **25**:83-125.
- Mansoori B, Mohammadi A, Davudian S, Shirjang S and Baradaran B (2017) The different mechanisms of cancer drug resistance: a brief review. *Adv Pharm Bull* **7**:339-348.
- Mao Y, Desai SD, Ting CY, Hwang J and Liu LF (2001) 26 S proteasome-mediated degradation of topoisomerase II cleavable complexes. *J Biol Chem* **276**:40652-40658.
- Marcato P, Dean CA, Liu RZ, Coyle KM, Bydoun M, Wallace M, Clements D, Turner C, Mathenge EG, Gujar SA, Giacomantonio CA, Mackey JR, Godbout R and Lee PW (2015) Aldehyde dehydrogenase 1A3 influences breast cancer progression via differential retinoic acid signaling. *Mol Oncol* **9**:17-31.
- Marquette C and Nabell L (2012) Chemotherapy-resistant metastatic breast cancer. *Curr Treat Options Oncol* **13**:263-275.

- Marteijn JA, Lans H, Vermeulen W and Hoeijmakers JHJ (2014) Understanding nucleotide excision repair and its roles in cancer and ageing. *Nat Rev Mol Cell Biol* **15**:465-481.
- Martin LP, Hamilton TC and Schilder RJ (2008) Platinum resistance: the role of DNA repair pathways. *Clin Cancer Res* **14**:1291-1295.
- Martinez-Farina CF and Jakeman DL (2015) Jadomycins, put a bigger ring in it: isolation of seven- to ten-membered ring analogues. *Chem Commun (Camb)* **51**:14617-14619.
- Martinez-Farina CF, McCormick N, Robertson AW, Clement H, Jee A, Ampaw A, Chan N-L, Syvitski RT and Jakeman DL (2015a) Investigations into the binding of jadomycin DS to human topoisomerase II β by WaterLOGSY NMR spectroscopy. *Org Biomol Chem* **13**:10324-10327.
- Martinez-Farina CF, Robertson AW, Yin H, Monro S, McFarland SA, Syvitski RT and Jakeman DL (2015b) Isolation and synthetic diversification of jadomycin 4-amino-1-phenylalanine. *J Nat Prod* **78**:1208-1214.
- Masood S (2016) Breast cancer subtypes: morphologic and biologic characterization. *Womens Health (Lond)* **12**:103-119.
- Mattioli R, Ilari A, Colotti B, Mosca L, Fazi F and Colotti G (2023) Doxorubicin and other anthracyclines in cancers: Activity, chemoresistance and its overcoming. *Mol Aspects Med* **93**:101205.
- Mayer EL and Burstein HJ (2007) Chemotherapy for metastatic breast cancer. *Hematol Oncol Clin North Am* **21**:257-272.
- McCormick DL, Madigan MJ and Moon RC (1985) Modulation of rat mammary carcinogenesis by indomethacin. *Cancer Research* **45**:1803-1808.
- McCormick DL and Moon RC (1983) Inhibition of mammary carcinogenesis by flurbiprofen, a non-steroidal antiinflammatory agent. *Br J Cancer* **48**:859-861.
- McDermott M, Eustace AJ, Busschots S, Breen L, Crown J, Clynes M, O'Donovan N and Stordal B (2014) In vitro development of chemotherapy and targeted therapy drug-resistant cancer cell lines: a practical guide with case studies. *Front Oncol* **4**:40.

- McKeown BT and Hurta RAR (2014) Magnolol affects expression of IGF-1 and associated binding proteins in human prostate cancer cells *in vitro*. *Anticancer Res* **34**:6333.
- McKeown BT and Hurta RAR (2015) Magnolol affects cellular proliferation, polyamine biosynthesis and catabolism-linked protein expression and associated cellular signaling pathways in human prostate cancer cells *in vitro*. *Funct Foods Health Dis* **5**:17-33.
- McKeown BT, McDougall L, Catalli A and Hurta RAR (2014) Magnolol causes alterations in the cell cycle in androgen insensitive human prostate cancer cells *in vitro* by affecting expression of key cell cycle regulatory proteins. *Nutr Cancer* **66**:1154-1164.
- McKeown BT, Relja NJ, Hall SR, Gebremeskel S, MacLeod JM, Veinotte CJ, Bennett LG, Ohlund LB, Sleno L, Jakeman DL, Berman JN, Johnston B and Goralski KB (2022) Pilot study of jadomycin B pharmacokinetics and anti-tumoral effects in zebrafish larvae and mouse breast cancer xenograft models. *Can J Physiol Pharmacol* **100**:1065-1076.
- Medema RH and Bos JL (1993) The role of p21ras in receptor tyrosine kinase signaling. *Crit Rev Oncog* **4**:615-661.
- Melvin MS, Tomlinson JT, Saluta GR, Kucera GL, Lindquist N and Manderville RA (2000) Double-strand DNA cleavage by copper-prodigiosin. *J Am Chem Soc* **122**:6333-6334.
- Meresse P, Dechaux E, Monneret C and Bertounesque E (2004) Etoposide: discovery and medicinal chemistry. *Curr Med Chem* **11**:2443-2466.
- Mesner PWJ, Budihardjo II and Kaufmann SH (1997) Chemotherapy-induced apoptosis, in *Advances in Pharmacology* (Kaufmann SH ed) pp 461-499, Academic Press.
- Michaelis L and Menten ML (1913) Die kinetik der invertinwirkung *Biochem Z* **49**:333-369.
- Michaelis L, Menten ML, Johnson KA and Goody RS (2011) The original Michaelis constant: translation of the 1913 Michaelis-Menten paper. *Biochemistry* **50**:8264-8269.
- Miki Y, Swensen J, Shattuck-Eidens D, Futreal PA, Harshman K, Tavtigian S, Liu Q, Cochran C, Bennett LM, Ding W and et al. (1994) A strong candidate for the breast and ovarian cancer susceptibility gene BRCA1. *Science* **266**:66-71.

- Millikan RC, Newman B, Tse CK, Moorman PG, Conway K, Dressler LG, Smith LV, Labbok MH, Geradts J, Bensen JT, Jackson S, Nyante S, Livasy C, Carey L, Earp HS and Perou CM (2008) Epidemiology of basal-like breast cancer. *Breast Cancer Res Treat* **109**:123-139.
- Mirabelli P, Coppola L and Salvatore M (2019) Cancer cell lines are useful model systems for medical research. *Cancers (Basel)* **11**:1098.
- Mirzoyan Z, Sollazzo M, Allocca M, Valenza AM, Grifoni D and Bellosta P (2019) *Drosophila melanogaster*: a model organism to study cancer. *Front Genet* **10**:51.
- Mitchener MM, Hermanson DJ, Shockley EM, Brown HA, Lindsley CW, Reese J, Rouzer CA, Lopez CF and Marnett LJ (2015) Competition and allostery govern substrate selectivity of cyclooxygenase-2. *Proc Natl Acad Sci U S A* **112**:12366-12371.
- Miyake K, Mickley L, Litman T, Zhan Z, Robey R, Cristensen B, Brangi M, Greenberger L, Dean M, Fojo T and Bates SE (1999) Molecular cloning of cDNAs which are highly overexpressed in mitoxantrone-resistant cells: demonstration of homology to ABC transport genes. *Cancer Res* **59**:8-13.
- Mizutani H, Tada-Oikawa S, Hiraku Y, Kojima M and Kawanishi S (2005) Mechanism of apoptosis induced by doxorubicin through the generation of hydrogen peroxide. *Life Sci* **76**:1439-1453.
- Molina MA, Codony-Servat J, Albanell J, Rojo F, Arribas J and Baselga J (2001) Trastuzumab (herceptin), a humanized anti-Her2 receptor monoclonal antibody, inhibits basal and activated Her2 ectodomain cleavage in breast cancer cells. *Cancer Res* **61**:4744-4749.
- Molto E and Sheldrick P (2018) Paleo-oncology in the Dakhleh Oasis, Egypt: case studies and a paleoepidemiological perspective. *Int J Paleopathol* **21**:96-110.
- Monro SMA, Cottreau KM, Spencer C, Wentzell JR, Graham CL, Borissow CN, Jakeman DL and McFarland SA (2011) Copper-mediated nuclease activity of jadomycin B. *Bioorg Med Chem* **19**:3357-3360.
- Montemurro F, Nuzzolese I and Ponzzone R (2020) Neoadjuvant or adjuvant chemotherapy in early breast cancer? *Expert Opin Pharmacother* **21**:1071-1082.
- Moudi M, Go R, Yien CY and Nazre M (2013) Vinca alkaloids. *Int J Prev Med* **4**:1231-1235.

- Mougalian SS, Soulos PR, Killelea BK, Lannin DR, Abu-Khalaf MM, DiGiovanna MP, Sanft TB, Pusztai L, Gross CP and Chagpar AB (2015) Use of neoadjuvant chemotherapy for patients with stage I to III breast cancer in the United States. *Cancer* **121**:2544-2552.
- Mucci LA, Hjelmborg JB, Harris JR, Czene K, Havelick DJ, Scheike T, Graff RE, Holst K, Möller S, Unger RH, McIntosh C, Nuttall E, Brandt I, Penney KL, Hartman M, Kraft P, Parmigiani G, Christensen K, Koskenvuo M, Holm NV, Heikkilä K, Pukkala E, Skytthe A, Adami H-O, Kaprio J and Collaboration for the Nordic Twin Study of Cancer (2016) Familial risk and heritability of cancer among twins in nordic countries. *JAMA* **315**:68-76.
- Mulay IL, Roy R, Knox BE, Suhr NH and Delaney WE (1971) Trace-metal analysis of cancerous and non-cancerous human tissues. *J Nat Cancer Inst* **47**:1-13.
- Najafi M, Mortezaee K and Majidpoor J (2019) Cancer stem cell (CSC) resistance drivers. *Life Sci* **234**:116781.
- Nelson-Rees WA, Daniels DW and Flandermeyer RR (1981) Cross-contamination of cells in culture. *Science* **212**:446-452.
- Newman DJ and Cragg GM (2020) Natural products as sources of new drugs over the nearly four decades from 01/1981 to 09/2019. *J Nat Prod* **83**:770-803.
- Nigro JM, Baker SJ, Preisinger AC, Jessup JM, Hosteller R, Cleary K, Signer SH, Davidson N, Baylin S, Devilee P, Glover T, Collins FS, Weslon A, Modali R, Harris CC and Vogelstein B (1989) Mutations in the p53 gene occur in diverse human tumour types. *Nature* **342**:705-708.
- Nitiss JL (2009) Targeting DNA topoisomerase II in cancer chemotherapy. *Nat Rev Cancer* **9**:338-350.
- Noble RL (1990) The discovery of the vinca alkaloids—chemotherapeutic agents against cancer. *Biochem Cell Biol* **68**:1344-1351.
- Noble RL, Beer CT and Cutts JH (1958) Role of chance observations in chemotherapy: Vinca rosea. *Ann N Y Acad Sci* **76**:882-894.
- Nugoli M, Chuchana P, Vendrell J, Orsetti B, Ursule L, Nguyen C, Birnbaum D, Douzery EJP, Cohen P and Theillet C (2003) Genetic variability in MCF-7 sublines: evidence of rapid genomic and RNA expression profile modifications. *BMC Cancer* **3**:13.

- O'Callaghan G and Houston A (2015) Prostaglandin E2 and the EP receptors in malignancy: possible therapeutic targets? *Br J Pharmacol* **172**:5239-5250.
- O'Shaughnessy J, Koeppen H, Xiao Y, Lackner MR, Paul D, Stokoe C, Phippen J, Jr., Krekow L, Holmes FA, Vukelja S, Lindquist D, Sedlacek S, Rivera R, Brooks R, McIntyre K, Brownstein C, Hoersch S, Blum JL and Jones S (2015) Patients with slowly proliferative early breast cancer have low five-year recurrence rates in a phase III adjuvant trial of capecitabine. *Clin Cancer Res* **21**:4305-4311.
- Oda M, Ueno T, Kasai N, Takahashi H, Yoshida H, Sugawara F, Sakaguchi K, Hayashi H and Mizushima Y (2002) Inhibition of telomerase by linear-chain fatty acids: a structural analysis. *Biochem J* **367**:329-334.
- Odes EJ, Randolph-Quinney PS, Steyn M, Throckmorton Z, Smilg JS, Zipfel B, Augustine TN, de Beer F, Hoffman JW, Franklin RD and Berger LR (2016) Earliest hominin cancer: 1.7-million-year-old osteosarcoma from Swartkrans Cave, South Africa. *S Afr J Sci* **112**:5.
- Ozaki T and Nakagawara A (2011) Role of p53 in cell death and human cancers. *Cancers (Basel)* **3**:994-1013.
- Pandya S and Moore RG (2011) Breast development and anatomy. *Clin Obstet Gynecol* **54**:91-95.
- Papanicolaou GN and Traut HF (1941) The diagnostic value of vaginal smears in carcinoma of the uterus. *Am J Obstet Gynecol* **42**:193-206.
- Paradiso A, Mangia A, Chiriatti A, Tommasi S, Zito A, Latorre A, Schittulli F and Lorusso V (2005) Biomarkers predictive for clinical efficacy of taxol-based chemotherapy in advanced breast cancer. *Ann Oncol* **16**:iv14-iv19.
- Patel A (2020) Benign vs malignant tumors. *JAMA Oncol* **6**:1488-1488.
- Patel HK and Bihani T (2018) Selective estrogen receptor modulators (SERMs) and selective estrogen receptor degraders (SERDs) in cancer treatment. *Pharmacol Ther* **186**:1-24.
- Pathak SK, Sharma RA, Steward WP, Mellon JK, Griffiths TRL and Gescher AJ (2005) Oxidative stress and cyclooxygenase activity in prostate carcinogenesis: targets for chemopreventive strategies. *Eur J Cancer* **41**:61-70.

- Pavel M, Renna M, Park SJ, Menzies FM, Ricketts T, Füllgrabe J, Ashkenazi A, Frake RA, Lombarte AC, Bento CF, Franze K and Rubinsztein DC (2018) Contact inhibition controls cell survival and proliferation via YAP/TAZ-autophagy axis. *Nat Commun* **9**:2961.
- Pavithra N, Bannikoppa PS, Uthappa S, Kurpad AV and Mani I (2018) Plasma fatty acid composition and estimated desaturase activities reflect dietary patterns in subjects with metabolic syndrome. *Indian J Clin Biochem* **33**:290-296.
- Paweł S, Konrad P, Adam M, Marek P, Jerzy K, Maciej Z, Dawid M, Marcin D, Tserenchunt G, Manfred D and Hermann L (2008) Positive correlation between cyclooxygenase 2 and the expression of ABC transporters in non-small cell lung cancer. *Anticancer Res* **28**:2967.
- Peddi PF and Hurvitz SA (2014) Ado-trastuzumab emtansine (T-DM1) in human epidermal growth factor receptor 2 (HER2)-positive metastatic breast cancer: latest evidence and clinical potential. *Ther Adv Med Oncol* **6**:202-209.
- Pegram MD, Finn RS, Arzoo K, Beryt M, Pietras RJ and Slamon DJ (1997) The effect of HER-2/neu overexpression on chemotherapeutic drug sensitivity in human breast and ovarian cancer cells. *Oncogene* **15**:537-547.
- Perez EA (2008) Cardiac toxicity of ErbB2-targeted therapies: what do we know? *Clin Breast Cancer* **8 Suppl 3**:S114-120.
- Perou CM, Sørlie T, Eisen MB, van de Rijn M, Jeffrey SS, Rees CA, Pollack JR, Ross DT, Johnsen H, Akslen LA, Fluge Ø, Pergamenschikov A, Williams C, Zhu SX, Lønning PE, Børresen-Dale A-L, Brown PO and Botstein D (2000) Molecular portraits of human breast tumours. *Nature* **406**:747-752.
- Piria R (1838) Sur la composition de la salicine et quelques-unes de ses réactions. *CR Acad Sci* **6**:620-624.
- Pizer ES, Thupari J, Han WF, Pinn ML, Chrest FJ, Frehywot GL, Townsend CA and Kuhajda FP (2000) Malonyl-coenzyme-A is a potential mediator of cytotoxicity induced by fatty-acid synthase inhibition in human breast cancer cells and xenografts. *Cancer Res* **60**:213-218.
- Pommier Y, Nussenzweig A, Takeda S and Austin C (2022) Human topoisomerases and their roles in genome stability and organization. *Nat Rev Mol Cell Biol* **23**:407-427.

- Porkka K, Blomqvist C, Rissanen P, Elomaa I and Pyrhönen S (1994) Salvage therapies in women who fail to respond to first-line treatment with fluorouracil, epirubicin, and cyclophosphamide for advanced breast cancer. *J Clin Oncol* **12**:1639-1647.
- Prates C, Sousa S, Oliveira C and Ikram S (2011) Prostate metastatic bone cancer in an Egyptian Ptolemaic mummy, a proposed radiological diagnosis. *Int J Paleopathol* **1**:98-103.
- Prihantono and Faruk M (2021) Breast cancer resistance to chemotherapy: when should we suspect it and how can we prevent it? *Ann Med Surg (Lond)* **70**:102793.
- Procópio RE, Silva IR, Martins MK, Azevedo JL and Araújo JM (2012) Antibiotics produced by *Streptomyces*. *Braz J Infect Dis* **16**:466-471.
- Prowell TM and Davidson NE (2004) What is the role of ovarian ablation in the management of primary and metastatic breast cancer today? *Oncologist* **9**:507-517.
- Pulaski BA and Ostrand-Rosenberg S (1998) Reduction of established spontaneous mammary carcinoma metastases following immunotherapy with major histocompatibility complex class II and B7.1 cell-based tumor vaccines. *Cancer Res* **58**:1486-1493.
- Pulaski BA and Ostrand-Rosenberg S (2000) Mouse 4T1 breast tumor model. *Curr Protoc Immunol* **39**:20.22.21-20.22.16.
- Pulvertaft RJV (1964) Cytology of Burkitt's Tumour (African lymphoma). *Lancet* **283**:238-240.
- Qiu S, Yang B, Li Z, Li S, Yan H, Xin Z, Liu J, Zhao X, Zhang L, Xiang W and Wang W (2024) Building a highly efficient *Streptomyces* super-chassis for secondary metabolite production by reprogramming naturally-evolved multifaceted shifts. *Metab Eng* **81**:210-226.
- Qu J, Zhao X, Wang J, Liu C, Sun Y, Cai H and Liu J (2018) Plasma phospholipase A2 activity may serve as a novel diagnostic biomarker for the diagnosis of breast cancer. *Oncol Lett* **15**:5236-5242.
- Quinn JE, Kennedy RD, Mullan PB, Gilmore PM, Carty M, Johnston PG and Harkin DP (2003) BRCA1 functions as a differential modulator of chemotherapy-induced apoptosis. *Cancer Res* **63**:6221-6228.

- Rae JM, Creighton CJ, Meck JM, Haddad BR and Johnson MD (2007) MDA-MB-435 cells are derived from M14 melanoma cells--a loss for breast cancer, but a boon for melanoma research. *Breast Cancer Res Treat* **104**:13-19.
- Rajkumar-Calkins AS, Szalat R, Dreze M, Khan I, Frazier Z, Reznichenkov E, Schnorenberg MR, Tsai YF, Nguyen H, Kochupurakkal B, D'Andrea AD, Shapiro GI, Lazaro JB and Mouw KW (2019) Functional profiling of nucleotide excision repair in breast cancer. *DNA Repair (Amst)* **82**:102697.
- Randolph-Quinney PS, Williams SA, Steyn M, Meyer MR, Smilg JS, Churchill SE, Odes EJ, Augustine T, Tafforeau P and Berger LR (2016) Osteogenic tumour in Australopithecus sediba: Earliest hominin evidence for neoplastic disease. *S Afr J Sci* **112**:1-7.
- Reader J, Holt D and Fulton A (2011) Prostaglandin E2 EP receptors as therapeutic targets in breast cancer. *Cancer Metastasis Rev* **30**:449-463.
- Reardon JT, Vaisman A, Chaney SG and Sancar A (1999) Efficient nucleotide excision repair of cisplatin, oxaliplatin, and Bis-aceto-ammine-dichloro-cyclohexylamine-platinum(IV) (JM216) platinum intrastrand DNA diadducts. *Cancer Res* **59**:3968-3971.
- Regulski M, Regulska K, Prukała W, Piotrowska H, Stanisiz B and Murias M (2016) COX-2 inhibitors: a novel strategy in the management of breast cancer. *Drug Discov Today* **21**:598-615.
- Reya T, Morrison SJ, Clarke MF and Weissman IL (2001) Stem cells, cancer, and cancer stem cells. *Nature* **414**:105-111.
- Riccardi C and Nicoletti I (2006) Analysis of apoptosis by propidium iodide staining and flow cytometry. *Nat Protoc* **1**:1458-1461.
- Riis M (2020) Modern surgical treatment of breast cancer. *Ann Med Surg (Lond)* **56**:95-107.
- Riss TL, Moravec RA, Niles AL, Duellman S, Benink HA, Worzella TJ and Minor L (2013) *Cell Viability Assays*. Eli Lilly & Company and the National Center for Advancing Translational Sciences, Bethesda, MD.
- Rix U, Zheng J, Remsing Rix LL, Greenwell L, Yang K and Rohr J (2004) The dynamic structure of jadomycin B and the amino acid incorporation step of its biosynthesis. *J Am Chem Soc* **126**:4496-4497.

- Robertson AW, MacLeod JM, MacIntyre LW, Forget SM, Hall SR, Bennett LG, Correa H, Kerr RG, Goralski KB and Jakeman DL (2018) Post Polyketide Synthase Carbon–Carbon Bond Formation in Type-II PKS-Derived Natural Products from *Streptomyces venezuelae*. *The Journal of Organic Chemistry* **83**:1876-1890.
- Robertson AW, Martinez-Farina CF, Smithen DA, Yin H, Monro S, Thompson A, McFarland SA, Syvitski RT and Jakeman DL (2015) Eight-membered ring-containing jadomycins: implications for non-enzymatic natural products biosynthesis. *J Am Chem Soc* **137**:3271-3275.
- Robey RW, Massey PR, Amiri-Kordestani L and Bates SE (2010) ABC transporters: unvalidated therapeutic targets in cancer and the CNS. *Anticancer Agents Med Chem* **10**:625-633.
- Robey RW, Pluchino KM, Hall MD, Fojo AT, Bates SE and Gottesman MM (2018) Revisiting the role of ABC transporters in multidrug-resistant cancer. *Nat Rev Cancer* **18**:452-464.
- Roell KR, Reif DM and Motsinger-Reif AA (2017) An introduction to terminology and methodology of chemical synergy-perspectives from across disciplines. *Front Pharmacol* **8**:158.
- Rohr J and Thiericke R (1992) Angucycline group antibiotics. *Nat Prod Rep* **9**:103-137.
- Rojas P, Jung-Cook H, Ruiz-Sánchez E, Rojas-Tomé IS, Rojas C, López-Ramírez AM and Reséndiz-Albor AA (2022) Historical aspects of herbal use and comparison of current regulations of herbal products between Mexico, Canada and the United States of America. *Int J Environ Res Public Health* **19**:15690.
- Rosadi F, Fiorentini C and Fabbri A (2016) Bacterial protein toxins in human cancers. *Pathog Dis* **74**:ftv105.
- Rothschild BM, Tanke DH, Helbling M and Martin LD (2003) Epidemiologic study of tumors in dinosaurs. *Naturwissenschaften* **90**:495-500.
- Ruan Y, Poirier A, Yong J, Garner R, Sun Z, Than J and Brenner DR (2023) Long-term projections of cancer incidence and mortality in Canada: the OncoSim all cancers model. *Prev Med* **168**:107425.
- Rubens RD, Sexton S, Tong D, Winter PJ, Knight RK and Hayward JL (1980) Combined chemotherapy and radiotherapy for locally advanced breast cancer. *Eur J Cancer (1965)* **16**:351-356.

- Russel FG, Koenderink JB and Masereeuw R (2008) Multidrug resistance protein 4 (MRP4/ABCC4): a versatile efflux transporter for drugs and signalling molecules. *Trends Pharmacol Sci* **29**:200-207.
- Russell PJ, Bennett S and Stricker P (1998) Growth factor involvement in progression of prostate cancer. *Clin Chem* **44**:705-723.
- Russo IH and Russo J (1996) Mammary gland neoplasia in long-term rodent studies. *Environ Health Perspect* **104**:938-967.
- Sagi SA, Weggen S, Eriksen J, Golde TE and Koo EH (2003) The non-cyclooxygenase targets of non-steroidal anti-inflammatory drugs, Lipoxygenases, peroxisome proliferator-activated receptor, inhibitor of kappa B kinase, and NF kappa B, do not reduce amyloid beta production. *J Biol Chem* **278**:31825-31830.
- Sajjad H, Imtiaz S, Noor T, Siddiqui YH, Sajjad A and Zia M (2021) Cancer models in preclinical research: a chronicle review of advancement in effective cancer research. *Animal Model Exp Med* **4**:87-103.
- Schapira M, Totrov M and Abagyan R (1999) Prediction of the binding energy for small molecules, peptides and proteins. *J Mol Recognit* **12**:177-190.
- Schatz A, Bugle E and Waksman SA (1944) Streptomycin, a substance exhibiting antibiotic activity against gram-positive and gram-negative bacteria. *Proc Soc Exp Biol Med* **55**:66-69.
- Scherer WF, Syverton JT and Gey GO (1953) Studies on the propagation in vitro of poliomyelitis viruses. IV. Viral multiplication in a stable strain of human malignant epithelial cells (strain HeLa) derived from an epidermoid carcinoma of the cervix. *J Exp Med* **97**:695-710.
- Schneider E, Horton JK, Yang CH, Nakagawa M and Cowan KH (1994) Multidrug resistance-associated protein gene overexpression and reduced drug sensitivity of topoisomerase II in a human breast carcinoma MCF7 cell line selected for etoposide resistance. *Cancer Res* **54**:152-158.
- Schofield MJ and Hsieh P (2003) DNA mismatch repair: molecular mechanisms and biological function. *Annu Rev Microbiol* **57**:579-608.
- Schwartz GK and Shah MA (2005) Targeting the cell cycle: a new approach to cancer therapy. *J Clin Oncol* **23**:9408-9421.

- Seidman A, Hudis C, Pierri MK, Shak S, Paton V, Ashby M, Murphy M, Stewart SJ and Keefe D (2002) Cardiac dysfunction in the trastuzumab clinical trials experience. *J Clin Oncol* **20**:1215-1221.
- Sekhon-Loodu S, Ziaullah and Rupasinghe HP (2015) Docosahexaenoic acid ester of phloridzin inhibit lipopolysaccharide-induced inflammation in THP-1 differentiated macrophages. *Int Immunopharmacol* **25**:199-206.
- Shah C, Vicini F, Shaitelman SF, Hepel J, Keisch M, Arthur D, Khan AJ, Kuske R, Patel R and Wazer DE (2018) The American Brachytherapy Society consensus statement for accelerated partial-breast irradiation. *Brachytherapy* **17**:154-170.
- Shan M, Sharif EU and O'Doherty GA (2010) Total synthesis of jadomycin A and a carbasugar analogue of jadomycin B. *Angew Chem Int Ed* **49**:9492-9495.
- Shapiro S, Strax P and Venet L (1971) Periodic breast cancer screening in reducing mortality from breast cancer. *JAMA* **215**:1777-1785.
- Shirling EB and Gottlieb D (1969) Cooperative description of type cultures of *Streptomyces*. IV. Species descriptions from the second, third and fourth studies. *Int J Syst Evol Microbiol* **19**:391-512.
- Si SY (2020) *Personal Communication*
- Siegel RL, Miller KD, Wagle NS and Jemal A (2023) Cancer statistics, 2023. *CA Cancer J Clin* **73**:17-48.
- Simmons DL, Botting RM and Hla T (2004) Cyclooxygenase isozymes: the biology of prostaglandin synthesis and inhibition. *Pharmacol Rev* **56**:387-437.
- Slamon DJ, Clark GM, Wong SG, Levin WJ, Ullrich A and McGuire WL (1987) Human breast cancer: correlation of relapse and survival with amplification of the HER-2/neu oncogene. *Science* **235**:177-182.
- Smadel JE and Jackson EB (1947) Chloromycetin, an antibiotic with chemotherapeutic activity in experimental rickettsial and viral infections. *Science* **106**:418-419.
- Smith IE and Dowsett M (2003) Aromatase inhibitors in breast cancer. *N Engl J Med* **348**:2431-2442.
- Smith KL, Dang C and Seidman AD (2006) Cardiac dysfunction associated with trastuzumab. *Expert Opin Drug Saf* **5**:619-629.

- Smith WL and Malkowski MG (2019) Interactions of fatty acids, nonsteroidal anti-inflammatory drugs, and coxibs with the catalytic and allosteric subunits of cyclooxygenases-1 and -2. *J Biol Chem* **294**:1697-1705.
- Smyth MJ, Dunn GP and Schreiber RD (2006) Cancer immunosurveillance and immunoediting: the roles of immunity in suppressing tumor development and shaping tumor immunogenicity, in *Advances in Immunology* pp 1-50, Academic Press.
- Snezhkina AV, Kudryavtseva AV, Kardymon OL, Savvateeva MV, Melnikova NV, Krasnov GS and Dmitriev AA (2019) ROS generation and antioxidant defense systems in normal and malignant cells. *Oxid Med Cell Longev* **2019**:6175804.
- Sobel RE and Sadar MD (2005) Cell lines used in prostate cancer research: a compendium of old and new lines--part 1. *J Urol* **173**:342-359.
- Soule HD, Vazquez J, Long A, Albert S and Brennan M (1973) A human cell line from a pleural effusion derived from a breast carcinoma. *J Natl Cancer Inst* **51**:1409-1416.
- Standring S (2016) *Gray's Anatomy: The Anatomical Basis of Clinical Practice*. Elsevier Limited.
- Stewart L, Redinbo MR, Qiu X, Hol WGJ and Champoux JJ (1998) A model for the mechanism of human topoisomerase I. *Science* **279**:1534-1541.
- Strax P, Venet L, Shapiro S and Gross S (1967) Mammography and clinical examination in mass screening for cancer of the breast. *Cancer* **20**:2184-2188.
- Strouhal E and Kritscher H (1990) Neolithic case of a multiple myeloma from Mauer (Vienna, Austria). *Anthropologie (Brno)* **28**:79-87.
- Sugimoto Y and Narumiya S (2007) Prostaglandin E receptors. *J Biol Chem* **282**:11613-11617.
- Sung H, Ferlay J, Siegel RL, Laversanne M, Soerjomataram I, Jemal A and Bray F (2021) Global cancer statistics 2020: GLOBOCAN estimates of incidence and mortality worldwide for 36 cancers in 185 countries. *CA Cancer J Clin* **71**:209-249.
- Swaby RF, Sharma CGN and Jordan VC (2007) SERMs for the treatment and prevention of breast cancer. *Rev Endocr Metab Disord* **8**:229-239.

- Syvitski RT, Borissow CN, Graham CL and Jakeman DL (2006) Ring-opening dynamics of jadomycin A and B and Dalomycin T. *Org Lett* **8**:697-700.
- Szczuraszek K, Materna V, Halon A, Mazur G, Wróbel T, Kuliczkowski K, Maciejczyk A, Zabel M, Drag M, Dietel M, Lage H and Surowiak P (2009) Positive correlation between cyclooxygenase-2 and ABC-transporter expression in non-Hodgkin's lymphomas. *Oncol Rep* **22**:1315-1323.
- Tai HH (2011) Prostaglandin catabolic enzymes as tumor suppressors. *Cancer Metastasis Rev* **30**:409-417.
- Tajima T, Akagi Y, Kumamoto T, Suzuki N and Ishikawa T (2012) Synthesis of jadomycin A and related jadomycin aglycons: structural re-examination of jadomycins S and T may be needed. *Tetrahedron Lett* **53**:383-387.
- Tchatchou S, Wirtenberger M, Hemminki K, Sutter C, Meindl A, Wappenschmidt B, Kiechle M, Bugert P, Schmutzler RK, Bartram CR and Burwinkel B (2007) Aurora kinases A and B and familial breast cancer risk. *Cancer Lett* **247**:266-272.
- Tesarova P (2012) Breast cancer in the elderly-should it be treated differently? *Rep Pract Oncol Radiother* **18**:26-33.
- Thienpont B, Van Dyck L and Lambrechts D (2016) Tumors smother their epigenome. *Mol Cell Oncol* **3**:e1240549.
- Thompson HJ and Singh M (2000) Rat models of premalignant breast disease. *J Mammary Gland Biol Neoplasia* **5**:409-420.
- Timoshenko AV, Chakraborty C, Wagner GF and Lala PK (2006) COX-2-mediated stimulation of the lymphangiogenic factor VEGF-C in human breast cancer. *Br J Cancer* **94**:1154-1163.
- Tönisen F, Perrin L, Bayarmagnai B, van den Dries K, Cambi A and Gligorijevic B (2017) EP4 receptor promotes invadopodia and invasion in human breast cancer. *Eur J Cell Biol* **96**:218-226.
- Totrov M and Abagyan R (1999) Derivation of sensitive discrimination potential for virtual ligand screening, in *Proceedings of the third annual international conference on Computational molecular biology* pp 312–320, Association for Computing Machinery, Lyon, France.
- Tremont A, Lu J and Cole JT (2017) Endocrine therapy for early breast cancer: updated review. *Ochsner J* **17**:405-411.

- Turley H, Comley M, Houlbrook S, Nozaki N, Kikuchi A, Hickson ID, Gatter K and Harris AL (1997) The distribution and expression of the two isoforms of DNA topoisomerase II in normal and neoplastic human tissues. *Br J Cancer* **75**:1340-1346.
- Turnbull C and Rahman N (2008) Genetic predisposition to breast cancer: past, present, and future. *Ann Rev Genomics Hum Genet* **9**:321-345.
- Valko M, Jomova K, Rhodes CJ, Kuča K and Musílek K (2016) Redox- and non-redox-metal-induced formation of free radicals and their role in human disease. *Archives of Toxicology* **90**:1-37.
- van Engeland M, Nieland LJ, Ramaekers FC, Schutte B and Reutelingsperger CP (1998) Annexin V-affinity assay: a review on an apoptosis detection system based on phosphatidylserine exposure. *Cytometry* **31**:1-9.
- Vann KR, Oviatt AA and Osheroff N (2021) Topoisomerase II poisons: converting essential enzymes into molecular scissors. *Biochemistry* **60**:1630-1641.
- Vassilomanolakis M, Koumakis G, Barbounis V, Demiri M, Panopoulos C, Chrissohoou M, Apostolikas N and Efremidis AP (2005) First-line chemotherapy with docetaxel and cisplatin in metastatic breast cancer. *Breast* **14**:136-141.
- Vaux DL, Cory S and Adams JM (1988) Bcl-2 gene promotes haemopoietic cell survival and cooperates with c-myc to immortalize pre-B cells. *Nature* **335**:440-442.
- Vavrova A, Jansova H, Mackova E, Machacek M, Haskova P, Tichotova L, Sterba M and Simunek T (2013) Catalytic inhibitors of topoisomerase II differently modulate the toxicity of anthracyclines in cardiac and cancer cells. *PLoS One* **8**:e76676.
- Vecchio AJ, Orlando BJ, Nandagiri R and Malkowski MG (2012) Investigating substrate promiscuity in cyclooxygenase-2: the role of Arg-120 and residues lining the hydrophobic groove. *J Biol Chem* **287**:24619-24630.
- Veinotte CJ, Dellaire G and Berman JN (2014) Hooking the big one: the potential of zebrafish xenotransplantation to reform cancer drug screening in the genomic era. *Dis Model Mech* **7**:745-754.
- Verma H, Narendra G, Raju B, Singh PK and Silakari O (2022) Dihydropyrimidine dehydrogenase-mediated resistance to 5-Fluorouracil: mechanistic investigation and solution. *ACS Pharmacol Transl Sci* **5**:1017-1033.

- Vermeulen K, Van Bockstaele DR and Berneman ZN (2003) The cell cycle: a review of regulation, deregulation and therapeutic targets in cancer. *Cell Prolif* **36**:131-149.
- Vessby B, Gustafsson IB, Tengblad S, Boberg M and Andersson A (2002) Desaturation and elongation of Fatty acids and insulin action. *Ann N Y Acad Sci* **967**:183-195.
- Voelcker G (2020) The mechanism of action of cyclophosphamide and its consequences for the development of a new generation of oxazaphosphorine cytostatics. *Sci Pharm* **88**:42.
- Vogel WH, Minhas A and Baumrucker S (2020) Dihydropyrimidine dehydrogenase deficiency: to screen or not to screen? *J Adv Pract Oncol* **11**:68-73.
- Vonderheide RH, Domchek SM and Clark AS (2017) Immunotherapy for breast cancer: what are we missing? *Clin Cancer Res* **23**:2640-2646.
- Waks AG and Winer EP (2019) Breast cancer treatment: a review. *JAMA* **321**:288-300.
- Walker OL, Dahn ML, Power Coombs MR and Marcato P (2021) The prostaglandin E2 pathway and breast cancer stem cells: evidence of increased signaling and potential targeting. *Front Oncol* **11**:791696.
- Wang J and Xu B (2019) Targeted therapeutic options and future perspectives for HER2-positive breast cancer. *Signal Transduct Target Ther* **4**:34.
- Wang L, White RL and Vining LC (2002) Biosynthesis of the dideoxysugar component of jadomycin B: genes in the jad cluster of *Streptomyces venezuelae* ISP5230 for l-digitoxose assembly and transfer to the angucycline aglycone. *Microbiology* **148**:1091-1103.
- Wang R, Lv Q, Meng W, Tan Q, Zhang S, Mo X and Yang X (2014) Comparison of mammosphere formation from breast cancer cell lines and primary breast tumors. *J Thorac Dis* **6**:829-837.
- Wang X, Zhang H and Chen X (2019) Drug resistance and combating drug resistance in cancer. *Cancer Drug Resist* **2**:141-160.
- Wani MC, Taylor HL, Wall ME, Coggon P and McPhail AT (1971) Plant antitumor agents. VI. Isolation and structure of taxol, a novel antileukemic and antitumor agent from *Taxus brevifolia*. *J Am Chem Soc* **93**:2325-2327.
- Warburg O (1956a) On respiratory impairment in cancer cells. *Science* **124**:269-270.

- Warburg O (1956b) On the origin of cancer cells. *Science* **123**:309-314.
- Warburg OH (1930) *The Metabolism of Tumours: Investigations from the Kaiser Wilhelm Institute for Biology, Berlin-Dahlem*. Constable & Company Limited, London, UK.
- Watson JD and Crick FHC (1953) Molecular structure of nucleic acids: a structure for deoxyribose nucleic acid. *Nature* **171**:737-738.
- Wells C (1963) Ancient Egyptian pathology. *J Laryngol Otol* **77**:261-265.
- Wenger SL, Senft JR, Sargent LM, Bamezai R, Bairwa N and Grant SG (2004) Comparison of established cell lines at different passages by karyotype and comparative genomic hybridization. *Biosci Rep* **24**:631-639.
- Wertman J, Veinotte CJ, Dellaire G and Berman JN (2016) The zebrafish xenograft platform: evolution of a novel cancer model and preclinical screening tool. *Adv Exp Med Biol* **916**:289-314.
- Willems E, Dedobbeleer M, Digregorio M, Lombard A, Lumapat PN and Rogister B (2018) The functional diversity of Aurora kinases: a comprehensive review. *Cell Div* **13**:7.
- Witsch E, Sela M and Yarden Y (2010) Roles for growth factors in cancer progression. *Physiology (Bethesda)* **25**:85-101.
- Woessner RD, Mattern MR, Mirabelli CK, Johnson RK and Drake FH (1991) Proliferation- and cell cycle-dependent differences in expression of the 170 kilodalton and 180 kilodalton forms of topoisomerase II in NIH-3T3 cells. *Cell Growth Differ* **2**:209-214.
- Woodruff HB (2014) Selman A. Waksman, winner of the 1952 Nobel Prize for physiology or medicine. *Appl Environ Microbiol* **80**:2-8.
- Woodward DF, Jones RL and Narumiya S (2011) International union of basic and clinical pharmacology. LXXXIII: classification of prostanoid receptors, updating 15 years of progress. *Pharmacol Rev* **63**:471-538.
- Wooster R, Bignell G, Lancaster J, Swift S, Seal S, Mangion J, Collins N, Gregory S, Gumbs C and Micklem G (1995) Identification of the breast cancer susceptibility gene BRCA2. *Nature* **378**:789-792.

- Wu Z, Li S, Cai Y, chen F, Chen Y and Luo X (2020) Synergistic action of doxorubicin and 7-Ethyl-10-hydroxycamptothecin polyphosphorylcholine polymer prodrug. *Colloids Surf B Biointerfaces* **189**:110741.
- Xu S, Zhou W, Ge J and Zhang Z (2018) Prostaglandin E2 receptor EP4 is involved in the cell growth and invasion of prostate cancer via the cAMP-PKA/PI3K-Akt signaling pathway. *Mol Med Rep* **17**:4702-4712.
- Yadav R, Kumar Y, Dahiya D and Bhatia A (2022) Claudins: the newly emerging targets in breast cancer. *Clin Breast Cancer* **22**:737-752.
- Yalaza M, İnan A and Bozer M (2016) Male breast cancer. *J Breast Health* **12**:1-8.
- Yan SH (2013) An early history of human breast cancer: West meets East. *Chin J Cancer* **32**:475-477.
- Yang H, Villani RM, Wang H, Simpson MJ, Roberts MS, Tang M and Liang X (2018) The role of cellular reactive oxygen species in cancer chemotherapy. *J Exp Clin Cancer Res* **37**:266.
- Yang K, Han L, Ayer SW and Vining LC (1996) Accumulation of the angucycline antibiotic rabelomycin after disruption of an oxygenase gene in the jadomycin B biosynthetic gene cluster of *Streptomyces venezuelae*. *Microbiology* **142**:123-132.
- Yang R, Han Y, Guan X, Hong Y, Meng J, Ding S, Long Q and Yi W (2023) Regulation and clinical potential of telomerase reverse transcriptase (TERT/hTERT) in breast cancer. *Cell Commun Signal* **21**:218.
- Yang X and Yu B (2013) Total synthesis of jadomycins B, S, T, and ILEVS1080. *Chem Eur J* **19**:8431-8434.
- Yao Y and Dai W (2014) Genomic instability and cancer. *J Carcinog Mutagen* **5**:1000163.
- Yeo HS, Shehzad A and Lee YS (2012) Prostaglandin E2 blocks menadione-induced apoptosis through the Ras/Raf/Erk signaling pathway in promonocytic leukemia cell lines. *Mol Cells* **33**:371-378.
- Yousefnia S, Ghaedi K, Seyed Forootan F and Nasr Esfahani MH (2019) Characterization of the stemness potency of mammospheres isolated from the breast cancer cell lines. *Tumor Biol* **41**:1010428319869101.

- Yuan C, Sidhu RS, Kuklev DV, Kado Y, Wada M, Song I and Smith WL (2009) Cyclooxygenase allosterism, fatty acid-mediated cross-talk between monomers of cyclooxygenase homodimers. *J Biol Chem* **284**:10046-10055.
- Zeliha KP, Dilek O, Ezgi O, Halil K, Cihan U and Gul O (2020) Association between ABCB1, ABCG2 carrier protein and COX-2 enzyme gene polymorphisms and breast cancer risk in a Turkish population. *Saudi Pharm J* **28**:215-219.
- Zeng L, Li W and Chen CS (2020) Breast cancer animal models and applications. *Zool Res* **41**:477-494.
- Zhang N, Fu JN and Chou TC (2016) Synergistic combination of microtubule targeting anticancer fludelson with cytoprotective panaxytriol derived from panax ginseng against MX-1 cells in vitro: experimental design and data analysis using the combination index method. *Am J Cancer Res* **6**:97-104.
- Zhang S, Guo N, Wan G, Zhang T, Li C, Wang Y, Wang Y and Liu Y (2019) pH and redox dual-responsive nanoparticles based on disulfide-containing poly(β -amino ester) for combining chemotherapy and COX-2 inhibitor to overcome drug resistance in breast cancer. *J Nanobiotechnol* **17**:109.
- Zheng J-T, Rix U, Zhao L, Mattingly C, Adams V, Chen Q, Rohr J and Yang K-Q (2005) Cytotoxic activities of new jadomycin derivatives. *J Antibiot* **58**:405-408.
- Zwelling LA, Hinds M, Chan D, Mayes J, Sie KL, Parker E, Silberman L, Radcliffe A, Beran M and Blick M (1989) Characterization of an amsacrine-resistant line of human leukemia cells. Evidence for a drug-resistant form of topoisomerase II. *J Biol Chem* **264**:16411-16420.

Appendix A: Copyright Permissions

A.1: License for Figure 1.1



This is a License Agreement between Mr. Brendan T. McKeown ("User") and Copyright Clearance Center, Inc. ("CCC") on behalf of the Rightsholder identified in the order details below. The license consists of the order details, the Marketplace Permissions General Terms and Conditions below, and any Rightsholder Terms and Conditions which are included below.
All payments must be made in full to CCC in accordance with the Marketplace Permissions General Terms and Conditions below.

Order Date	22-Jan-2024	Type of Use	Republish in a thesis/dissertation
Order License ID	1440464-1	Publisher	Elsevier Health Sciences
ISBN-13	9780702052309	Portion	Chart/graph/table/figure

LICENSED CONTENT

Publication Title	Gray's Anatomy : The Anatomical Basis of Clinical Practice	Country	United Kingdom of Great Britain and Northern Ireland
Author/Editor	Standingr, Susan	Rightsholder	Elsevier Science & Technology Journals
Date	09/25/2015	Publication Type	Book
Language	English		

REQUEST DETAILS

Portion Type	Chart/graph/table/figure	Distribution	Worldwide
Number of Charts / Graphs / Tables / Figures Requested	3	Translation	Original language of publication
Format (select all that apply)	Print, Electronic	Copies for the Disabled?	No
Who Will Republish the Content?	Academic institution	Minor Editing Privileges?	Yes
Duration of Use	Life of current edition	Incidental Promotional Use?	No
Lifetime Unit Quantity	Up to 499	Currency	CAD
Rights Requested	Main product		

NEW WORK DETAILS

Title	Jadomycin B Affects Cyclooxygenase-2 Related Signalling and Acts Synergistically with Celecoxib to Kill Human Breast Cancer Cells	Institution Name	Dalhousie University
Instructor Name	Dr. Kerry Goralski	Expected Presentation Date	2024-03-25

ADDITIONAL DETAILS

Order Reference Number	Figure 1.1 of new work	The Requesting Person / Organization to Appear on the License	Mr. Brendan T. McKeown
------------------------	------------------------	---	------------------------

REQUESTED CONTENT DETAILS

Title, Description or Numeric Reference of the Portion(s)	Figure 53.22, Figure 53.23A, Figure 53.23B, Figure 53.24	Title of the Article / Chapter the Portion Is From	Chapter 53: Chest wall and breast
Editor of Portion(s)	N/A	Author of Portion(s)	Standingr, Susan
Volume / Edition	41	Issue, if Republishing an Article From a Serial	N/A
Page or Page Range of Portion	946-948	Publication Date of Portion	2015-09-25

RIGHTSHOLDER TERMS AND CONDITIONS

Elsevier publishes Open Access articles in both its Open Access journals and via its Open Access articles option in subscription journals, for which an author selects a user license permitting certain types of reuse without permission. Before proceeding please check if the article is Open Access on <http://www.sciencedirect.com> and refer to the user license for the individual article. Any reuse not included in the user license terms will require permission. You must always fully and appropriately credit the author and source. If any part of the material to be used (for example, figures) has appeared in the Elsevier publication for which you are seeking permission, with credit or acknowledgement to another source it is the responsibility of the user to ensure their reuse complies with the terms and conditions determined by the rights holder. Please contact permissions@elsevier.com with any queries.

Marketplace Permissions General Terms and Conditions

The following terms and conditions ("General Terms"), together with any applicable Publisher Terms and Conditions, govern User's use of Works pursuant to the Licenses granted by Copyright Clearance Center, Inc. ("CCC") on behalf of the applicable Rightsholders of such Works through CCC's applicable Marketplace transactional licensing services (each, a "Service").

1) Definitions. For purposes of these General Terms, the following definitions apply:

"License" is the licensed use the User obtains via the Marketplace platform in a particular licensing transaction, as set forth in the Order Confirmation.

"Order Confirmation" is the confirmation CCC provides to the User at the conclusion of each Marketplace transaction. "Order Confirmation Terms" are additional terms set forth on specific Order Confirmations not set forth in the General Terms that can include terms applicable to a particular CCC transactional licensing service and/or any Rightsholder-specific terms.

"Rightsholder(s)" are the holders of copyright rights in the Works for which a User obtains licenses via the Marketplace platform, which are displayed on specific Order Confirmations.

"Terms" means the terms and conditions set forth in these General Terms and any additional Order Confirmation Terms collectively.

"User" or "you" is the person or entity making the use granted under the relevant License. Where the person accepting the Terms on behalf of a User is a freelancer or other third party who the User authorized to accept the General Terms on the User's behalf, such person shall be deemed jointly a User for purposes of such Terms.

"Work(s)" are the copyright protected works described in relevant Order Confirmations.

2) Description of Service. CCC's Marketplace enables Users to obtain Licenses to use one or more Works in accordance with all relevant Terms. CCC grants Licenses as an agent on behalf of the copyright rightsholder identified in the relevant Order Confirmation.

3) Applicability of Terms. The Terms govern User's use of Works in connection with the relevant License. In the event of any conflict between General Terms and Order Confirmation Terms, the latter shall govern. User acknowledges that Rightsholders have complete discretion whether to grant any permission, and whether to place any limitations on any grant, and that CCC has no right to supersede or to modify any such discretionary act by a Rightsholder.

4) Representations; Acceptance. By using the Service, User represents and warrants that User has been duly authorized by the User to accept, and hereby does accept, all Terms.

5) Scope of License; Limitations and Obligations. All Works and all rights therein, including copyright rights, remain the sole and exclusive property of the Rightsholder. The License provides only those rights expressly set forth in the terms and conveys no other rights in any Works

6) General Payment Terms. User may pay at time of checkout by credit card or choose to be invoiced. If the User chooses to be invoiced, the User shall: (i) remit payments in the manner identified on specific invoices, (ii) unless otherwise specifically stated in an Order Confirmation or separate written agreement, Users shall remit payments upon receipt of the relevant invoice from CCC, either by delivery or notification of availability of the invoice via the Marketplace platform, and (iii) if the User does not pay the invoice within 30 days of receipt, the User

A.2: License for Table 1.2

RightsLink - Your Account

2024-01-21, 11:41 PM

JOHN WILEY AND SONS LICENSE TERMS AND CONDITIONS

Jan 21, 2024

This Agreement between Mr. Brendan McKeown ("You") and John Wiley and Sons ("John Wiley and Sons") consists of your license details and the terms and conditions provided by John Wiley and Sons and Copyright Clearance Center.

License Number	5713961161980
License date	Jan 21, 2024
Licensed Content Publisher	John Wiley and Sons
Licensed Content Publication	CA: A Cancer Journal for Clinicians
Licensed Content Title	Breast Cancer Statistics, 2022
Licensed Content Author	Rebecca L. Siegel, Ahmedin Jemal, Adair Minihan, et al
Licensed Content Date	Oct 3, 2022
Licensed Content Volume	72
Licensed Content Issue	6
Licensed Content Pages	18
Type of Use	Dissertation/Thesis
Requestor type	University/Academic
Format	Print and electronic
Portion	Figure/table
Number of figures/tables	1
Will you be translating?	No
Title of new work	Jadomycin B Affects Cyclooxygenase-2 Related Signalling and Acts Synergistically with Celecoxib to Kill Human Breast Cancer Cells
Institution name	Dalhousie University
Expected presentation date	Mar 2024
Order reference number	Table 1.2 of new work
Portions	I would like to reproduce Table 2 from this original work, describing the age-specific 10-year probability of breast cancer diagnosis or death
Requestor Location	Mr. Brendan McKeown College of Pharmacy Dalhousie University 5968 College Street Halifax, NS B3H 4R2 Canada Attn: Mr. Brendan McKeown
Publisher Tax ID	EU826007151
Total	0.00 CAD
Terms and Conditions	

<https://s100.copyright.com/MyAccount/viewPrintableLicenseDetails?ref=8423616e-f428-4583-a2df-f50f74c44281>

Page 1 of 4

A.3: License for Tables 1.3 and 1.4

RightsLink - Your Account

2024-01-22, 12:20 AM

JOHN WILEY AND SONS LICENSE TERMS AND CONDITIONS

Jan 21, 2024

This Agreement between Mr. Brendan McKeown ("You") and John Wiley and Sons ("John Wiley and Sons") consists of your license details and the terms and conditions provided by John Wiley and Sons and Copyright Clearance Center.

License Number	5713980607109
License date	Jan 21, 2024
Licensed Content Publisher	John Wiley and Sons
Licensed Content Publication	Histopathology
Licensed Content Title	pathological prognostic factors in breast cancer. I. The value of histological grade in breast cancer: experience from a large study with long-term follow-up
Licensed Content Author	C.W. ELSTON, I.O. ELLIS
Licensed Content Date	Apr 3, 2007
Licensed Content Volume	19
Licensed Content Issue	5
Licensed Content Pages	8
Type of Use	Dissertation/Thesis
Requestor type	University/Academic
Format	Print and electronic
Portion	Figure/table
Number of figures/tables	2
Will you be translating?	No
Title of new work	Jadomycin B Affects Cyclooxygenase-2 Related Signalling and Acts Synergistically with Celecoxib to Kill Human Breast Cancer Cells
Institution name	Dalhousie University
Expected presentation date	Mar 2024
Order reference number	Tables 1.3 and 1.4 of new work
Portions	I would like to reproduce Table 1, describing the semiquantitative method for assessing histological grade, and adapt the portion of text at the bottom left of page 405 into a table describing the determination of histological grade based on score
Requestor Location	Mr. Brendan McKeown College of Pharmacy Dalhousie University 5968 College Street Halifax, NS B3H 4R2 Canada Attn: Mr. Brendan McKeown
Publisher Tax ID	EU826007151

<https://s100.copyright.com/MyAccount/viewPrintableLicenseDetails?ref=40734cbf-87ad-4c25-8c4d-dddc3aff1b73>

Page 1 of 4

A.4: License for Tables 1.5, 1.6, 1.7, and 1.8

RightsLink - Your Account

2024-01-22, 12:29 AM

JOHN WILEY AND SONS LICENSE TERMS AND CONDITIONS

Jan 21, 2024

This Agreement between Mr. Brendan McKeown ("You") and John Wiley and Sons ("John Wiley and Sons") consists of your license details and the terms and conditions provided by John Wiley and Sons and Copyright Clearance Center.

License Number	5713981113203
License date	Jan 21, 2024
Licensed Content Publisher	John Wiley and Sons
Licensed Content Publication	CA: A Cancer Journal for Clinicians
Licensed Content Title	Breast Cancer—Major changes in the American Joint Committee on Cancer eighth edition cancer staging manual
Licensed Content Author	Armando E. Giuliano, James L. Connolly, Stephen B. Edge, et al
Licensed Content Date	Mar 14, 2017
Licensed Content Volume	67
Licensed Content Issue	4
Licensed Content Pages	14
Type of Use	Dissertation/Thesis
Requestor type	University/Academic
Format	Print and electronic
Portion	Figure/table
Number of figures/tables	4
Will you be translating?	No
Title of new work	Jadomycin B Affects Cyclooxygenase-2 Related Signalling and Acts Synergistically with Celecoxib to Kill Human Breast Cancer Cells
Institution name	Dalhousie University
Expected presentation date	Mar 2024
Order reference number	Tables 1.5, 1.6, 1.7, and 1.8 of new work
Portions	I would like to reproduce Table 2 (Definition of primary tumor), Table 3 (Definition of regional lymph nodes), Table 4 (Definition of distant metastasis), and Table 5 (TNM anatomic stage groups) of this work
Requestor Location	Mr. Brendan McKeown College of Pharmacy Dalhousie University 5968 College Street Halifax, NS B3H 4R2 Canada Attn: Mr. Brendan McKeown
Publisher Tax ID	EU826007151

<https://s100.copyright.com/MyAccount/viewPrintableLicenseDetails?ref=beacce09-f8cc-4ffc-bded-d97d45dd51cf>

Page 1 of 4

A.5: License for Table 1.9

RightsLink - Your Account

2024-01-22, 12:47 AM

SPRINGER NATURE LICENSE TERMS AND CONDITIONS

Jan 21, 2024

This Agreement between Mr. Brendan McKeown ("You") and Springer Nature ("Springer Nature") consists of your license details and the terms and conditions provided by Springer Nature and Copyright Clearance Center.


License Number	5713990704324
License date	Jan 21, 2024
Licensed Content Publisher	Springer Nature
Licensed Content Publication	Breast Cancer Research
Licensed Content Title	Choosing the right cell line for breast cancer research
Licensed Content Author	Deborah L Holliday et al
Licensed Content Date	Aug 12, 2011
Type of Use	Thesis/Dissertation
Requestor type	academic/university or research institute
Format	print and electronic
Portion	figures/tables/illustrations
Number of figures/tables/illustrations	1
Will you be translating?	no
Circulation/distribution	1 - 29
Author of this Springer Nature content	no
Title of new work	Jadomycin B Affects Cyclooxygenase-2 Related Signalling and Acts Synergistically with Celecoxib to Kill Human Breast Cancer Cells
Institution name	Dalhousie University
Expected presentation date	Mar 2024
Order reference number	Table 1.9 of new work
Portions	I would like to reproduce Table 1 (Molecular classification of breast carcinoma) with alterations
Requestor Location	Mr. Brendan McKeown College of Pharmacy Dalhousie University 5968 College Street Halifax, NS B3H 4R2 Canada Attn: Mr. Brendan McKeown
Total	0.00 CAD
Terms and Conditions	


Springer Nature Customer Service Centre GmbH Terms and Conditions

<https://s100.copyright.com/MyAccount/viewPrintableLicenseDetails?ref=cac175d5-8feb-4a0f-b127-ce895f522747>

Page 1 of 5

Appendix A.6: Creative Commons Attribution for Figure 1.2

BM ⓘ 🔍



Selective estrogen receptor modulators (SERMs) and selective estrogen receptor degraders (SERDs) in cancer treatment

Author: Hitisha K. Patel, Teeru Bihani
Publication: Pharmacology & Therapeutics
Publisher: Elsevier
Date: June 2018

© 2018 The Authors. Published by Elsevier Inc.

Creative Commons Attribution-NonCommercial-No Derivatives License (CC BY NC ND)

This article is published under the terms of the [Creative Commons Attribution-NonCommercial-No Derivatives License \(CC BY NC ND\)](#). For non-commercial purposes you may copy and distribute the article, use portions or extracts from the article in other works, and text or data mine the article, provided you do not alter or modify the article without permission from Elsevier. You may also create adaptations of the article for your own personal use only, but not distribute these to others. You must give appropriate credit to the original work, together with a link to the formal publication through the relevant DOI, and a link to the Creative Commons user license above. If changes are permitted, you must indicate if any changes are made but not in any way that suggests the licensor endorses you or your use of the work.

Permission is not required for this non-commercial use. For commercial use please continue to request permission via RightsLink.

BACK

CLOSE WINDOW

© 2024 Copyright - All Rights Reserved | [Copyright Clearance Center, Inc.](#) | [Privacy statement](#) | [Data Security and Privacy](#) | [For California Residents](#) | [Terms and Conditions](#)
Comments? We would like to hear from you. E-mail us at customercare@copyright.com

Appendix A.7: Creative Commons License



CC BY-NC-ND 4.0 DEED

Attribution-NonCommercial-NoDerivs 4.0 International

Canonical URL : <https://creativecommons.org/licenses/by-nc-nd/4.0/>


[See the legal code](#)


You are free to:


Share — copy and redistribute the material in any medium or format

The licensor cannot revoke these freedoms as long as you follow the license terms.

Under the following terms:

 **Attribution** — You must give [appropriate credit](#), provide a link to the license, and [indicate if changes were made](#). You may do so in any reasonable manner, but not in any way that suggests the licensor endorses you or your use.

 **NonCommercial** — You may not use the material for [commercial purposes](#).

 **NoDerivatives** — If you [remix, transform, or build upon](#) the material, you may not distribute the modified material.


No additional restrictions — You may not apply legal terms or [technological measures](#) that legally restrict others from doing anything the license permits.

Notices:

You do not have to comply with the license for elements of the material in the public domain or where your use is permitted by an applicable [exception or limitation](#).

No warranties are given. The license may not give you all of the permissions necessary for your intended use. For example, other rights such as [publicity](#), [privacy](#), or [moral rights](#) may limit how you use the material.

Appendix A.8: Creative Commons Terms for Table 1.10



HOME | ABOUT | ARCHIVE | SUBMIT | SUBSCRIBE | ADVERTISE | AUTHOR INFO | CONTACT | HELP

Institution: DALHOUSIE UNIVERSITY Sign In via User Name/Password

Advanced Search

Permissions

1. Articles not designated as Open Access are distributed exclusively by Cold Spring Harbor Laboratory Press for the first six months after the full-issue publication date (see [Terms](#) for complete details). After six months, they are available under a Creative Commons License ([Attribution-NonCommercial 4.0 International License](#)).

Authors of these non-Open Access articles retain copyright in the articles but grant Cold Spring Harbor Laboratory Press exclusive publishing rights for six months following full-issue publication. This grant of rights includes the rights to publish, reproduce, distribute, display, and store the article in all formats; to translate the article into other languages; to create adaptations, summaries, extracts, or derivations of the article; and to license others to do any or all of the above.

2. Articles that carry the Open Access designation are immediately distributed under one of two Creative Commons Licenses: (i) [Creative Commons Attribution-NonCommercial 4.0 International License \(CC-BY-NC\)](#) or (ii) [Creative Commons Attribution 4.0 International License \(CC-BY\)](#). The CC-BY license permits commercial use, including reproduction, adaptation, and distribution of the article provided the original author and source are credited. *Please note specific licensing information within article of interest.*

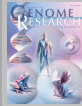
3. To request permission to reproduce/adapt artwork from *Genome Research* elsewhere (e.g., in other publications) during the first six months after full-issue publication, [click here](#).

4. Please contact [Copyright Clearance Center](#) to request permission to photocopy articles or for use in a coursepack during the first six months after full-issue publication.

5. To request permission for any other use, including for commercial purposes, [click here](#).

Current Issue

December 2023, 33 (12)



From the Cover

- Sperm chromatin organization and gene expression
- Long-read CAGE sequencing
- Vertebrate selfing
- Genetic privacy
- MBD4-associated germline hypermutation

Alert me to new issues of *Genome Research*

- [Advance Online Articles](#)
- [Submit a Manuscript](#)
- [Editorial Board](#)
- [Permissions](#)
- [E-mail Alerts & RSS Feeds](#)
- [Recommend to Your Library](#)
- [Job Opportunities](#)

AACR

Home | About | Archive | Submit | Subscribe | Advertise | Author Info | Contact | Help

Print ISSN: 1088-9051
Online ISSN: 1549-5469

Copyright © 2024 by Cold Spring Harbor Laboratory Press

Appendix A.9: License for Figure 1.6E

RightsLink - Your Account

2024-01-22, 1:17 AM

ELSEVIER LICENSE TERMS AND CONDITIONS

Jan 22, 2024

This Agreement between Mr. Brendan McKeown ("You") and Elsevier ("Elsevier") consists of your license details and the terms and conditions provided by Elsevier and Copyright Clearance Center.

License Number	5714000951821
License date	Jan 22, 2024
Licensed Content Publisher	Elsevier
Licensed Content Publication	Trends in Microbiology
Licensed Content Title	Streptomyces Exploration: Competition, Volatile Communication and New Bacterial Behaviours
Licensed Content Author	Stephanie E. Jones, Marie A. Elliot
Licensed Content Date	Jul 1, 2017
Licensed Content Volume	25
Licensed Content Issue	7
Licensed Content Pages	10
Start Page	522
End Page	531
Type of Use	reuse in a thesis/dissertation
Portion	figures/tables/illustrations
Number of figures/tables/illustrations	1
Format	both print and electronic
Are you the author of this Elsevier article?	No
Will you be translating?	No
Title of new work	Jadomycin B Affects Cyclooxygenase-2 Related Signalling and Acts Synergistically with Celecoxib to Kill Human Breast Cancer Cells
Institution name	Dalhousie University
Expected presentation date	Mar 2024
Order reference number	Figure 1.6E of new work
Portions	I would like to reproduce Figure 1A, depicting The Classic Streptomyces Life Cycle, from this original work
Requestor Location	Mr. Brendan McKeown College of Pharmacy Dalhousie University 5968 College Street Halifax, NS B3H 4R2 Canada

<https://s100.copyright.com/MyAccount/viewPrintableLicenseDetails?ref=6ef36bb5-5c94-4c64-a5b9-8f50a6b08edf>

Page 1 of 5

Appendix A.10: License Agreement for Tables 1.11, 1.12 and Figure 1.8

RightsLink - Your Account

2024-01-25, 3:56 PM

JOHN WILEY AND SONS LICENSE TERMS AND CONDITIONS

Jan 25, 2024

This Agreement between Mr. Brendan McKeown ("You") and John Wiley and Sons ("John Wiley and Sons") consists of your license details and the terms and conditions provided by John Wiley and Sons and Copyright Clearance Center.

License Number	5716061453725
License date	Jan 25, 2024
Licensed Content Publisher	John Wiley and Sons
Licensed Content Publication	Pharmacology Research & Perspectives
Licensed Content Title	Jadomycins: A potential chemotherapy for multi-drug resistant metastatic breast cancer
Licensed Content Author	Kerry B. Goralski, Brendan T. McKeown, Esther P. Bonitto
Licensed Content Date	Oct 27, 2021
Licensed Content Volume	9
Licensed Content Issue	6
Licensed Content Pages	15
Type of Use	Dissertation/Thesis
Requestor type	Author of this Wiley article
Format	Print and electronic
Portion	Figure/table
Number of figures/tables	2
Will you be translating?	No
Title of new work	Jadomycin B Affects Cyclooxygenase-2 Related Signalling and Acts Synergistically with Celecoxib to Kill Human Breast Cancer Cells
Institution name	Dalhousie University
Expected presentation date	Mar 2024
Order reference number	Tables 1.11 and 1.12, and Figure 1.8 in new work
Portions	I would like to adapt Table 2 to include updated information in the IC50 values of all published studies on jadomycin cytotoxicity in cancer cells, and adapt Figure 5 to summarize the previously proposed mechanisms of action of jadomycins in breast cancer
Requestor Location	Mr. Brendan McKeown College of Pharmacy Dalhousie University 5968 College Street Halifax, NS B3H 4R2 Canada Attn: Mr. Brendan McKeown
Publisher Tax ID	EU826007151
Total	0.00 CAD

<https://s100.copyright.com/MyAccount/viewPrintableLicenseDetails?ref=dab8ce46-b4a8-4064-8712-0c1288ef8e2e>

Page 1 of 4

Appendix A.11: License Agreement for Figure 1.9

RightsLink - Your Account

2024-01-22, 1:02 AM

SPRINGER NATURE LICENSE TERMS AND CONDITIONS

Jan 22, 2024

This Agreement between Mr. Brendan McKeown ("You") and Springer Nature ("Springer Nature") consists of your license details and the terms and conditions provided by Springer Nature and Copyright Clearance Center.

License Number	5714000068532
License date	Jan 22, 2024
Licensed Content Publisher	Springer Nature
Licensed Content Publication	Nature Reviews Molecular Cell Biology
Licensed Content Title	Human topoisomerases and their roles in genome stability and organization
Licensed Content Author	Yves Pommier et al
Licensed Content Date	Feb 28, 2022
Type of Use	Thesis/Dissertation
Requestor type	academic/university or research institute
Format	print and electronic
Portion	figures/tables/illustrations
Number of figures/tables/illustrations	1
Would you like a high resolution image with your order?	no
Will you be translating?	no
Circulation/distribution	1 - 29
Author of this Springer Nature content	no
Title of new work	Jadomycin B Affects Cyclooxygenase-2 Related Signalling and Acts Synergistically with Celecoxib to Kill Human Breast Cancer Cells
Institution name	Dalhousie University
Expected presentation date	Mar 2024
Order reference number	Figure 1.9 of new work
Portions	I would like to reproduce Figure 1 from this original work, depicting topological problems solved by human topoisomerases
Requestor Location	Mr. Brendan McKeown College of Pharmacy Dalhousie University 5968 College Street Halifax, NS B3H 4R2 Canada Attn: Mr. Brendan McKeown

<https://s100.copyright.com/MyAccount/viewPrintableLicenseDetails?ref=52357fcb-0cfb-44cd-927a-43beb58ac276>

Page 1 of 5

Appendix A.12: License Agreement for Figure 1.10



This is a License Agreement between Brendan T. McKeown ("User") and Copyright Clearance Center, Inc. ("CCC") on behalf of the Rightsholder identified in the order details below. The license consists of the order details, the Marketplace Permissions General Terms and Conditions below, and any Rightsholder Terms and Conditions which are included below. All payments must be made in full to CCC in accordance with the Marketplace Permissions General Terms and Conditions below.

Order Date	25-Jan-2024	Type of Use	Republish in a thesis/dissertation
Order License ID	1442272-1	Publisher	Pioneer Bioscience Publishing Company
ISSN	2218-676X	Portion	Chart/graph/table/figure

LICENSED CONTENT

Publication Title	Translational cancer research	Country	China
Date	01/01/2012	Rightsholder	Nancy International Ltd Subsidiary AME Publishing Company
Language	English	Publication Type	Journal

REQUEST DETAILS

Portion Type	Chart/graph/table/figure	Distribution	Worldwide
Number of Charts / Graphs / Tables / Figures Requested	1	Translation	Original language of publication
Format (select all that apply)	Print, Electronic	Copies for the Disabled?	No
Who Will Republish the Content?	Academic institution	Minor Editing Privileges?	No
Duration of Use	Current edition and up to 5 years	Incidental Promotional Use?	No
Lifetime Unit Quantity	Up to 499	Currency	CAD
Rights Requested	Main product		

NEW WORK DETAILS

Title	Jadomycin B Affects Cyclooxygenase-2 Related Signalling and Acts Synergistically with Celecoxib to Kill Human Breast Cancer Cells	Institution Name	Dalhousie University
Instructor Name	Dr. Kerry Goralski	Expected Presentation Date	2024-03-25

ADDITIONAL DETAILS

Order Reference Number	Figure 1.10 in new work	The Requesting Person / Organization to Appear on the License	Brendan T. McKeown
------------------------	-------------------------	---	--------------------

REQUESTED CONTENT DETAILS

Title, Description or Numeric Reference of the Portion(s)	Figure 1: Summary schematic of TOP2-mediated DNA cleavage and re-ligation and of the formation of DNA double-strand breaks caused by TOP2 poisons.	Title of the Article / Chapter the Portion is From	ZATT, TDP2, and SUMO2: breaking the tie that binds TOP2 to DNA
Editor of Portion(s)	N/A	Author of Portion(s)	Steven R. Hall and Kerry Brennan Goralski
Volume / Edition	7	Issue, if Republishing an Article From a Serial	Supplement 4
Page or Page Range of Portion	S440	Publication Date of Portion	2018-02-02

RIGHTSHOLDER TERMS AND CONDITIONS

It is the responsibility of the users' to identify the copyright holder of any materials. If the user has any doubts, please contact the publisher at permissions@amegroups.com. For illustrations owned by Ms. Croce, please contact beth@bioperspective.com.

Marketplace Permissions General Terms and Conditions

The following terms and conditions ("General Terms"), together with any applicable Publisher Terms and Conditions, govern User's use of Works pursuant to the Licenses granted by Copyright Clearance Center, Inc. ("CCC") on behalf of the applicable Rightsholders of such Works through CCC's applicable Marketplace transactional licensing services (each, a "Service").

1) **Definitions.** For purposes of these General Terms, the following definitions apply:

"License" is the licensed use the User obtains via the Marketplace platform in a particular licensing transaction, as set forth in the Order Confirmation.

"Order Confirmation" is the confirmation CCC provides to the User at the conclusion of each Marketplace transaction. "Order Confirmation Terms" are additional terms set forth on specific Order Confirmations not set forth in the General Terms that can include terms applicable to a particular CCC transactional licensing service and/or any Rightsholder-specific terms.

"Rightsholder(s)" are the holders of copyright rights in the Works for which a User obtains licenses via the Marketplace platform, which are displayed on specific Order Confirmations.

"Terms" means the terms and conditions set forth in these General Terms and any additional Order Confirmation Terms collectively.

"User" or "you" is the person or entity making the use granted under the relevant License. Where the person accepting the Terms on behalf of a User is a freelancer or other third party who the User authorized to accept the General Terms on the User's behalf, such person shall be deemed jointly a User for purposes of such Terms.

"Work(s)" are the copyright protected works described in relevant Order Confirmations.

2) **Description of Service.** CCC's Marketplace enables Users to obtain Licenses to use one or more Works in accordance with all relevant Terms. CCC grants Licenses as an agent on behalf of the copyright rightsholder identified in the relevant Order Confirmation.

3) **Applicability of Terms.** The Terms govern User's use of Works in connection with the relevant License. In the event of any conflict between General Terms and Order Confirmation Terms, the latter shall govern. User acknowledges that Rightsholders have complete discretion whether to grant any permission, and whether to place any limitations on any grant, and that CCC has no right to supersede or to modify any such discretionary act by a Rightsholder.

4) **Representations; Acceptance.** By using the Service, User represents and warrants that User has been duly authorized by the User to accept, and hereby does accept, all Terms.

5) **Scope of License; Limitations and Obligations.** All Works and all rights therein, including copyright rights, remain the sole and exclusive property of the Rightsholder. The License provides only those rights expressly set forth in the terms and conveys no other rights in any Works

6) **General Payment Terms.** User may pay at time of checkout by credit card or choose to be invoiced. If the User chooses to be invoiced, the User shall: (i) remit payments in the manner

Appendix A.13: License for Figure 4.18

RightsLink - Your Account

2024-01-25, 10:24 PM

SPRINGER NATURE LICENSE TERMS AND CONDITIONS

Jan 25, 2024

This Agreement between Mr. Brendan McKeown ("You") and Springer Nature ("Springer Nature") consists of your license details and the terms and conditions provided by Springer Nature and Copyright Clearance Center.

License Number	5716220545454
License date	Jan 25, 2024
Licensed Content Publisher	Springer Nature
Licensed Content Publication	Indian Journal of Clinical Biochemistry
Licensed Content Title	Plasma Fatty Acid Composition and Estimated Desaturase Activities Reflect Dietary Patterns in Subjects with Metabolic Syndrome
Licensed Content Author	N. Pavithra et al
Licensed Content Date	Jul 22, 2017
Type of Use	Thesis/Dissertation
Requestor type	academic/university or research institute
Format	print and electronic
Portion	figures/tables/illustrations
Number of figures/tables/illustrations	1
Will you be translating?	no
Circulation/distribution	1 - 29
Author of this Springer Nature content	no
Title of new work	Jadomycin B Affects Cyclooxygenase-2 Related Signalling and Acts Synergistically with Celecoxib to Kill Human Breast Cancer Cells
Institution name	Dalhousie University
Expected presentation date	Mar 2024
Order reference number	Figure 4.18 of new work
Portions	Figure 1 depicting the desaturation/chain elongation involved in biosynthesis of n-6 and n-3 fatty acids.
Requestor Location	Mr. Brendan McKeown College of Pharmacy Dalhousie University 5968 College Street Halifax, NS B3H 4R2 Canada Attn: Mr. Brendan McKeown
Total	0.00 CAD

<https://s100.copyright.com/MyAccount/viewPrintableLicenseDetails?ref=ba790e83-d36f-4faf-91ef-44abf8d59a4e>

Page 1 of 5

Appendix B:Supplementary Figures

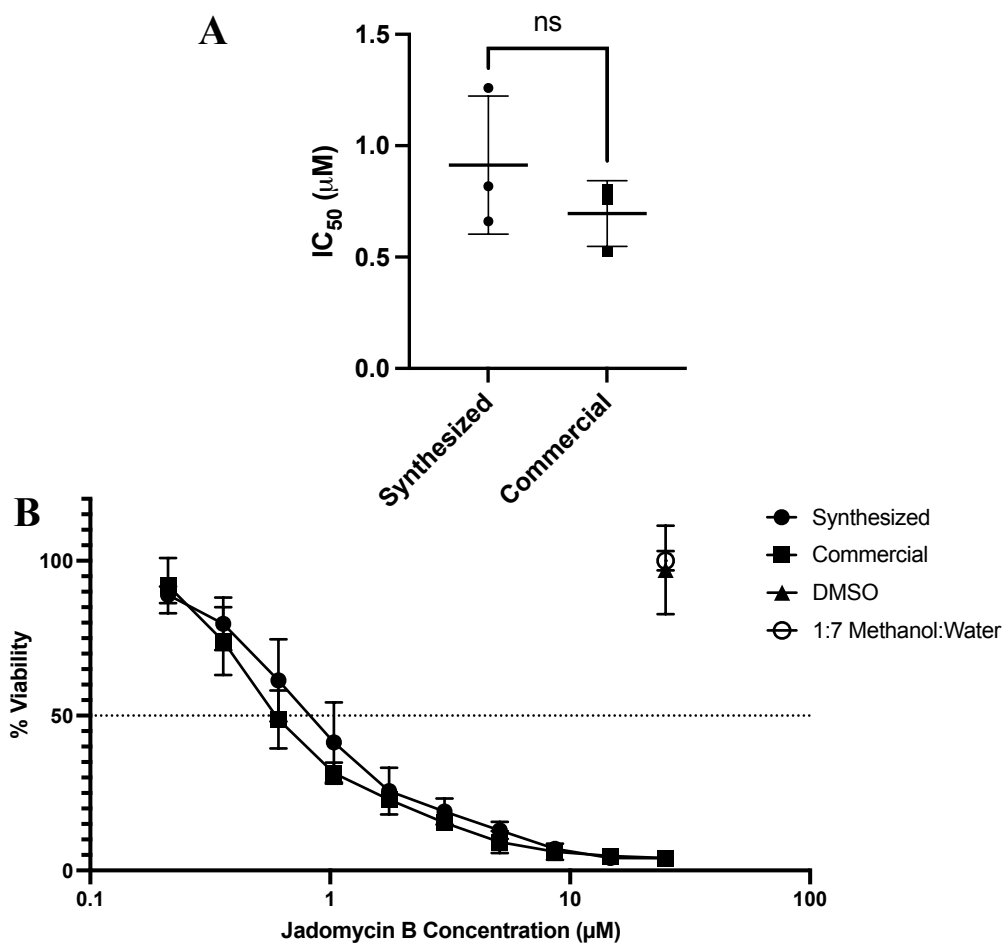


Figure B.1: Graphical Representation of IC₅₀ Values Reported in Table 4.1

231-CON cells were exposed to jadomycin B. (0.21-25 μM) for 72 h. Calculated IC₅₀ values (A) for jadomycin B synthesized by our research group or purchased commercially are not significantly different (unpaired t-test, P=0.34, n=3). IC₅₀s were calculated using (B) dose response curves generated from datapoints representing the mean value of triplicate assays, each consisting of a mean of quadruplicate technical replicates and expressed as % viability of untreated controls. Vehicle control for commercial (DMSO) and synthesized (1:7 methanol:water) are included at concentrations equivalent to those present in 25 μM jadomycin B samples. Error bars are mean ± standard deviation.

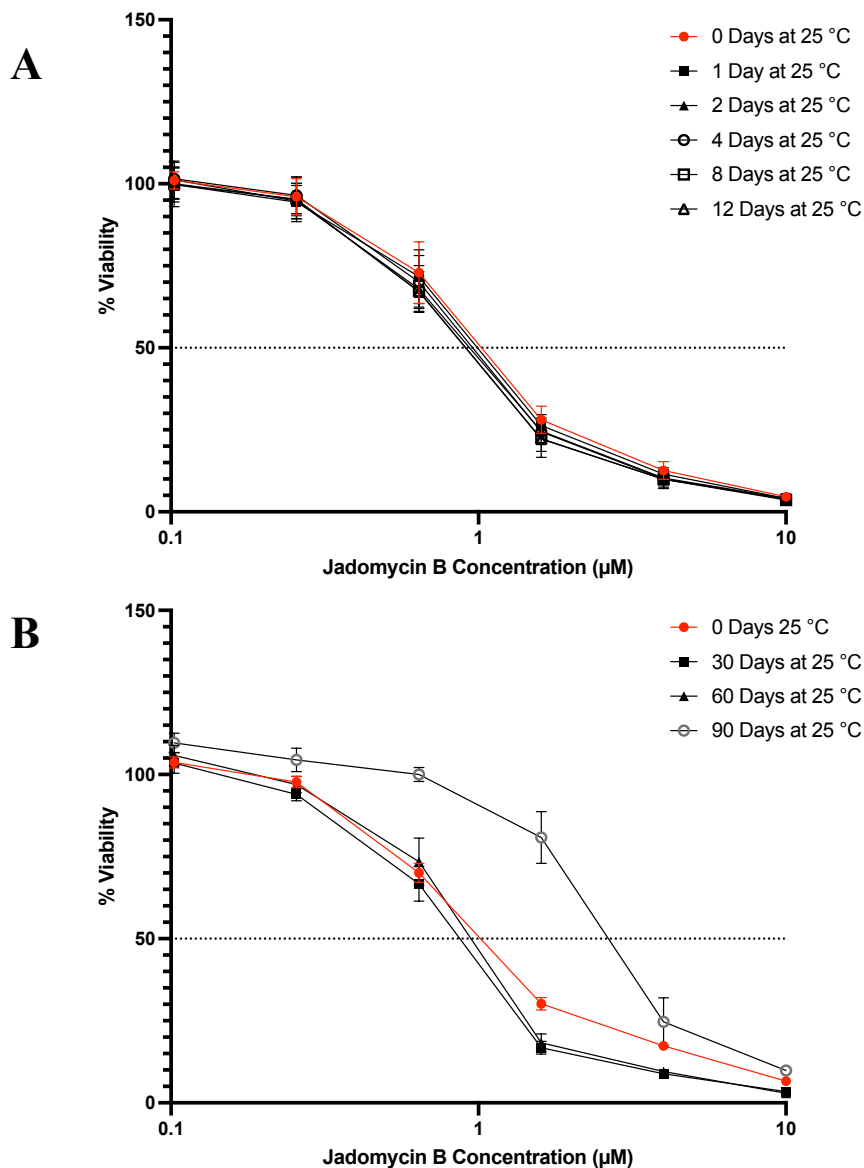


Figure B.2: Dose Response Curves for Jadomycin B Aged at 25 °C

Dose response curves for 231-CON cells exposed to jadomycin B (0.1-4.0 μM) for 72 h. Comparisons were made between groups consisting of jadomycin B exposure following aging for (A) 0, 1, 2, 4, 8, and 12 days or (B) 0, 30, 60, or 90 days at 25 °C (with unaged jadomycin B highlighted in red). IC_{50}s in **Figure 4.1** were calculated using dose response curves generated from datapoints representing the mean value of quadruplicate assays, each consisting of a mean of quadruplicate technical replicates and expressed as % viability of untreated controls. Error bars are mean \pm standard deviation.

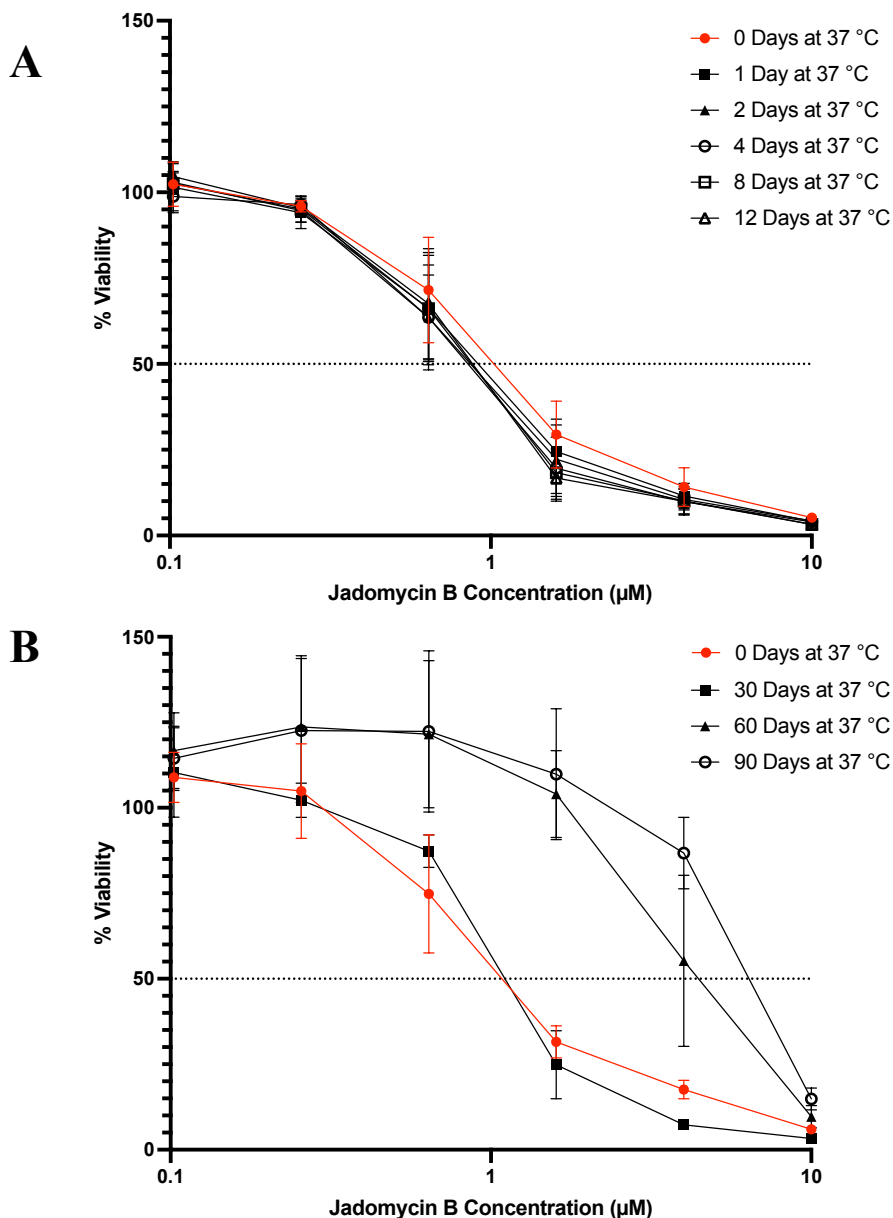


Figure B.3: Dose Response Curves for Jadomycin B Aged at 37 °C

Dose response curves for 231-CON cells exposed to jadomycin B (0.1-4.0 μM) for 72 h. Comparisons were made between groups consisting of jadomycin B exposure following aging for (A) 0, 1, 2, 4, 8, and 12 days or (B) 0, 30, 60, or 90 days at 37 °C (with unaged jadomycin B highlighted in red). IC_{50} s in **Figure 4.1** were calculated using dose response curves generated from datapoints representing the mean value of quadruplicate assays, each consisting of a mean of quadruplicate technical replicates and expressed as % viability of untreated controls. Error bars are mean \pm standard deviation.

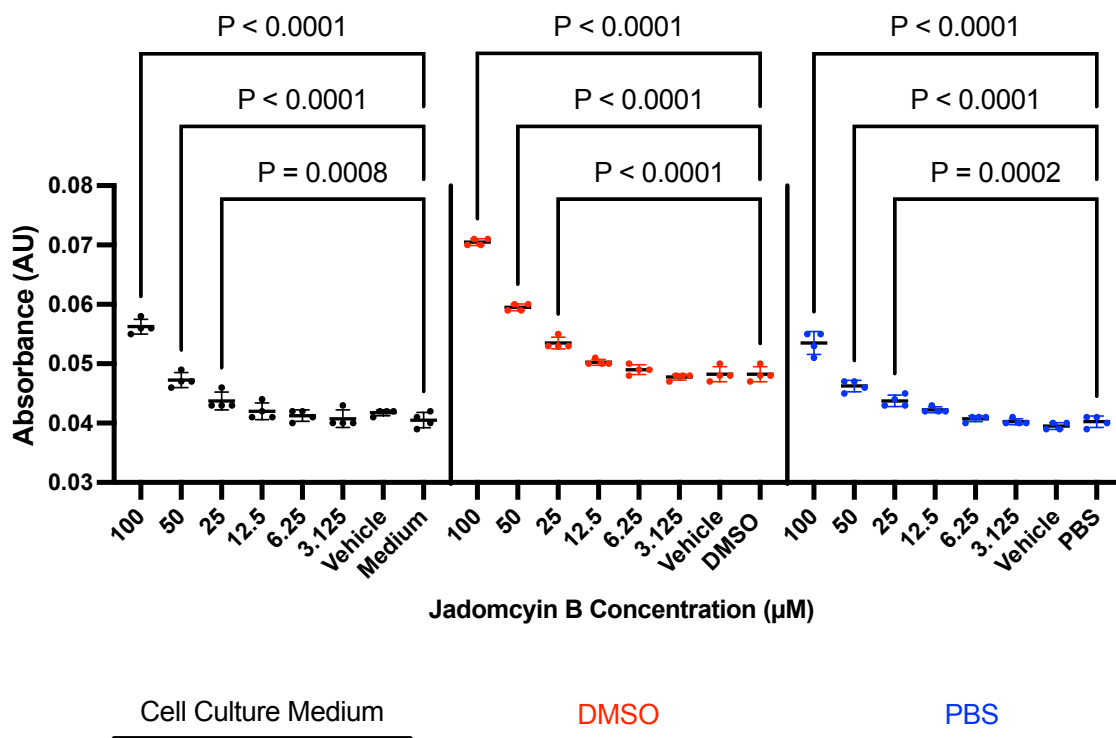


Figure B.4: Jadomycin B Absorbance at 550 nm

Absorbance measured in absorbance units (AU) of jadomycin B at 550 nm across a range of biologically relevant concentrations (3.125-100 µM). Absorbance was measured for jadomycin B dissolved in DMSO and diluted in cell culture medium (black), DMSO (red), or phosphate buffered saline (blue). Each datapoint represents the mean value of quadruplicate measurements. Significant difference from diluent alone is indicated by reported p-value ($P \leq 0.05$) as determined by two-way ANOVA, followed by Bonferroni's multiple comparison test. Error bars are mean \pm standard deviation.

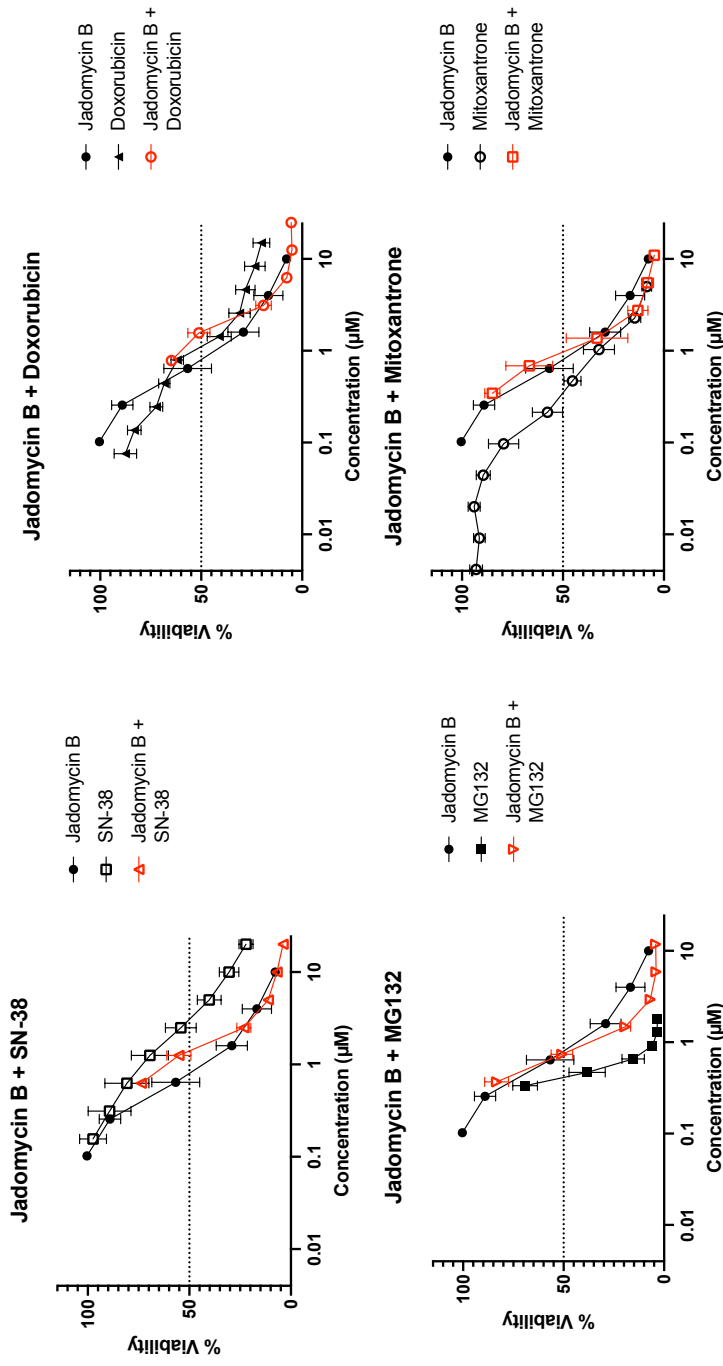


Figure B.5: Dose Response Curves for Combination Index Calculations Involving Jadomycin B

Dose response curves for 231-CON cells exposed to combinations of jadomycin B with doxorubicin, mitoxantrone, SN-38, or MG132 for 48 h (single agents in black, with combination in red). Values were entered into CompuSyn Software to generate data reported in **Table 4.2** based on calculations described in **section 1.7.4.2**. Representative dose response curves were generated from datapoints representing the mean value of at least quadruplicate assays, each consisting of a mean of quadruplicate technical replicates and expressed as % viability of untreated controls. Error bars are mean \pm standard deviation.

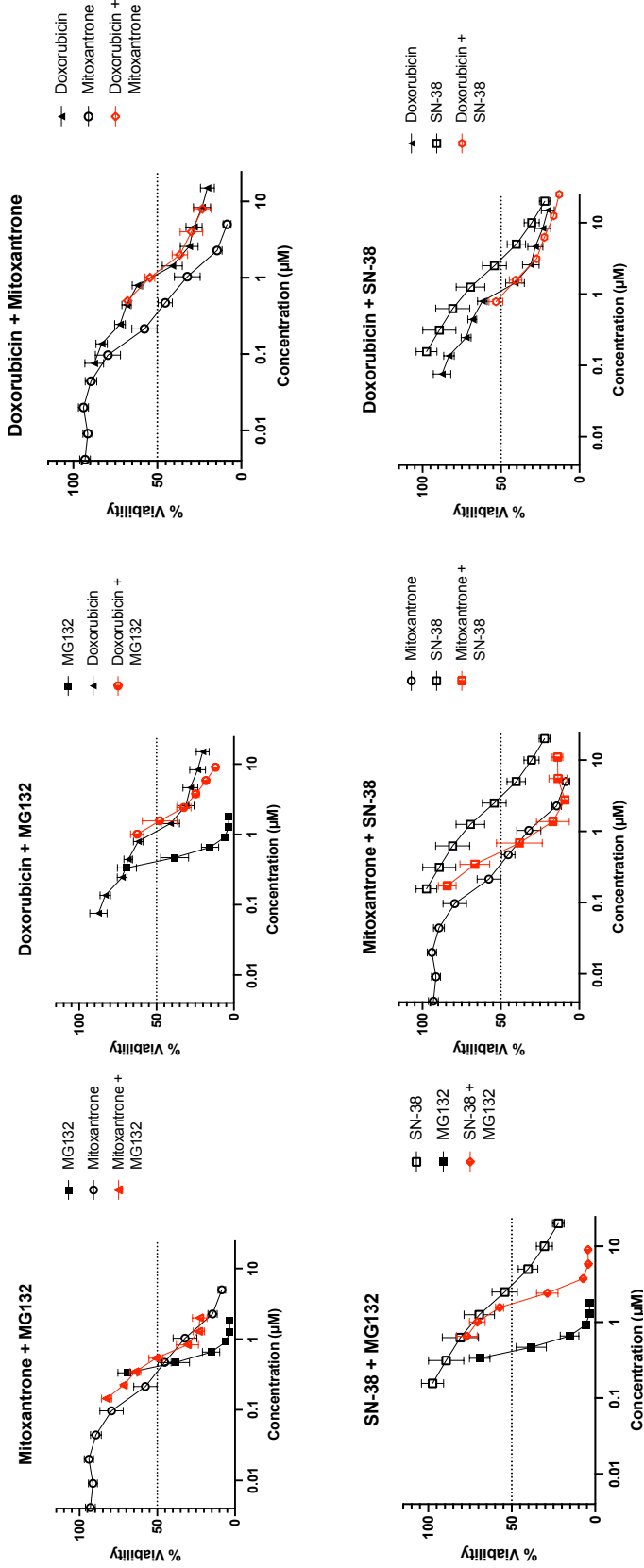
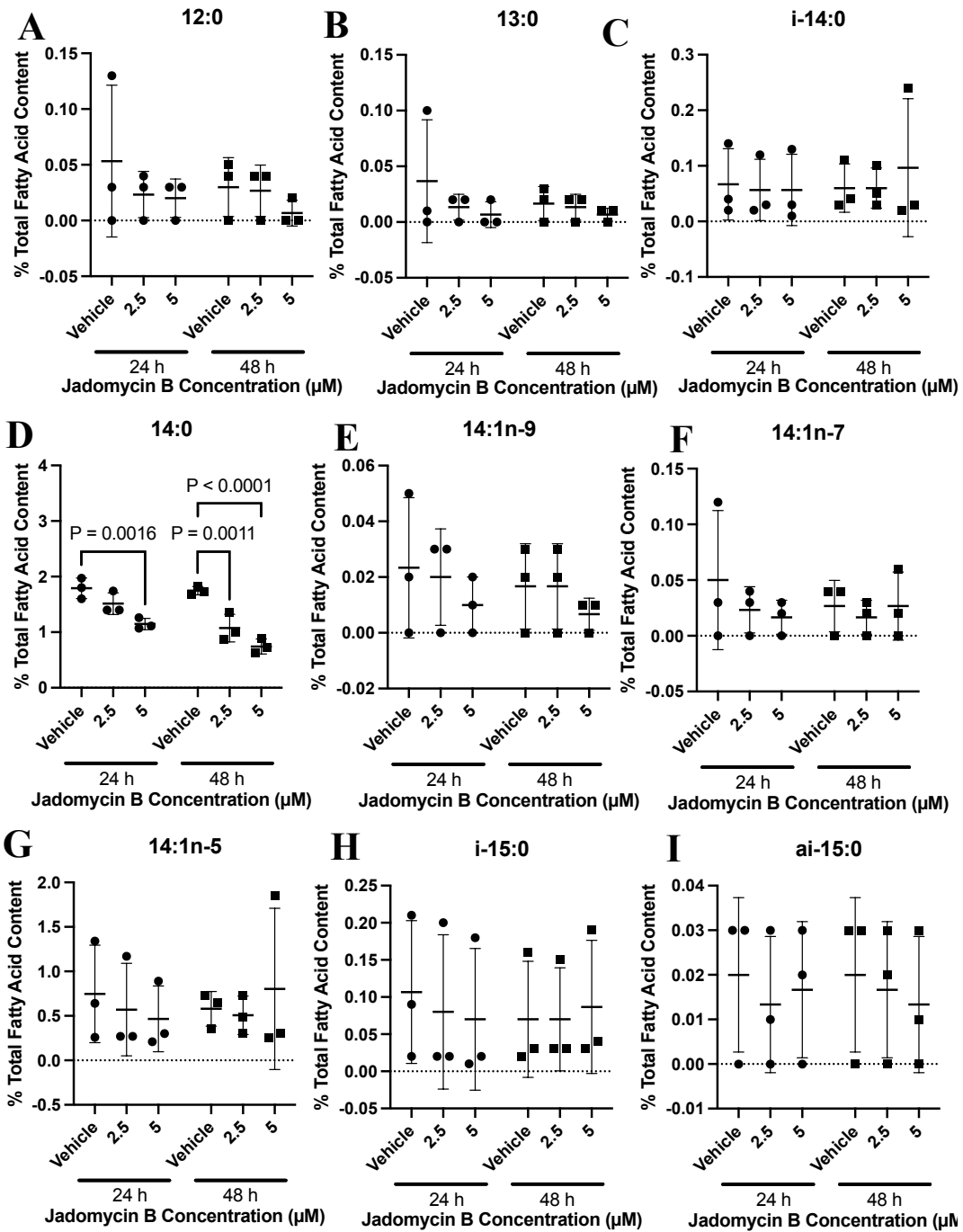
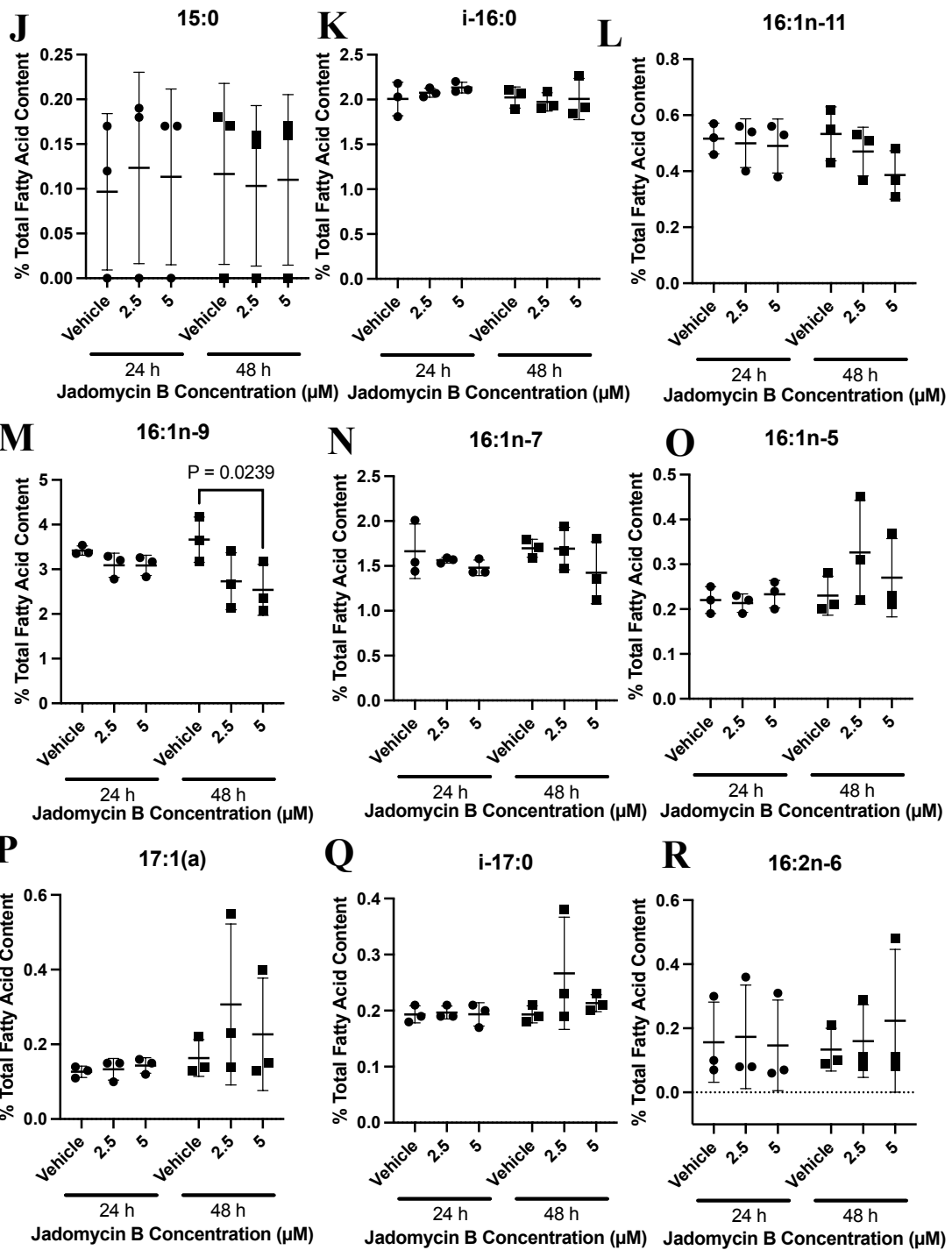
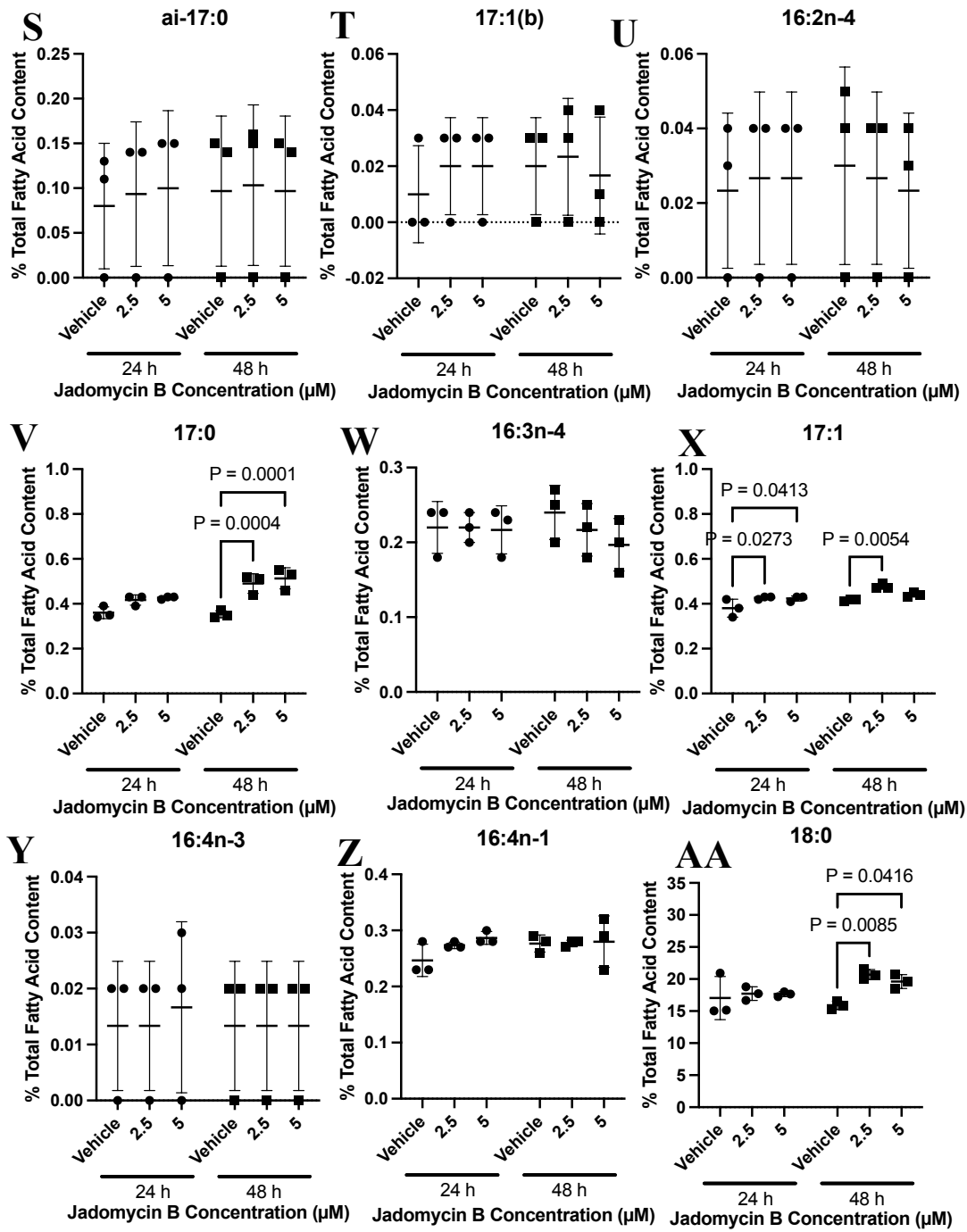


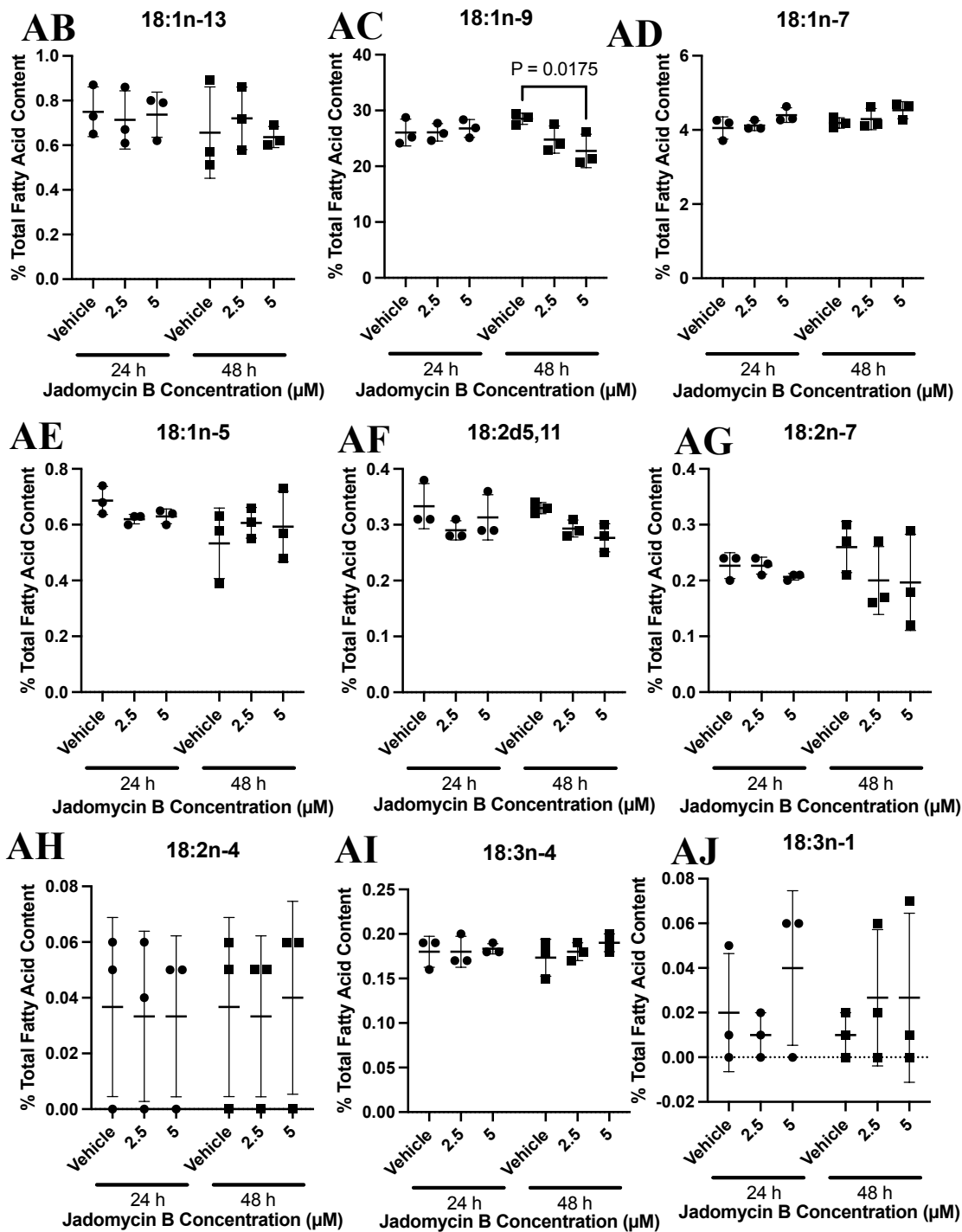
Figure B.6: Dose Response Curves for All Other Combination Index Calculations

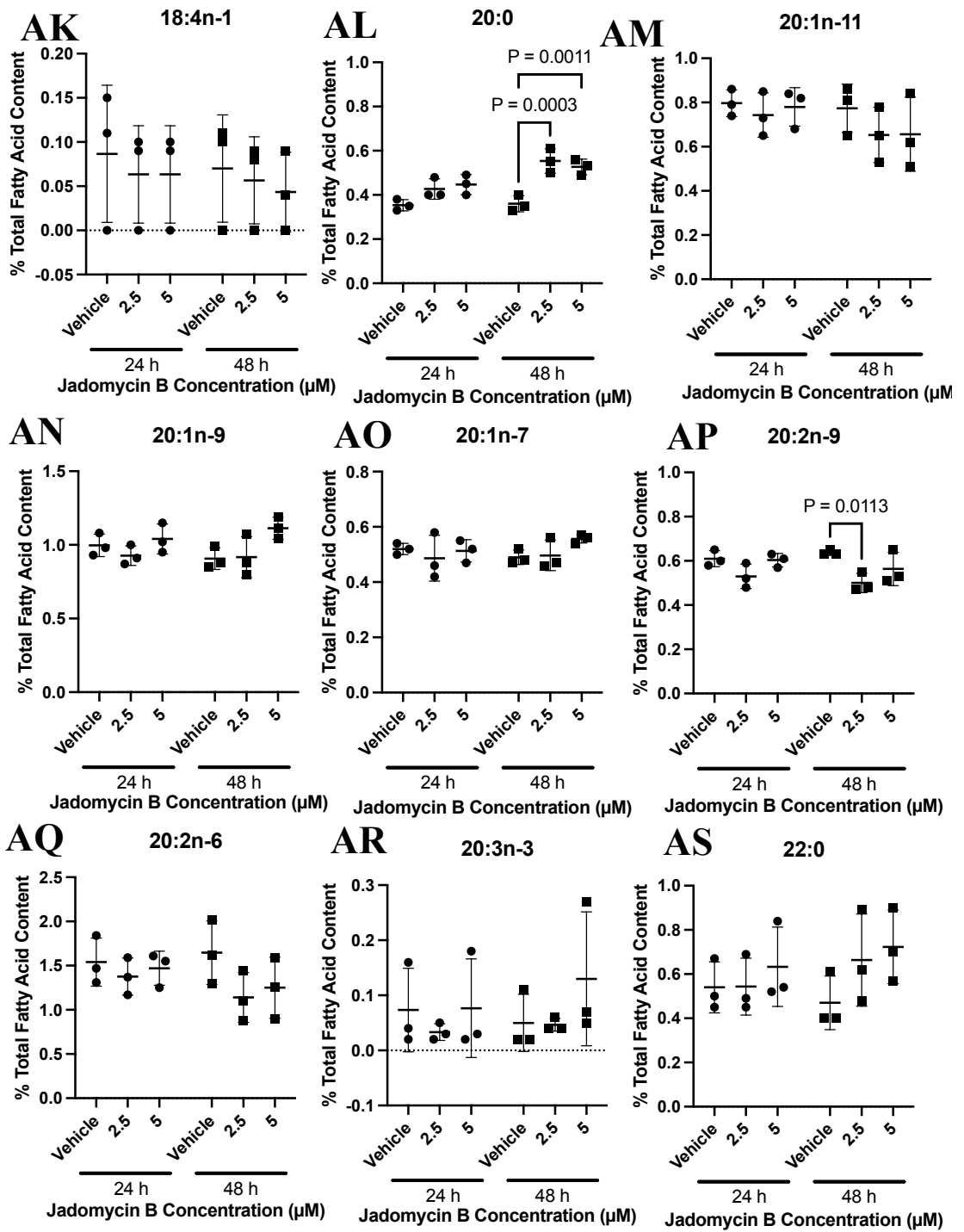
Dose response curves for 231-CON cells exposed to combinations of doxorubicin, mitoxantrone, SN-38, and MG132 for 48 h (single agents in black, with combination in red). Values were entered into CompuSyn Software to generate data reported in **Table 4.2** based on calculations described in **section 1.7.4.2**. Representative dose response curves were generated from











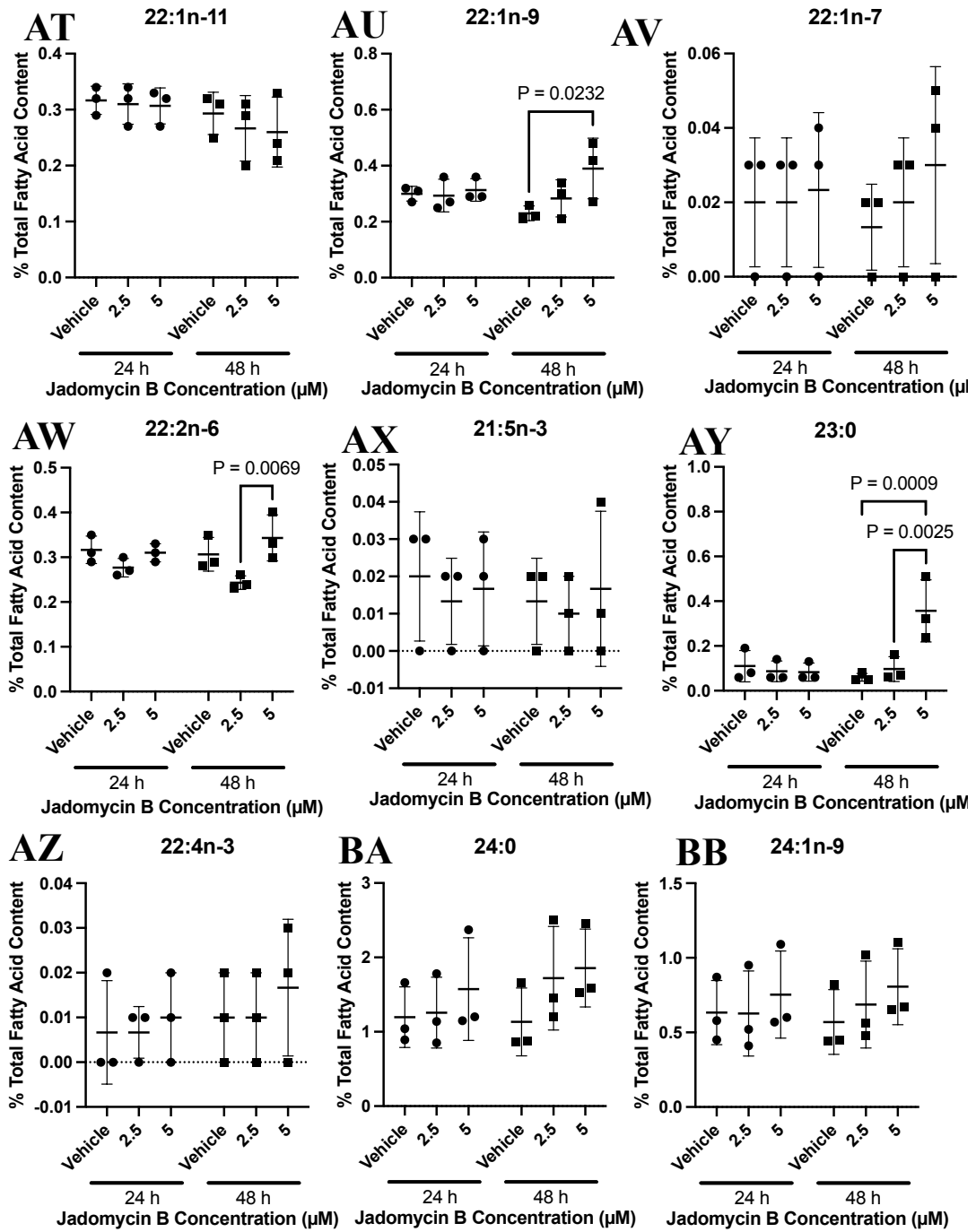


Figure B.7: Changes in Other Cellular Levels of Fatty Acids Following Exposure to Jadomycin B

Levels of other fatty acids in 231-CON cells treated with jadomycin B (2.5 or 5 μ M) for 24 or 48 h as measured by GCFID. In addition to those fatty acids analyzed in **Figures 4.21, 4.22, and 4.23**, the following fatty acids were also detected: **(A)** 12:0, **(B)** 13:0, **(C)** i-14:0, **(D)** 14:0, **(E)** 14:1n-9, **(F)** 14:1n-7, **(G)** 14:1n-5, **(H)** i-15:0, **(I)** ai-15:0, **(J)** 15:0, **(K)** i-16:0, **(L)** 16:1n-11, **(M)** 16:1n-9, **(N)** 16:1n-7, **(O)** 16:1n-5, **(P)** 17:1(a), **(Q)** i-17:0, **(R)** 16:2n-6, **(S)** ai-17:0, **(T)** 17:1(b), **(U)** 16:2n-4, **(V)** 17:0, **(W)** 16:3n-4, **(X)** 17:1, **(Y)** 16:4n-3, **(Z)** 16:4n-1, **(AA)** 18:0, **(AB)** 18:1n-13, **(AC)** 18:1n-9, **(AD)** 18:1n-7, **(AE)** 18:1n-5, **(AF)** 18:2d5,11, **(AG)** 18:2n-7, **(AH)** 18:2n-4, **(AI)** 18:3n-4, **(AJ)** 18:3n-1, **(AK)** 18:4n-1, **(AL)** 20:0, **(AM)** 20:1n-11, **(AN)** 20:1n-9, **(AO)** 20:1n-7, **(AP)** 20:2n-9, **(AQ)** 20:2n-6, **(AR)** 20:3n-3, **(AS)** 22:0, **(AT)** 22:1n-11, **(AU)** 22:1n-9, **(AV)** 22:1n-7, **(AW)** 22:2n-6, **(AX)** 21:5n-3, **(AY)** 23:0, **(AZ)** 22:4n-3, **(BA)** 24:0, and **(BB)** 24:1n-9.

Datapoints represent the mean value of triplicate assays, expressed as percent of total cellular fatty acid content and compared to vehicle (DMSO) treated cells. Significant difference is indicated by reported p-value ($P \leq 0.05$) as determined by two-way ANOVA, followed by Bonferroni's multiple comparison test. Error bars are mean \pm standard deviation. (Figures on previous pages)

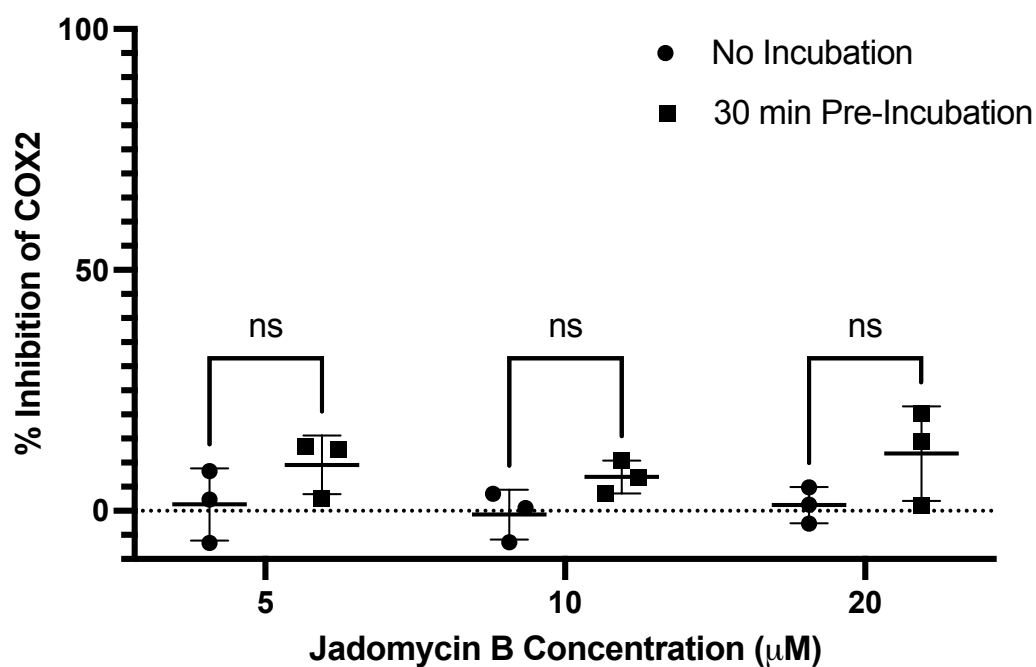


Figure B.8: Pre-Incubation of Jadomycin B with COX2 Does Not Affect Enzyme Inhibition

Percent inhibition of purified COX2 enzyme activity in the presence of jadomycin B (5-20 µM) added simultaneously with enzyme substrate (arachidonic acid) or 30 minutes prior to substrate introduction. Datapoints represent the mean value of triplicate assays. No significant difference between the conditions was observed, as determined by two-way ANOVA followed by Bonferroni's multiple comparison test. Error bars are mean ± standard deviation.

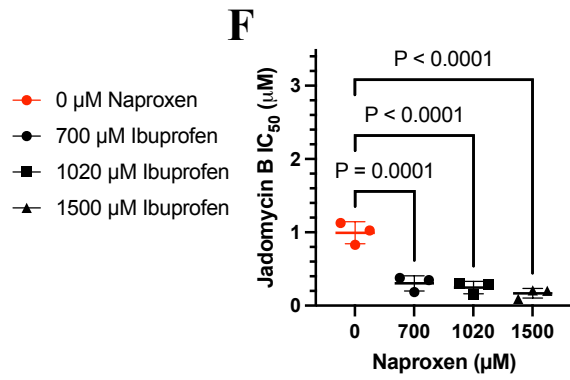
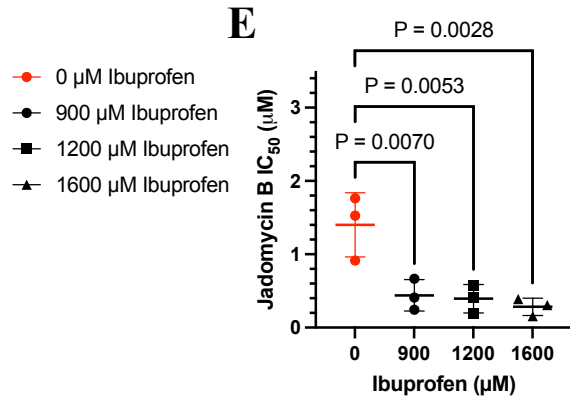
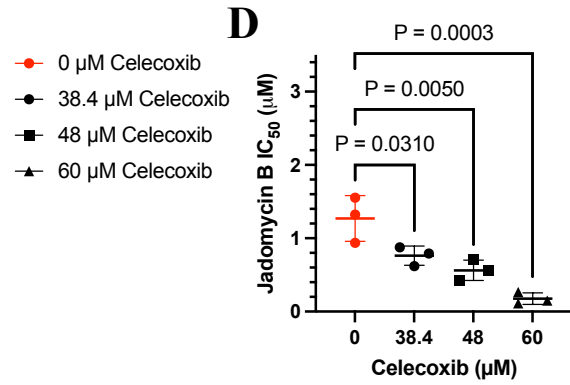
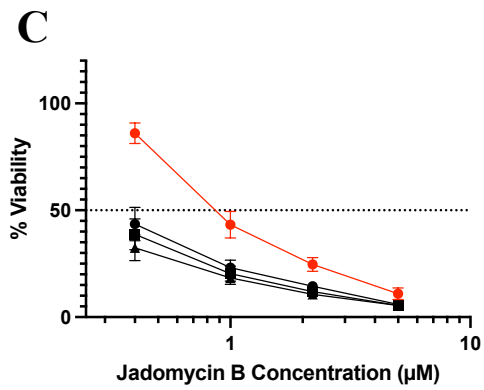
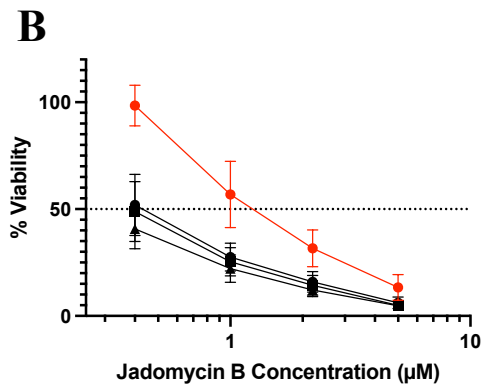
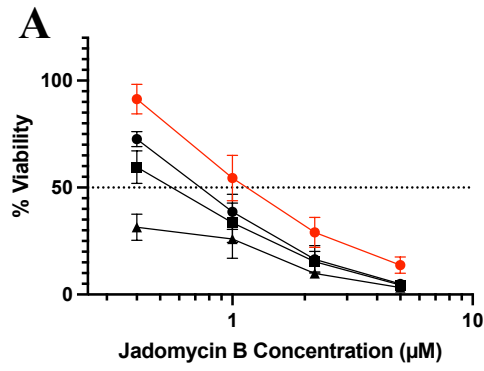


Figure B.9: Synergistic Activity of Jadomycins with Celecoxib, Naproxen, and Ibuprofen in 231-CON cells

Dose response curves and calculated IC₅₀ values, respectively, for combinations of jadomycin B (0-5 μM) and (A, D) celecoxib (0-60 μM), (B, E) ibuprofen (0-1600 μM), and (C, F) naproxen (0-1500 μM) in 231-CON cells used to determine synergy as presented in **Figure 4.29** and **Tables C.13, C.14, and C.15**. Each datapoint represents the mean value of triplicate assays, each consisting of quadruplicate technical replicates ± standard deviation. For IC₅₀ values, significant difference from jadomycin B alone (highlighted in red) is indicated by reported p-value ($P \leq 0.05$) as determined by two-way ANOVA followed by Bonferroni's multiple comparison test. (Figures on previous page)

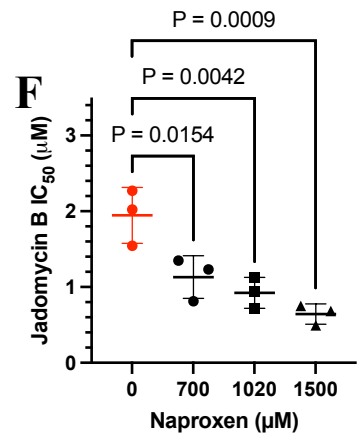
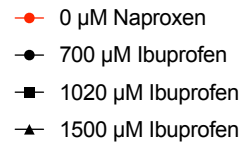
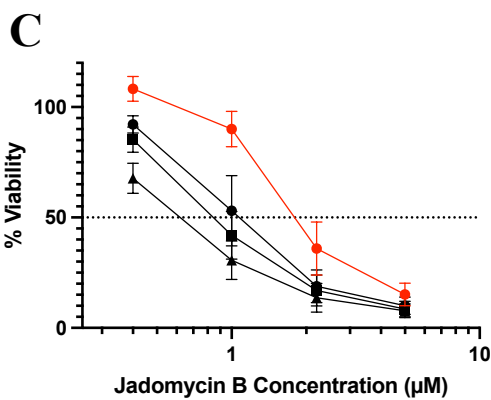
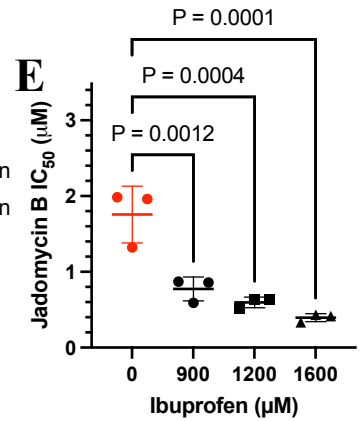
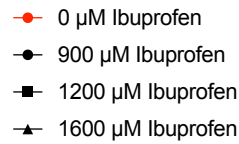
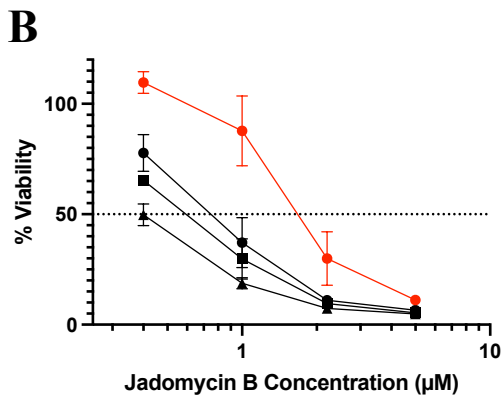
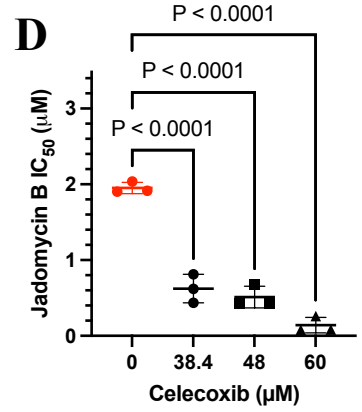
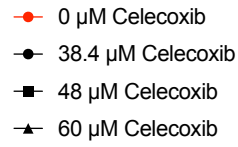
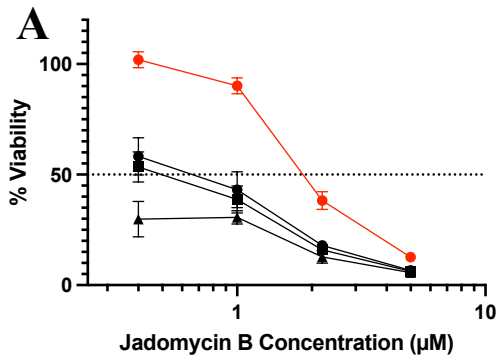


Figure B.10: Synergistic Activity of Jadomycins with Celecoxib, Naproxen, and Ibuprofen in 231-JB cells

Dose response curves and calculated IC₅₀ values, respectively, for combinations of jadomycin B (0-5 μM) and (A, D) celecoxib (0-60 μM), (B, E) ibuprofen (0-1600 μM), and (C, F) naproxen (0-1500 μM) in 231-JB cells used to determine synergy as presented in **Figure 4.30** and **Tables C.16, C.17, and C.18**. Each datapoint represents the mean value of triplicate assays, each consisting of quadruplicate technical replicates ± standard deviation. For IC₅₀ values, significant difference from jadomycin B alone (highlighted in red) is indicated by reported p-value ($P \leq 0.05$) as determined by two-way ANOVA followed by Bonferroni's multiple comparison test. (Figures on previous page)

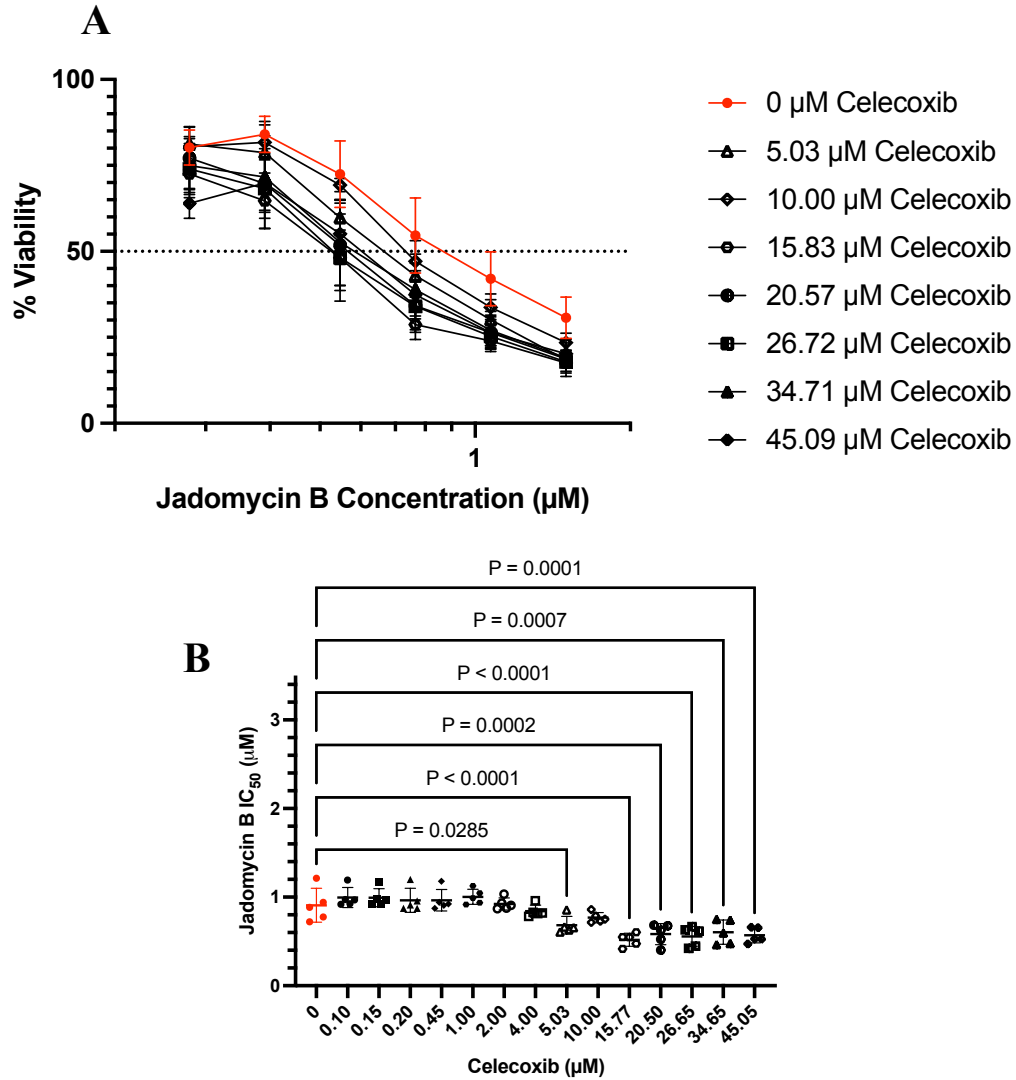


Figure B.11: Synergistic Activity of Jadomyjcins with Celecoxib Across an Expanded Range of Concentrations in 231-CON cells

Dose response curves (A) and calculated IC_{50} values (B) for combinations of jadomyjcins B (0-1.5 μ M) and celecoxib (0-45 μ M) in 231-CON cells used to determine synergy as presented in **Figure 4.32A**. Only those dose response curves with statistically significant differences in IC_{50} have been included in A. Each datapoint represents the mean value of quintuplicate assays, each consisting of quadruplicate technical replicates \pm standard deviation. For IC_{50} values, significant difference from jadomyjcins B alone (highlighted in red) is indicated by reported p-value ($P \leq 0.05$) as determined by two-way ANOVA followed by Bonferroni's multiple comparison test.

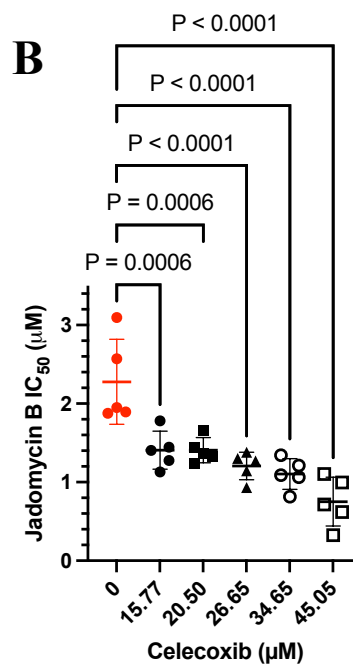
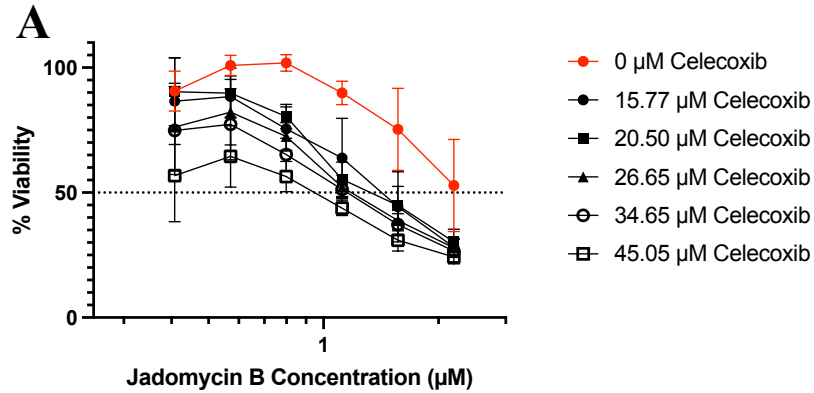


Figure B.12: Synergistic Activity of Jadomycins with Celecoxib Across an Expanded Range of Concentrations in 231-JB cells

Dose response curves (A) and calculated IC₅₀ values (B) for combinations of jadomycin B (0-2.2 µM) and celecoxib (0-45 µM) in 231-JB cells used to determine synergy as presented in **Figure 4.32B**. Each datapoint represents the mean value of quintuplicate assays, each consisting of quadruplicate technical replicates ± standard deviation. For IC₅₀ values, significant difference from jadomycin B alone (highlighted in red) is indicated by reported p-value ($P \leq 0.05$) as determined by two-way ANOVA followed by Bonferroni's multiple comparison test.

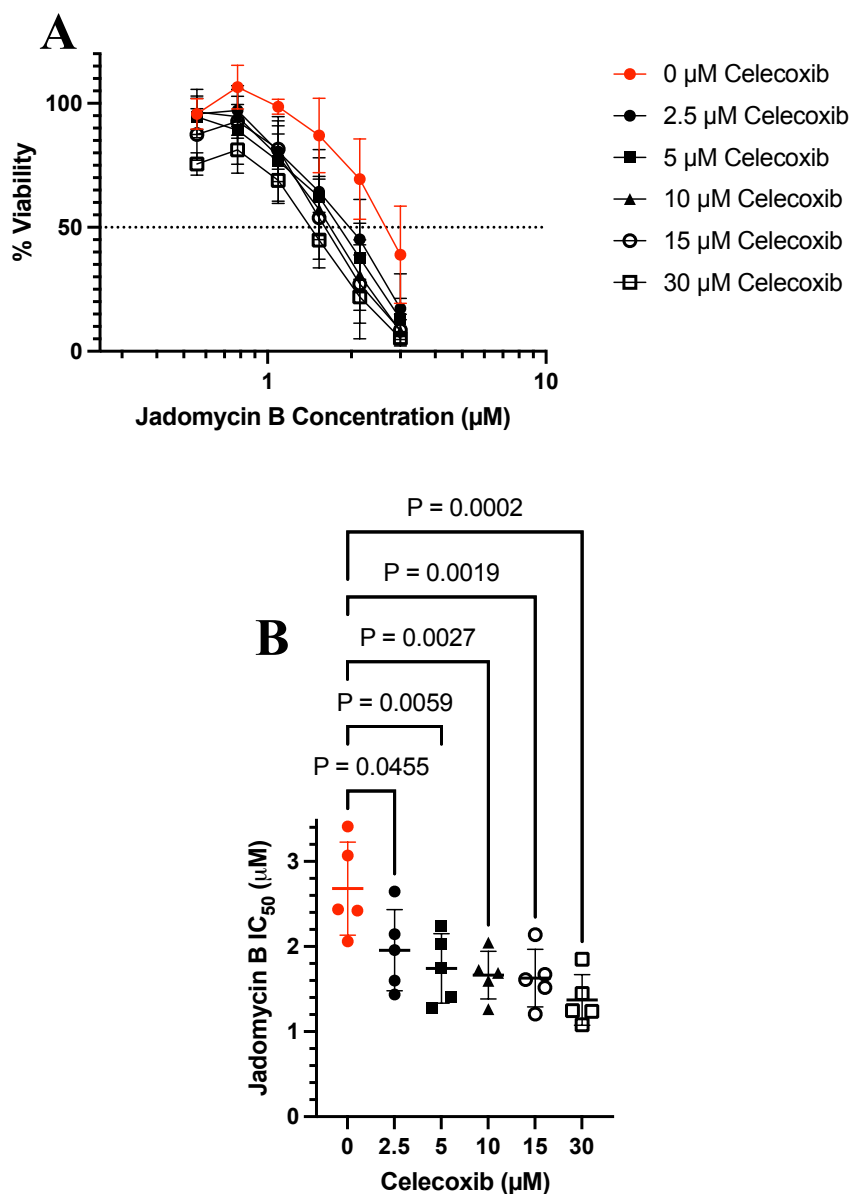


Figure B.13: Synergistic Activity of Jadomycins with Celecoxib in MCF-7 cells

Dose response curves (**A**) and calculated IC_{50} values (**B**) for combinations of jadomycin B (0-3 μM) and celecoxib (0-30 μM) in MCF-7 cells used to determine synergy as presented in **Figure 4.31** and **Table C.19**. Each datapoint represents the mean value of quintuplicate assays, each consisting of quadruplicate technical replicates \pm standard deviation. For IC_{50} values, significant difference from jadomycin B alone (highlighted in red) is indicated by reported p-value ($P \leq 0.05$) as determined by two-way ANOVA followed by Bonferroni's multiple comparison test.

Appendix C:Supplementary Tables

Table C.1: Interpolated Dose Reduction Index Values for a Combination of Jadomycin B and Doxorubicin

Dose reduction index values, reflecting fold change in dose needed to achieve a specific fraction affected in 231-CON cells were calculated using CompuSyn from the median effect parameters described in **Table 4.2**.

Fraction Affected (f_a)	Drug Used Alone		Dose Reduction Index (fold reduction in dose) When Used in Combination	
	<i>Test Compound</i>	<i>TOP2 Poison</i>	Jadomycin B	Doxorubicin
	Jadomycin B (μM)	Doxorubicin (μM)		
0.05	0.23	0.01	6.96	0.29
0.1	0.37	0.05	5.62	0.47
0.15	0.48	0.09	4.92	0.64
0.2	0.60	0.16	4.45	0.79
0.25	0.71	0.25	4.10	0.95
0.3	0.83	0.36	3.81	1.12
0.35	0.95	0.52	3.57	1.29
0.4	1.08	0.72	3.36	1.48
0.45	1.23	0.98	3.17	1.69
0.5	1.38	1.33	2.99	1.92
0.55	1.56	1.81	2.82	2.18
0.6	1.77	2.48	2.66	2.48
0.65	2.01	3.42	2.50	2.85
0.7	2.31	4.86	2.34	3.29
0.75	2.69	7.14	2.18	3.86
0.8	3.20	11.09	2.01	4.64
0.85	3.95	18.89	1.82	5.79
0.9	5.23	38.31	1.59	7.78
0.95	8.22	120.06	1.28	12.51
0.97	11.33	270.63	1.10	17.54
Average			3.16	3.68

Table C.2: Interpolated Dose Reduction Index Values for a Combination of Jadomycin B and Mitoxantrone

Dose reduction index values, reflecting fold change in dose needed to achieve a specific fraction affected in 231-CON cells were calculated using CompuSyn from the median effect parameters described in **Table 4.2**.

Fraction Affected (f_a)	Drug Used Alone		Dose Reduction Index (fold reduction in dose) When Used in Combination	
	<i>Test Compound</i> Jadomycin B (μM)	<i>TOP2 Poison</i> Mitoxantrone (μM)	Jadomycin B	Mitoxantrone
0.05	0.23	0.01	2.07	0.63
0.1	0.37	0.02	1.91	0.99
0.15	0.48	0.03	1.82	1.30
0.2	0.60	0.05	1.75	1.60
0.25	0.71	0.08	1.70	1.90
0.3	0.83	0.11	1.66	2.21
0.35	0.95	0.15	1.62	2.54
0.4	1.08	0.20	0.16	2.89
0.45	1.23	0.26	1.55	3.26
0.5	1.38	0.34	1.51	3.68
0.55	1.56	0.44	1.48	4.15
0.6	1.77	0.57	1.45	4.69
0.65	2.01	0.76	1.42	5.34
0.7	2.31	1.02	1.38	6.12
0.75	2.69	1.42	1.35	7.11
0.8	3.20	2.07	1.31	8.45
0.85	3.95	3.27	1.26	10.42
0.9	5.23	6.00	1.20	13.75
0.95	8.22	16.00	1.11	21.52
0.97	11.33	32.12	1.04	29.91
Average			1.44	6.62

Table C.3: Interpolated Dose Reduction Index Values for a Combination of Jadomycin B and SN-38

Dose reduction index values, reflecting fold change in dose needed to achieve a specific fraction affected in 231-CON cells were calculated using CompuSyn from the median effect parameters described in **Table 4.2**.

Fraction Affected (f_a)	Drug Used Alone		Dose Reduction Index (fold reduction in dose) When Used in Combination	
	<i>Test Compound</i> Jadomycin B (μM)	<i>TOP1 Poison</i> SN-38 (μM)	Jadomycin B	SN-38
0.05	0.23	0.17	3.91	2.88
0.1	0.37	0.38	3.38	3.47
0.15	0.48	0.61	3.09	3.90
0.2	0.60	0.88	2.89	4.25
0.25	0.71	1.19	2.73	4.57
0.3	0.83	1.55	2.6	4.87
0.35	0.95	1.97	2.49	5.16
0.4	1.08	2.46	2.39	5.44
0.45	1.23	3.05	2.30	5.73
0.5	1.38	3.77	2.21	6.02
0.55	1.56	4.65	2.13	6.33
0.6	1.77	5.77	2.04	6.67
0.65	2.01	7.22	1.96	7.04
0.7	2.31	9.17	1.88	7.45
0.75	2.69	11.94	1.79	7.94
0.8	3.20	16.14	1.69	8.53
0.85	3.95	23.27	1.58	9.31
0.9	5.23	37.81	1.45	10.46
0.95	8.22	82.82	1.25	12.61
0.97	11.33	144.69	1.13	14.41
Average			2.24	6.85

Table C.4: Interpolated Dose Reduction Index Values for a Combination of Jadomycin B and MG132

Dose reduction index values, reflecting fold change in dose needed to achieve a specific fraction affected in 231-CON cells were calculated using CompuSyn from the median effect parameters described in **Table 4.2**.

Fraction Affected (f_a)	Drug Used Alone		Dose Reduction Index (fold reduction in dose) When Used in Combination	
	<i>Test Compound</i>	<i>Proteasome Inhibitor</i>	Jadomycin B	MG132
	Jadomycin B (μM)	MG132 (μM)		
0.05	0.23	0.12	2.9	8.53
0.1	0.37	0.16	2.69	6.73
0.15	0.48	0.20	2.57	5.81
0.2	0.60	0.23	2.48	5.20
0.25	0.71	0.25	2.41	4.75
0.3	0.83	0.28	2.35	4.39
0.35	0.95	0.30	2.30	4.08
0.4	1.08	0.33	2.25	3.81
0.45	1.23	0.36	2.21	3.57
0.5	1.38	0.39	2.16	3.35
0.55	1.56	0.42	2.12	3.15
0.6	1.77	0.45	2.07	2.95
0.65	2.01	0.49	2.03	2.75
0.7	2.31	0.54	1.98	2.56
0.75	2.69	0.59	1.94	2.37
0.8	3.20	0.66	1.88	2.16
0.85	3.95	0.76	1.82	1.93
0.9	5.23	0.91	1.73	1.67
0.95	8.22	1.21	1.61	1.32
0.97	11.33	1.49	1.52	1.11
Average			2.15	3.61

Table C.5: Interpolated Dose Reduction Index Values for a Combination of Doxorubicin and Mitoxantrone

Dose reduction index values, reflecting fold change in dose needed to achieve a specific fraction affected in 231-CON cells were calculated using CompuSyn from the median effect parameters described in **Table 4.2**.

Fraction Affected (f_a)	Drug Used Alone		Dose Reduction Index (fold reduction in dose) When Used in Combination	
	<i>TOP2 Poison</i>	<i>TOP2 Poison</i>	Doxorubicin	Mitoxantrone
	Doxorubicin (μM)	Mitoxantrone (μM)		
0.05	0.01	0.01	0.80	5.73
0.1	0.05	0.02	0.87	5.33
0.15	0.09	0.03	0.92	5.10
0.2	0.16	0.05	0.96	4.93
0.25	0.25	0.08	1.00	4.80
0.3	0.36	0.11	1.03	4.68
0.35	0.52	0.15	1.06	4.58
0.4	0.72	0.20	1.08	4.49
0.45	0.98	0.26	1.11	4.40
0.5	1.33	0.34	1.14	4.32
0.55	1.81	0.44	1.17	4.23
0.6	2.48	0.57	1.20	4.15
0.65	3.42	0.76	1.23	4.07
0.7	4.86	1.02	1.26	3.98
0.75	7.14	1.42	1.30	3.88
0.8	11.09	2.07	1.35	3.78
0.85	18.89	3.27	1.40	3.65
0.9	38.31	6.00	1.49	3.49
0.95	120.06	16.00	1.63	3.25
0.97	270.63	32.12	1.74	3.09
Average			1.19	4.30

Table C.6: Interpolated Dose Reduction Index Values for a Combination of Doxorubicin and SN-38

Dose reduction index values, reflecting fold change in dose needed to achieve a specific fraction affected in 231-CON cells were calculated using CompuSyn from the median effect parameters described in **Table 4.2**.

Fraction Affected (f_a)	Drug Used Alone		Dose Reduction Index (fold reduction in dose) When Used in Combination	
	<i>TOP2 Poison</i>	<i>TOPI Poison</i>	Doxorubicin	SN-38
	Doxorubicin (μM)	SN-38 (μM)		
0.05	0.01	0.17	4.75	82.65
0.1	0.05	0.38	4.14	50.35
0.15	0.09	0.61	3.8	37.04
0.2	0.16	0.88	3.56	29.40
0.25	0.25	1.19	3.38	24.29
0.3	0.36	1.55	3.23	20.56
0.35	0.52	1.97	3.09	17.67
0.4	0.72	2.46	2.98	15.34
0.45	0.98	3.05	2.87	13.39
0.5	1.33	3.77	2.76	11.72
0.55	1.81	4.65	2.66	10.26
0.6	2.48	5.77	2.56	8.96
0.65	3.42	7.22	2.46	7.77
0.7	4.86	9.17	2.36	6.68
0.75	7.14	11.94	2.26	5.66
0.8	11.09	16.14	2.14	4.67
0.85	18.89	23.27	2.01	3.71
0.9	38.31	37.81	1.84	2.73
0.95	120.06	82.82	1.61	1.66
0.97	270.63	144.69	1.46	1.17
Average			2.80	17.78

Table C.7: Interpolated Dose Reduction Index Values for a Combination of Doxorubicin and MG132

Dose reduction index values, reflecting fold change in dose needed to achieve a specific fraction affected in 231-CON cells were calculated using CompuSyn from the median effect parameters described in **Table 4.2**.

Fraction Affected (f_a)	Drug Used Alone		Dose Reduction Index (fold reduction in dose) When Used in Combination	
	<i>TOP2 Poison</i>	<i>Proteasome Inhibitor</i>	Doxorubicin	MG132
	Doxorubicin (μM)	MG132 (μM)		
0.05	0.01	0.12	0.16	10.59
0.1	0.05	0.16	0.26	7.27
0.15	0.09	0.20	0.34	5.75
0.2	0.16	0.23	0.43	4.82
0.25	0.25	0.25	0.51	4.17
0.3	0.36	0.28	0.60	3.68
0.35	0.52	0.30	0.70	3.28
0.4	0.72	0.33	0.80	2.94
0.45	0.98	0.36	0.91	2.65
0.5	1.33	0.39	1.03	2.40
0.55	1.81	0.42	1.17	2.17
0.6	2.48	0.45	1.34	1.95
0.65	3.42	0.49	1.53	1.75
0.7	4.86	0.54	1.77	1.56
0.75	7.14	0.59	2.08	1.38
0.8	11.09	0.66	2.49	1.19
0.85	18.89	0.76	3.11	1.00
0.9	38.31	0.91	4.17	0.79
0.95	120.06	1.21	6.71	0.54
0.97	270.63	1.49	9.41	0.41
Average			1.98	3.01

Table C.8: Interpolated Dose Reduction Index Values for a Combination of Mitoxantrone and SN-38

Dose reduction index values, reflecting fold change in dose needed to achieve a specific fraction affected in 231-CON cells were calculated using CompuSyn from the median effect parameters described in **Table 4.2**.

Fraction Affected (f_a)	Drug Used Alone		Dose Reduction Index (fold reduction in dose) When Used in Combination	
	<i>TOP2 Poison</i>	<i>TOP1 Poison</i>	Mitoxantrone	SN-38
	Mitoxantrone (μM)	SN-38 (μM)		
0.05	0.01	0.17	3.74	9.05
0.1	0.02	0.38	4.32	8.60
0.15	0.03	0.61	4.73	8.34
0.2	0.05	0.88	5.06	8.15
0.25	0.08	1.19	5.35	7.99
0.3	0.11	1.55	5.62	7.86
0.35	0.15	1.97	5.87	7.73
0.4	0.20	2.46	6.12	7.62
0.45	0.26	3.05	6.37	7.52
0.5	0.34	3.77	6.62	7.42
0.55	0.44	4.65	6.89	7.32
0.6	0.57	5.77	7.16	7.22
0.65	0.76	7.22	7.47	7.11
0.7	1.02	9.17	7.81	7.01
0.75	1.42	11.94	8.20	6.89
0.8	2.07	16.14	8.67	6.76
0.85	3.27	23.27	9.28	6.60
0.9	6.00	37.81	10.16	6.40
0.95	16.00	82.82	11.74	6.08
0.97	32.12	144.69	13.02	5.87
Average			7.21	7.38

Table C.9: Interpolated Dose Reduction Index Values for a Combination of Mitoxantrone and MG132

Dose reduction index values, reflecting fold change in dose needed to achieve a specific fraction affected in 231-CON cells were calculated using CompuSyn from the median effect parameters described in **Table 4.2**.

Fraction Affected (f_a)	Drug Used Alone		Dose Reduction Index (fold reduction in dose) When Used in Combination	
	<i>TOP2 Poison</i>	<i>Proteasome Inhibitor</i>	Mitoxantrone	MG132
	Mitoxantrone (μM)	MG132 (μM)		
0.05	0.01	0.12	0.35	6.12
0.1	0.02	0.16	0.49	4.25
0.15	0.03	0.20	0.60	3.40
0.2	0.05	0.23	0.69	2.87
0.25	0.08	0.25	0.79	2.49
0.3	0.11	0.28	0.88	2.20
0.35	0.15	0.30	0.97	1.97
0.4	0.20	0.33	1.06	1.78
0.45	0.26	0.36	1.16	1.61
0.5	0.34	0.39	1.27	1.46
0.55	0.44	0.42	1.39	1.32
0.6	0.57	0.45	1.52	1.20
0.65	0.76	0.49	1.66	1.08
0.7	1.02	0.54	1.84	0.96
0.75	1.42	0.59	2.05	0.85
0.8	2.07	0.66	2.32	0.74
0.85	3.27	0.76	2.70	0.63
0.9	6.00	0.91	3.31	0.50
0.95	16.00	1.21	4.58	0.35
0.97	32.12	1.49	5.77	0.27
Average			1.77	1.80

Table C.10: Interpolated Dose Reduction Index Values for a Combination of SN-38 and MG132

Dose reduction index values, reflecting fold change in dose needed to achieve a specific fraction affected in 231-CON cells were calculated using CompuSyn from the median effect parameters described in **Table 4.2**.

Fraction Affected (f_a)	Drug Used Alone		Dose Reduction Index (fold reduction in dose) When Used in Combination	
	<i>TOPI Poison</i>	<i>Proteasome Inhibitor</i>	SN-38	MG132
	SN-38 (μM)	MG132 (μM)		
0.05	0.17	0.12	0.63	3.62
0.1	0.38	0.16	0.94	3.28
0.15	0.61	0.20	1.2	3.09
0.2	0.88	0.23	1.44	2.95
0.25	1.19	0.25	1.67	2.84
0.3	1.55	0.28	1.91	2.75
0.35	1.97	0.30	2.16	2.67
0.4	2.46	0.33	2.42	2.59
0.45	3.05	0.36	2.70	2.52
0.5	3.77	0.39	3.00	2.46
0.55	4.65	0.42	3.33	2.39
0.6	5.77	0.45	3.72	2.33
0.65	7.22	0.49	4.16	2.27
0.7	9.17	0.54	4.70	2.20
0.75	11.94	0.59	5.37	2.13
0.8	16.14	0.66	6.25	2.05
0.85	23.27	0.76	7.52	1.96
0.9	37.81	0.91	9.61	1.84
0.95	82.82	1.21	14.27	1.67
0.97	144.69	1.49	18.92	1.56
Average			4.80	2.46

Table C.11: Expression Changes Found with Human Cancer Drug Target Array

Changes in gene expression found with the QIAGEN 84 gene Human Cancer Drug Targets PCR Array. Fold change in 231-JB cells is normalized to expression in 231-CON cells. Results are reported from a single array, therefore no statistical analysis was conducted. (Table on following pages)

Gene	Description	Fold Change
<i>ABCC1</i>	ATP-binding cassette, sub-family C, member 1	1.010897038
<i>AKT1</i>	V-akt murine thymoma viral oncogene homolog 1	1.092923574
<i>AKT2</i>	V-akt murine thymoma viral oncogene homolog 2	1.051178557
<i>ATF2</i>	Activating transcription factor 2	1.382649475
<i>AURKA</i>	Aurora kinase A	0.958236247
<i>AURKB</i>	Aurora kinase B	0.872546722
<i>AURKC</i>	Aurora kinase C	1.947245706
<i>BCL2</i>	B-cell CLL/lymphoma 2	0.881610942
<i>BIRC5</i>	Baculoviral IAP repeat containing 5	0.599740679
<i>CDC25A</i>	Cell division cycle 25 homolog A	1.549377496
<i>CDK1</i>	Cyclin-dependent kinase 1	0.458677724
<i>CDK2</i>	Cyclin-dependent kinase 2	0.79619183
<i>CDK4</i>	Cyclin-dependent kinase 4	1.083402772
<i>CDK5</i>	Cyclin-dependent kinase 5	1.009857791
<i>CDK7</i>	Cyclin-dependent kinase 7	1.269423143
<i>CDK8</i>	Cyclin-dependent kinase 8	0.732675491
<i>CDK9</i>	Cyclin-dependent kinase 9	1.06299328
<i>CTSB</i>	Cathepsin B	1.151796346
<i>CTSD</i>	Cathepsin D	2.246709932
<i>CTSL1</i>	Cathepsin L1	3.593310599
<i>CTSS</i>	Cathepsin S	3.952843127
<i>EGFR</i>	Epidermal growth factor receptor	1.174491449
<i>ERBB2</i>	V-erb-b2 erythroblastic leukemia viral oncogene homolog 2	0.96373238
<i>ERBB3</i>	V-erb-b2 erythroblastic leukemia viral oncogene homolog 3	0.678785764
<i>ERBB4</i>	V-erb-a erythroblastic leukemia viral oncogene homolog 4	2.942628948
<i>ESR1</i>	Estrogen receptor 1	0.779607118
<i>ESR2</i>	Estrogen receptor 2	3.506429932
<i>FIGF</i>	C-fos induced growth factor	1.764126586
<i>FLT1</i>	Fms-related tyrosine kinase 1	1.358119056
<i>FLT4</i>	Fms-related tyrosine kinase 4	3.332027304
<i>GRB2</i>	Growth factor receptor-bound protein 2	0.948627485
<i>GSTP1</i>	Glutathione S-transferase pi 1	0.958945951
<i>HDAC1</i>	Histone deacetylase 1	1.129475578
<i>HDAC11</i>	Histone deacetylase 11	0.604279684
<i>HDAC2</i>	Histone deacetylase 2	0.829305906
<i>HDAC3</i>	Histone deacetylase 3	0.82461565
<i>HDAC4</i>	Histone deacetylase 4	1.953467656
<i>HDAC6</i>	Histone deacetylase 6	1.320742887
<i>HDAC7</i>	Histone deacetylase 7	0.847596439
<i>HDAC8</i>	Histone deacetylase 8	0.781216666
<i>HIF1A</i>	Hypoxia inducible factor 1, alpha subunit	1.25541196
<i>HRAS</i>	V-Ha-ras Harvey rat sarcoma viral oncogene homolog	1.079215566
<i>HSP90AA1</i>	Heat shock protein 90kDa alpha, class A member 1	0.9085313
<i>HSP90B1</i>	Heat shock protein 90kDa beta, member 1	0.968421061
<i>IGF1</i>	Insulin-like growth factor 1	2.216015405
<i>IGF1R</i>	Insulin-like growth factor 1 receptor	1.043335116

Gene	Description	Fold Change
<i>IGF2</i>	Insulin-like growth factor 2	0.562534329
<i>IRF5</i>	Interferon regulatory factor 5	1.423748845
<i>KDR</i>	Kinase insert domain receptor	0.633945065
<i>KIT</i>	V-kit Hardy-Zuckerman 4 feline sarcoma viral oncogene homolog	2.380650347
<i>KRAS</i>	V-Ki-ras2 Kirsten rat sarcoma viral oncogene homolog	0.761943158
<i>MDM2</i>	Mdm2 p53 binding protein homolog	1.212049209
<i>MDM4</i>	Mdm4 p53 binding protein homolog	1.292983863
<i>MTOR</i>	Mechanistic target of rapamycin	1.008883633
<i>NFKB1</i>	Nuclear factor kappa light polypeptide gene enhancer in B-cells 1	1.033402984
<i>NRAS</i>	Neuroblastoma RAS viral oncogene homolog	1.004846263
<i>NTN3</i>	Netrin 3	1.8984995
<i>PARP1</i>	Poly (ADP-ribose) polymerase 1	1.021619956
<i>PARP2</i>	Poly (ADP-ribose) polymerase 2	0.981964693
<i>PARP4</i>	Poly (ADP-ribose) polymerase family, member 4	1.025472521
<i>PDGFRA</i>	Platelet-derived growth factor receptor, alpha polypeptide	0.656841528
<i>PDGFRB</i>	Platelet-derived growth factor receptor, beta polypeptide	0.446833181
<i>PGR</i>	Progesterone receptor	1.482563473
<i>PIK3C2A</i>	Phosphoinositide-3-kinase, class 2, alpha polypeptide	0.940811361
<i>PIK3C3</i>	Phosphoinositide-3-kinase, class 3	0.948893403
<i>PIK3CA</i>	Phosphoinositide-3-kinase, catalytic, alpha polypeptide	0.719468312
<i>PLK1</i>	Polo-like kinase 1	0.888311406
<i>PLK2</i>	Polo-like kinase 2	0.852597739
<i>PLK3</i>	Polo-like kinase 3	1.569650812
<i>PLK4</i>	Polo-like kinase 4	0.792983598
<i>PRKCA</i>	Protein kinase C, alpha	1.067051239
<i>PRKCB</i>	Protein kinase C, beta	0.619662544
<i>PRKCD</i>	Protein kinase C, delta	1.929366691
<i>PRKCE</i>	Protein kinase C, epsilon	0.881176297
<i>PTGS2</i>	Prostaglandin-endoperoxide synthase 2	22.3276901
<i>RHOA</i>	Ras homolog gene family, member A	0.836649043
<i>RHOB</i>	Ras homolog gene family, member B	2.202829966
<i>TERT</i>	Telomerase reverse transcriptase	0.329027462
<i>TNKS</i>	Tankyrase, TFR1-interacting ankyrin-related ADP-ribose polymerase	1.340088767
<i>TOP2A</i>	Topoisomerase II alpha 170kDa	0.913660199
<i>TOP2B</i>	Topoisomerase II beta 180kDa	1.004871505
<i>TP53</i>	Tumor protein p53	1.358332741
<i>TXN</i>	Thioredoxin	1.457911321
<i>TXNRD1</i>	Thioredoxin reductase 1	2.11729119
<i>ACTB</i>	Actin, beta	0.843435868
<i>B2M</i>	Beta-2-microglobulin	1.147079387
<i>GAPDH</i>	Glyceraldehyde-3-phosphate dehydrogenase	1.442532803
<i>HPRT1</i>	Hypoxanthine phosphoribosyltransferase 1	0.926159993
<i>RPLP0</i>	Ribosomal protein, large, P0	0.773646818

Table C.12: Jadomycin B and Celecoxib Act Synergistically to Inhibit COX2

Synergy scores \pm standard deviation were calculated using SynergyFinder 3.0 to determine if jadomycin B and celecoxib act synergistically in combination in a purified enzyme assay. Synergy scores represent fold change from expected effect if the two molecules were acting additively, therefore, scores > 10 denote synergy, < -10 denote antagonism, and < 10 but > -10 denote additivity. Scores were calculated from triplicate assays. Graphical reported in **Figure 4.26**.

		Celecoxib Concentration (μM)			
		0.05	0.10	0.15	0.20
Jadomycin B Concentration (μM)	1.00	4.17 \pm 5.28	3.97 \pm 6.22	13.97 \pm 0.44	12.29 \pm 1.16
	2.50	8.91 \pm 1.36	3.03 \pm 8.58	12.43 \pm 3.92	13.32 \pm 0.98
	5.00	15.74 \pm 9.90	10.70 \pm 2.98	20.46 \pm 1.74	14.76 \pm 0.72
	10.00	12.00 \pm 2.86	13.04 \pm 7.35	26.73 \pm 1.63	13.14 \pm 0.62
	20.00	10.71 \pm 3.06	15.04 \pm 7.32	20.27 \pm 0.81	12.75 \pm 0.36

Table C.13: Synergy Scores for Jadomycin B and Celecoxib in 231-CON Cells

Synergy scores were calculated using SynergyFinder 3.0 to determine if jadomycin B (0-5 μ M) and celecoxib (0-60 μ M) act in combination to elicit synergistic changes in cellular viability in 231-CON cells. Synergy scores represent fold change from expected effect if the two molecules were acting additively, therefore, scores > 10 denote synergy, < -10 denote antagonism, and < 10 but > -10 denote additivity. Scores were calculated from triplicate assays. Graphical results are presented in **Figure 4.29**.

Jadomycin B Concentration (μ M)	Celecoxib Concentration (μ M)									
	0.10	0.15	0.20	0.45	1.00	2.00	4.00	5.03		
0.28	-1.60 \pm 7.12	-6.56 \pm 5.50	-5.82 \pm 6.28	-6.61 \pm 3.98	-6.61 \pm 2.97	0.17 \pm 4.07	-5.12 \pm 1.93	9.63 \pm 4.92		
0.39	-1.04 \pm 3.90	0.29 \pm 4.33	2.42 \pm 4.25	-2.31 \pm 4.03	4.16 \pm 4.39	4.64 \pm 3.94	1.34 \pm 3.46	15.33 \pm 9.08		
0.40	-	-	-	-	-	-	-	-		
0.55	3.03 \pm 6.34	4.10 \pm 5.93	6.32 \pm 6.62	7.86 \pm 8.90	3.09 \pm 9.85	5.96 \pm 2.41	7.16 \pm 4.94	25.16 \pm 13.84		
0.77	8.23 \pm 10.64	8.70 \pm 10.89	12.54 \pm 12.50	11.75 \pm 12.14	9.19 \pm 7.19	15.81 \pm 5.78	12.54 \pm 5.69	29.81 \pm 14.77		
1.00	-	-	-	-	-	-	-	-		
1.07	6.54 \pm 8.64	6.22 \pm 7.28	8.72 \pm 10.27	9.39 \pm 8.00	3.36 \pm 3.57	10.61 \pm 3.99	12.31 \pm 3.58	22.54 \pm 7.48		
1.50	6.08 \pm 0.80	7.22 \pm 1.78	8.83 \pm 1.86	7.61 \pm 1.33	4.64 \pm 1.60	7.31 \pm 2.37	8.33 \pm 1.76	16.98 \pm 1.39		
2.20	-	-	-	-	-	-	-	-		
5.00	-	-	-	-	-	-	-	-		

Jadomycin B Concentration (μ M)	Celecoxib Concentration (μ M)									
	10.00	15.83	20.57	26.72	34.71	38.40	45.09	48.00	60.00	
0.28	6.71 \pm 2.92	10.77 \pm 6.91	3.54 \pm 9.17	9.24 \pm 7.43	7.32 \pm 7.81	-	7.17 \pm 4.35	-	-	
0.39	7.78 \pm 5.08	16.39 \pm 8.06	14.32 \pm 7.81	12.36 \pm 11.66	4.33 \pm 11.95	-	3.73 \pm 8.48	-	-	
0.40	-	-	-	-	-	13.68 \pm 3.55	-	10.93 \pm 7.70	4.80 \pm 6.15	
0.55	14.77 \pm 1.95	25.61 \pm 8.08	22.19 \pm 13.10	26.34 \pm 12.72	21.89 \pm 12.56	-	13.95 \pm 8.95	-	-	
0.77	23.73 \pm 6.02	33.33 \pm 4.38	29.37 \pm 6.99	29.79 \pm 7.63	18.74 \pm 7.67	-	18.38 \pm 7.05	-	-	
1.00	-	-	-	-	-	15.07 \pm 8.21	-	18.87 \pm 9.26	-2.30 \pm 9.00	
1.07	17.00 \pm 2.23	22.80 \pm 1.85	18.72 \pm 3.82	20.83 \pm 4.38	16.59 \pm 5.55	-	13.65 \pm 4.58	-	-	
1.50	12.49 \pm 2.75	15.04 \pm 2.46	14.47 \pm 2.60	15.44 \pm 3.26	9.44 \pm 5.47	-	8.41 \pm 3.16	-	-	
2.20	-	-	-	-	-	9.83 \pm 6.44	-	7.56 \pm 4.86	1.51 \pm 2.18	
5.00	-	-	-	-	-	7.45 \pm 1.64	-	6.13 \pm 1.88	1.92 \pm 1.02	

Table C.14: Synergy Scores for Jadomycin B and Ibuprofen in 231-CON Cells

Synergy scores were calculated using SynergyFinder 3.0 to determine if jadomycin B (0-5 μM) and ibuprofen (0-1600 μM) act in combination to elicit synergistic changes in cellular viability in 231-CON cells. Synergy scores represent fold change from expected effect if the two molecules were acting additively, therefore, scores > 10 denote synergy, < -10 denote antagonism, and < 10 but > -10 denote additivity. Scores were calculated from triplicate assays. Graphical results are presented in **Figure 4.29**.

		Ibuprofen Concentration (μM)		
		900	1200	1600
Jadomycin B Concentration (μM)	0.40	49.71 ± 14.3	35.62 ± 14.0	17.51 ± 9.27
	1.00	36.54 ± 6.53	29.63 ± 6.25	17.93 ± 6.41
	2.20	18.86 ± 4.79	16.15 ± 4.64	9.32 ± 3.11
	5.00	5.97 ± 2.69	5.40 ± 1.93	2.91 ± 1.86

Table C.15: Synergy Scores for Jadomycin B Naproxen in 231-CON Cells

Synergy scores were calculated using SynergyFinder 3.0 to determine if jadomycin B (0-5 μ M) and naproxen (0-1500 μ M) act in combination to elicit synergistic changes in cellular viability in 231-CON cells. Synergy scores represent fold change from expected effect if the two molecules were acting additively, therefore, scores > 10 denote synergy, < -10 denote antagonism, and < 10 but > -10 denote additivity. Scores were calculated from triplicate assays. Graphical results are presented in **Figure 4.29**.

		Naproxen Concentration (μ M)		
		700	1020	1500
Jadomycin B Concentration (μ M)	0.40	43.84 \pm 7.85	45.87 \pm 7.17	39.53 \pm 6.05
	1.00	20.11 \pm 3.52	21.23 \pm 3.58	17.56 \pm 3.04
	2.20	11.94 \pm 1.66	13.64 \pm 1.58	11.45 \pm 1.08
	5.00	6.63 \pm 1.06	7.03 \pm 1.02	4.72 \pm 0.88

Table C.16: Synergy Scores for Jadomycin B and Celecoxib in 231-JB Cells

Synergy scores were calculated using SynergyFinder 3.0 to determine if jadomycin B (0-5 μ M) and celecoxib (0-60 μ M) act in combination to elicit synergistic changes in cellular viability in 231-JB cells. Synergy scores represent fold change from expected effect if the two molecules were acting additively, therefore, scores > 10 denote synergy, < -10 denote antagonism, and < 10 but > -10 denote additivity. Scores were calculated from triplicate assays. Graphical results are presented in **Figure 4.30**.

	Celecoxib Concentration (μ M)							
	15.77	20.50	26.65	34.65	38.40	45.05	48.00	60.00
0.40	-	-	-	-	9.41 \pm 8.46	-	2.48 \pm 6.79	8.43 \pm 8.01
0.41	2.53 \pm 17.38	-4.38 \pm 13.54	10.13 \pm 17.4	3.62 \pm 17.60	-	18.41 \pm 18.4	-	-
0.57	5.00 \pm 8.25	-7.40 \pm 10.0	3.78 \pm 13.12	5.74 \pm 14.26	-	11.47 \pm 12.2	-	-
0.80	21.07 \pm 8.84	6.43 \pm 4.90	18.18 \pm 5.50	13.78 \pm 6.50	-	17.59 \pm 6.05	-	-
1.00	-	-	-	-	22.49 \pm 8.10	-	18.14 \pm 6.17	1.10 \pm 2.97
1.12	29.07 \pm 15.8	26.76 \pm 6.86	31.70 \pm 4.80	24.45 \pm 3.53	-	26.30 \pm 2.92	-	-
1.57	34.54 \pm 14.0	23.95 \pm 7.64	28.99 \pm 4.11	25.96 \pm 4.43	-	26.24 \pm 4.31	-	-
2.19	14.15 \pm 2.03	9.94 \pm 5.06	10.29 \pm 3.89	9.58 \pm 4.71	-	9.64 \pm 2.76	-	-
2.20	-	-	-	-	11.60 \pm 0.47	-	7.20 \pm 0.42	2.09 \pm 2.78
5.00	-	-	-	-	3.31 \pm 0.73	-	1.11 \pm 0.39	-1.47 \pm 0.39

Table C.17: Synergy Scores for Jadomycin B and Ibuprofen in 231-JB Cells

Synergy scores were calculated using SynergyFinder 3.0 to determine if jadomycin B (0-5 μM) and ibuprofen (0-1600 μM) act in combination to elicit synergistic changes in cellular viability in 231-JB cells. Synergy scores represent fold change from expected effect if the two molecules were acting additively, therefore, scores > 10 denote synergy, < -10 denote antagonism, and < 10 but > -10 denote additivity. Scores were calculated from triplicate assays. Graphical results are presented in **Figure 4.30**.

		Ibuprofen Concentration (μM)		
		900	1200	1600
Jadomycin B Concentration (μM)	0.40	7.79 ± 8.30	9.65 ± 2.20	5.47 ± 4.96
	1.00	39.38 ± 11.3	37.21 ± 9.07	34.77 ± 2.57
	2.20	19.97 ± 2.05	18.70 ± 1.31	13.28 ± 0.81
	5.00	2.66 ± 0.42	2.85 ± 0.19	1.22 ± 0.48

Table C.18: Synergy Scores for Jadomycin B and Naproxen in 231-JB Cells

Synergy scores were calculated using SynergyFinder 3.0 to determine if jadomycin B (0-5 μM) and naproxen (0-1500 μM) act in combination to elicit synergistic changes in cellular viability in 231-JB cells. Synergy scores represent fold change from expected effect if the two molecules were acting additively, therefore, scores > 10 denote synergy, < -10 denote antagonism, and < 10 but > -10 denote additivity. Scores were calculated from triplicate assays. Graphical results are presented in **Figure 4.30**.

		Naproxen Concentration (μM)		
		700	1020	1500
Jadomycin B Concentration (μM)	0.40	1.78 ± 3.95	5.74 ± 5.73	0.68 ± 6.88
	1.00	26.98 ± 15.9	37.85 ± 10.8	30.32 ± 6.56
	2.20	19.86 ± 7.49	20.99 ± 7.00	17.07 ± 6.56
	5.00	3.12 ± 3.89	3.93 ± 3.48	1.50 ± 3.08

Table C.19: Synergy Scores for Jadomycin B and Celecoxib in MCF-7 Cells

Synergy scores were calculated using SynergyFinder 3.0 to determine if jadomycin B (0-3 μM) and celecoxib (0-30 μM) act in combination to elicit synergistic changes in cellular viability in MCF-7 cells. Synergy scores represent fold change from expected effect if the two molecules were acting additively, therefore, scores > 10 denote synergy, < -10 denote antagonism, and < 10 but > -10 denote additivity. Scores were calculated from triplicate assays. Graphical results are presented in **Figure 4.32**.

		Celecoxib Concentration (μM)				
		2.50	5.00	10.00	15.00	30.00
Jadomycin B Concentration (μM)	0.56	-11.90 ± 6.28	-13.98 ± 8.38	-14.46 ± 9.16	-2.62 ± 10.46	1.93 ± 4.51
	0.78	-12.95 ± 10.04	-6.19 ± 13.75	-9.16 ± 11.03	2.88 ± 6.86	0.21 ± 9.43
	1.09	4.83 ± 7.08	2.77 ± 16.24	3.14 ± 12.32	6.87 ± 13.15	10.14 ± 9.38
	1.53	11.84 ± 17.03	19.55 ± 15.73	20.94 ± 12.19	33.38 ± 16.71	31.40 ± 11.17
	2.14	13.41 ± 16.11	27.00 ± 13.99	27.14 ± 14.24	40.50 ± 15.84	38.49 ± 16.97
	3.00	16.13 ± 14.05	15.55 ± 8.36	18.32 ± 4.69	20.76 ± 6.40	18.57 ± 2.46